THE PROCEEDINGS OF THE PHYSICAL SOCIETY

Section A

VOL. 63, PART 3 1 March 1950 No. 363 A

CONTENTS

PAGE

Mr. E. B. ANDREWS and Dr. R. F. BARROW. The Band Spectrum of GeF . 185

Mr. B. A. BILBY. On the Interactions of Dislocations and Solute Atoms . . 191

Dr. R. J. BENZIE and Dr. A. H. COOKE. Spin-Lattice Relaxation in some Paramagnetic Salts 201

Dr. R. J. BENZIE and Dr. A. H. COOKE. Specific Heats of some Paramagnetic Salts at Temperatures near 1° K. 213

Dr. D. G. E. MARTIN and Dr. H. O. W. RICHARDSON. The 'External' Photoelectron Spectrum and the Intensities of the γ-Rays of Thorium (B+C+C″) 223

Dr. H. O. W. RICHARDSON. Ellis and Aston's Theory of the Height of a Photoelectron Line 234

Prof. L. JÁNOSSY. Note on the Fluctuation Problem of Cascades 241

Dr. NORA PAGE. Some Observations on the Nuclear Disintegrations caused by Cosmic Rays in Photographic Emulsions 250

Dr. K. J. LE COUTEUR. The Evaporation Theory of Nuclear Disintegrations . 259

Mr. C. H. COLLIE, Dr. P. F. D. SHAW and Mr. H. J. GALE. The Correction of Specific β-Radioactivity for Self-Absorption 282

Dr. D. K. C. MACDONALD. The Magneto-Resistance of the Alkali Metals . 290

Letters to the Editor:

- Mr. E. R. RAE. The Radiations of Praseodymium–142 292
- Mr. R. M. LITTAUER. The Angular Distribution of Gamma-Rays from ^{7}Li(p, p′)^{7}Li* 294
- Prof. K. SITTE. On the Production of Penetrating Showers in Nuclear Collisions 295
- Mr. G. R. EVANS and Mr. T. C. GRIFFITH. Some Decay Effects of Mesons in Penetrating Showers observed in a High-Pressure Wilson Cloud Chamber 296
- Mr. D. M. EVANS and Dr. H. WILMAN. Epitaxial Strain and Disorientation in Crystals Growing on Single-Crystal Substrates 298

Corrigendum 299

Reviews of Books 300

Contents for Section B 302

Abstracts for Section B 303

Price to non-members 10*s.* net, by post 6*d.* extra. Annual subscription: £5 5*s.*
Composite subscription for both Sections A and B £9 9*s.*

Published by
THE PHYSICAL SOCIETY
1 Lowther Gardens, Prince Consort Road, London S.W.7

PROCEEDINGS OF THE PHYSICAL SOCIETY

The *Proceedings* is now published monthly in two Sections.

ADVISORY BOARD

Chairman: The President of the Physical Society (S. Chapman, M.A., D.Sc., F.R.S.).

E. N. da C. Andrade, Ph.D., D.Sc., F.R.S.
Sir Edward Appleton, G.B.E., K.C.B., D.Sc., F.R.S.
L. F. Bates, Ph.D., D.Sc.
P. M. S. Blackett, M.A., F.R.S.
Sir Lawrence Bragg, O.B.E., M.A., Sc.D., D.Sc., F.R.S.
Sir James Chadwick, D.Sc., Ph.D., F.R.S.
Lord Cherwell of Oxford, M.A., Ph.D., F.R.S.
Sir John Cockcroft, C.B.E., M.A., Ph.D., F.R.S.
Sir Charles Darwin, K.B.E., M.C., M.A., Sc.D., F.R.S.
N. Feather, Ph.D., F.R.S.
G. I. Finch, M.B.E., D.Sc., F.R.S.
D. R. Hartree, M.A., Ph.D., F.R.S.
N. F. Mott, M.A., F.R.S.
M. L. Oliphant, Ph.D., D.Sc., F.R.S.
F. E. Simon, C.B.E., M.A., D.Phil., F.R.S.
T. Smith, M.A., F.R.S.
Sir George Thomson, M.A., D.Sc., F.R.S.

Papers for publication in the *Proceedings* should be addressed to the Hon. Papers Secretary, Dr. H. H. Hopkins, at the Office of the Physical Society, 1 Lowther Gardens, Prince Consort Road, London S.W.7. Telephone : KENsington 0048, 0049.

Detailed Instructions to Authors were included in the February 1948 issue of the *Proceedings*; separate copies can be obtained from the Secretary-Editor.

BULLETIN ANALYTIQUE

Publication of the Centre National de la Recherche Scientifique, France

The *Bulletin Analytique* is an abstracting journal which appears monthly in two parts, Part I covering scientific and technical papers in the mathematical, chemical and physical sciences and their applications, Part II the biological sciences.

The *Bulletin*, which started on a modest scale in 1940 with an average of 10,000 abstracts per part, now averages 35 to 40,000 abstracts per part. The abstracts summarize briefly papers in scientific and technical periodicals received in Paris from all over the world and cover the majority of the more important journals in the world scientific press. The scope of the *Bulletin* is constantly being enlarged to include a wider selection of periodicals.

The *Bulletin* thus provides a valuable reference book both for the laboratory and for the individual research worker who wishes to keep in touch with advances in subjects bordering on his own.

A specially interesting feature of the *Bulletin* is the microfilm service. A microfilm is made of each article as it is abstracted and negative microfilm copies or prints from microfilm can be purchased from the editors.

The subscription rates for Great Britain are 4,000 frs. (£5) per annum for each part. Subscriptions can also be taken out to individual sections of the *Bulletin* as follows :

	frs.	
Pure and Applied Mathematics—Mathematics—Mechanics	550	14/6
Astronomy—Astrophysics—Geophysics	700	18/-
General Physics—Thermodynamics—Heat-Optics—Electricity and Magnetism	900	22/6
Atomic Physics—Structure of Matter	325	8/6
General Chemistry—Physical Chemistry	325	8/6
Inorganic Chemistry — Organic Chemistry — Applied Chemistry—Metallurgy	1,800	45/-
Engineering Sciences	1,200	30/-
Mineralogy—Petrography—Geology—Paleontology ..	550	14/6
Biochemistry—Biophysics—Pharmacology	900	22/6
Microbiology—Virus and Phages	600	15/6
Animal Biology—Genetics—Plant Biology	1,800	45/-
Agriculture—Nutrition and the Food Industries	550	14/6

Subscriptions can be paid directly to the editors : Centre National de la Recherche Scientifique, 18, rue Pierre-Curie, Paris 5ème. (Compte-chèque-postal 2,500–42, Paris), or through Messrs. H. K. Lewis & Co. Ltd., 136, Gower Street, London W.C. 1.

PHILIPS Electron Microscope

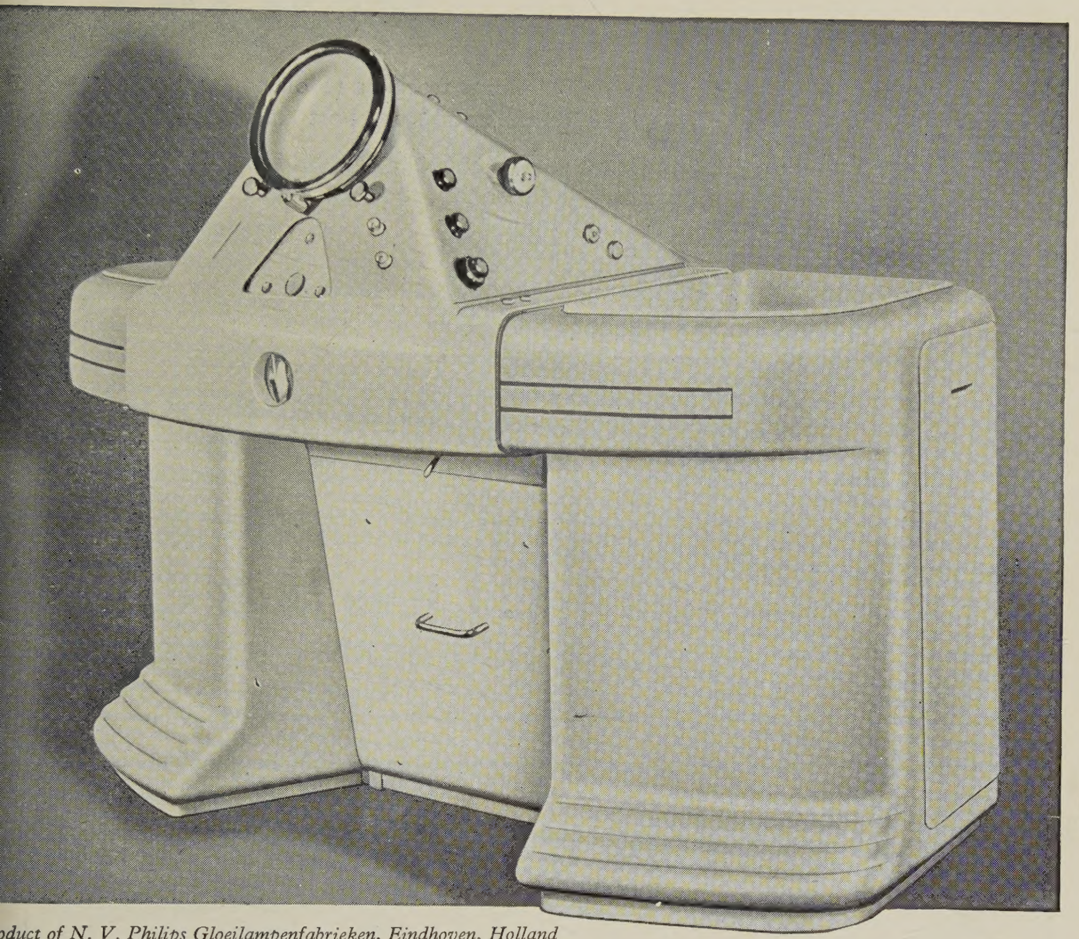

oduct of N. V. Philips Gloeilampenfabrieken, Eindhoven, Holland

- Acceleration voltage up to 100 kV.
- Magnification range continuously variable between 1,000 and 60,000 diameters.
- Photographic enlargement up to 150,000 diameters.
- Stereo-micrographs obtainable.
- Special self-sealing airlock for specimen holder
- Film camera for obtaining micrographs.
- Focussing device and quick electronic alignment.
- Apertures adjustable and removable for cleaning without dismantling.
- Large *final* image screen of 8-in. diameter.
- Microscope tube not sensitive to vibration.
- No special foundations required.
- Suitable to work in any climate and at any altitude.

PHILIPS ELECTRICAL
LIMITED

MAKERS OF : INDUSTRIAL X-RAY EQUIPMENT · ELECTRONIC APPARATUS · LAMPS & LIGHTING EQUIPMENT · ARC & RESISTANCE WELDING PLANT & ELECTRODES · SOUND AMPLIFYING INSTALLATIONS · MAGNETIC FILTERS · BATTERY CHARGERS & RECTIFIERS

USTRIAL X-RAY DEPT., CENTURY HOUSE, SHAFTESBURY AVENUE, LONDON, W.C.2.
(XB490)

SCIENTIFIC BOOKS

Messrs. H. K. LEWIS can supply from stock or to order any book on the Physical and Chemical Sciences. Catalogues post free on request.

FOREIGN DEPARTMENT : Select stock. Books not in stock obtained under Board of Trade licence.

SECOND-HAND SCIENTIFIC BOOKS. 140 GOWER STREET. An extensive stock of books in all branches of Pure and Applied Science may be seen in this department. Large and small collections bought. Back volumes of Scientific Journals.

SCIENTIFIC LENDING LIBRARY

Annual subscription from One Guinea. *Details of terms and prospectus free on request.*

THE LIBRARY CATALOGUE revised to December 1943, containing a classified index of authors and subjects: to subscribers 12*s*. 6*d*. net, to non-subscribers 25*s*. net, postage 9*d*. **Supplement** from 1944 to December 1946. To subscribers 2*s*. 6*d*. net; to non-subscribers 5*s*. net; postage 4*d*. **Bi-monthly List of Additions, free on application.**

Telephone : EUSton 4282

Telegrams : "Publicavit, Westcent, London"

H. K. LEWIS & Co. Ltd

136 GOWER STREET, LONDON, W.C

Business hours: 9 a.m. to 5 p.m., Saturdays to 1 p.m.

BALDWIN GAMMA-RADIATION DETECTOR

Type P.P.

A light-weight tropicalized dry-battery-operated G.M. detector with aural and visual indication for prospecting and surveying all radio-active minerals, including lost radium containers, etc. Cold-cathode tubes only are used, thus the battery load is negligible and the life equal to the shelf life.

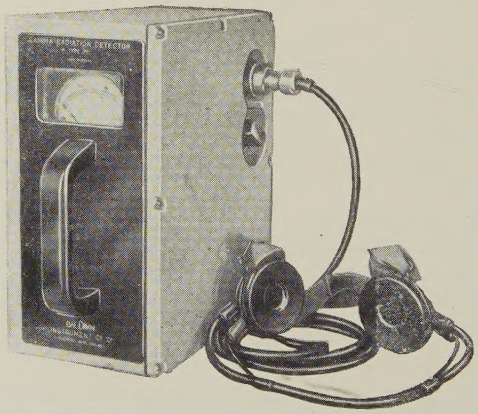

Finds Radium and other Radio-active materials

Write for Leaflet PS. 120

May be carried in the hand or slung on the body

BATTERY LIFE APPROXIMATELY 6–12 MONTHS

BALDWIN INSTRUMENT Co. Ltd.,

DARTFORD, KENT *Telephone :* DARTFORD 2989

F. C. Robinson & Partners Ltd., 308 Deansgate, Manchester, 3, Northern Agents

MICROID FLASK SHAKER

A new variable speed "wrist-action" shaker—silent, portable and efficient

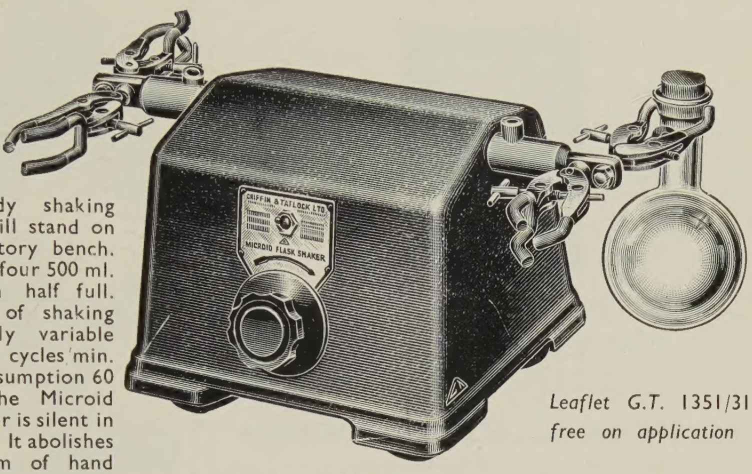

This handy shaking machine will stand on the laboratory bench. Total load, four 500 ml. flasks each half full. Frequency of shaking continuously variable up to 500 cycles/min. Power consumption 60 watts. The Microid Flask Shaker is silent in operation. It abolishes the tedium of hand shaking. It can find a use in every chemical laboratory.

Leaflet G.T. 1351/31 free on application

DELIVERY EX-STOCK

GRIFFIN and TATLOCK Ltd

Established as Scientific Instrument Makers in 1826

LONDON Kemble St., W.C.2.
MANCHESTER 19 Cheetham Hill Rd., 4.
GLASGOW 45 Renfrew St., C.2.
EDINBURGH 7 Teviot Place, 1.
BIRMINGHAM: STANDLEY BELCHER & MASON LTD., Church Street, 3.

HIGH VACUUM GAUGES NOW AVAILABLE

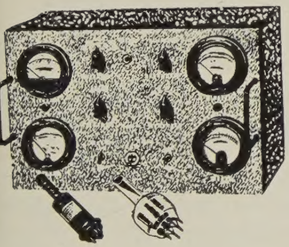

☛ THE B.A.R. THERMOCOUPLE-IONISATION GAUGE CONTROL. The newly developed Thermocouple-Ionisation Gauge Control, complete with Thermocouple and Ionisation Gauges, covers the pressure range from 2× 10⁻⁷ mm. to 1mm. Hg. Operation is dependable and simple. Ranges are 10⁻³–1mm. and 0–5, 0–1·0, 0–0·1, 0–0·01 microns. The unit is removable from its cabinet for incorporation in a central panel.

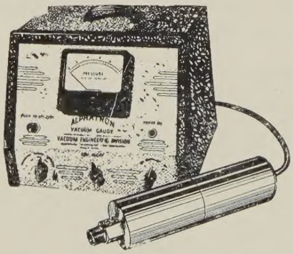

THE B.A.R. ALPHATRON is an ionisation type vacuum gauge using the ionising power of alpha-particles from a radium source to measure total pressure of any gas, vapour or mixed atmosphere from 1 μ to 10 mm. Hg with instantaneous linear response. The B.A.R. Alphatron is quickly available from batches now in production. ☛

BRITISH AMERICAN RESEARCH LTD.
SOCIATED WITH NATIONAL RESEARCH CORPORATION, BOSTON AND CAMBRIDGE, MASSACHUSETTS)

DESIGNERS AND MANUFACTURERS OF HIGH VACUUM GAUGES · VALVES · SEALS DIFFUSION PUMPS · STILLS · FURNACES · COATING EQUIPMENT AND DEHYDRATION PLANT

HILLINGTON · GLASGOW · S.W.2

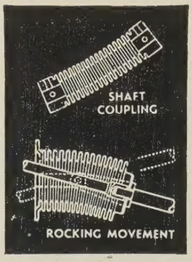
PLEASE tell us of OTHER applications

Drayton 'Hydroflex' Metal Bellows are an essential component part in Automatic coolant regulation . . Movement for pressure change . . Packless gland to seal spindle in high vacua . . Reservoir to accept liquid expansion . . Dashpot or delay device . . Barometric measurement or control . . Pressurised couplings where vibration or movement is present . . Dust seal to prevent ingress of dirt . . pressure reducing valves . . Hydraulic transmission . . Distance thermostatic control . . Low torque flexible coupling . . Pressure sealed rocking movement . . Pressurised rotating shaft seals . . Aircraft pressurised cabin control . . Refrigeration expansion valves . . Thermostatic Steam Traps . . Pressure amplifiers . . Differential pressure measurements . . Thermostatic operation of louvre or damper.

for HYDRAULICALLY FORMED

Seamless, one-piece, metal bellows combining the properties of a compression spring able to withstand repeated flexing, a packless gland and a container which can be hermetically sealed. Made by a process unique in this country, they are tough, resilient, with a uniformity of life, performance and reliability in operation unobtainable by any other method.

Drayton METAL BELLOWS

Write for List No. V800-1 **DRAYTON REGULATOR & INSTRUMENT CO. LTD.,**
WEST DRAYTON, MIDDLESEX. West Drayton 2611 B.8

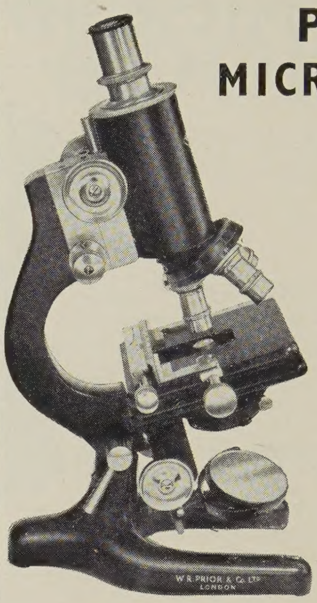

PRIOR MICROSCOPE

PRE EMINEN
IN
DESIGN
PERFORMAN
WORKMANSH
STABILITY
AND
PRICE

Literature on Request

W. R. PRIOR & CO. LT
28A DEVONSHIRE STREET, LONDON, W

PROCEEDINGS OF THE PHYSICAL SOCIETY

ADVERTISEMENT RATES

The *Proceedings* are divided into two parts, A and B. The charge for insertion is £18 for a full page in either Section A or Section B, £30 for a full page for insertion of the same advertisement in both Sections. The corresponding charges for part pages are :

½ page	£9 5 0	£15 10 0
¼ page	£4 15 0	£8 0 0
⅛ page	£2 10 0	£4 5 0

Discount is 20% for a series of six similar insertions and 10% for a series of three.

The printed area of the page is $8\frac{1}{2}'' \times 5\frac{1}{2}''$, and the screen number is 120.

Copy should be received at the Offices of the Physical Society six weeks before the date of publication of the *Proceedings*.

PAST ISSUES
OF THE
PROCEEDINGS OF THE PHYSICAL SOCIETY
AND THE
TRANSACTIONS OF THE OPTICAL SOCIETY

Your attention is drawn to the fact that as from 1st January 1950 **Messrs. Wm. Dawson & Sons Ltd.,** 102 Wigmore Street, London W.C. 1, are acting as agents for all issues of the *Proceedings of the Physical Society* up to and including 1947, and the *Transactions of the Optical Society*, Volumes 1–33.

Orders for these publications should be addressed to Messrs. Wm. Dawson direct.

The current volume and the two previous years of the *Proceedings* and all special publications are obtainable from the **Offices of the Society** in the normal way.

REPORT OF AN
INTERNATIONAL CONFERENCE
ON
FUNDAMENTAL PARTICLES
AND
LOW TEMPERATURES
HELD AT
The Cavendish Laboratory,
Cambridge
on 22–27 *July* 1946

Volume I 200 pages
FUNDAMENTAL PARTICLES
Volume II 184 pages
LOW TEMPERATURES

Price of each volume (in paper covers) 15*s*., *inclusive of postage*

Orders, with remittances, should be sent to
THE PHYSICAL SOCIETY
1 Lowther Gardens, Prince Consort Road,
London S.W.7

RESONANT ABSORBERS AND REVERBERATION

Report of the
1947 SUMMER SYMPOSIUM
OF THE
ACOUSTICS GROUP
OF THE
PHYSICAL SOCIETY

together with the Inaugural Address of the Group:
ACOUSTICS AND SOME ALLIED STUDIES
by ALEXANDER WOOD

57 pages. **7*s*. 6*d*.** ; by post **8*s*.**

Orders, with remittances, to be sent to
THE PHYSICAL SOCIETY
1 Lowther Gardens, Prince Consort Road,
London S.W.7

COST OF THE 'PROCEEDINGS'

Fellows and Student-Members of the Society may care to be reminded that for their annual subscription they are entitled to one Section of the *Proceedings*, either A or B, and that the other Section may be obtained for a further payment of 30*s*. per annum.

HANDBOOK OF
SCIENTIFIC INSTRUMENTS
AND APPARATUS,
1950
5*s*.; *by post* 6*s*.
To be published at the beginning of March

Copies of last year's Handbook are available, price 5*s*.

Orders, with remittances, should be sent to
THE PHYSICAL SOCIETY
1 Lowther Gardens, Prince Consort Rd., London S.W.7

SYMPOSIUM ON NOISE AND SOUND TRANSMISSION

Report of the
1948 SUMMER SYMPOSIUM
OF THE
ACOUSTICS GROUP
OF THE
PHYSICAL SOCIETY

200 pages. **17*s*. 6*d*.**; by post **18*s*.**

(Price **10*s*. 6*d*.**, by post **11*s*.**, to Fellows of the Society and Members of the Acoustics Group)

Now ready

Orders, with remittances, to be sent to
THE PHYSICAL SOCIETY
1 Lowther Gardens, Prince Consort Road,
London S.W.7

THE PHYSICAL SOCIETY

NOTES ON THE PREPARATION OF PAPERS

The following instructions refer to the main points which have to be considered in the preparation of a paper for publication, and authors offering papers to the Physical Society for publication are asked to conform to these recommendations.

MANUSCRIPTS

Manuscripts should be typed in *double* spacing on paper not wider than 8 in. and not longer than 13 in. Only one side of the paper should be used, and a margin of 1–1½ in. should be left. As alterations in the text cannot be allowed once the paper is set up in type, authors should aim at absolute clarity of meaning and of typing, and should check the typescript carefully before submission.

Title and Sectional Headings.

The title should be as concise as is compatible with lucidity. Papers are usually divided into sections beginning with §1. Introduction, and ending with § . Conclusion.

Abstract.

An abstract is printed at the beginning of the paper; it should state briefly the general aspects of the subject on which new information is presented and the main conclusions reached and final numerical results obtained. The abstract is placed immediately after the title, name(s) of author(s), and place of employment of author(s). The " title and abstract " page should be submitted in duplicate.

Mathematics.

It is not necessary to give detailed derivations of mathematical expressions and formulae in a published paper when the work is straightforward; it is quite sufficient to indicate the method of treatment and the final results. When interested readers are likely to find the argument difficult to follow, fuller treatment is called for. Extraordinary care should be taken with mathematical scripts, especially for expressions in the least complicated; legible long-hand is preferable to typing.

References.

In the text bibliographical references are made by giving the name of the author and the year of publication in brackets, e.g. (Jones 1942), and details are given in the last section, " References ", where the references are arranged in alphabetical order of authors' names and in date order for each author.

DRAWINGS

Drawings should be in Indian ink on tracing cloth, tracing paper or white card, with lettering in soft pencil. The drawings should in general be sufficiently large to allow of reduction in printing, and the lines should therefore be bold; the frame lines of graphs should be slightly finer than those of the plotted curves. Essential photographs can be reproduced as plates, but they should be avoided when possible because of their expense. If authors are unable to submit drawings in the required form, arrangements can be made for these to be drawn and the cost price charged to the author. If the drawings are made on tracing cloth or paper, it is advisable to send a set of prints with the MS. so that the originals may not be handled unduly.

Full details are available in the Society's " Instructions to Authors ", obtainable from the Secretary–Editor, The Physical Society, 1 Lowther Gardens, Prince Consort Road, London S.W. 7.

THE PHYSICAL SOCIETY

MEMBERSHIP

Membership of the Society is open to all who are interested in Physics:

Fellowship. A candidate for election to Fellowship must as a rule be recommended by three Fellows, to two of whom he is known personally. Fellows may attend all meetings of the Society, are entitled to receive Publications 1 (either Section A or Section B), 4 and 5 below, and may obtain the other publications at much reduced rates.

Student Membership. A candidate for election to Student Membership must be between 18 and 26 years of age and must be recommended from personal knowledge by a Fellow. Student Members may attend all meetings of the Society, are entitled to receive Publications 1 (either Section A or Section B) and 4, and may obtain the other publications at much reduced rates.

Books and periodicals may be read in the Society's Library, and a limited number of books may be borrowed by Fellows and Student Members on application to the Honorary Librarian.

Fellows and Student Members may become members of the *Colour Group*, the *Optical Group*, the *Low-Temperature Group* and the *Acoustics Group* (specialist Groups formed in the Society) without payment of additional annual subscription.

PUBLICATIONS

1. *The Proceedings of the Physical Society*, published monthly in two Sections, contains original papers, lectures by specialists, reports of discussions and of demonstrations, and book reviews. Section A contains papers mainly on atomic and sub-atomic subjects; Section B contains papers on macroscopic physics.

2. *Reports on Progress in Physics*, published annually, is a comprehensive review by qualified physicists.

3. *The Handbook of the Physical Society's Annual Exhibition of Scientific Instruments and Apparatus.* This Exhibition is recognized as the most important function of its kind, and the Handbook is a valuable book of reference.

4. *The Bulletin*, issued at frequent intervals during the session, informs members of programmes of future meetings and of the business of the Society generally.

5. *Physics Abstracts* (*Science Abstracts A*), published monthly in association with the Institution of Electrical Engineers, covers the whole field of contemporary physical research.

6. *Electrical Engineering Abstracts* (*Science Abstracts B*), published monthly in association with the Institution of Electrical Engineers, covers the whole field of contemporary research in electrical engineering.

7. *Special Publications*, critical monographs and reports on special subjects prepared by experts or committees, are issued from time to time.

MEETINGS

At approximately monthly intervals throughout each annual session, meetings are held for the reading and discussion of papers, for lectures, and for experimental demonstrations. Special lectures include : the *Guthrie Lecture*, in memory of the founder of the Society, given annually by a physicist of international reputation; the *Thomas Young Oration*, given biennially on an optical subject; the *Charles Chree Address*, given biennially on Geomagnetism, Atmospheric Electricity, or a cognate subject; and the biennial *Rutherford Memorial Lecture*. A Summer Meeting is generally held each year at a provincial centre, and from time to time meetings are arranged jointly with other Societies for the discussion of subjects of common interest.

Each of the four specialist Groups holds about five meetings in each session.

SUBSCRIPTIONS

Fellows pay an Entrance Fee of £1 1*s*. and an Annual Subscription of £3 3*s*. Student Members pay only an Annual Subscription of 15*s*. Second Section of *Proceedings* 30*s*. No entrance fee is payable by a Student Member on transfer to Fellowship.

Further information may be obtained from the Secretary-Editor
at the Office of the Society :

1 Lowther Gardens, Prince Consort Road, London S.W. 7
Telephone: KENsington 0048, 0049

CAMBRIDGE "SPOT" GALVANOMETER

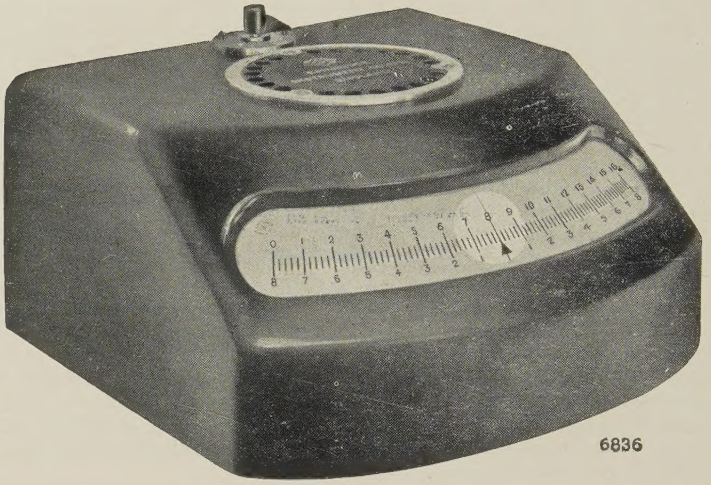

Resistance Ohms	Scale Length	Sensitivity mm on scale per μA.	Period	External resistance to give critical damping
30	160 mm	19	2 secs	150 ohms
50	160 mm	30	2 secs	500 ohms
450	160 mm	170	2 secs	14,000 ohms

THIS comprises an exceptionally robust and sensitive reflecting galvanometer mounted together with a suitable lamp and radial scale in a compact case, effecting a considerable saving in space, and eliminating the trouble of setting up. It requires no special levelling and is not affected by ordinary vibration. The instrument may be operated from mains or battery.

PROMPT DELIVERY FROM STOCK.

Full details are given in ***SHEET 271-L.*** *May we send you a copy ?*

CAMBRIDGE INSTRUMENT COMPANY LTD.
13, GROSVENOR PLACE, LONDON, S.W.1.
WORKS: LONDON & CAMBRIDGE.

THE PROCEEDINGS OF
THE PHYSICAL SOCIETY

Section A

Vol. 63, Part 3 — 1 March 1950 — No. 363 A

The Band Spectrum of GeF

By E. B. ANDREWS and R. F. BARROW
Physical Chemistry Laboratory, University of Oxford

MS. received 10*th August* 1949

ABSTRACT. Two band-systems attributed to GeF have been observed in emission from a discharge through a stream of GeF_4 vapour. Vibrational analyses of both systems have been made and the following constants derived :

State	ν_e	ω_e	$x_e\omega_e$ (cm^{-1})
? $^2\Sigma$	35007·4	800·4	$4{\cdot}1_5$
? $^2\Sigma$	23316·8	413·5	$1{\cdot}0_5$
$^2\Pi_{3/2}$	935	665·8	$2{\cdot}8_3$
$^2\Pi_{1/2}$	0	664·5	$2{\cdot}7_4$

A brief discussion of the results, and a comparison between the force-constants of the mono- and tetra-halides of the group IV–B elements, is given.

§ 1. INTRODUCTION

THE diatomic halides of the group IV–B elements form a series in which it may be expected that the study of the variation in bond properties in going from fluorine to iodine and from carbon to lead—both among themselves and in comparison with the tetrahalides—may be of some interest. GeF is one such molecule for which there appears to be no experimental information. It might be expected to give rise to an ultra-violet band-system, $^2\Sigma - {}^2\Pi$, analogous to those of GeCl and GeBr (Jevons, Bashford and Briscoe 1937), and also to a system, perhaps $^2\Delta - {}^2\Pi$, similar to that recently found for GeCl in the near ultra-violet (Barrow and Lagerqvist 1949).

The present work shows that GeF does indeed emit two band-systems. One, in the ultra-violet region, probably corresponds to the $^2\Sigma - {}^2\Pi$ systems of GeCl and GeBr; the second, in the visible region, has however no analogue in GeCl, but appears to be similar to the least refrangible system of SnF (Yuasa 1939). The lower state of both transitions is almost certainly the ground-state, $^2\Pi$. For the $^2\Pi_{3/2} - {}^2\Pi_{1/2}$ separation we find 935 cm^{-1}, in excellent agreement with the value of 940 cm^{-1} predicted by Howell (1945).

§ 2. EXPERIMENTAL

A simple quartz discharge-tube fitted with molybdenum wire electrodes was used. GeF_4 was produced by heating solid $BaGeF_6$ (Dennis and Laubengayer 1927) contained in a side-arm. A discharge at about 0·25 amp., 1,000 v., was sufficient to produce an intense violet-coloured source in which the bands attributed to GeF were observed.

The systems were photographed in about 20 minutes on a Hilger E1 spectrograph with glass and quartz optics. One system, degraded to the violet, lies in the region λλ 2600–3100 A., the other has its strong bands in the region λλ 3900–5200 A., and is degraded to the red.

Interference due to other spectra was slight, and limited to SiF and, to a lesser extent, OH. GeO bands were observed on the short wavelengths side of the ultra-violet system. Ge, H, Mo and Si lines which appeared on the plates were used as standards in computing wavelengths: their values were taken from the M.I.T. Wavelength Tables (1939).

§ 3. APPEARANCE OF THE BANDS

Reproductions of spectrograms of the two systems are given in the Plate.

(i) *The Ultra-violet System*

The system splits clearly into two sub-systems, so that each band consists of two sub-bands. Each sub-band possesses two heads, one P-like and the other Q-like. Near the origins the separation of these two heads is about 10 cm^{-1}. The rotational structure is only partially resolved near the origins. Away from the origins, the heads become progressively more complex in appearance and more than two heads are observed for each sub-band. The separations of these heads are of the order of magnitude expected for a vibrational effect arising from the Ge isotopes.

(ii) *The Visible System*

This is similar to the ultra-violet system, except that the bands degrade to the red. Near the origin, the R-like heads are separated from the Q-like heads by about 5 cm^{-1}.

§ 4. VIBRATIONAL ANALYSIS

No particular difficulties were encountered in the analyses, which were facilitated by the strengths of the 0,0 bands and by the vibrational isotope effect. The data are set out in Deslandres schemes in Tables 1 and 2. In deriving the vibrational constants given in Table 3, only the figures for the Q-like heads were used: the ν_e values were got from these heads of the 0,0 bands by correcting for zero-point energy.

A Birge-Sponer extrapolation gives 4·9 ev. for the dissociation energy of the ground state. This fits reasonably with the value of 4·3 ev. for GeCl. Similar extrapolations for the upper states lead to considerably higher dissociation limits, but they are much less certain and it is hardly possible to say more than that the higher excited state probably gives one or more excited atoms on dissociation.

§ 5. DISCUSSION

There is little doubt that the bands arise from transitions between states of GeF. The nature of the source, the appearance of the bands and the fact that the derived constants are of the order of magnitude expected all lead to this conclusion.

Whilst the lower state is almost certainly the $^2\Pi$ ground state, all that can definitely be concluded about the upper states is that both appear to show very small,

Table 1. Band-head Data for Ultra-violet System of GeF
(Figures in parentheses are visual relative intensities)

					Sub-system (ii)								
3			35825·9 (0) *2790·46*										
			773·2										
2	35713·0 (0) *2799·28*	660·3	35052·7 (3) *2852·02*										
	782·8		783·4										
1	34930·2 (5) *2862·02*	660·9	34269·3 (2) *2917·21*	655·5	33613·8 (4) *2974·11*	649·3	32964·5 (3) *3032·69*	641·4	32323·1 (0) *3092·87*				
	790·5		791·0		789·9								
0 ↑ v′	34139·7 (10) *2928·29*	661·4	33478·3 (6) *2986·15*	654·4	32823·9 (4) *3045·68*								
					Sub-system (i)								
6									37097 (0) *2694·9*				
5					37652 (0) *2655·2*	657	36994·7 (0) *2702·29*						
					773·0								
4					36878·7 (1) *2710·79*				35592·3 (0) *2808·78*				34315 (0) *2913·3*
					764·3								
3			36769·2 (0) *2718·87*	654·8	36114·4 (2) *2768·17*	648·0	35466·4 (0) *2818·75*						
			779·2				775·6						
2	36648·3 (0) *2727·84*	658·3	35990·0 (4) *2777·73*				34690·8 (0) *2881·77*	643·0	34047·8 (2) *2936·20*	635·3	33412·5 (2) *2992·02*		
	782·6		783·3				782·8		788·4		788·5		
1	35865·7 (6) *2787·36*	659·0	35206·7 (2) *2839·54*	654·0	34552·7 (4) *2893·29*	654·7	33898·0 (3) *2949·18*	638·6	33259·4 (3) *3005·80*	635·4	32624·0 (0) *3064·35*		
	790·7		791·8		793·0		791·8		789·7				
0 ↑ v′	35075·0 (9) *2850·20*	660·1	34414·9 (6) *2904·88*	655·2	33759·7 (4) *2961·25*	653·5	33106·2 (3) *3019·71*	636·5	32469·7 (1) *3078·90*				
$v'' \rightarrow$	0		1		2		3		4		5		6

if not zero, doublet separations: to identify them as $^2\Sigma$ would be consistent with the apparent structure of the bands. Some support to the view that these excited states of GeF are $^2\Sigma$ comes from a comparison with SnF. GeCl is remarkably similar in spectroscopic properties to SnCl, and we might expect the fluorides also to be similar. Of the five stable excited states of SnF known (Jenkins and Rochester 1937, Yuasa 1939), it appears that the two lowest excited states are probably analogous to the two states of GeF, thus:

GeF		SnF	
ν_e, ev.	k'/k''	ν_e, ev.	k'/k''
4·34	1·45	4·23	1·34
2·89	0·39	2·50	0·51

k is the force-constant.

Both these states of SnF have been supposed to be $^2\Sigma$, so it appears that the similarity of the tin and germanium compounds extends at least partly to the

Table 2. Band-head Data for Visible System of GeF

Sub-system (ii)

v' ↑	v'' → 0		1		2		3		4		5
8	25487·4 (0) *3922·40*										
	391·7										
7	25095·7 (0) *3983·62*										
	393·1										
6	24702·6 (1) *4047·01*										
	401·9										
5	24300·7 (2) *4113·96*										
	409·9										
4	23890·8 (3) *4184·53*	658·9	23231·9 (2) *4303·23*				21921·1 (2) *4560·54*				
	405·6										
3	23485·2 (4) *4256·81*				22165·3 (1) *4510·29*				20863·8 (1) *4791·66*		
	407·4				406·9						
2	23077·8 (6) *4331·96*				21758·4 (4) *4594·64*	649·1	21109·3 (1) *4735·93*				19832·6 (0) *5040·80*
	412·0						406·1				409·7
1	22665·8 (7) *4410·70*	660·9	22004·9 (3) *4543·19*				20703·2 (2) *4828·83*	644·5	20058·7 (2) *4983·99*	635·8	19422·9 (1) *5147·14*
	410·3		407·6				412·3		410·0		
0	22255·5 (7) *4492·02*	658·2	21597·3 (8) *4628·92*	655·7	20941·8 (6) *4773·80*	650·9	20290·9 (3) *4926·95*	642·2	19648·7 (1) *5087·98*		

PROC. PHYS. SOC. VOL. 63, PT. 3—A (E. B. ANDREWS AND R. F. BARROW)

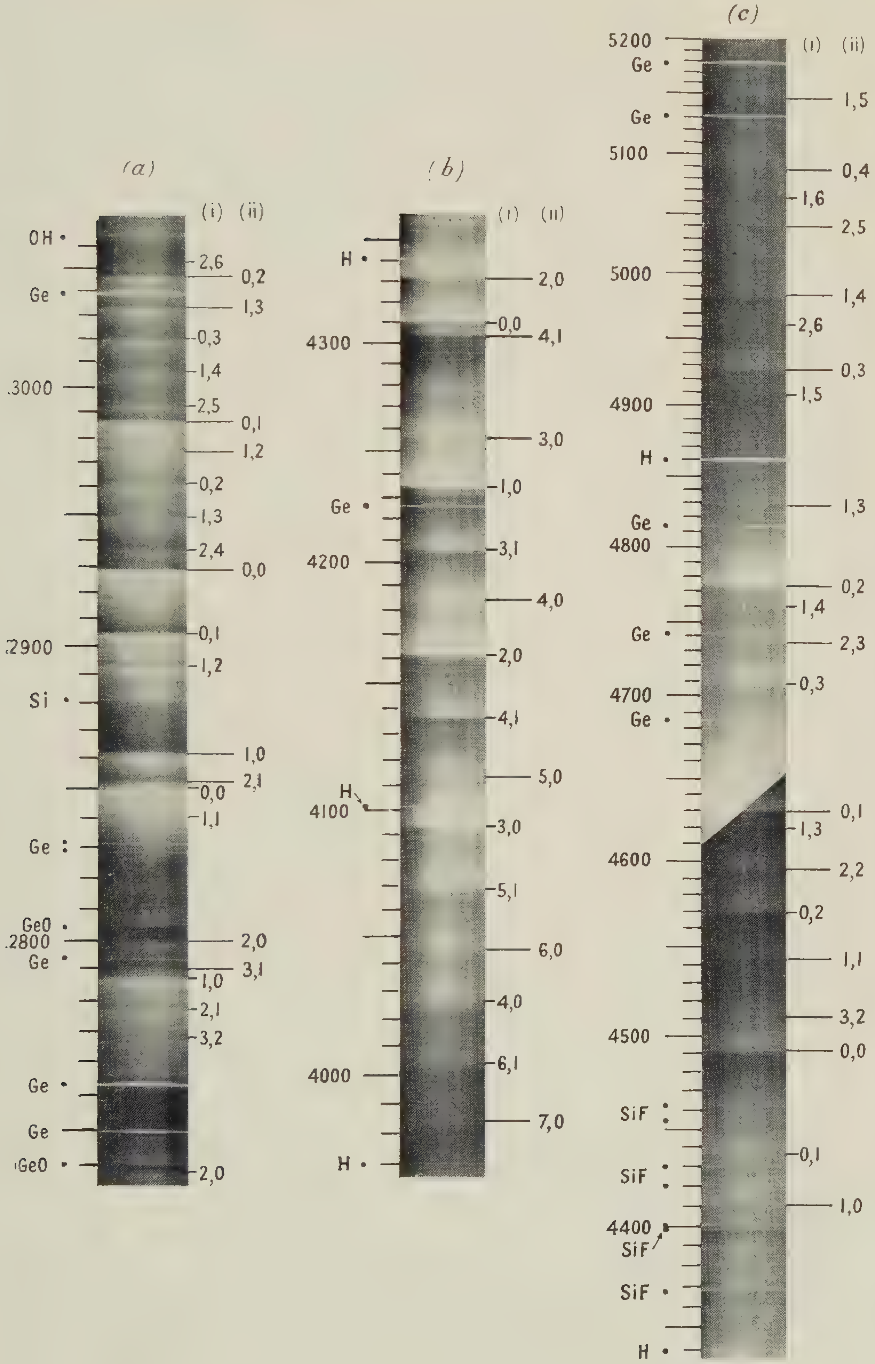

Prism spectrograms of (*a*) ultra-violet system, (*b*, *c*) visible system, of GeF.

Table 2 (*cont.*)

Sub-system (i)

v' ↑	v'' → 0		1		2		3		4		5		6
7			25367·5 (0) *3940·94*										
			402·8										
6			24964·7 (1) *4004·52*										
			395·5										
5	25227·9 (0) *3962·76*	658·7	24569·2 (1) *4069·00*										
	403·8		403·8										
4	24824·1 (2) *4027·21*	658·7	24165·4 (3) *4136·98*				22840·3 (0) *4380·08*						
	405·0		405·4										
3	24419·1 (4) *4093·99*	659·1	23760·0 (3) *4207·57*						21810·8 (0) *4583·60*				
	404·8		405·0										
2	24014·3 (6) *4163·01*	659	23355 (0) *4280·0*										20140 (0) *4963·8*
	410·9												404
1	23603·4 (7) *4235·48*						21633·4 (3) *4621·21*	637·0	20996·4 (2) *4761·39*	628	20368 (1) *4908·4*	632·0	19736 (0) *5065·6*
	411·7						406·8		413·8				
0	23191·7 (8) *4310·68*	659·3	22532·4 (9) *4436·82*	653·1	21879·3 (6) *4569·26*	652·7	21226·6 (3) *4709·76*	644·0	20582·6 (1) *4857·13*				

Table 3

State	ν_e	ω_e	$x_e\omega_e$ (cm^{-1})
? $^2\Sigma$	35007·4	800·4	$4{\cdot}1_5$
? $^2\Sigma$	23316·8	413·5	$1{\cdot}0_5$
$^2\Pi_{3/2}$	935	665·8	$2{\cdot}8_3$
$^2\Pi_{1/2}$	0	664·5	$2{\cdot}7_4$

fluorides. It is therefore probable that transitions involving more highly-excited states of GeF at wavelengths less than 2500 A. await discovery.

Finally it is of interest to compare the force-constants of the diatomic halides with those for the corresponding tetrahalides. On general grounds it might be expected that the valency bonds should increase in strength in passing from MX to MX_4, because the hybridized orbitals in MX_4 are likely to be stronger than those in MX. This is supported by the experimental values of the internuclear distances in SiF ($r_0 = 1{\cdot}60$ A., Eyster 1937) and in SiF_4 ($r = 1{\cdot}54$ A., Maxwell 1940). However, as Heath and Linnett (1948a, b) have emphasized, repulsion between non-bonded atoms is important, particularly of course when the central atom is small, and the derivation of the bond-stretching constant k_1 from the totally symmetric vibration ν_1 becomes dependent upon the law of interaction between the X atoms. In the table below are given for $k_1(MX_4)$, (i) the values calculated with the simple valency force field, 'S.V.F.F.' (Herzberg 1945), (ii) the values calculated by Heath and Linnett (1948 b) using the orbital valency force field, 'O.V.F.F.', and including the effect of repulsion between non-bonded atoms.

It is hardly possible to conclude from these figures alone which set of force-constants for the tetrahalides is the more likely to be correct. But either set shows what seems to be a significant decrease in the ratio $k(MX_4)/k(MX)$ in the direction F to Br for a given metal; moreover the ratios determined with the (O.V.F.F + repulsion) force-constants decrease in addition in the direction Sn to Si for a given halogen. No doubt there are considerable changes in the bond-type in the two series of molecules, but it seems significant that both these trends are in the direction expected if there is repulsion in the tetrahalides, varying with the sizes of M and of X – repulsion which weakens the bond in the tetrahalides relative to that in the diatomic halides. The figures for the carbon–chlorine bond follow the trend observed with the (O.V.F.F. + repulsion) figures in the series Sn to Si, except that here k_1 for CCl_4 is much smaller—as calculated in either way—than would be expected by comparison with CCl (Horie 1939). The ratios $k_1(CCl_4)/k(CCl)$ are (i) 1·11 according to S.V.F.F., (ii) 0·47 according to (O.V.F.F. + repulsion). The bond in CCl_4 appears therefore to be abnormally weak—a conclusion which is also reached by the force-constant analysis of Heath and Linnett (1948 a). It is unfortunate that similar comparison cannot, for lack of data, at present be made for the other carbon halides.

Table 4

	Values of k				Ratios $\frac{k(MX_4)}{k(MX)}$		
	Si	Ge	Sn		Si	Ge	Sn
$-F$	4·89	3·92	3·31				
$-F_4$ (i)	7·16	5·72*	4·83*	(i)	1·46	—	—
$-F_4$ (ii)	5·7 †	—	—	(ii)	1·17	—	—
$-Cl$	2·63	2·33	1·96				
$-Cl_4$ (i)	3·75	3·27	2·80	(i)	1·43	1·40	1·43
$-Cl_4$ (ii)	2·58	2·44	2·30	(ii)	0·98	1·05	1·17
$-Br$	2·21	1·97	1·73				
$-Br_4$ (i)	2·92	2·58	2·28	(i)	1·32	1·31	1·32
$-Br_4$ (ii)	2·03	1·95	1·85	(ii)	0·92	1·01	1·07

* Estimated, with $k(i)(MX_4)/k(MX) = 1{\cdot}46$; this gives $\nu_1 \sim 715$ cm^{-1} for GeF_4, 655 for SnF_4.

† Heath and Linnett (1948 a).

A further attack on this problem might be made by comparing the energy changes for the processes $MX_{4g} \rightarrow M_g + 4X_g$, ($E_1$), with those for $MX_g \rightarrow M_g + X_g$, ($E_2$). Unfortunately the data at present available are not sufficiently reliable to detect any general trends such as are revealed by the force-constants. Nevertheless, the average value for the ratio E_1/E_2 for Si–F, Si–Cl, Si–Br, Ge–Cl, Sn–Cl and Sn–Br is 4·$_5$. Although the interpretation of E_1/E_2 is not simple (Skinner 1949), it appears again that the bonds in these tetrahalides are somewhat, but not much, stronger than those in the monohalides. This result may therefore be regarded as some support for the Heath–Linnette force-constants given in Table 4.

REFERENCES

Barrow, R. F., and Lagerqvist, A., 1949, *Ark. Fys.*, **1**, No. 8.
Dennis, L. M., and Laubengayer, A. W., 1927, *Z. phys. Chem.*, **130**, 520.
Eyster, E. H., 1937, *Phys. Rev.*, **51**, 1078.
Heath, D. F., and Linnett, J. W., 1948 a, *Trans. Faraday Soc.*, **44**, 561 ; 1948 b, *Ibid.*, **44**, 878.
Herzberg, G., 1945, *Infra-red and Raman Spectra of Polyatomic Molecules* (New York : van Nostrand), p. 167.
Horie, T., 1939, *Proc. Phys. Math. Soc., Japan*, **21**, 143.
Howell, H. G., 1945, *Proc. Phys. Soc.*, **57**, 37.
Jenkins, F. A., and Rochester, G. D., 1937, *Phys. Rev.*, **52**, 1135.
Jevons, W., Bashford, L. A., and Briscoe, H. V. A., 1937, *Proc. Phys. Soc.*, **49**, 532.
Maxwell, L. R., 1940, *J. Opt. Soc. Amer.*, **30**, 375.
M.I.T. Wavelength Tables, 1939 (London : Chapman and Hall).
Skinner, H. A., 1949, *Trans. Faraday Soc.*, **45**, 20.
Yuasa, T., 1939, *Proc. Phys. Math. Soc., Japan*, **21**, 497.

On the Interactions of Dislocations and Solute Atoms

By B. A. BILBY
Department of Metallurgy, University of Birmingham

Communicated by N. F. Mott; *MS. received 25th July* 1949

ABSTRACT. An extension of the reciprocal theorem of Colonetti is given and with it a general expression derived for the elastic energy of a multiply-connected solid containing sources of internal stress and subjected to external forces. The terms in the energy which depend on the relative position of a selected source of stress with respect to the field of all the others can be separated. The expression is used to estimate approximately the interaction energy between parallel edge dislocations with arbitrary slip vectors, between parallel screw dislocations and between an edge dislocation and a solute atom causing a spherical distortion of the lattice.

§ 1. INTRODUCTION

Dislocations and solute atoms are sources of internal stress in a crystal and interact because of their associated stress fields. The interaction energy of a given source in a stress field is the change in energy of the system, including both work done by external forces and changes in the elastic energy of the crystal, which accompanies the introduction of the source. When the interaction energy depends on the position of the source, forces of strain interaction arise. Estimates of the interaction energy may be obtained by treating the crystal as a continuous elastic solid and using the linear elasticity theory. This theory does not permit the estimation of the energy near to the dislocation lines, since the displacements become singular there. These lines are therefore excluded by small cylinders drawn about them, and we assume with Koehler (1941) that the energy of the material inside these cylinders is unaffected by the presence of other sources of stress, so that the interaction energy arising from changes in the elastic energy of the solid is determined by elastic energy changes outside these regions. We also assume that the nature of each source of stress is unaffected by the presence of the others; that is, each source will produce in the surrounding medium certain displacements and stresses, and these can be combined everywhere by the Principle of Superposition. The interaction calculated in this way will be a sufficient approximation if the sources are not too close together.

Interaction energies have been deduced by Cottrell by imagining that one source is 'expanded' in the field of another. Thus, for a solute atom causing a spherical distortion of the lattice in a stress field σ_{ij} (the boundary conditions being unspecified) the interaction energy W is given (Cottrell 1948) as

$$W = -\tfrac{4}{3}\pi\epsilon\rho^3(\sigma_{11}+\sigma_{22}+\sigma_{33}), \qquad \ldots\ldots(1)$$

where ρ is the radius of the solvent atom and $\rho(1+\epsilon)$ that of the solute. This is obtained by assuming that W is equal to the work done by the local forces due to the stress field acting over a spherical surface of radius ρ surrounding the solute atom when the radius of this surface becomes $\rho(1+\epsilon)$. The stress field is assumed constant over the spherical surface, and also constant during the 'expansion'. When σ_{ij} is due to a positive edge dislocation of strength λ_0 situated at the origin in an infinite medium, and (t, ψ) are the polar coordinates of the solute atom, (1) becomes

$$W = \tfrac{4}{3}\mu\epsilon\rho^3\lambda_0\left(\frac{1+f}{1-f}\right)\frac{\sin\psi}{t}, \qquad \ldots\ldots(2)$$

where μ is the shear modulus and f is Poisson's ratio. For a positive edge dislocation at the origin and a parallel negative one at (t, ψ), both of strength λ_0, Cottrell (1949) finds for the interaction energy

$$W = \frac{\mu\lambda_0^2}{2\pi(1-f)}(\ln L - \ln t + \cos^2\psi), \qquad \ldots\ldots(3)$$

where L is the radius of a large cylinder containing the dislocations. The second dislocation is imagined to be made by making a cut perpendicular to the slip vectors (that is, in the x_2x_3 plane) and introducing an extra half-plane of atoms. W is assumed to be the work done by the forces of the first dislocation field acting on the surfaces of the cut when the two sides suffer the required relative displacement. The expression (3) leads to interaction forces:

$$\left.\begin{aligned} F_t &= -\frac{\partial W}{\partial t} = -\frac{\mu\lambda_0^2}{2\pi(1-f)}\frac{1}{t}, \\ F_\psi &= -\frac{1}{t}\frac{\partial W}{\partial\psi} = -\frac{\mu\lambda_0^2}{2\pi(1-f)}\frac{\sin 2\psi}{t}. \end{aligned}\right\} \qquad \ldots\ldots(4)$$

The F_t force is identical with that obtained by Koehler (1941), but the function of (t, ψ) in the F_ψ force is multiplied by a different constant. The result (4) has been confirmed by Eshelby (private communication). In an unpublished note Cottrell has shown that a result differing from (3) only by an additive constant is obtained by taking a section parallel to the x_1x_3 plane and sliding the two sides of the cut over each other in the slip direction.

In these estimates stresses for an edge dislocation in an infinite medium ($L \to \infty$) with tractions applied to the inner boundary were used (see Koehler 1941). It was considered that other contributions to the interaction energy were of a higher order. We now derive a general expression for the elastic energy of a multiply-connected solid containing sources of internal stress under definite boundary conditions on the stress fields. Under certain conditions integrals of the type considered by Cottrell arise as the leading interaction terms in this expression.

§ 2. GENERAL EXPRESSION FOR THE ELASTIC ENERGY

Suppose that an elastic solid B occupies a cyclic space Γ, N times connected, which is bounded by a surface S. Let $A^{(r)}$, $r=1, 2, 3, \ldots . (N-1)$, be a set of $(N-1)$ surfaces lying in Γ such that, if barriers are drawn along them, the space Γ is reduced to a singly-connected one. If a cut is made in such a solid along one of the surfaces $A^{(r)}$, the two surfaces of the cut given a small relative displacement as rigid bodies, and the two sides then rejoined, elastic material being added or removed if necessary in this operation, the solid contains a 'dislocation' (Volterra 'distortion') across $A^{(r)}$ and is in a state of strain even if no external forces are acting. It has been shown by Volterra (1907) that if the body is in a state of strain

$$e_{ij}=\tfrac{1}{2}\left(\frac{\partial u_j}{\partial x_i}+\frac{\partial u_i}{\partial x_j}\right),$$

due to given dislocations across the surfaces $A^{(r)}$, and to the action of external body forces $f_i(x_1, x_2, x_3)$ per unit volume and of external surface forces, the elastic energy E may be written

$$2E=\iiint_{\Gamma} f_i u_i d\Gamma+\iint_{S} t_i^{(\nu)} u_i dS+\sum_{r=1}^{(N-1)} \iint_{A^{(r)}} t_i^{(\nu)}[u_i^{(\alpha)}-u_i^{(\beta)}]dA^{(r)}. \qquad \ldots\ldots(5)$$

Here $u_i(x_1, x_2, x_3)$ and $t_i^{(\nu)}(x_1, x_2, x_3)=\sigma_{ij}\nu_j$ are the components along the three coordinate axes $(i=1, 2, 3)$ of the displacement, and the traction across a surface whose normal is $\boldsymbol{\nu}$ respectively, and $\sigma_{ij}(x_1, x_2, x_3)$ is the stress tensor. In order to avoid confusion with tensor suffixes, letters distinguishing a particular quantity of a similar set are placed as superscripts in brackets; letters in brackets after the tensor suffixes denote the usual functional dependence. The letters α and β denote the two sides of each of the surfaces $A^{(r)}$ and the positive normal $\boldsymbol{\nu}$ is assumed to be directed outwards from the solid at each point of S, and hence on the surfaces $A^{(r)}$ from the side α to the side β.

Extensions to such a multiply-connected solid of the Reciprocal Theorem of Betti have been given by Volterra (1907) and by Colonetti (1915). It is not difficult to prove a general reciprocal formula which includes these extensions as special cases. This result is required in the deduction of the expression for the energy and does not seem to have been stated explicitly before.

Suppose that two states of strain $e_{ij}^{(1)}$ and $e_{ij}^{(2)}$ are separately produced in the body B by given systems of dislocations across the surfaces $A^{(r)}$, and by the action of given body forces and surface tractions, $f_i^{(1)}$, $f_i^{(2)}$ and $t_i^{(\nu, 1)}$, $t_i^{(\nu, 2)}$, respectively. Let $u_i^{(1)}$ and $u_i^{(2)}$ be the corresponding displacements. Then the expression

$$\iiint_{\Gamma} f_i^{(1)} u_i^{(2)} d\Gamma+\iint_{S} t_i^{(\nu, 1)} u_i^{(2)} dS+\overset{(N-1)}{\underset{r=1}{\Sigma_1}} \iint_{A^{(r)}} t_i^{(\nu, 1)}[u_i^{(\alpha, 2)}-u_i^{(\beta, 2)}]dA^{(r)} \qquad \ldots\ldots(6)$$

may be transformed by the divergence theorem into

$$\iiint_{\Gamma} \sigma_{ij}^{(1)} \frac{\partial u_i^{(2)}}{\partial x_j} d\Gamma=\iiint_{\Gamma} \frac{\partial W(1)}{\partial e_k^{(1)}} e_k^{(2)} d\Gamma, \qquad k=1, 2, 3, \ldots . 6$$

where $W(1)$ is the strain energy function expressed in terms of $e_k^{(1)}$, and the suffix contractions $1=11$, $2=22$, $3=33$, $4=23$, $5=31$, $6=12$ are made. This last expression is, by a general property of quadratic functions, symmetrical in the two sets of strain components $e_k^{(1)}$, $e_k^{(2)}$. Thus, denoting the expression (6), regarded as a function of its numerical superscripts, by $F(1,2)$, we have

$$F(1,2)=F(2,1), \qquad \ldots\ldots(7)$$

which is the formula required. If $f_i^{(1)}=f_i^{(2)}=0$ in Γ and $t_i^{(\nu,1)}=t_i^{(\nu,2)}=0$ on S, this reduces to Volterra's equation (2), (Volterra 1907, p. 432). If $f_i^{(2)}=0$ in Γ, $t_i^{(\nu,2)}=0$ on S, $u_i^{(1)}$ is single-valued, and $u_i^{(2)}$ is discontinuous across only one of the surfaces $A^{(r)}$, the theorem of Colonetti is obtained.

We now suppose that the multiple-connectivity of the solid B arises from the removal of small cylinders of material about certain lines (which may extend across the whole solid or be closed in themselves), and also that there are within the solid singly-connected spaces not occupied by elastic material, bounded by closed surfaces G. The cylindrical surfaces C and the surfaces G together with the external surface H form the outer boundary S of the solid. In such a solid elastic displacements can be considered which are multi-valued about the lines enclosed by the cylinders, and singular on these lines, and also singular at points within the surfaces G. A given source of stress (p) is then specified by defining the tractions or displacements on one of the surfaces G, or the discontinuity in displacement across one of the surfaces $A^{(r)}$ (or the tractions on H if it is an external source of stress). The displacement $u_i^{(p)}$ defining the state of the solid when this source acts depends, of course, on the boundary conditions on all the other surfaces, and on any body forces $f_i^{(p)}$ which are present. The energy $E^{(p)}$ when the source (p) acts is given by equation (5) with $u_i^{(p)}$ replacing u_i, $f_i^{(p)}$ replacing f_i and $t_i^{(\nu,p)}$ replacing $t_i^{(\nu)}$ respectively. If the displacement functions $u_i^{(p)}$ are known for a number of sources separately, the energy $\mathscr{E}$ when they all act simultaneously is given by a similar expression in which the body forces, displacements and surface tractions are everywhere the sum of the corresponding quantities for each source separately. If we now select one of the sources defined by $u_i^{(a)}$ and denote the sum of the displacements of all the others by $u_i^{(R)}$, and the corresponding body forces and surface tractions similarly, the energy $\mathscr{E}$ may be written down by means of (5) and is easily transformed using the reciprocal relation (7) into the two equivalent expressions:

$$\mathscr{E}=E^{(a)}+E^{(R)}+\iiint_{\Gamma} f_i^{(a)}u_i^{(R)}d\Gamma+\iint_{S} t_i^{(\nu,a)}u_i^{(R)}dS$$

$$+\sum_{r=1}^{(N-1)}\iint_{A^{(r)}} t_i^{(\nu,a)}[u_i^{(\alpha,R)}-u_i^{(\beta,R)}]dA^{(r)} \qquad \ldots\ldots(8)$$

$$=E^{(a)}+E^{(R)}+\iiint_{\Gamma} f_i^{(R)}u_i^{(a)}d\Gamma+\iint_{S} t_i^{(\nu,R)}u_i^{(a)}dS$$

$$+\sum_{r=1}^{(N-1)}\iint_{A^{(r)}} t_i^{(\nu,R)}[u_i^{(\alpha,a)}-u_i^{(\beta,a)}]dA^{(r)}. \qquad \ldots\ldots(9)$$

Here $E^{(a)}$ and $E^{(R)}$ denote the energy when the displacements are $u_i^{(a)}$ and $u_i^{(R)}$ respectively. The energy when all the sources act together is thus expressed in terms of the elastic fields associated with the separate action of the sources of stress (a) and (R). In using the formulae to calculate the energy in any problem, the arbitrary boundary conditions for all the sources must be suitably chosen so that, on superposition, the final boundary conditions are those required. In the examples usually considered the body forces are relatively unimportant and it is assumed in the subsequent discussion that they are zero. The energy is then expressed as the sum of a number of surface integrals, and it is possible to examine the relative importance of these terms, and to separate those whose value depends on the relative position of the sources (a) and (R). The interaction energy can thus be found without evaluating a volume integral of the strain energy directly.

When the boundary conditions are chosen in a special way a simple interpretation can be given to the various terms. If $u_i^{(a)}$ is the displacement produced by the source (a) alone in an infinite medium, it does not depend on the position of (a) with respect to the surfaces G, C, although the maintenance of such a displacement when these surfaces are present requires the application of tractions to them. Thus $E^{(a)}$ is a true 'self-energy' term. Under similar conditions on $u_i^{(R)}$, $E^{(R)}$ is also a self-energy term, while the remaining terms are interaction terms. In general, however, all the terms give rise to interactions because $u_i^{(a)}$, for example, depends on the relative position of the surfaces G, C and H with respect to the source (a). Thus in a finite solid sources will in any case interact indirectly as they change their position with respect to the outer boundary.

It may be noted that the formulae (8) and (9) may be obtained by imagining that cuts are made initially along all the surfaces $A^{(r)}$ so that the solid B becomes singly-connected. Then to produce the displacements $u_i^{(\nu)}$ additional equal and opposite tractions have to be applied to the two faces of each cut to keep them in juxtaposition (or in a dislocated position if $u_i^{(\nu)}$ is due to a dislocation across one of them). A direct appeal to the reciprocal theorem for singly-connected solids can then be made, and the expressions for the energy reduce to those given, since the extra integrals vanish over the surfaces to which the additional tractions are applied.

§ 3. THE INTERACTION ENERGY OF TWO PARALLEL EDGE DISLOCATIONS WITH ARBITRARY SLIP VECTORS

Dislocation (1) is taken along the axis of a cylindrical crystal of radius L, and dislocation (2) at a position $x_1=X_1=t\cos\psi$, $x_2=X_2=t\sin\psi$, where $(x_1, x_2)\equiv(R,\Phi)$ are coordinates with the centre of the cylinder as origin (Figure 1). Outside small cylinders C_1, C_2 of radius r_0 drawn about the dislocation lines, the crystal is treated as a continuous elastic solid which becomes singly-connected if cuts are made along $A^{(1)}$ and $A^{(2)}$, and the interaction energy is calculated in the limit when $L\to\infty$. The total elastic energy per unit length along the dislocation lines when the two dislocations are present is, by (8),

$$\mathscr{E}=E^{(1)}+E^{(2)}+\iint_{(H+C_1+C_2)} t_i^{(\nu,1)}u_i^{(2)}dS+\iint_{A^{(2)}} t_i^{(\nu,1)}[u_i^{(\alpha,2)}-u_i^{(\beta,2)}]dA^{(2)}, \qquad \ldots\ldots(10)$$

where the superscripts refer to the fields when the two dislocations are present separately, and H is the outer cylindrical surface. It is assumed that tractions are applied over the plane ends of the cylinder in order to maintain plane strain $(u_3^{(1)}=u_3^{(2)}=0)$ and the integrals over these surfaces are therefore zero. The integral over the surface $A^{(1)}$ is zero because $u_i^{(2)}$ is not discontinuous there.

The boundary conditions on the fields of stress $\sigma_{ij}^{(1)}$ and $\sigma_{ij}^{(2)}$ are chosen as follows. We assume that neither dislocation produces a discontinuity in the field of the other, and hence that tractions are required on C_1 to maintain $u_i^{(2)}$ and on C_2 to maintain $u_i^{(1)}$. This assumption is made because, although Hooke's law is no longer valid inside C$_1$ and C$_2$, there are in reality no holes in the lattice there. We assume that $t_i^{(\nu,1)}=0$ on C$_1$ and H, and that $t_i^{(\nu,2)}=0$ on C$_2$ and H. Taking the material to be isotropic, the state of stress (1) is then defined by a stress function (Timpe 1905):

$$\chi^{(1)}=\gamma\left\{-R\ln R+\frac{R^3}{2(L^2+r_0{}^2)}-\frac{L^2r_0{}^2}{2(L^2+r_0{}^2)}\frac{1}{R}\right\}(\lambda_1 l_1\sin\Phi), \qquad \ldots\ldots(11)$$

where the slip vector of dislocation (1) has components $(\lambda_1 l_1, 0, 0)$, and where $\gamma=\mu(\lambda+\mu)/(\lambda+2\mu)\pi$, λ and μ being Lamé's elastic constants. We denote the three terms in $\chi^{(1)}$ by P, H and C, the last two being introduced to make $t_i^{(\nu,1)}=0$ on H and C$_1$ respectively. The slip vector of dislocation (2) is assumed to have components $(\lambda_2 m_1, \lambda_2 m_2, 0)$.

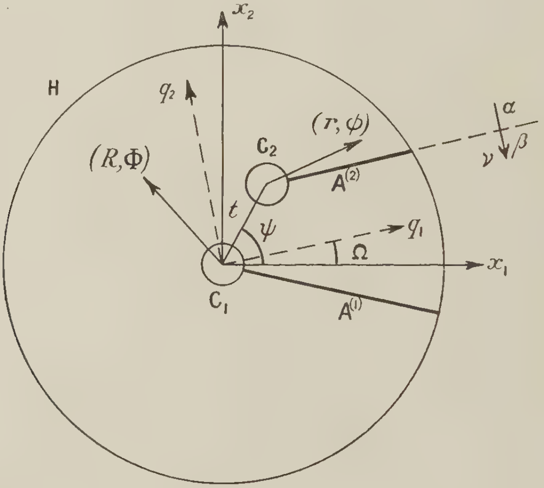

Figure 1.

When $L\to\infty$, $E^{(1)}$ and $E^{(2)}$ become self-energy terms, and with these assumptions the interaction energy arises from the A$^{(2)}$ and C$_2$ integrals. Taking the surface A$^{(2)}$ at an angle Ω to Ox_1 and neglecting terms of the form r_0/t, the contribution to the integral from the P term in $\chi^{(1)}$ is, when $L\to\infty$,

$$W_1=\lambda_1\lambda_2 l_1\gamma[m_1\{\ln L-\ln t-\sin^2\psi+\sin^2\Omega\}+m_2\{\tfrac{1}{2}\sin 2\psi-\tfrac{1}{2}\sin 2\Omega\}]. \qquad \ldots\ldots(12)$$

The H term gives

$$W_2=\lambda_1\lambda_2 l_1\gamma[m_1\{-\tfrac{1}{2}-\sin^2\Omega\}+m_2\{\tfrac{1}{2}\sin 2\Omega\}], \qquad \ldots\ldots(13)$$

while the C term is at most of the form $r_0{}^2/t^2$.

To evaluate the C$_2$ integral we require the values of $u_i^{(2)}$ on C$_2$. We assume that when $L\to\infty$, the value of the C$_2$ integral calculated from these values does not differ significantly from that calculated using values of $u_i^{(2)}$ corresponding to a stress function of the same form as $\chi^{(1)}$, but with $(\lambda_1 l_1\sin\Phi)$ replaced by $\lambda_2(m_1\sin\phi-m_2\cos\phi)$, and R replaced by r, where (r,ϕ) are polar coordinates with (X_1, X_2) as origin. Thus $u_i^{(2)}$ on C_2 is of the form $\{\ln r_0 + f(\phi)\}$ when $L \to \infty$. On C_2 the tractions $t_i^{(\nu, 1)}$ are of the form $1/t$, so that the C_2 integral is at most of the form r_0/t.

Thus, neglecting terms of order r_0/t, the interaction energy is

$$W = \lambda_1 \lambda_2 l_1 \gamma [m_1\{\infty \text{ const.} - \ln t - \sin^2 \psi\} + m_2\{\tfrac{1}{2} \sin 2\psi\}], \quad \ldots\ldots(14)$$

which is independent of Ω. When $m_2 = 0$, $l_1 = +1$, $m_1 = -1$, $\lambda_1 = \lambda_2 = \lambda_0$, this expression leads to the same interaction forces as (3), which is obtained from (12) by making the additional substitution $\Omega = \pi/2$. The forces are

$$F_t = \frac{\lambda_1 \lambda_2 l_1 m_1 \gamma}{t},$$

$$F_\psi = \frac{\lambda_1 \lambda_2 l_1 \gamma}{t} [m_1 \sin 2\psi - m_2 \cos 2\psi]. \quad \ldots\ldots(15)$$

Thus when $m_1 = 0$, and the slip vectors are perpendicular, the leading term in the radial force is at most of the form $(r_0/t)(1/t)$.

If we use only the P term in $\chi^{(1)}$, the C_1 and H integrals in (10) no longer vanish but they contribute to the interaction energy terms of higher order than the $A^{(2)}$ integral (12), which thus gives, apart from additive finite constants, the interaction energy. This now depends on Ω, but gives the correct forces for any constant Ω except $\Omega = \psi$. To obtain the energy in this case, it is necessary to include the H term in $\chi^{(1)}$ which gives (13).* The energy of the system depends on where the surface $A^{(2)}$ is taken when only the P term is used, because equilibrium can then be maintained only when external forces are acting. When such forces are present, the integrals of the tractions across any two surfaces $A^{(2)}$ and $A^{(2)\prime}$ which are equivalent (that is, which can be transformed into each other by continuous variation without passing out of the solid) are not necessarily equal, since these tractions are no longer the only forces keeping the elastic material between the surfaces in equilibrium.

In this example the leading term in the interaction energy is the $A^{(2)}$ integral in (10). If we put

$$x_1 = q_1 \cos \Omega - q_2 \sin \Omega; \qquad x_2 = q_1 \sin \Omega + q_2 \cos \Omega;$$

$$Q_1 = t \cos(\psi - \Omega); \qquad Q_2 = t \sin(\psi - \Omega),$$

so that (q_1, q_2) are coordinates parallel and perpendicular to $A^{(2)}$, then the leading term in the force in the Q_1 direction (Q_2 constant) when the dislocation (2) is at (Q_1, Q_2) can be written down by inserting the values $q_1 = Q_1$, $q_2 = Q_2$ in the $A^{(2)}$ integrand. This gives for the force in the direction of the surface $A^{(2)}$

$$t_i^{(\nu, 1)}(Q_1, Q_2)[u_i^{(\alpha, 2)} - u_i^{(\beta, 2)}]. \quad \ldots\ldots\ldots(16)$$

By choosing two surfaces at right angles the force in two perpendicular directions, and hence the force in any direction, can be found. For this rule to be valid no contributions of comparable order must be made to the energy by integrals other than a 'cut' integral, that is, an integral over a plane surface such that a cut along it would serve to introduce the dislocation. Further, if the force is to be independent of the surface, the energy must not depend on where this surface is taken.

---

* The author is indebted to Mr. F. R. N. Nabarro for this remark.

§ 4. THE INTERACTION ENERGY OF TWO PARALLEL SCREW DISLOCATIONS

We assume as before that neither dislocation produces a discontinuity in the field of the other. Then, taking the dislocation lines as in Figure 1, we assume the following stresses and displacements (Burgers 1939):

$$u_3^{(1)}=(\lambda_1/2\pi)\Phi\,; \qquad u_3^{(2)}=(\lambda_2/2\pi)(\phi-\Omega)\,;$$
$$\sigma_{23}^{(1)}=(\mu\lambda_1/2\pi)(\cos\Phi/R)\,; \qquad \sigma_{31}^{(1)}=-(\mu\lambda_1/2\pi)(\sin\Phi/R). \qquad \ldots\ldots (17)$$

The other stresses and displacements are zero. Tangential tractions are required on the plane ends of the cylinders, H_1 and H_2, to maintain $u_i^{(1)}$ but $t_i^{(\nu,1)}=0$ on H and C_1. Tractions are required on C_1, H, H_1 and H_2 to maintain $u_i^{(2)}$. We again assume that the interaction energy calculated using this $u_i^{(2)}$ does not differ significantly when $L\to\infty$ from that found when a displacement making $t_i^{(\nu,2)}=0$ on H and C_2 is used. The energy $\mathscr{E}$ stored outside the cylinders C_1 and C_2 is now given by (10) where the tractions and displacements are those obtained from (17) and the S integral extends over $H_1+H_2+C_2$. On H_1, $t_i^{(\nu,1)}=\sigma_{i3}^{(1)}$, and thus this integral and the corresponding one over H_2, are both zero. On C_2 the stresses $\sigma_{ij}^{(1)}$ are of the form $1/t$, so that the C_2 integral is at most of the form r_0/t. Neglecting terms of the form r_0/t, therefore, the interaction energy reduces to a 'cut' integral, and the leading term of the interaction force in the 'cut' direction may be deduced from (16). Taking $A^{(2)}$ at an angle Ω to Ox_1 the force in the Q_1 direction is

$$\frac{\mu\lambda_1\lambda_2}{2\pi}\frac{\cos(\psi-\Omega)}{t}, \qquad \ldots\ldots (18)$$

giving a force in the x_1 direction proportional to $\cos(\psi)$ when $\Omega=0$ and an x_2 force proportional to $\sin(\psi)$ when $\Omega=\pi/2$, and hence a total force

$$\mu\lambda_1\lambda_2/2\pi t \qquad \ldots\ldots (19)$$

in the ψ direction. Evaluating the $A^{(2)}$ integral and taking the limit as $L\to\infty$, we find, neglecting terms of the form r_0/t, that its value is

$$(\mu\lambda_1\lambda_2/2\pi)(\ln L-\ln t).$$

This is independent of Ω and leads to the force (19).

§ 5. INTERACTION OF AN EDGE DISLOCATION AND A SOLUTE ATOM

It is assumed that the dislocation lies along the axis of a cylindrical crystal (Figure 2); the plane ends H_1 and H_2 are $x_3=+M_1$, and $x_3=-N_1$. The centre of the solute atom is taken at

$$x_1=R\cos\Phi=t\cos\psi,$$
$$x_2=R\sin\Phi=t\sin\psi,$$
$$x_3=0.$$

Outside a small cylinder C of radius r_0 about the axis the continuum approximation is made and the crystal treated as an elastic solid which becomes singly-connected if a cut is made along a surface A. The stress function for the dislocation alone is taken to be that of (11) with $\lambda_1 l_1=\lambda_0$. Thus no discontinuity is assumed to arise in the dislocation field due to the presence of the solute atom, that is, the elastic constants of the latter are assumed to be the same as those of the surrounding lattice. Tractions on H_1, H_2 and G, the surface of a spherical hole of radius ρ about (t,ψ), are required to maintain this state of stress. The model of the solute atom, assumed spherical, is of a larger sphere of (similar) elastic material forced into the hole of radius ρ about (t, ψ). We assume for the field of the solute atom alone

$$u_i^{(2)} = \delta\left(\frac{y_i}{r^3}\right), \qquad \ldots\ldots(20)$$

where $$y_1 = r \sin\theta \cos\phi, \quad y_2 = r \sin\theta \sin\phi, \quad y_3 = r \cos\theta \qquad \ldots\ldots(21)$$

are coordinates with (t, ψ) as origin. No discontinuity in the solute atom field thus occurs on C. Tractions on G, C, H, H_1, H_2 are required to maintain this displacement, and we again assume that when L, M_1, $N_1 \to \infty$ the interaction energy calculated using $u_i^{(2)}$ does not differ significantly from that obtained using a displacement making $t_i^{(\nu, 2)} = 0$ on H, H_1 and H_2. We show later that the energy integrals arising from the presence of tractions on these outer surfaces tend to zero as L, M_1, $N_1 \to \infty$. The constant $\delta = \epsilon\rho^3$, where ϵ is the parameter defining the final radius of the solute atom in an infinite medium (Mott and Nabarro 1940).

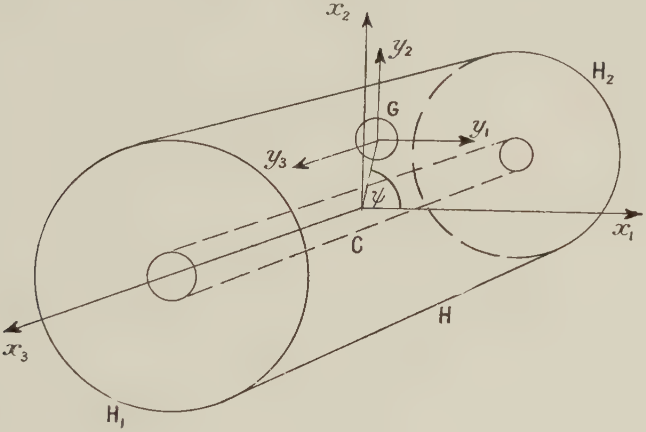

Figure 2.

For the energy of the material outside G and C when both the dislocation and solute atom are present, (8) and (9) give

$$\mathscr{E} = E^{(1)} + E^{(2)} + \iint_G t_i^{(\nu, 1)} u_i^{(2)} dG + \iint_{(H_1+H_2)} t_i^{(\nu, 1)} u_i^{(2)} dS \qquad \ldots\ldots(22)$$

$$= E^{(1)} + E^{(2)} + \iint_S t_i^{(\nu, 2)} u_i^{(1)} dS + \iint_A t_i^{(\nu, 2)} [u_i^{(\alpha, 1)} - u_i^{(\beta, 1)}] dA, \qquad \ldots\ldots(23)$$

where in (23) $S = C + G + H + H_1 + H_2$. It can be seen immediately from (22) that the interaction term is given by the integral considered by Cottrell, provided that the second integral makes a contribution of higher order. On H_1 the stresses $\sigma_{ij}^{(1)}$ are of the form $1/R$ and the displacements $u_i^{(2)}$ of the form $1/M_1^2$. Thus the H_1 integral (and similarly the H_2 integral) tends to zero as L, M_1, $N_1 \to \infty$. On G we expand the stresses $\sigma_{ij}^{(1)}$ by the binomial theorem in powers of ρ/t, the expansions converging uniformly in θ and ϕ when $\rho < t(\sqrt{2} - 1)$. Integrating and neglecting terms of the form $(\rho/t)(1/t)$, the expression in equation (1) results, the stresses in this formula being $\sigma_{ii}^{(1)}(t, \psi)$.

Using the reciprocal expression (23) to calculate the energy, we obtain the same result. The important contributions come from the integrals over G and A, the others being either zero or of higher order. After partial integration of the $\tan^{-1}$ term, the G integrand may be expanded in powers of ρ/t. When $L\to\infty$, and terms of the form $(\rho/t)(1/t)$ are neglected, this integral is

$$-\frac{16}{3}\frac{\delta\mu^2\lambda_0}{\lambda+2\mu}\frac{\sin\psi}{t}. \qquad \ldots\ldots(24)$$

Neglecting similar terms, and taking the surface A at an angle Ω to the x_1x_3 plane, the A integral is

$$4\delta\mu\lambda_0\frac{\sin\psi}{t}, \qquad \ldots\ldots(25)$$

which is independent of Ω. In the C integral we perform the x_3 integration, take the limit, and expand the Φ integrand; thus the integral is at most of the form $(r_0/t)(1/t)$. The integrals over H, H_1 and H_2, which arise because we use a displacement which does not make $t_i^{(\nu,2)}=0$ on these surfaces, all tend to zero as L, M_1, $N_1\to\infty$; for the stresses $\sigma_{ij}^{(2)}$ are of the form $1/r^3$ and the displacement $u_i^{(1)}$ at most of the form $\ln L$.

Thus the energy $\mathscr{E}$, neglecting terms of the form $(\rho/t)(1/t)$ and $(r_0/t)(1/t)$, is the sum of (24) and (25) which is equal to the expression in equation (2). The formula (2) thus gives that part of the elastic energy of the material outside the surfaces G and C which depends on the position of the solute atom. The displacement of the surface of the original spherical hole when the sphere of similar material is inserted is $u_i^{(2)}$ when the dislocation field is negligible, and in this condition a certain elastic energy is stored within G. When the dislocation field is no longer negligible, the displacement of this surface is $u_i^{(1)}+u_i^{(2)}$, and $u_i^{(1)}$ is a function of the position of the atom in the dislocation field. Since the final tractions are $t_i^{(\nu,1)}+t_i^{(\nu,2)}$ the change in the elastic energy of the material inside G due to the presence of the dislocation field is

$$\iint_G t_i^{(\nu,2)}u_i^{(1)}dG,$$

where on account of the theorem of virtual work we have neglected the work done by the tractions $t_i^{(\nu,1)}$. (This work is easily shown to be of higher order in this example.) This expression is exactly the G integral in (23) with the sign reversed, since the normal now points outwards from the centre of the sphere, and is thus equal to minus the expression (24). Therefore, when changes in the energy of the material inside G are included, (25) gives the interaction energy. This is greater by a factor $[3(1-f)/(1+f)]=3/2$ when $f=1/3$, than the expression (2).

ACKNOWLEDGMENTS

The work was carried out under the general supervision of Professor D. Hanson, to whom the author is indebted for his interest and support. The author wishes to thank Dr. A. H. Cottrell for suggesting the problem and, together with Mr. F. R. N. Nabarro, for valuable discussions during the progress of the work.

REFERENCES

Burgers, J. M., 1939, *Proc. K. Ned. Akad. Wet.*, **42**, 293.

Colonetti, G., 1915, *Rend. Cont. Real. Acc. Lincei*, **24** (1), 404.

Cottrell, A. H., 1948, *Report on the Strength of Solids* (London: Physical Society), p. 30; 1949, *The Theory of Dislocations, Progress in Metal Physics*, Vol. I (London: Butterworth Scientific Publications).

Koehler, J. S., 1941, *Phys. Rev.*, **60**, 397.

Mott, N. F., and Nabarro, F. R. N., 1940, *Proc. Phys. Soc.*, **52**, 86.

Timpe, A., 1905, *Z. Math. und Phys.*, **52**, 348.

Volterra, V., 1907, *Ann. Ecole Norm. Sup.*, Sér. 3, **24**, 404.

Spin-Lattice Relaxation in some Paramagnetic Salts

By R. J. BENZIE and A. H. COOKE
Clarendon Laboratory, Oxford

MS. received 29*th August* 1949

ABSTRACT. The magnetization of a paramagnetic salt is a relaxation process with a relaxation time depending on the external field and temperature. Measurements have been made with the object of determining relaxation times at various fields and temperatures in the liquid helium range. A description of the apparatus is given.

The results show that paramagnetic relaxation is a complex phenomenon, and suggest that in any one specimen it must be described in terms of a distribution of relaxation times rather than a single relaxation time. In general we find that relaxation times are of the order of 10^{-2} sec., with a temperature dependence according to a power of $1/T$ between 2 and 3, while increasing with the external field H according to a power of H between 0 and 1.

§ 1. INTRODUCTION

In the statistical theory of paramagnetism the state of magnetization of a paramagnetic substance under given conditions of temperature and magnetic field is calculated by considering the statistical equilibrium of an assembly of magnetic dipoles. Since the classical work of Langevin (1905), the theory has been elaborated to take into account the quantization of the magnetic energy levels and the interactions of the dipoles with one another and with their surroundings (Van Vleck 1932, 1937, Hebb and Purcell 1937.) It is essentially an equilibrium theory; to each set of external conditions there corresponds an equilibrium distribution of the dipoles, and an equilibrium magnetic moment of the assembly. If now the magnetic field is suddenly changed, a new equilibrium must be set up. This requires changes in the energies of the individual dipoles, which can occur only if some mechanism for energy transfer exists. In general the new equilibrium will not be attained instantaneously; the rate of approach to it can be described in terms of one or more relaxation times, introduced by equations of the form

$$\frac{dM}{dt}=\frac{M_0-M}{\tau}.$$

Here M is the magnetic moment of the specimen along a given direction, M_0 is the equilibrium value of M, and τ is a relaxation time.

Interest in these time effects first arose from their analogy with dielectric relaxation. Waller (1932) was the first to make a study of specifically paramagnetic relaxation. Subsequently Kronig (1939) and Van Vleck (1940) introduced further ideas which have given a general qualitative understanding of the subject. The pioneer of experimental research in this field was Gorter (1936), whose first experiments were carried out at Haarlem in 1935 and 1936. The introduction of the adiabatic demagnetization method of attaining very low temperatures (Giauque and MacDougall 1933) stimulated interest in relaxation effects at very low temperatures, since demagnetization experiments would not be fruitful if relaxation times were very long, which was the prediction of Heitler and Teller (1936) from an elaboration of Waller's theory.

§ 2. THE MECHANISM OF PARAMAGNETIC RELAXATION

In paramagnetic crystals the magnetic dipoles to be considered are the electron spins of the magnetic ions, the interaction of the electric field of the crystalline lattice with the orbital magnetic moments being so strong that no changes of orbital moment can occur at ordinary temperatures, so that the orbital magnetism is 'quenched'. Paramagnetic relaxation in these crystals includes two separate phenomena: spin relaxation, which is concerned with the attainment of equilibrium within the spin system, and spin–lattice relaxation, which is concerned with the interchange of energy between the spin system and the crystal lattice of the salt. Each spin is subject to a fluctuating magnetic field due to its neighbours; interchange of energy among the spins may be regarded as arising from absorption or induced emission in this field. The resulting spin relaxation time is of the order of 10^{-9} sec. independent of temperature. The spin–lattice relaxation time, on the other hand, is highly temperature dependent; it is of the order of 10^{-7} sec. at room temperature and 10^{-2} sec. at 1° K. for most paramagnetic salts. In the first suggested mechanism for spin–lattice relaxation (Waller 1932), the changes in the electric field of the salt's crystalline lattice, due to its distortion by thermal vibration, were considered to act directly on the interaction field of the spins. This gave relaxation times of the order of $10^{11}/H^2$ sec. at liquid hydrogen temperatures—far longer than are found experimentally. Kronig (1939) however showed that the indirect action of the crystalline electric field on the spins through the spin–orbit coupling is much stronger than its direct action, and derived theoretically relaxation times of the correct order of magnitude.

Transfer of energy between the spins and the lattice can take place by two processes—a 'first order process' in which a whole quantum of the lattice waves is absorbed or emitted, and a 'Raman process', analogous to the Raman scattering of light waves, in which inelastic scattering of lattice waves takes place with exchange of energy between the spin system and the lattice. According to Fierz (1938) and Kronig (1939) the number of Raman processes is proportional to T^2 for $T \gg \theta$ and to T^7 for $T \ll \theta$, where θ is the Debye characteristic temperature of the lattice. The number of first order processes is proportional to T. Kronig (1939) found that for caesium titanium alum (for $T \ll \theta$) the first order processes gave rise to a transition probability $B \simeq 10^{-10} H^4 T$ sec^{-1}, and the Raman processes a probability $D \simeq 10^{-9} H^2 T^7$ sec^{-1}. The relaxation times so predicted are extremely short under the experimental conditions usually employed; the experimental values are however considerably shorter. Caesium titanium alum is a less typical case than potassium chrome alum, on which calculations have been made by Van Vleck (1940). Here the calculated relaxation times are of the correct order of magnitude both at liquid air temperatures, where the Raman processes are the more important, and at liquid helium temperatures, where the direct effects should predominate; but neither the temperature dependence nor the field dependence is correctly predicted. The relaxation time at liquid helium temperatures varies more rapidly with temperature than the law $\tau \simeq A/T$ where A is independent of temperature, and it increases with increasing magnetic field, instead of decreasing, as the theory predicts.

§ 3. THE SCOPE OF THE PRESENT EXPERIMENTS

The experiments described in this paper are concerned with spin–lattice relaxation only, being carried out at frequencies in the audio-frequency range at liquid helium temperatures. At these frequencies the spin system may be regarded as being always in internal equilibrium. It was hoped to obtain more definite results on the temperature and field dependence of the spin–lattice relaxation times of representative paramagnetic salts, and also to determine the magnetic specific heats of these salts. As the experiments progressed it was found that the phenomena were more complex than has been supposed till now. Not only do different samples prepared from the same material give different relaxation times, but the behaviour of a single specimen cannot be described in terms of a single relaxation time. On the other hand, experiments on different specimens of the same material, having quite different relaxation behaviour, yield the same value for the specific heat.

§ 4. THE MEASUREMENT OF RELAXATION TIMES

The theory of spin–lattice relaxation measurements is based on the fact that provided the spin system is in internal equilibrium (as is certainly the case in audio-frequency measurements) it can be treated as a thermodynamic entity separate from the crystal lattice, whose temperature may differ from that of the lattice (Casimir and du Pré 1938). Measurements are made by applying a large steady magnetic field and a small parallel oscillatory field to the salt, and measuring the oscillatory component of the susceptibility. (The presence of the large field is essential, since otherwise the energy changes associated with magnetization are small, and can be absorbed in the spin system without spin–lattice relaxation effects coming into play.) The temperature of the spin system oscillates with the field, but if the period is sufficiently long compared with the relaxation time, the spin temperature will never differ materially from the lattice temperature (supposed constant) and the isothermal susceptibility χ_T will be measured. If on the other hand the period is too short to allow of the exchange of energy of magnetization between the spin system and the lattice, another value will be obtained, which we may call the adiabatic value χ_S. At intermediate periods relaxation effects will be observed.

The amplitude of the temperature oscillations of the spin system and thus the value of χ_S will clearly depend on the heat capacity of the spin system. There are two important thermodynamic relations which are independent of any further assumption about the relaxation time:

$$\frac{\chi_T}{\chi_S} = \frac{C_H}{C_I} \qquad \ldots\ldots(1)$$

and

$$C_H - C_I = T\left(\frac{\partial I}{\partial T}\right)_H^2 \Big/ \chi_T. \qquad \ldots\ldots(2)$$

Here I is the magnetization, and C_H and C_I are the specific heats *of the spin system* at constant field and at constant magnetization respectively. It is clear that if χ_T, χ_S and $(\partial I/\partial T)_H$ are determined, the specific heats C_H and C_I can be found. This is the basis of the specific heat measurements to be described in a later paper. The relaxation measurements and the specific heat measurements were carried out in the same set of experiments.

(i) *The Casimir–du Pré Equations*

Casimir and du Pré (1938) have considered the case when the period of the oscillatory field is comparable with the relaxation time. Their treatment assumes that the relaxation may be ascribed to a single relaxation time τ. If the magnetic field is represented by $H+he^{i\omega t}$, the susceptibility may be expressed as $\chi'-i\chi''$. Then

$$\chi' = \chi_T\left(A+(1-A)\frac{1}{1+\omega^2\tau^2}\right) \qquad \ldots\ldots(3)$$

and

$$\chi'' = \chi_T\left((1-A)\frac{\omega\tau}{1+\omega^2\tau^2}\right) \qquad \ldots\ldots(4)$$

where $A=C_I/C_H=\chi_S/\chi_T$.

As Casimir, Bijl and du Pré point out (1941), χ', χ'', χ_S and χ_T satisfy the relation

$$\{\chi'-\tfrac{1}{2}(\chi_T+\chi_S)\}^2+\chi''^2=\tfrac{1}{4}(\chi_T-\chi_S)^2, \qquad \ldots\ldots(5)$$

which represents a circle in the χ', χ'' plane with its centre at $\{\tfrac{1}{2}(\chi_T+\chi_S), 0\}$ and radius $\tfrac{1}{2}(\chi_T-\chi_S)$. From equations (3) and (4) another relation may be obtained, viz.

$$\chi_T-\chi'=\omega\tau\chi''. \qquad \ldots\ldots(6)$$

Equations (5) and (6) may be used to test the validity of the Casimir–du Pré assumptions. A graph of χ' against χ'' for different frequencies at the same field and temperature should give a semi-circle, while a graph of $\chi_T-\chi'$ against $\omega\chi''$ should give a straight line. If the assumption of a single relaxation time is valid, its value can at once be found.

(ii) *The Measurement of χ' and χ''*

The measurements to be made, then, are determinations of χ' and χ'' at different frequencies, which cover as much of the relaxation range as possible. Liquid helium temperatures are particularly suitable for the investigation of spin–lattice relaxation. The values of susceptibility are very much bigger than at liquid air or hydrogen temperatures, a consideration which is quite important for such magnetically dilute salts as the cupric Tutton salts. Also, the values of the relaxation time at helium temperatures are normally such that most of the relaxation range can be covered at low audio frequencies, at which it is a relatively simple matter to make simultaneous measurements of χ' and χ''.

The method used was essentially that of Casimir, Bijl and du Pré (1941). The specimen was surrounded by a mutual inductance, the primary of which carried the oscillatory magnetizing current. Changes in the magnetization of the specimen produced changes in the induced voltage in the secondary. The voltage due to the in-phase component of magnetization was compensated by a second mutual inductance with its primary and secondary respectively in series with those of the coil round the specimen. The difference ΔM between the value of the compensating inductance and its zero value in the absence of the specimen gave χ' in arbitrary units. The voltage due to the out-of-phase component of magnetization was balanced by a potentiometer device in which a voltage was fed into the secondary circuit from a tapping across a resistance in the primary circuit (Hartshorn's method). When the difference of this resistance from its zero was ΔR, and the frequency $\omega/2\pi$, $\Delta R/\omega$ gave χ'' in the same units as χ'.

(iii) *The Values of* χ_T *and* χ_S

In general χ_S could be determined without difficulty from relaxation measurements in which χ has nearly the adiabatic value, χ_S. Usually a small extrapolation has to be made. This is done on the (χ', χ'') diagram, some specimens of which are shown in Figure 3; these give typical examples of extrapolations to χ_S.

As the relaxation times were too long, it was not possible to obtain χ_T in other than zero magnetic field, when, as remarked above, spin–lattice relaxation does not come into play. The difference between χ_T in zero field and its value in field H was always small, and was calculated from the Brillouin function:

$$\chi_\mathrm{T} = \chi_{\mathrm{T},\,H=0}(1 - \lambda H^2/T^2)$$

where

$$\lambda = \frac{1}{80}\left(\frac{\mu g}{\boldsymbol{k}}\right)^2 \frac{(2j+1)^4 - 1}{j(j+1)},$$

Here μ is the Bohr magneton, g the Landé factor, $\boldsymbol{k}$ Boltzmann's constant and j the effective angular momentum quantum number, which, owing to 'quenching' of the orbital moment, is usually different from the value for the free ion.

It was desirable to obtain χ_T thus rather than by an effectively static measurement (e.g. by a ballistic galvanometer method) as it was inconvenient to change over from A.C. to D.C. measurements and, further, it was difficult to hold the field current for the field H sufficiently steady to take accurate ballistic galvanometer readings.

§ 5. THE APPARATUS

The form of apparatus used is shown in Figure 1; Figure 2 shows the electrical circuit diagrammatically. Small crystals of the salt investigated were normally contained in a spheroidal container A of Perspex, 40 mm. long and 10 mm. diameter internally, which stood in the glass cryostat B, suspended by two tubes C and D which were joined by platinum–glass seals to the expansion chamber of a small Simon expansion helium liquefier. (In the measurements on the copper Tutton salts, in which demagnetizing effects were unimportant on account of

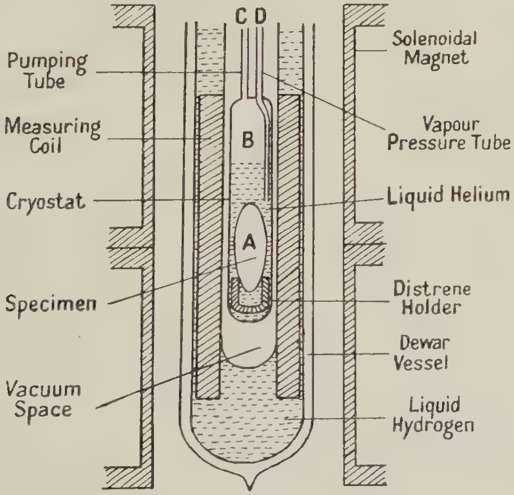

Figure 1. The apparatus.

the small susceptibility of the salts, the Perspex container was omitted, and a larger volume of salt was used.) The cryostat and liquefier were enclosed in a vacuum case, of which the part surrounding the cryostat was of glass, attached to the metal part above by a copper–glass seal. The entire vacuum case was surrounded by liquid hydrogen in a Dewar vessel. Susceptibility measurements were made by means of a compensated mutual inductance (immersed in the liquid hydrogen) of the type described by Casimir, Bijl and du Pré (1941). This system employs two primary coils with the numbers of turns in the inverse ratio of their cross-sectional areas, and three secondaries of which the two end coils are wound in opposition to the centre coil and compensate its mutual inductance with the primaries. The arrangement has the advantages that in the absence of a specimen of salt the mutual inductance between the primary and secondary systems is almost zero, that the external field is very small, so that eddy currents in the surrounding solenoid are minimized, and that it produces a highly uniform field at the specimen.

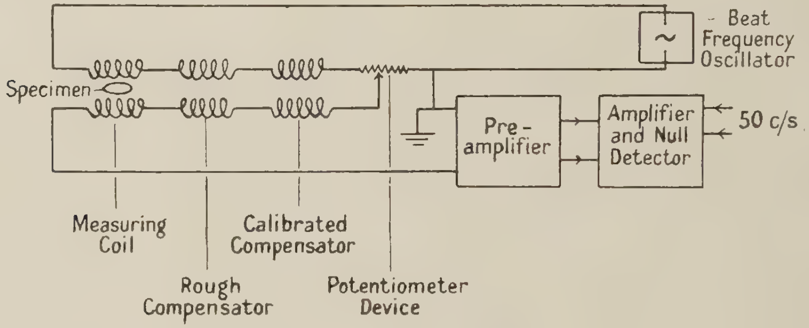

Figure 2. The electrical circuit.

The mutual inductance measurement was made by Hartshorn's method (Figure 2), the mutual inductance being compensated by an equal and opposite inductance provided by a system consisting of a 4-decade mutual inductance set (graduated in arbitrary units of approximately 0·153 μH.), and a potentiometer device. The latter consisted of 24 steps of 0·1 ohm and a 0·1 ohm slide wire, shunted to give dividing factors of 10 and 100. The shunts served the double purpose of reducing to a negligible quantity the inductive feed from primary to secondary and increasing the accuracy of reading. The primary circuit could be fed with frequencies of 12·5, 20, 33·3, 75, 175, 500 and 950 c/s. from a "Birmingham Sound Reproducers" beat-frequency oscillator, the frequencies being checked against a standard 50 c/s. The secondary circuit was connected to a detector consisting of a "General Radio" cathode-ray null detector preceded by a two-stage battery-operated pre-amplifier. Both the null detector and pre-amplifier were tuned by twin-Tee feedback networks. The limit of sensitivity of the detector was 1 μV. The primary current used was generally 0·1 amp. which produced an oscillatory field of about 4 oersted at the specimen. Parallel steady fields up to 1,000 oersted were produced by an external iron-free solenoid, the limit being set by the heating of the coil. The solenoid was excited by a battery of accumulators, and the current was measured by a potentiometer and standard resistance.

§ 6. PROCEDURE

Each experiment began with the measurement of the susceptibility of the paramagnetic salt at different temperatures. The mutual inductance of the measuring coil was first determined with the specimen at liquid oxygen temperature, then at liquid hydrogen temperature. Helium was then liquefied in the expansion chamber of the Simon liquefier, and sufficient helium condensed into the cryostat to cover the specimen. The mutual inductance was then measured at different temperatures in the helium range, the helium vapour pressure being measured by a manometer connected to tube D, which dips into the liquid, while the temperature of the helium bath was reduced by evaporating the helium by a pump connected to tube C. By connecting successively a mercury manometer, an oil manometer, and a McLeod gauge to tube D, the measurement of the susceptibility of the specimen could be made at temperatures down to about 0·95° K. This part of the experiment serves to establish the exact law of variation of the susceptibility of the specimen with temperature, after which it could be used as a secondary thermometer which could at any time be checked against the vapour pressure thermometer. In most of the experiments a complete calibration was made only at a single frequency, check measurements at the other frequencies being made at the hydrogen boiling point, the helium λ-point, and at the temperatures at which relaxation measurements were made.

With the cryostat maintained at a constant temperature by pumping helium through tube C at a suitable rate, mutual inductance measurements were made at the different frequencies in zero external field and in two or three different values of steady field. For the specific heat measurements, which depend on the ratio $(\chi_T - \chi_S)/\chi_S$, fields were selected whenever possible to make this ratio approximately unity, so as to give the greatest accuracy in the measurement of the ratio. Measurements were not always made at all the available frequencies, but at enough to give the value of χ_S, and to give information on the spin–lattice relaxation time. At the higher temperatures of measurement it was sometimes impossible to secure adiabatic conditions with the frequencies we were able to employ; in this case measurements at a series of frequencies usually allowed a value of χ_S to be found by extrapolation with an accuracy better than 1%.

§ 7. RESULTS

In the course of the experiments it soon became apparent that the observed phenomena could not be explained in terms of a single relaxation time. Thus precise determination of values of relaxation times and their dependence on temperature and external field proved impossible, and conclusions are of a qualitative rather than a quantitative nature.

(i) *Test of the Casimir–du Pré Relations*

Tests of the Casimir–du Pré relations (3) and (4) are made in the ways already described. Plots of χ'' against χ' lie on a semicircle for only one salt at one temperature of measurement—manganese ammonium sulphate at 2·17° K. The curves obtained for the other salts may be roughly described as flattened semicircles which tail off to χ_T. Some examples are given in Figure 3. Even in the case of manganese ammonium sulphate at 2·17, however, the fact that a semicircle can be drawn accurately seems to be largely accidental, since it does not pass through χ_T, and the positions of the experimental points (χ', χ'') along the semi-circle do not agree with formulae (3) and (4); this comes out clearly in the plot of $(\chi_T - \chi')$ against $\omega\chi''$ (Figure 4) when a straight line is not obtained. None of the salts investigated gave a straight line on this method of presentation. In all the cases the curves obtained had a steadily decreasing slope.

Casimir, Bijl and du Pré (1941) obtained for the plot of χ'' against χ' for potassium chrome alum a semi-circle which, however, did not pass through χ_T. They did not consider this significant and suggested its cause to be a small amount of ferromagnetic impurity or a slight mechanical vibration of the coils. Neither of these suggestions is easily acceptable.

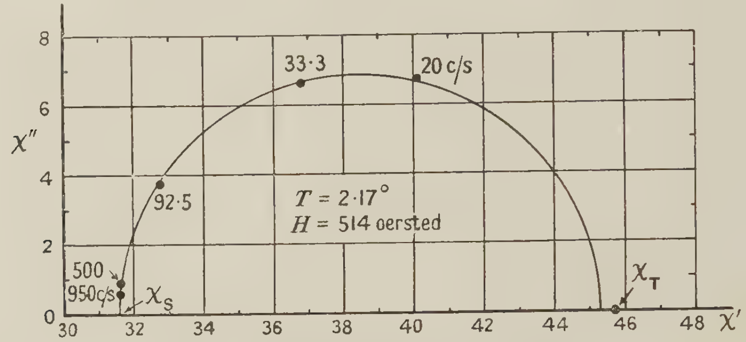

(a) Manganous Ammonium Sulphate

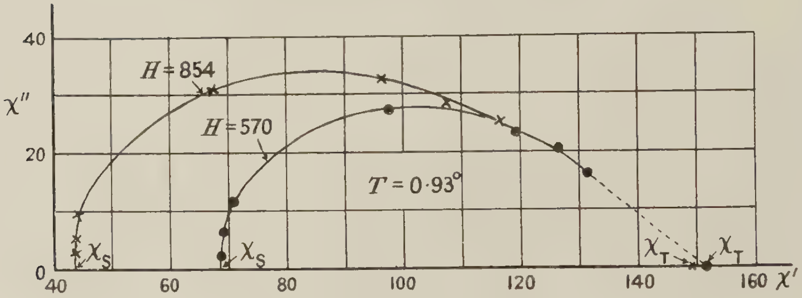

(b) Iron Ammonium Alum, Sample I.

Figure 3. χ', χ'' relaxation diagrams.

If relaxation phenomena were due to a single relaxation time τ, we should find from equations (3) and (4) $\tau = (\chi_T - \chi')/\omega\chi''$. Let us call this ratio τ_a—the apparent relaxation time—in an actual case. In any actual case it is found that τ_a is not constant but depends on ω. For any particular specimen, then, H and T are not sufficient to fix τ_a—another parameter is required; we have chosen $\chi''/(\chi_T - \chi')$, which specifies the position on the χ', χ'' relaxation diagram. Let us call this ratio p for convenience. If there is only a single relaxation time τ, then $p = 1/\omega\tau$. It may be expected that a reasonably true comparison of relaxation times will be obtained if comparisons are made of τ_a at similar positions on the 'circle diagram'. Table 1 gives values of τ_a with corresponding values of p for iron ammonium alum at 2·16° K. This set of results gives a typical example of the behaviour of τ_a.

A typical set of results (for a single crystal of iron ammonium alum) is given in Table 1, and a summary of all the results obtained is given in Table 2. τ_a is

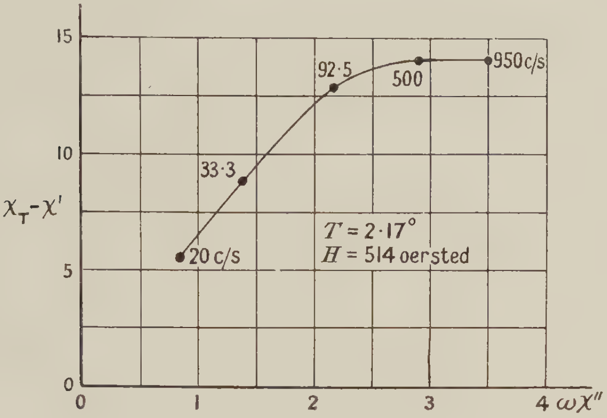

(a) Manganous Ammonium Sulphate

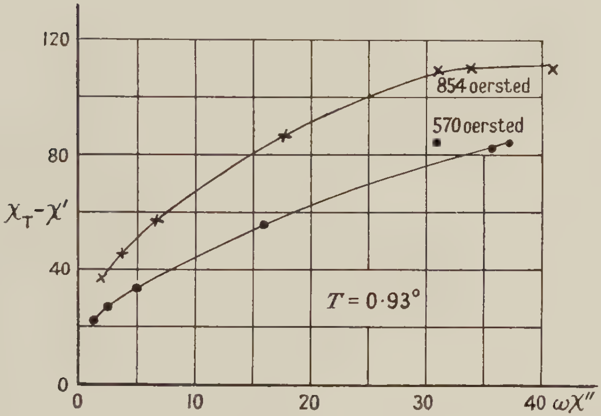

(b) Iron Ammonium Alum, Sample I.

Figure 4. $(\chi_T - \chi')$, $\omega\chi''$ relaxation diagrams.

Table 1. Relaxation Data for Iron Ammonium Alum (Sample 3)

T (° K.)	$\frac{\omega}{2\pi}$	H (oersted)	$\chi_T - \chi'$	$\omega\chi''$	τ_a (sec. $\times 10^{-3}$)	p
2·16	950	400	41·4	9·9	4·2	0·040
		570	60·2	12·8	4·7	0·036
		748	72·6	11·5	6·3	0·027
	500	400	40·5	9·6	4·2	0·076
		570	59·2	10·6	5·6	0·057
		748	71·7	10·4	7·0	0·045
	92·5	400	33·9	6·25	5·4	0·32
		570	52·6	7·74	6·8	0·25
		748	67·0	7·79	8·6	0·20
	33·3	400	23·7	2·84	8·4	0·57
		570	38·8	4·04	9·6	0·50
		748	52·7	4·59	11·5	0·42
	12·5	400	14·3	0·96	15	0·85
		570	24·9	1·56	16	0·80
		748	35·2	1·93	18	0·71

given for values of p as close to 0·1 as possible to make the values of τ_a comparable. All the samples were of Analar material. In the case of copper sulphate pentahydrate the relaxation time was too short for calculation in the same way as for the others—the ratio $(\chi_T - \chi')/\omega\chi''$ was rather indeterminate, both numerator and denominator being nearly zero. It was therefore obtained from the Casimir–du Pré formula for χ'', equation (4), using the value of C_I (0·23 at 1° K.) obtained by Ashmead (Duyckaerts 1942). τ is too short for a proper determination and it can only be given as being of the order of 10^{-5} sec. or less.

Table 2. Relaxation Times—Summary of Results

Salt*	T (° K.)	H (oersted)†	τ_a (sec. $\times 10^{-3}$)†	p
Iron ammonium alum : Sample 1	2·13	285–968	0·2– 0·4	0·5
	0·93	285–968	1·5– 4	0·1
Iron ammonium alum : Sample 2	1·30	400–795	0·3– 0·6	0·2
	0·91	343–841	1·4– 3·5	0·2
Iron ammonium alum : Sample 3	2·16	400–748	4 – 7·5	0·1
	0·94	400–748	44 –80	0·1
Iron ammonium alum : Sample 4	2·16	400–748	1·5– 2·5	0·1
	0·96	400–748	10 –20	0·02
Manganese ammonium sulphate	2·16	514–852	5 – 7	0·1
Chromium ammonium alum	2·16	684–908	4 – 5	0·1
	0·98	684–908	17 –20	0·1
Chromium caesium alum	2·15	396–678	0·8 –1·0	0·1
	0·96	396–678	13 –16	0·01
Nickel fluosilicate	0·96	400–748	0·9– 1·3	0·1
Gadolinium sulphate octohydrate	2·16	570–851	7 – 8	0·1
	0·99	570–851	50	0·1
Copper ammonium sulphate	2·18	286–428	10	0·1
	0·97	286–428	40 –50	0·05
Copper potassium sulphate	2·16	226–339	3 – 4	0·1
	1·0	226–339	18 –22	0·1
Copper rubidium sulphate	1·56	172–284	5	0·1
	0·98	172–284	15	0·1
Copper sulphate (pentahydrate)	1·0	700	$\sim 10^{-2}$	—

* Sample 1 of iron ammonium alum was a fine powder.
Sample 2 of iron ammonium alum was of small crystals, of average size about 10 mm³.
Sample 3 of iron ammonium was a single crystal.
Sample 4 of iron ammonium was a spheroid of compressed powder.

† Where, for example, H is given as 400–748 oersted and τ_a as $1{\cdot}5$–$2{\cdot}5 \times 10^{-3}$ sec. it may be taken roughly that τ_a varies from $1{\cdot}5 \times 10^{-3}$ sec. at 400 oersted to $2{\cdot}5 \times 10^{-3}$ sec. at 748 oersted.

(ii) *Effect of a 'Mixture' of Relaxation Times*

Let us consider the effect on τ_a of various different relaxation times throughout the sample. Suppose in the first place that the sample consists of n equal portions whose relaxation times are $\tau_1, \tau_2 \ldots . \tau_n$.

Then from formulae (3) and (4),

$$\tau_a = \frac{\chi_T - \chi'}{\omega\chi''} = \frac{1}{\omega}\frac{\sum\limits_{r=1}^{n}\frac{\omega^2\tau_r^2}{1+\omega^2\tau_r^2}}{\sum\limits_{r-1}^{n}\frac{\omega\tau_r}{1+\omega^2\tau_r^2}},$$

(1) when $\omega\tau \gg 1$ this reduces to

$$\tau_a = \frac{n}{\Sigma\frac{1}{\tau_r}} = \frac{1}{\overline{\left(\frac{1}{\tau}\right)}},$$

(2) when $\frac{1}{\omega\tau} \gg 1$ this reduces to

$$\tau_a = \frac{\Sigma\tau_r^2}{\Sigma\tau_r} = \frac{\overline{\tau^2}}{\bar{\tau}},$$

where $\bar{\tau}$ etc. indicate average values.

It will be apparent from these expressions that in case (1) a value of τ_a shorter than the average, $\bar{\tau}$, will be obtained, while in case (2) it will be larger than the average, $\bar{\tau}$. Whatever distribution of relaxation times is assumed this will still hold.

The departures from ideal behaviour indicated on the various methods of presentation are all of this nature. τ_a is long for the low frequency measurements, decreases steadily and becomes much shorter at high frequencies of measurement. This is most clearly seen on the $(\chi_T - \chi', \omega\chi'')$ presentation or from the behaviour of τ_a in Table 1. The finding of widely different relaxation times (by a factor of 20–30) for different samples of iron ammonium alum makes it appear very reasonable that any one sample should not have all its constituent parts with the same relaxation time. It is not clear how an analysis of the relaxation results into a distribution of relaxation times could be made when the (χ', χ'') relaxation diagrams do not fit any simple formula. While relaxation times are no doubt dependent on the chemical purity of a material, the indications are that differences between specimens cannot be attributed solely to this. Gorter (1947) has pointed out that the relaxation time has been found to alter on re-crystallization, and Casimir, Bijl and du Pré (1941) suggest that it depends on the 'physical purity' of the material.

The range of measurements and the complexity of the phenomenon do not permit any detailed conclusions to be drawn as to the dependence of τ on H and T. The actual values of H and T at which measurements were made are shown in Table 2. However, using τ_a at a value of p of 0·1 approximately, it appears that τ_a increases with H according to a low power of H, between 0 and a value less than 1. The dependence on T, also, can only be described very roughly. The variation of τ_a would fit roughly a dependence on $1/T$ according to a power between 2 and 3, being nearer the former for the cupric Tutton salts. The results for the four samples of iron ammonium alum do not show any clear dependence on the state of aggregation of the salt.

§8. CONCLUSIONS

It is not possible to describe spin–lattice relaxation effects in the paramagnetic salts studied at liquid helium temperatures by a single relaxation time. It is tentatively suggested that it might be possible to describe them by a 'mixture' of relaxation times. Dependence on H may be said roughly to be according to a power between 0 and 1, varying considerably from one salt to another, and on T according to T^{-n} where n is between 2 and 3. As proportionality to $1/T$ would be expected if the relaxation were the result of 'first order' processes only, this indicates that 'Raman processes' must still play a considerable part in relaxation between 1° and 2° K.

ACKNOWLEDGMENTS

We wish to thank Professor Lord Cherwell for extending to us the facilities of the Clarendon Laboratory, Professor F. E. Simon for his interest and encouragement, and Mr. L. E. Drain for many helpful suggestions. Grants were made by the Royal Society for the purchase of the beat-frequency oscillator and the null detector used in the experiments. One of us (R.J.B.) is indebted to the Ministry of Education for a maintenance grant.

REFERENCES

Casimir, H. B. G., Bijl, D., and du Pré, F. K., 1941, *Physica*, **8,** 449.
Casimir, H. B. G., and du Pré, F. K., 1938, *Physica*, **5,** 507.
Duyckaerts, G., 1942, *Mém. Soc. Roy. Sci., Liège*, 4^e^ série, tome VI, 195.
Fierz, M., 1938, *Physica*, **5,** 433.
Giauque, W. F., and MacDougall, D. P., 1933, *Phys. Rev.*, **43,** 768.
Gorter, C. J., 1936, *Physica*, **3,** 503; 1947, *Paramagnetic Relaxation* (Amsterdam : Elsevier Publishing Co.), Chapter III.
Hebb, M. H., and Purcell, E. M., 1937, *J. Chem. Phys.*, **5,** 338.
Heitler, W., and Teller, E., 1936, *Proc. Roy. Soc.* A, **155,** 629.
Kronig, R. de L., 1939, *Physica*, **6,** 33.
Langevin, P., 1905, *J. Phys. Radium*, **4,** 678, *Ann. Chim.* (*Phys.*), **5,** 70.
Van Vleck, J. H., 1932, *Electric and Magnetic Susceptibilities* (Oxford : University Press), Chapter XI ; 1937, *J. Chem. Phys.*, **5,** 320; 1940, *Phys. Rev.*, **57,** 426.
Waller, I., 1932, *Z. Phys.*, **79,** 370.

Specific Heats of some Paramagnetic Salts at Temperatures near 1° K.

By R. J. BENZIE and A. H. COOKE
Clarendon Laboratory, Oxford

MS. received 29th August 1949

ABSTRACT. The magnetic specific heats of gadolinium sulphate and of several salts of the iron group of transition elements have been measured at temperatures near 1° K. by a method depending on paramagnetic relaxation. The results obtained are analysed into contributions due to magnetic dipole coupling and interaction of the magnetic ions with the electric field of the crystalline lattice. Cases in which these contributions are insufficient to account for the observed specific heats are discussed.

§ 1. INTRODUCTION

Since the first successful application of the magnetic method of cooling by Giauque and MacDougall (1933) there have been many experiments employing the magnetic method to reach temperatures below 1° K., using a variety of paramagnetic salts as cooling agents. As is well known, the temperatures attained are measured in the first approximation on the 'magnetic temperature scale', obtained by the extrapolation of Curie's law of paramagnetism known to be valid at high temperatures, to the temperatures reached by adiabatic demagnetization. The two most important properties of the salts below 1° K. are therefore the entropy, whose temperature variation determines the temperature reached on demagnetization, and the magnetic susceptibility, which determines the relation of the magnetic temperature to the absolute temperature of the salt. In this paper we describe specific heat measurements on a number of paramagnetic salts in the temperature range 1° K. to 2° K., which provide the data for calculating the properties of the salts below 1° K. by the theoretical formulae given by Van Vleck (1937) and by Hebb and Purcell (1937). This information is obtained by the analysis of the specific heat into the contribution due to magnetic dipole interaction of the magnetic ions and that due to the splitting of their energy levels by the Stark effect of the electric field of the crystalline lattice. At the temperatures at which we have made measurements both effects contribute terms to the specific heat which vary as the inverse square of the temperature. The magnetic dipole interaction is calculable from the susceptibility, which can be measured at high temperatures. Our experiments then give the Stark splitting of the energy levels. Values of the splitting are derived for iron ammonium alum, manganous ammonium sulphate, gadolinium sulphate, nickel fluosilicate, two chromic alums and three cupric Tutton salts. It will be seen that besides the salts commonly used in magnetic cooling work, this list includes a number of others which have been recently investigated by radio-frequency spectroscopy (Bagguley *et al.* 1948). The interest here lies in the comparison of the spectroscopic determinations of the energy levels (made at relatively high temperatures) with the values derived from the specific heat measurements. In some of the cases in which this comparison is possible (chromium ammonium alum and chromium caesium alum) the values are in fair agreement, but in the copper Tutton salts, for which there is no Stark splitting of the spin-degenerate energy levels, the specific heat is much too large to be accounted for by magnetic interaction alone. The excess specific heat is attributed partly to exchange coupling of the magnetic ions and partly to hyperfine splitting of the nuclear energy levels.

§ 2. METHOD OF MEASUREMENT

The magnetic method of measuring specific heats (first described by de Haas and du Pré (1939)) which we have employed, consists essentially in the determination of the susceptibility of the magnetic ions of the salt under isothermal conditions and under adiabatic conditions. From these measurements the specific heat of the system of magnetic ions is obtained by a simple thermodynamic relation. The isothermal measurement is made in a straightforward way. The salt, normally in the form of small crystals, is immersed in a bath of liquid helium, and observations of the susceptibility of the salt are made from its influence on the mutual inductance of two coils that surround it. Measurement of the adiabatic susceptibility by isolating the salt from the helium bath would be difficult experimentally, and would, moreover, have the disadvantage for our purpose that the specific heat so determined would include the lattice specific heat of the salt, which in the helium temperature range is of the same order of magnitude as the specific heat of the magnetic ions. We can, however, measure the susceptibility under conditions in which no heat transfer is possible between the magnetic ions and the crystalline lattice of the salt, and so obtain the specific heat of the ions alone. To do this, use is made of the finite time of relaxation for thermal transfer from the magnetic ions to the surrounding heat bath formed by the crystal lattice and liquid helium. When a large steady field and a small parallel oscillatory field are supplied to the salt, the 'temperature' of the magnetic ions will oscillate with the field, rising as it increases and falling as it decreases. These oscillations of temperature will be reduced by heat transfer between the ions and the heat bath, and if the period of oscillation is sufficiently long the variations of magnetization will take place under practically isothermal conditions. If however the period of oscillation is very short compared with the time constant for heat transfer, the variations will be adiabatic. By measuring the influence of the salt on the mutual inductance of two coils surrounding it at low and at high frequencies it is thus in principle possible to determine the isothermal and adiabatic values of the magnetic susceptibility, $\chi_T = (\partial I/\partial H)_T$ and $\chi_S = (\partial I/\partial H)_S$, under identical conditions of field and temperature. In practice there are difficulties in doing this directly, but they are avoided as described below. The specific heat is related to these quantities by the thermodynamical equations

$$C_H/C_I = \chi_T/\chi_S$$

and

$$C_H - C_I = T\left(\frac{\partial I}{\partial T}\right)_H^2 \frac{1}{\chi_T},$$

from which we derive

$$C_I = \frac{T\left(\frac{\partial I}{\partial T}\right)_H^2 \chi_S}{\chi_T(\chi_T - \chi_S)}$$

where I is the magnetic moment per cm^3.

If the salt behaves as an ideal paramagnetic, i.e. if $I=f(H/T)$, then

$$\left(\frac{\partial I}{\partial T}\right)_{\mathrm{H}} = -\frac{H}{T}\left(\frac{\partial I}{\partial H}\right)_{\mathrm{T}} = -\frac{T}{H}\chi_{\mathrm{T}},$$

giving
$$C_{\mathrm{I}} = \frac{H^2\chi_{\mathrm{T}}\chi_{\mathrm{S}}}{T(\chi_{\mathrm{T}}-\chi\ )}.$$

(The specific heat at constant magnetization, C_{I}, is a more convenient quantity than that at constant field, C_{H}, since for an ideal paramagnetic C_{I} is independent of the magnetic field at a given temperature. It is equal to the value of C_{H} at $H=0$.)

In practice the assumption that the salt behaves as an ideal paramagnetic is not realized. Interaction and demagnetizing effects cause the magnetization to obey the equation $I=f\{H/(T-\beta)\}$ rather than $I=f(H/T)$. Moreover, it is normally difficult to determine the value of χ_{T} in a magnetic field due to the relaxation time being too long, and so χ_{T} is usually measured in zero field, where relaxation effects do not affect the measurement, since $\chi_{\mathrm{T}}=\chi_{\mathrm{S}}$ at $H=0$. It is then necessary to correct for the effect of saturation in order to arrive at the value of χ_{T} in a field H. This correction is always small and has on occasion been checked by a ballistic galvanometer comparison of χ_{T} in field H with its value in zero field. If the relaxation time is too short, it may not be possible to obtain the value of χ_{S} from a measurement at a single frequency, but it may be derived without difficulty from measurements at several frequencies which nearly give the adiabatic condition by making an extrapolation to χ_{S} as described in the preceding paper on paramagnetic relaxation (Benzie and Cooke 1950).

For a substance obeying the equation $\chi_{\mathrm{T}}=C/(T-\beta)$,

$$C_{\mathrm{I}} = \frac{CT}{(T-\beta)^3}H^2\frac{\chi_{\mathrm{S}}}{\chi_{\mathrm{T}}-\chi_{\mathrm{S}}}.$$

Including the saturation correction

$$\chi_{\mathrm{T,\,H}} = \chi_{\mathrm{T,\,0}}(1-\lambda H^2/T^2),$$

and ignoring terms in λ to a power higher than the first, we have

$$C_{\mathrm{I}} = \frac{CT}{(T-\beta)^3}H^2\frac{\chi_{\mathrm{S}}}{\chi_{\mathrm{T,\,0}}-\chi_{\mathrm{S}}(1+\lambda H^2/T^2)}$$

or
$$\frac{C_{\mathrm{I}}T^2}{\boldsymbol{R}} = \frac{C}{\boldsymbol{R}}\left(\frac{T}{T-\beta}\right)^3\frac{H^2}{\chi_{\mathrm{T,\,0}}/\chi_{\mathrm{S}}-(1+\lambda H^2/T^2)}.$$

Here
$$C = \frac{\boldsymbol{R}}{3}\left(\frac{g\mu}{\boldsymbol{k}}\right)^2 j(j+1),$$

and
$$\lambda = \frac{1}{80}\left(\frac{g\mu}{\boldsymbol{k}}\right)^2\frac{(2j+1)^4-1}{j(j+1)},$$

where C is the Curie constant for the salt, μ the Bohr magneton, g the Landé splitting factor, $\boldsymbol{k}$ Boltzmann's constant, and j the effective angular momentum of the ion, which owing to 'quenching' of the orbital component has a 'spin-only' value for the salts we have investigated. $\boldsymbol{R}$ is the gas constant.

It will be seen that since we know the value of the Curie constant, which is well established for all the salts we have used, the experiment is reduced to the determination of the ratio of χ_{S} to $\chi_{\mathrm{T,\,0}}$. It is not necessary to know β and λ very accurately as they occur only in correction terms.

§3. THE APPARATUS AND PROCEDURE

Details of the apparatus and procedure during the experiment are given in the preceding paper (Benzie and Cooke 1950).

§4. RESULTS

The main source of the specific heats which we have measured is usually the Stark splitting of the spin-degenerate energy levels of the magnetic ions in the crystalline electric field of the lattice (Hebb and Purcell 1937). To derive the values of such splittings we must first calculate the component of specific heat due to magnetic dipole interaction from the formula given by Van Vleck (1937), viz.

$$C_{\mathrm{m}}T^2/\boldsymbol{R}=\tfrac{1}{6}Q\tau^2,$$

where $\tau/3$ is the Curie constant per unit volume and Q is a factor depending on the lattice arrangement of the magnetic ions. Taking this to be a face-centred cubic arrangement for the alums, $Q=14{\cdot}4$ and $C_{\mathrm{m}}T^2/\boldsymbol{R}=2{\cdot}4\tau^2$. Assuming that the Tutton salts have the same crystal structure as magnesium ammonium sulphate (Hofmann 1931), with crystallographic axes in the ratio 3 : 4 : 2, Q is 16·8 giving $C_{\mathrm{m}}T^2/\boldsymbol{R}=2{\cdot}8\tau^2$.

In the absence of any other contribution to the specific heat, the remainder after subtracting the magnetic interaction contribution can be attributed to the Stark splitting. It is shown below however that the values of Stark splitting so derived are consistently greater than those determined spectroscopically. The discrepancy may be explained by the presence of exchange interaction, which contributes to the specific heat. Evidence of the presence of exchange interaction is provided by the magnetic behaviour of the salts. Several of them are found to obey a Curie–Weiss law with a Weiss constant which is not wholly attributable to magnetic dipole interaction.

Iron Ammonium Alum.

As an example of the method of working, the results of an experiment on a specimen of iron ammonium alum are given in some detail. This specimen was a spheroid of fine compressed powder, for which the value of Weiss constant β, calculated from the Lorentz internal field and demagnetizing effects, was 0·05°. This agreed with experiment without the addition of any Weiss constant due to exchange effects.

Experiments on two other specimens, one a loosely packed fine powder, and the other consisting of small crystals of about 10 mm^3 average size, gave values of $C_{\mathrm{I}}T^2/\boldsymbol{R}$ at 0·93° K. of 0·0144 and 0·0143 respectively. In both cases the relaxation time was too short for values to be obtained at higher temperatures.

The Fe^{+++} ion is in a ^{6}S state. If we assume that the water molecules surrounding each ion produce an electric field of cubic symmetry, the six-fold degenerate level will split into one of two-fold and one of four-fold degeneracy (Van Vleck and Penney 1934). The partition function per ion is then

$$Z=2\{1+2\exp(-\delta/\boldsymbol{k}T)\}$$

where δ is the energy separation of the levels. At temperatures high compared with $\delta/\boldsymbol{k}$ this leads to a contribution to the specific heat given by

$$CT^2/\boldsymbol{R}=(2/9)(\delta/\boldsymbol{k})^2.$$

With this arrangement of energy levels the deviation of $C_{\mathrm{I}}T^2/\boldsymbol{R}$ from this square law value is $+3\%$ at 2° K. and $+6\%$ at 1° K. if δ is taken positive and $-3{\cdot}5\%$ and

-7% if δ is taken negative. Our measurements, however, show a variation of less than 1% between 2·2° K. and 0·96° K. This is more consistent with the assumption of the splitting of the six-fold spin degenerate level into three equally spaced doublets, giving a partition function

$$Z=2\{1+\exp(-\tfrac{1}{2}\delta/\boldsymbol{k}T)+\exp(-\delta/\boldsymbol{k}T)\},$$

which would result in a calculated falling off of $C_\mathrm{I}T^2/\boldsymbol{R}$ by 0·5% from 2° K. to 1° K. Further evidence of the near-constancy of $C_\mathrm{I}T^2/\boldsymbol{R}$ down to 1% is found in the agreement of the present measurement with the most recent determination—by Broer (Gorter 1947)—at liquid air temperature; Broer's value of $C_\mathrm{I}T^2/C$ is 0·27. With the assumption of three equally spaced doublets the high temperature value of $CT^2/\boldsymbol{R}$ due to the splitting is $\frac{1}{6}(\delta/\boldsymbol{k})^2$, where δ is the overall splitting. This leads to a value of 0·23 for $\delta/\boldsymbol{k}$.

Table 1

T (° K.)	H (oe.)	$\chi_{\mathrm{T},0}-\chi_\mathrm{S}$	χ_S	r	$\lambda\frac{H^2}{T^2}$	$\frac{H^2}{r_1}$	$\left(\frac{T}{T-\beta}\right)^3$	$\frac{C_\mathrm{I}T^2}{\boldsymbol{R}}$	$\frac{C_\mathrm{I}T^2}{C}$	$\frac{\delta}{\boldsymbol{k}}$ ( )
						$\times 10^5$		$\times 10^{-2}$	$\times 10^5$	
2·16	400	42·5	66·5	0·639	0·001	2·50	1·074	1·43	2·70	0·20
	570	61·5	47·5	1·295	0·002	2·51				
	748	74·5	34·5	2·161	0·004	2·53				
1·31	400	73·8	111·2	0·663	0·003	2·42	1·123	1·43	2·70	
	570	106·6	78·4	1·360	0·006	2·40				
	748	128·7	56·3	2·284	0·011	2·40				
0·96	400	104·3	149·0	0·700	0·006	2·30	1·172	1·42	2·69	
	570	148·7	104·6	1·421	0·013	2·31				
	748	178·7	74·6	2·395	0·021	2·29				

The values given for the χ's are actually mutual inductance measurements, but these are proportional to the susceptibility, and are therefore taken as susceptibilities in arbitrary units; $r=(\chi_{\mathrm{T},0}-\chi_\mathrm{S})/\chi_\mathrm{S}$; $r_1=r-\lambda H^2/T^2$.

A crystalline field of symmetry less than cubic would lead to a greater removal of degeneracy than that found by Van Vleck and Penney, and would make the splitting into three doublets possible. That the crystalline field in the alums has a component with symmetry less than cubic is clear from the existence of a splitting of the spin degenerate levels of the chrome alums—there would be no such splitting in a purely cubic field (Hebb and Purcell 1937).

It would be unwise to draw definite conclusions as to the arrangement of the split levels from our results, but it does seem certain that the split levels are three doublets, rather than one doublet and one quadruplet, and that the spacing is not far from being equal.

Preliminary spectroscopic measurements by Bagguley *et al.* (1948) suggest however that the overall splitting is less than 0·1 cm^{-1}. If this is the case we must conclude that the theory we have assumed in deriving $\delta/\boldsymbol{k}$ is inadequate but we are unable to offer any explanation of the discrepancy. It is hardly possible that exchange interaction could account for the difference.

Table 2 summarizes the results of specific heat measurements on different substances. Besides the value of $C_\mathrm{I}T^2/\boldsymbol{R}$, we give the value of $C_\mathrm{I}T^2/C$, where C is the Curie constant for the substance. Gorter in his book *Paramagnetic*

Relaxation (1947) gives most specific heat results in terms of this quantity—it is his "b/C". The value of the crystalline splitting of the energy levels, deduced by the same procedure as for iron alum, is also given. The results for the different substances are discussed in the notes below.

Table 2

Substance	T (° K.)	$\frac{C_I T^2}{R}$	$\frac{C_I T^2}{C}$	$\frac{\delta}{k}$ (°)	Spin	$\frac{C_I}{R}$
			$\times 10^6$			
Iron ammonium alum	2·16	0·0143	0·270	0·20	5/2	—
Sample C	1·31	0·0143	0·270			
	0·96	0·0142	0·269			
Sample A	0·93	0·0144				
Sample B	0·93	0·0143				
Manganous ammonium sulphate	2·17	0·0331	0·63	0·32	5/2	—
	0·95	0·0330	0·63			
Ammonium chrome alum	2·16	0·0370	1·64	0·38	3/2	—
	1·54	0·0365	1·61			
	1·27	0·0361	1·60			
	0·97	0·0354	1·57			
Caesium chrome alum	2·16	0·0109	0·481	0·20	3/2	—
	1·82	0·0108	0·480			
	1·60	0·0108	0·480			
	1·02	0·0106	0·473			
Nickel fluosilicate	0·95	0·0139	0·89	0·23	1	—
Gadolinium sulphate	2·165	0·305	3·24	1·35	7/2	0·065
	1·50	0·274	2·92			0·122
	1·20	0·242	2·58			0·168
	1·055	0·228	2·42			0·204
	0·994	0·217	2·30			0·220

Substance	T (° K.)	$\frac{C_I T^2}{R}$	$\frac{C_I T^2}{C}$	Weiss constant	Spin	$\frac{(C_I - C_m)T^2}{R}$
		$\times 10^{-4}$	$\times 10^5$			$\times 10^{-4}$
Copper ammonium sulphate	2·18	8·701	1·62	0	1/2	7·4
	1·81	8·70	1·62			7·4
	1·59	8·69	1·62			7·4
	1·30	8·55	1·59			7·2
	0·97	8·43	1·57			7·1
Copper rubidium sulphate	1·56	3·36	0·61	0	1/2	2·1
	1·35	3·33	0·61			2·0
	1·104	3·30	0·60			2·0
	0·98	3·30	0·60			2·0
Copper potassium sulphate	2·16	5·95	1·11	0·035 ±0·005	1/2	4·7
	1·49	6·01	1·12			
	1·28	5·93	1·10			
	1·016	5·98	1·11			

Manganous Ammonium Sulphate.

The specimen was a loosely packed powder contained in an ellipsoidal shell. The value of $0{\cdot}63 \times 10^6$ for b/C is in satisfactory agreement with the value of $0{\cdot}64 \times 10^6$ quoted by Gorter (1947) presumably obtained at liquid air temperature. The value of $\delta/\boldsymbol{k}$ is obtained by assuming that the ^{6}S ground state is split by the crystalline electric field into a two-fold and a four-fold level. The value obtained agrees with that deduced from measurements below 1° K. (Cooke 1949), but as Bleaney and Ingram (to be published) have detected a nuclear hyperfine structure in the paramagnetic resonance spectrum of much diluted manganous salts, the value of $\delta/\boldsymbol{k}$ may be too high, since our experiments would not distinguish between the electronic and nuclear splittings. In addition, there will probably be an appreciable contribution from exchange interaction, though it is likely to be small compared with the contributions from the splittings. The resolution of the nuclear and electronic specific heat anomalies would require experiments at temperatures of 0·1° K. or lower.

Chromic Alums.

The quenching of the orbital magnetic moment of the Cr^{+++} ion by the crystalline field converts the ^{4}F ground state effectively into ^{4}S. A crystalline field of symmetry lower than cubic causes splitting of this state into two doublets of energy separation δ (Hebb and Purcell 1937). As this is the maximum extent of splitting which an electric field can produce (Kramers 1930) there can only be one splitting associated with each ion. The specific heat associated with the splitting will be given by

$$C_{\mathrm{S}}T^2\,\boldsymbol{R} = \tfrac{1}{4}\left(\frac{\delta}{\boldsymbol{k}}\right)^2 \frac{4\exp(-\delta/\boldsymbol{k}T)}{\{1+\exp(-\delta/\boldsymbol{k}T)\}^2}.$$

At high temperatures ($\delta \ll \boldsymbol{k}T$) this reduces to $\tfrac{1}{4}(\delta/\boldsymbol{k})^2$.

Ammonium Chrome Alum.

The specimen was of loosely packed powder.

After allowing for the Lorentz and demagnetizing effects, and the effect of the Stark splitting on the susceptibility, a Weiss constant of $-0{\cdot}03$ was required to express the temperature dependence of the susceptibility of this salt.

The value of $C_{\mathrm{I}}T^2/\boldsymbol{R}$ fell with temperature, which is to be expected in the temperature range of our measurements, since $C_{\mathrm{S}}T^2/\boldsymbol{R}$ is constant only for temperatures high compared with $\delta/\boldsymbol{k}$. The fall from 2° to 1° is $3\tfrac{1}{2}$%, in close agreement with 3% calculated theoretically.

Paramagnetic resonance experiments at 77° K. and 20° K. by Bleaney and Penrose (1948) and Bleaney (1949) showed two splittings—0·45° and 0·34°. Since there can be only one splitting associated with each ion, we have to conclude that different ions in the unit cell have different splittings. To reconcile our results with those of Bleaney and Penrose would require three ions having the larger splitting to one ion having the smaller.

Caesium Chrome Alum.

Our experiments were made with a single crystal ground to a rough sphere. After the appropriate allowance had been made for the Lorentz and demagnetizing fields a Weiss constant of $-0{\cdot}02$ was found.

Our value of 0·20° for $\delta/\boldsymbol{k}$ compares with 0·19 from paramagnetic resonance data (Bleaney 1949).

Nickel Fluosilicate.

The specimen was in the form of a loose powder. A Weiss constant of 0·1 was found after allowance had been made for the Lorentz and demagnetizing effects.

This substance is of special interest for paramagnetic resonance work, as it has only one ion per unit cell. The ground state of the Ni^{+++} ion is $^3F_4$, but as a result of quenching of the orbital levels it is effectively in an S state but with a Landé g-factor of 2·27, due to the influence of the higher orbital levels. Assuming that the electric crystalline field splits the three spin levels into a singlet $j=0$ and a doublet $j=\pm 1$, we find the separation $\delta = 0{\cdot}23^\circ$. Penrose (Bagguley *et al.* 1948) found a single splitting of 0·17° at liquid hydrogen temperatures from paramagnetic resonance experiments. The Weiss constant of 0·1° for the salt implies the existence of exchange coupling, which will contribute to the specific heat (Opechowski 1937, 1948), accounting partly at least for the difference between the spectroscopic and our value of $\delta/\boldsymbol{k}$.

Gadolinium Sulphate Octohydrate.

The specimen, in the form of a loose powder in an ellipsoidal container, was prepared from gadolinium oxide kindly supplied by Dr. J. R. Marsh, of the Dyson Perrins Laboratory, Oxford.

For a substance of the high susceptibility and large Stark splitting which gadolinium sulphate possesses, the usual Curie–Weiss expression for the susceptibility is inadequate. It was found possible, however, to express it as $C/\{T-\beta(T)\}$, where $\beta(T)$ is a semi-empirical function of T, corresponding to a behaviour intermediate between what is given by the Onsager (1936) and Van Vleck (1937) improvements to the Lorentz internal field theory, together with a correction for the effect of the Stark splitting (Hebb and Purcell 1937). This necessitates a further correction factor $(1-d\beta/dT)^2$ to the expression for $C_I T^2/\boldsymbol{R}$.

Our values for the specific heat are in good agreement with those of other workers (Clark and Keesom 1935, de Haas and du Pré 1939, and van Dijk and Auer 1942) at liquid helium temperatures.

The ground state of the Gd^{+++} ion is ^8S, which is split by an electric field of cubic symmetry into two doubly degenerate levels and a four-fold degenerate level between them, the ratio of the two separations being 3 : 5 (Penney and Schlapp 1932). The partition function for one ion $Z=2\{1+2\exp(-3\delta/8\boldsymbol{k}T)+\exp(-\delta/\boldsymbol{k}T)\}$ where δ is the overall splitting, assuming that the four-fold level is nearer the lower of the other two, as this gives the better agreement with experiment (van Dijk and Auer 1942). The contribution to $C_I T^2/\boldsymbol{R}$ arising from the splitting

$$C_S T^2/\boldsymbol{R} = T^3 \frac{d^2}{dT^2}(T \ln Z)$$

cannot be replaced by its high temperature approximation between 1° and 2° K. as δ is too large, and the full calculation must therefore be made. The magnetic interaction specific heat has been calculated from an expression given by Hebb and Purcell (1937) as the approximate Van Vleck formula for $C_m T^2/\boldsymbol{R}$ given above also becomes inadequate.

Our value of 1·35° for $\delta/\boldsymbol{k}$ is chosen to fit the experimental value of specific heat at 2·16°, as the calculated magnetic specific heat should be quite reliable here.

The observed specific heat, however, falls off more rapidly than that calculated using this splitting, $C_I/\boldsymbol{R}$ being 0·22 instead of the calculated 0·25 at 1°. This may be either because the calculated value of the magnetic interaction specific heat is in error or because the assumed disposition of the split levels is wrong. This trend is further confirmed by the value of b/C found by de Vrijer, Volger and Gorter (1946)—$3{\cdot}9 \times 10^6$ at room temperature and liquid air temperature—which is equivalent to a splitting of 1·4°.

The Copper Tutton Salts.

The ground state of the Cu^{++} ion is $^2D_{5/2}$, but the orbital degeneracy is completely removed by the crystalline electric field. The distance of the higher orbital levels is such that they have a second-order effect on the susceptibility in that $g = 2{\cdot}19 \pm 0{\cdot}01$. Otherwise the susceptibility has the spin-only value.

The copper salts are of particular interest because, the Cu^{++} ion having only one electron spin, there can be no splitting of the spin levels by the crystalline electric field (Kramers 1930). There is therefore no Stark specific heat. It was thought that the specific heat could therefore be analysed into contributions due to exchange interaction and to magnetic dipole interaction, and that, as the magnetic interaction contribution is calculable with fair accuracy, information on the exchange interaction could be obtained. In fact it transpired that the situation is less simple. The discovery by Penrose (1949) of a nuclear hyperfine structure with an overall splitting of the order of 0·02 cm^{-1} in very dilute cupric salts made it clear that this splitting will contribute appreciably to the specific heat.

The Ammonium, Potassium and Rubidium Copper Tutton Salts.

All the specimens were in the form of loosely packed powders. After allowing for the Lorentz and demagnetizing effects the ammonium and rubidium salts obeyed Curie's law exactly down to 1° K. A Weiss constant of 0·01 would have been easily detectable. In the case of the potassium salt a Weiss constant of $0{\cdot}035 \pm 0{\cdot}005$ was found.

The value of $C_I T^2/\boldsymbol{R}$ found for the potassium salt ($6{\cdot}0 \times 10^{-4}$) disagrees with the value of $6{\cdot}8 \times 10^{-4}$ found by de Klerk (1946) below 1° K., but it is in good agreement with $6{\cdot}1 \times 10^{-4}$ found by Garrett (1949), also below 1° K.

In all three cases the specific heat considerably exceeds the value attributable to magnetic interaction ($C_m T^2/\boldsymbol{R} = 1{\cdot}3 \times 10^{-4}$ approx.), varying from about seven times in the case of the ammonium salt to 2½ times in the case of the rubidium salt. It seems reasonable to suppose that the contribution from the nuclear splitting is approximately the same in all three salts, and therefore, in the ammonium and potassium salts at least, the greatest part of the specific heat must be attributed to exchange interaction (Opechowski 1937, 1948).

A further series of experiments, using diluted copper Tutton salts, has been undertaken to elucidate the nuclear contribution to the specific heat.

ACKNOWLEDGMENTS

The authors wish to thank Professor Lord Cherwell for making available to them the facilities of the Clarendon Laboratory, Professor F. E. Simon for his interest and encouragement, and Drs. Bleaney and Bagguley for many helpful discussions. One of us (R.J.B.) wishes to thank the Ministry of Education for the provision of a maintenance grant.

REFERENCES

Bagguley, D. M. S., Bleaney, B., Griffiths, J. H. E., Penrose, R. P., and Plumpton, B. I., 1948, *Proc. Phys. Soc.*, **61,** 551.

Benzie, R. J., and Cooke, A. H., 1950, *Proc. Phys. Soc.* A, **63,** 201.

Bleaney, B., 1949, *Phys. Rev.* **75,** 1962.

Bleaney, B., and Penrose, R. P., 1948, *Proc. Phys. Soc.*, **60,** 395.

Casimir, H. B. G., de Haas, W. J., and de Klerk, D., 1939, *Physica*, **6,** 241.

Clark, C. W., and Keesom, W. H., 1935, *Physica*, **2,** 1075.

Cooke, A. H., 1949, *Proc. Phys. Soc.* A, **62,** 269.

van Dijk, H., and Auer, W. U., 1942, *Physica*, **9,** 785.

Garrett, C. G. B., 1949, *Nature, Lond.*, **163,** 956.

Giauque, W. F., and MacDougall, D. P., 1933, *Phys. Rev.*, **43,** 768.

Gorter, C. J., 1947, *Paramagnetic Relaxation* (Amsterdam : Elsevier Publishing Co.).

de Haas, W. J., and du Pré, F. K., 1939, *Physica*, **6,** 705.

Hebb, M. H., and Purcell, E. M., 1937, *J. Chem. Phys.*, **5,** 338.

Hofmann, W., 1931, *Z. Kristallogr.*, **78,** 279.

de Klerk, D., 1946, *Physica*, **12,** 513.

Kramers, H. A., 1930, *Proc. K. Ned. Akad. Wet.*, **33,** 959.

Onsager, L., 1936, *J. Amer. Chem. Soc.*, **58,** 1486.

Opechowski, W., 1937, *Physica*, **4,** 181; 1948, *Ibid.*, **14,** 237.

Penney, W. G., and Schlapp, A., 1932, *Phys. Rev.*, **41,** 194.

Penrose, R. P., 1949, *Nature, Lond.*, **163,** 992.

Van Vleck, J. H., 1937, *J. Chem. Phys.*, **5,** 320.

Van Vleck, J. H., and Penney, W. G., 1934, *Phil. Mag.*, **17,** 961.

de Vrijer, W. F., Volger, J., and Gorter, C. J., 1946, *Physica*, **11,** 412.

The 'External' Photoelectron Spectrum and the Intensities of the γ-Rays of Thorium (B + C + C″)

By D. G. E. MARTIN* and H. O. W. RICHARDSON†
* University of Liverpool † University of Edinburgh

Communicated by N. Feather; *MS. received 3rd October* 1949

ABSTRACT. The spectra of the photoelectrons ejected from various targets by the γ-rays of Th(B+C+C″) have been measured and the emission probabilities of the γ-rays of energy 0·238, 0·277, 0·299, 0·510, 0·582, 0·726, and 0·859 Mev. have been estimated. Using the known intensities of the internal conversion lines, coefficients of internal conversion have been found. The four low-energy rays seem to be magnetic dipole in character with some electric quadripole admixture, but the strong 0·582 Mev. ray of ^{208}Pb is predominantly electric quadripole. The possible spins of the nuclear levels are discussed.

§ 1. INTRODUCTION

The aim of the present work was to find the intensities of certain γ-rays of thorium (B + C + C″) in order to elucidate their multipole character and to check some contradictions in the literature. For example, Itoh and Watase (1941) found the 0·510 and 0·582 Mev. γ-rays of ^{208}Pb to have nearly equal intensity, whereas Thibaud (1926) and Johansson (1947) found their 'external' photoelectron lines to be in a ratio of about 1 : 3. The two latter authors have assigned to the G (0·277 Mev.) γ-ray of ^{208}Pb a photoelectron line of height about one-third that of the line due to the strong F (0·238 Mev.) γ-ray of ThB → C. So large an intensity would make the G γ-ray electric dipole in character.

The intensities have been calculated by using a modified form of the relation of Ellis and Aston (1930), which applies in the case of a thick target. The relation can be tested at quantum energies $h\nu$ of 0·238 and 2·62 Mev. because independent estimates of intensity for these two strong γ-rays are available from β-ray data. The theory seems to overestimate the intensity ratio of the high to the low energy γ-ray by about 50%, perhaps because a difference in the angular distributions of the photoelectrons ejected by hard and soft γ-rays may affect the probability of detection with our arrangement of source and target, shown in Figure 5 (*b*). In favour of this view is the fact that an even larger discrepancy has been found in some measurements using the alternative method of very thin targets.

The source consisted of about 60 mc. of radiothorium in thorium oxide carrier held in a copper tube 0·09 cm. thick and 3/16 in. outside diameter with soldered ends. A flat square target was waxed to a flattened part of the tube. The surface of the target, about 1·6 cm. wide, was inclined so that it made an angle of 22° with the central ray of the focused beam.

The magnetic spectrometer described by Martin, Richardson and Hsü (1948) was used, the magnetic field strength being obtained from the voltage generated in a coil rotating at constant speed. The β-ray counts were recorded with a scale of 32.

§ 2. THE SPECTRA

The spectra of the ejected electrons are shown in Figures 1 and 2, in which the notation resembles that used by Ellis (1932) for the internal conversion lines. For example, the F γ-ray of 0·238 MeV. ejects the F, I and J photoelectron groups from the K, L and M shells of the target atoms. The background due to γ-rays penetrating the lead shielding was about 1,800 counts/minute. To reduce statistical errors about 40,000 electrons were counted for each plotted point.

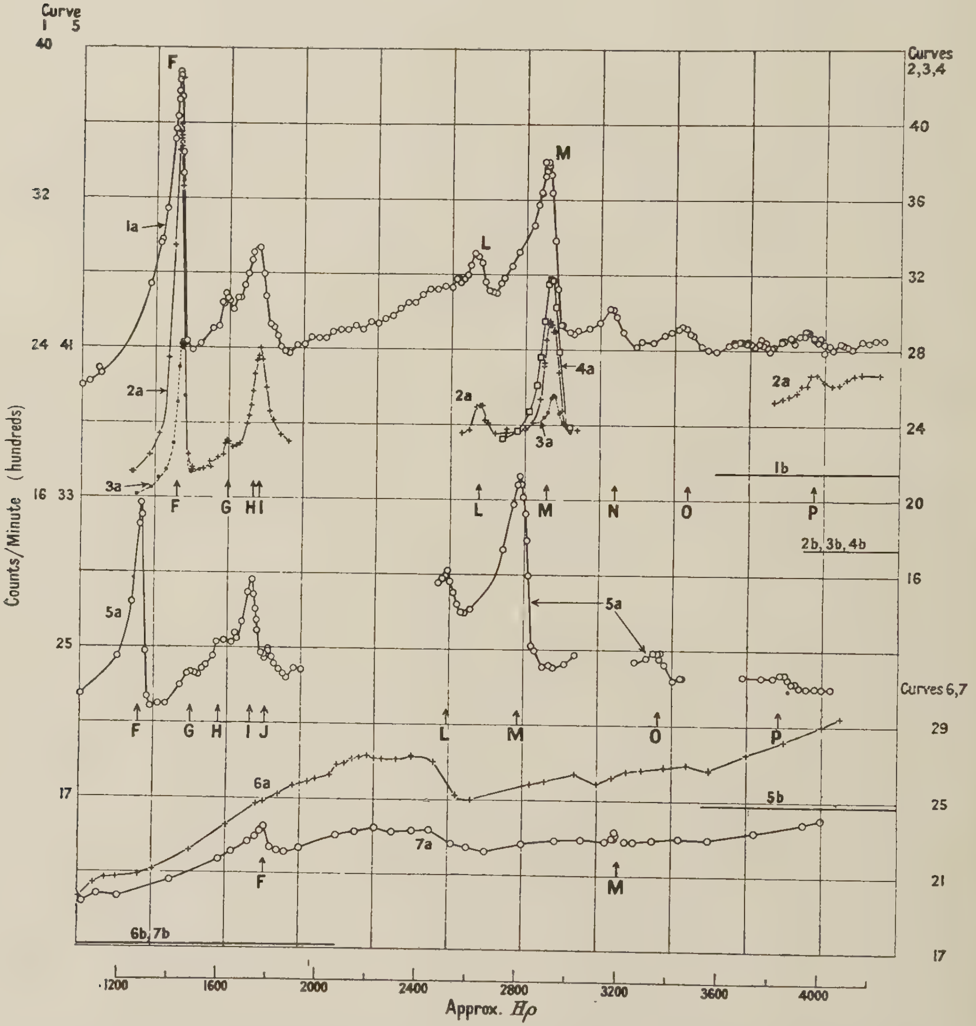

Figure 1. The photoelectron and Compton electron spectrum of RdTh and its products from targets of (1) 200 mg/cm^2, (2) 3·7 mg/cm^2, (3) 0·72 mg/cm^2, (4) 7·4 mg cm^2 gold, (5) thorium, (6) polythene and (7) copper. The γ-ray background for each curve is indicated by the letter b. The space between ordinate lines represents 400 counts/min.

The height of the line due to the 0·51 MeV. (L) γ-ray is about $\frac{1}{3}$ that of the 0·582 MeV. (M) ray while that of the 0·277 MeV. (G) ray is very small, about 1/10 that of the 0·238 MeV. (F) ray. The I and H lines, unresolved with gold, are just distinguishable with thorium, which also shows the J line. Curves 2, 3 and 4 show sharper lines from thin layers of gold mounted on an aluminium base.

As the thickness of gold is increased the added photoelectrons build up the low energy side of the line because they come from deeper layers in the target. The Compton recoil electron groups are well shown in curve 6 for polythene which, because of its low mean atomic number, emits few photoelectrons. With copper, curve 7, the F photoelectron line is already appreciable.

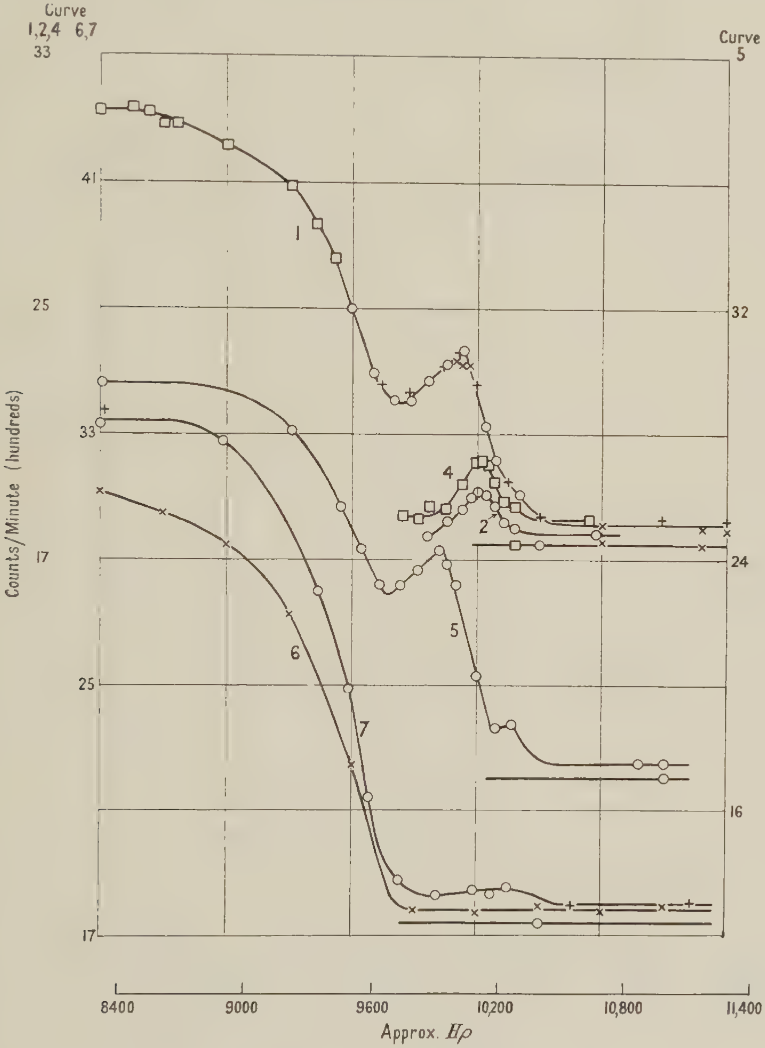

Figure 2. The spectrum near the 2·62 MeV. γ-ray lines.

‘Pre-absorption’ of the 0·238 MeV. γ-ray in the thick target of 200 mg/cm^2 of gold is shown by the fact that the F line is lower with that target than it is with one of 3·7 mg/cm^2 of the same material.

§3. ANALYSIS OF THE LINES FROM A THICK TARGET

The heights h of the line in counts/min. obtained after subtracting the underlying background are given in Table 1. The X line is corrected for the incompletely resolved Xa line from the L shell and the M line is corrected for the nearly coincident line ejected by the 0·51 MeV. γ-ray from the L shell, assuming

τ_K, the atomic absorption coefficient for the K shell, to be $4 \times \tau_L$. Above 0·34 MEV., τ_K has been interpolated from the curves of Hulme, McDougall, Buckingham and Fowler (1935). For the 0·238 MEV. γ-ray the formula of L. H. Gray (1930) for $Z = 82$ has been used:

$$\log(1{\cdot}25 \times \tau_K) = \log\lambda + 0{\cdot}48(\log\lambda)^2 - 24{\cdot}8684,$$

where λ is the wavelength in X.U. The values for gold and thorium were found by multiplying by $(Z/82)^4$ and, for the G and H rays, by interpolating between these values and the curves of Hulme *et al.*

Table. 1. Heights h of Photoelectron Lines from Thick Targets and Calculated γ-Ray Intensities BI^γ in Quanta per Disintegration

Nucleus		ThC	^{208}Pb	ThC	^{208}Pb	^{208}Pb	ThC′	^{208}Pb	^{208}Pb
γ-ray		F	G	H	L	M	O	P	X
$h\nu$ (MEV.)		0·238	0·277	0·299	0·510	0·582	0·726	0·859	2·62
$\tau_K \times 10^{23}$ (cm²/atom)	Au	12·5	8·8	7·2	1·90	1·39	0·86	0·61	0·104
	Th	21·1	14·8	12·2	3·21	2·38	1·49	1·06	0·184
h (counts/min.)	Au	1630	160	144	304	948	128	136	464
	Th	1200	112	176	304	1032	157	136	592
% loss in mica window	Au	3·6	2·2	1·5	0	—	—	—	—
	Th	5·0	3·0	2·2	0	—	—	—	—
γ-ray transmission	Au	0·50	0·57	0·61	0·78	0·82	0·83	0·85	0·925
	Th	0·35	0·43	0·49	0·73	0·76	0·81	0·83	0·913
Q	Au	31·4	26·4	24·6	17·0	16·2	15·0	14·5	14·6
	Th	35·6	28·7	26·1	17·2	16·0	14·8	14·3	14·3
I^γ (relative no. of quanta)	Au	0·85	0·075	—	0·19	0·66	0·11	0·14	1·00
	Th	0·94	0·068	0·10	0·17	0·64	0·11	0·11	1·00
Mean BI^γ		0·301	0·072	0·033	0·18	0·65	0·057	0·125	1·00

B corrects for the branching of the radioactive series at thorium C.

$$Q = \beta^{-3}\left(\ln\frac{Rm^2c^4\beta^4}{I^2Z^2(1-\beta^2)^{\frac{3}{2}}} + 1 - \beta^2\right).$$

The intensities I^γ in quanta per second relative to the 2·62 MEV. γ-ray have been calculated using a modification of the formula of Ellis and Aston (1930). Their relation for the height h_K of the line from the K shell may be put in the following form, derived elsewhere (Richardson 1950):

$$h_K = \frac{\text{constant} \times I^\gamma \tau_K H\rho\beta^3}{nZ\left(\ln\dfrac{Rm^2c^4\beta^4}{I^2Z^2(1-\beta^2)^{3/2}} + 1 - \beta^2\right)}, \qquad \ldots\ldots(1)$$

n is the number of atoms per cm³ in the target of atomic number Z and I is 13·5 electron volts. $H\rho e/c$ is the momentum of a photoelectron of velocity $v = \beta c$. $R = \Delta(H\rho)_0/H\rho$ where $\Delta(H\rho)_0$ is the distance in the spectrum between the peak of a line and its high energy limit.

As R is in the logarithm, its value is not critical. For our apparatus it was about 1/40 for all the lines, as can be seen from Figure 3, where the lines are plotted with the relative displacement in momentum as abscissa, and the fraction of peak height as ordinate. Identity in shape of the lines was shown by Ellis and Aston to imply that no large error will be produced by neglect of electron scattering in equation (1). The shapes can only be similar if scattering has reduced the heights of all the lines in the same ratio.

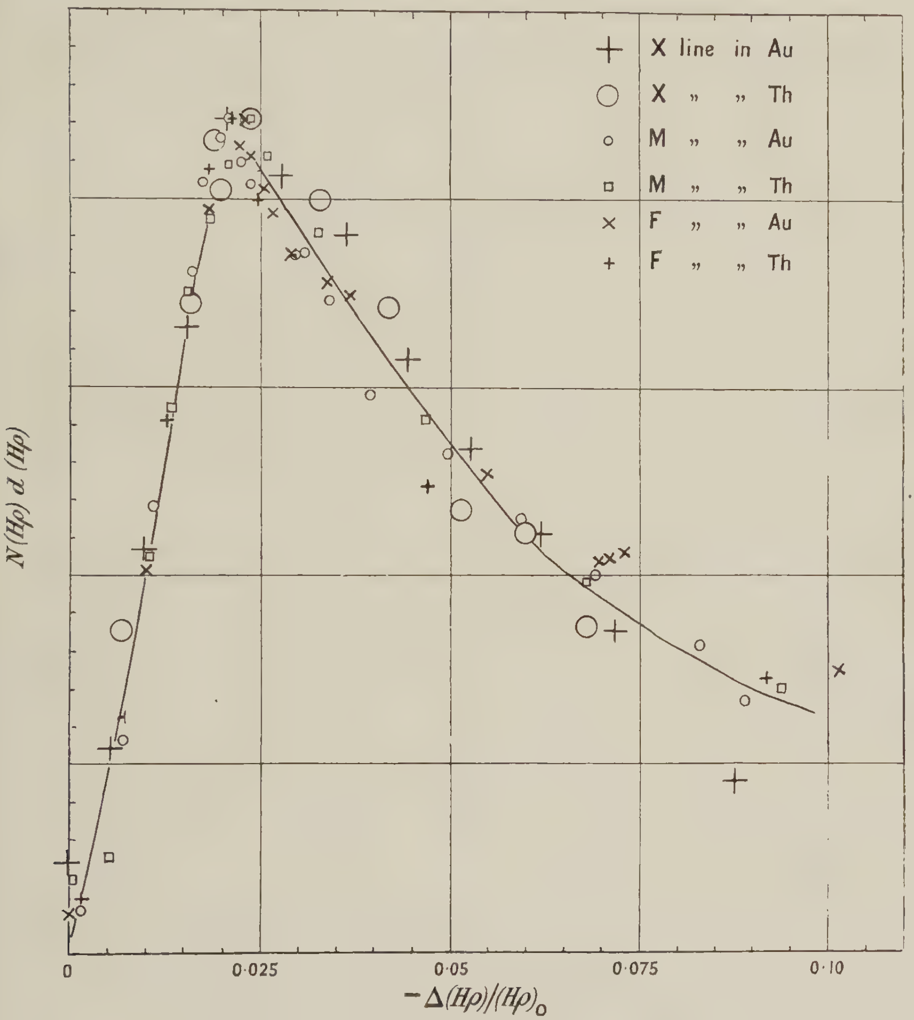

Figure 3. Comparison of the shapes of the strong photoelectron lines. $(H\rho)_0$ is the high energy limit of the line.

The table shows the correction for loss of β-rays in the mica window of the counter and also the fraction of the γ-rays transmitted to the target surface. This 'pre-absorption' is large for the soft γ-rays and is discussed in an appendix. It is subject to error owing to uncertainty in the density of the thorium oxide carrier. Tests with inactive samples of powdered oxide gave a most probable density of 2·7 gm/cm^3. An error here of 25% would give one of 10% in I^γ for the F γ-ray.

§4. LINES FROM THIN TARGETS

Deutsch, Elliot and Evans (1944) have pointed out that K photoelectrons from a very thin target should give lines in the momentum spectrum of area A given by

$$I^{\gamma}=cA/\tau_{K}, \qquad \ldots\ldots(2)$$

where c is a constant for the apparatus. Now τ_K as usually defined involves averaging the emission probability over all angles and (2) will only be true if any anisotropy in the photoelectron emission is evened out by the apparatus.

Table 2. Relative Intensities I^{γ} deduced by Equation (2) from the Lines from Thin Targets

Line	Target thickness (mg/cm^2)	γ-ray transmission	Uncorrected area of line	I^{γ} with M line as standard	I^{γ} with X line as standard
F	0·72	0·61	2050	0·49	—
F	3·7	0·61	7860	0·58	0·70
L	3·7	0·83	316	0·11	0·14
M	0·72	0·84	447	0·65	—
M	3·7	0·84	1400	0·65	0·78
M	7·4	0·84	2090	0·65	0·59
X	3·7	0·93	141	0·83	1·0
X	7·4	0·93	280	1·13	1·0

Values of cA/τ_K found with three thin gold targets are given in Table 2 with the constant c adjusted, first, to give the same I^{γ} for the strong M ray as the mean for thick targets in Table 1, and then, to give $I^{\gamma}=1{\cdot}0$ for the X γ-ray.

The values of I^{γ} for the F and L rays are markedly less than those found with thick targets. Except in the case of the 2·6 MeV. ray the area of the line does not increase in proportion to the target thickness, indicating an apparent absorption of photoelectrons coming from the deeper layers.

§5. COMPARISON WITH γ-RAY INTENSITIES DEDUCED FROM THE NATURAL β-SPECTRUM

The values of I^{γ} found for the 0·238 MeV. F γ-ray are less than that deducible from the known intensity of the β-transition to the 0·238 MeV. level of ThC, which has been estimated to be $0{\cdot}83 \pm 0{\cdot}03$ electrons per disintegration (Martin and Richardson 1948). Subtracting from this the experimental number of internal conversion electrons per disintegration, which is 0·39 according to Table 3, we are left with $0{\cdot}44 \pm 0{\cdot}03$ for the number BI^{γ} of γ-quanta escaping unconverted. This is 46% larger than the mean value 0·30 in Table 1 for thick targets and 2·2 times the mean value for thin targets in Table 2.

The larger discrepancy with thin targets suggests that a line of low energy suffers a greater reduction in area by scattering than does the comparison line of higher energy. The intensities from thick targets should be more reliable because the effect of scattering seems to be effectively corrected in equation (1).

Some of the 46% discrepancy with thick targets may be due to the variation with energy of θ, the most probable angle of ejection of the photoelectron from the atom. For a K photoelectron θ, measured from the direction of the incident quantum, is 90° for a soft γ-ray but, as Latyshev (1947) has shown, it falls to 9° for the 2·62 MeV. γ-ray in lead, because much forward momentum is transmitted to the electron.

The arrangement of source and target in Figure 5 may favour the detection of electrons emitted at small angles with the incident radiation. This would explain why the F line from the thinnest target of 0·7 mg/cm² is exceptionally weak because in such a target multiple scattering has little chance to even out the anisotropy.

In the absence of information on the energy variation of the discrepancy Table 3 gives (a) lower and (b) upper limits to the nuclear transition probabilities per disintegration p^γ where

$$p^\gamma = BI^\gamma + p_K{}^\beta + p_L{}^\beta + \dots \qquad \dots\dots(3)$$

The p^β are the numbers per disintegration of internal conversion electrons from the K, L etc. shells. The upper limit (b) assumes that all except the 2·62 MeV. γ-ray have true intensities BI^γ 46% higher than the mean value in Table 1, while the lower limit (a) applies no increase to BI^γ.

Table 3. Upper and Lower Limits (a) and (b) of the Experimental Internal Conversion Coefficients α_K compared with Theoretical Values for (c) Magnetic Dipole and (d) Electric Quadripole Radiation

γ-ray Nucleus		F ThC	G ^{208}Pb	H ThC	L ^{208}Pb	M ^{208}Pb	O ThC′	P ^{208}Pb	X ^{208}Pb
β-line strengths	$p_K{}^\beta$	31·3	2·64	1·17	1·84	1·34	0·106	0·262	0·178
	$p_L{}^\beta$	5·7	0·42	0·2	—	0·36	—	—	—
Transitions per disintegration p^γ	Σp^β	38·8	3·2	1·44	2·18	1·82	0·127	0·314	0·214
	(a)	69	10	4·7	20	67	5·9	13	100
	(b)	83	14	6·2	29	97	8·5	19	100
α_K, from experiment	(a)	45	26	24	9	2·0	1·8	2	0·18
	(b)	37·7	19	19	6·4	1·38	1·3	1·4	0·18
α_K, from theory	(c1)	32·5	24	21	7·1	—	—	—	—
	(d1)	12·5	8·5	7	2·2	2·1	1·36	0·92	0·15
	(c2)	44	34	32	10·2	7·5	5·4	3·1	0·20
	(d2)	10	7·2	6·2	2·0	1·58	1·13	0·77	0·10

Values expressed as percentages.

§ 6. THE INTERNAL CONVERSION COEFFICIENTS α_K

In Table 3 the experimental and theoretical coefficients are compared, using the definition $\alpha_K = p_K{}^\beta / p^\gamma$.

The values of p^β for the H, I + Ia, J + Ja, Jb and N lines are from Flammersfeld (1939) and for the rest from Martin and Richardson (1948). Feather, Kyles and Pringle (1948) have found $p^\beta = 28·8\%$ for the F line which gives $\alpha_K(a) = 43\%$ and $\alpha_K(b) = 34·7\%$.

The theoretical values in rows (c1) and (d1) are from the curves of Hulme, Mott, Oppenheimer and Taylor (1936), while (c2) and (d2) are from the comprehensive unpublished tables of Rose, Goertzel, Spinrad, Harr and Strong (1950).

We have assumed that the tables give the quantity $\alpha_K{}^0 = p_K{}^\beta / BI^\gamma$ and that $\alpha_K = \alpha_K{}^0 BI^\gamma / p^\gamma = \alpha_K{}^0 / (1 + 1{\cdot}24\alpha_K{}^0)$.

Both the experimental values (a) and (b) of α_K for the F γ-ray are larger than the 32·5% for pure magnetic dipole (M.D.) radiation given by the earlier theory. The discrepancy is of opposite sign according to the new theory in which the value of 44% in row (c2) is 17% higher than the experimental value (b) of 37·7%. The difference renders doubtful the hypothesis of Feather and Richardson (1948) that the ground level of ThC has zero spin quantum number I, because this makes the F γ-ray pure magnetic dipole, the only radiation allowed by the spin and parity selection rules for a $1 \rightarrow 0$ transition. However, the difference is probably within the limits of error.

Turning to the γ-rays of ^{208}Pb, the new theory indicates that the 2·62 MeV. (X) γ-ray is pure M.D. corresponding to $\Delta I = 1 \rightarrow 0$, rather than pure electric quadripole (E.Q.) as would be required by the alternative possibility that $\Delta I = 2 \rightarrow 0$*. Thus the first excited state should have $I = 1$.

This result makes it possible to eliminate two of the three alternative sets of values of I previously suggested for the levels of ^{208}Pb (Richardson 1948), all assumed to have the same parity. The remaining set of values is shown in Figure 4 which gives spin changes $\Delta I = 0, -1, -2, -2$ for the G, L, M and P γ-rays, respectively. According to the new theory the experimental values of α_K for the G and L rays are definitely lower than for pure M.D. radiation. This is consistent with the admixture of some E.Q. radiation which is to be expected for transitions between levels of high spin. The lower value of α_K for the strong 0·582 MeV. (M) ray is in satisfactory agreement with the value for E.Q. radiation appropriate to the larger spin change of two units, which forbids the emission of M.D. radiation. The experimental values of α_K for the 0·859 MeV. (P) γ-ray which also has $\Delta I = 3 \rightarrow 1$ are, however, not in good agreement with the value for E.Q. radiation, but suggest a mixed radiation corresponding to $\Delta I = \pm 1$ or 0. It is probable that the discrepancy is within the experimental error in measuring the weak internal and external conversion lines due to this γ-ray. Similarly the weak 0·726 MeV. (O) γ-ray of ThC′ has a multipole character which may be either pure E.Q. or mixed.

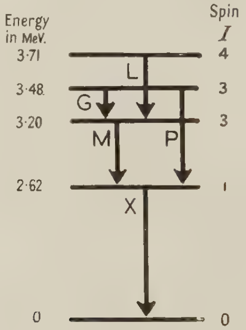

Figure 4.

---

* We are indebted to Dr. B. B. Kinsey for drawing our attention to this point and to the existence of the new calculation.

APPENDIX

THE CORRECTION FOR γ-RAY TRANSMISSION LOSS

In the general case of γ-ray absorption multiple Compton scattering must be considered, but in our problem it can be ignored because γ-quanta which have been scattered once will usually have lost enough energy to prevent their photoelectrons from contributing to the height h of the lines.

We have for the total linear absorption coefficient

$$\mu=\tau+\kappa+\sigma,$$

where τ represents the total photoelectric absorption assumed to be 5/4 times the absorption in the K shell, κ is the coefficient for pair production and σ is that for loss by scattering from a parallel beam of γ-rays, as given by the Klein–Nishina formula. κ and σ have been taken from the data of Sizoo and Coumou (1936) and Sizoo and Willemsen (1938).

We assume that photoelectrons ejected from any two points on the flat surface of the target have equal probability of entering the counter so that the number counted from an element of area $d\sigma$ of the surface is proportional to $I d\sigma$, where I is the intensity of radiation at the element. I is reduced by absorption in the thorium oxide, the copper tube and the target. $\int I\, d\sigma$ is evaluated over the surface, firstly for the actual case with absorption and secondly for the ideal case with no absorption. The ratio of the two integrals is the transmission term given in Tables 1 and 2.

To evaluate $\int I\, d\sigma$ the volume source is replaced by five parallel linear sources whose mid-points are shown at A, B, C, D, E in Figure 5 (c). The target surface is also broken up into seven equidistant lines parallel to the tube axis. Consider a source line n and a target line m a distance d_{nm} apart (Figure 5 (a)). Then I at Q due to an element dy_1 of the source line at P is proportional to

$$\{dy_1 \exp(-\Sigma\mu_i d_i \sec\theta)\}/d_{nm}^2 \sec^2\theta,$$

where $\Sigma\mu_i d_i \sec\theta$ is the sum of the absorption exponents for the media between P and Q. The rate N_{nm} of emission of photoelectrons from the mth target line due to the nth source line is

$$N_{nm}=\frac{\text{constant}}{d_{nm}}\int_0^{L_1} dy_n \int_0^{L_2} d\theta \exp(-\Sigma\mu_i d_i \sec\theta). \qquad \ldots\ldots(4)$$

Equation (4) has been integrated numerically for each value of nm for the 0·238 and 0·582 MeV. γ-rays.

In combining the N_{nm} the accuracy may be improved by using, where possible, a numerical integration formula instead of simple addition. Thus the seven N_{nm} for each source line n are combined by the Newton–Cotes formula, and Simpson's rule has been used for combining the three discrete sources at B, E and D to find the emission due to the area marked 1 in Figure 5 (c). The rule approximates to the true z-variation of the emission due to a source on the line BD by fitting a parabola through the three known points.

The x-variation of the emission is almost linear, the value of N_{Em} being near the mean of N_{Am} and N_{Cm}. Thus the combined areas 2 give an emission proportional to that of a line source at B′ whose emission can be read off from the fitted parabola. A similar substitution can be made for the areas 3. Weights proportional to the areas have been used in combining the zones 1, 2 and 3.

The transmission found in this way did not differ by more than 3% from the value given for a single line source through E, the origin of coordinates. For the remaining γ-rays therefore the transmission was interpolated by a more approximate method, equivalent to using a single line source through E.

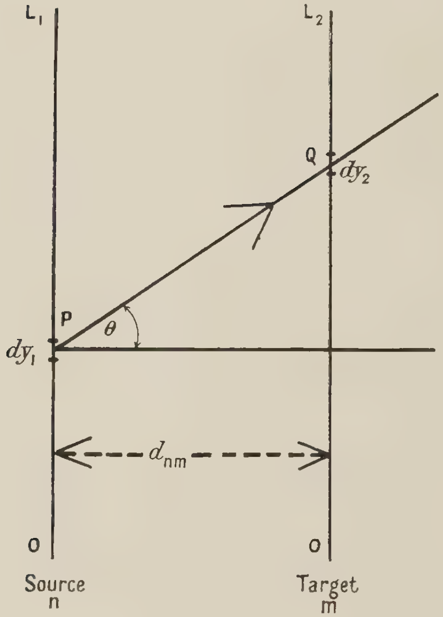

Figure 5 (*a*).

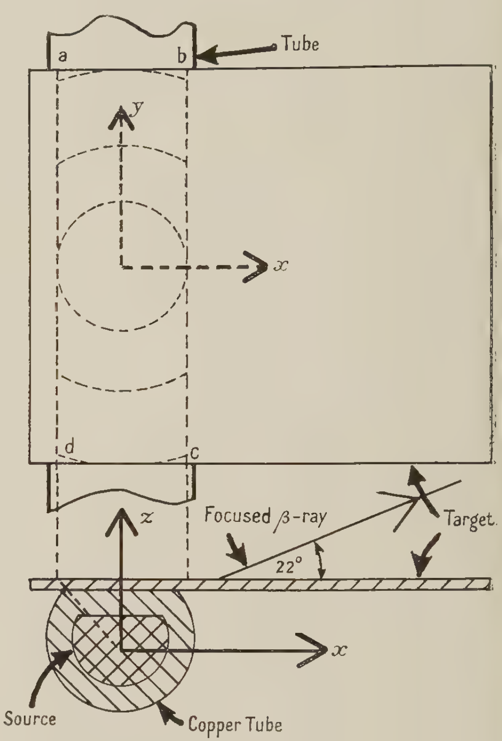

Figure 5 (*b*).

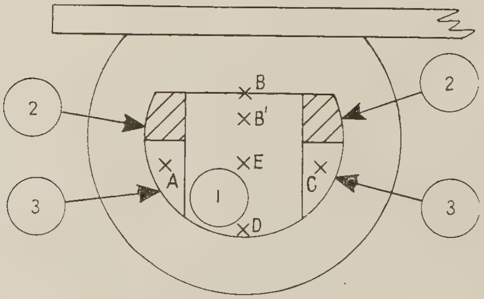

Figure 5 (*c*).

The source is first replaced by a single radiant point at E and we find the number N_1 of photoelectrons from the part abcd of the target in contact with the flattened part of the tube, where the absorber consists of parallel layers. Let ϕ be the angle between the ray from E and the z axis (the normal to the target surface). Then

$$N_1 = \text{constant} \times \int \{d\sigma \exp(\Sigma - \mu_i d_i \sec\phi)\}/z^2 \sec^2\phi \qquad \ldots\ldots(5)$$

and $d\sigma = 2\pi z^2 \tan\phi \sec^2\phi \, d\phi$. Denote the integral in (5) by I and put $\eta = \Sigma\mu_i d_i \sec\phi$.

Integrating over a disc between 0 and ϕ,

$$I=2\pi\int_{\Sigma\mu_i d_i}^{\eta} e^{-\eta}\,d\eta/\eta$$

$$=2\pi\{\mathrm{Ei}[-\Sigma\mu_i d_i]-\mathrm{Ei}[-\eta]\}, \qquad \ldots\ldots(6)$$

where $\mathrm{Ei}[-x]=\int_x^\infty e^{-x}\,dx/x$, the exponential integral.

In the case of no absorption, $I=2\pi\int\tan\phi\,d\phi=2\pi\ln\sec\phi$.

To find N over the rectangle abcd, I is found for discs of the three radii shown dotted in Figure 5 (b) and the three contributions to N_1 are weighted in proportion to the fraction of the complete disc or annulus lying inside abcd. To extend the calculation from a radiant point to a radiant line, N_1 is next found for a single point at one end of the line. To do this I is evaluated for a fourth disc of radius equal to the length of the source and the contributions of the four zones are reweighted and added. The values of N_1 for sources at the centre and ends of the line are then integrated by Simpson's rule to represent the line source.

The number N_2 of photoelectrons from the parts of the target not in contact with the copper tube was found by numerical integration of

$$N_2=\text{constant}\times\iint\frac{dx\,dy}{x^2+y^2+z^2}\exp-\left(\frac{a}{z}+\frac{b}{(x^2+z^2)^{\frac{1}{2}}}\right)(x^2+y^2+z^2)^{\frac{1}{2}}, \qquad \ldots\ldots(7)$$

where $a=\Sigma\mu_i d_i$ for the target and $b=\Sigma\mu_i d_i$ for the source and tube. The result for a radiant point at the origin was extended to a line in the way used for N_1.

ACKNOWLEDGMENTS

The authors wish to express their thanks to Mr. I. A. D. Lewis and other colleagues at the George Holt Physics Laboratory, Liverpool, for their help, and also to the Ministry of Supply for the source of radiothorium.

REFERENCES

Deutsch, M., Elliott, M. G., and Evans, R. D., 1944, *Rev. Sci. Instrum.*, **15,** 178.

Ellis, C. D., 1932, *Proc. Roy. Soc.* A, **138,** 318.

Ellis, C. D., and Aston, G. H., 1930, *Proc. Roy. Soc.* A, **129,** 180.

Feather, N., Kyles, J., and Pringle, R. W., 1948, *Proc. Phys. Soc.*, **61,** 466.

Feather, N., and Richardson, H. O. W., 1948, *Proc. Phys. Soc.*, **61,** 452.

Flammersfeld, A., 1939, *Z. Phys.*, **114,** 227.

Gray, L. H., 1930, *Proc. Camb. Phil. Soc.*, **27,** 103.

Hulme, H. R., McDougall, J., Buckingham, R. A., and Fowler, R. H., 1935, *Proc. Roy. Soc.* A, **149,** 131.

Hulme, H. R., Mott, N. F., Oppenheimer, F., and Taylor, H. M., 1936, *Proc. Roy. Soc.* A, **155,** 315.

Itoh, J., and Watase, Y., 1941, *Proc. Phys. Math. Soc., Japan*, **23,** 142.

Johansson, A., 1947, *Ark. Mat. Astr. Fys.*, **34A,** No. 9.

Latyshev, G. D., 1947, *Rev. Mod. Phys.*, **19,** 132.

Martin, D. G. E., Richardson, H. O. W., and Hsü, Y. K., 1948, *Proc. Phys. Soc.*, **60,** 466.

Martin, D. G. E., and Richardson, H. O. W., 1948, *Proc. Roy. Soc.* A, **195,** 287.

Richardson, H. O. W., 1948, *Nature, Lond.*, **161,** 516; 1950, *Proc. Phys. Soc.* A, **63,** 234.

Rose, M. E., Goertzel, G., Spinrad, B., Harr, J., and Strong, P., 1950, *U.S. Atomic Energy Commission*, Report AEC U-550.

Sizoo, G. J., and Coumou, D. J., 1936, *Physica*, **3,** 921.

Sizoo, G. J., and Willemsen, H., 1938, *Physica*, **5,** 100.

Thibaud, J., 1926, *Ann. Phys., Paris*, **5,** 73.

Ellis and Aston's Theory of the Height of a Photoelectron Line

By H. O. W. RICHARDSON
Department of Natural Philosophy, University of Edinburgh

Communicated by N. Feather; MS. received 3rd October 1949

ABSTRACT. The formula of Ellis and Aston relating the intensity of a γ-ray to the height of its photoelectron line produced from a thick target is revised using the quantum-mechanical theory of stopping power. The effects of multiple scattering, bremsstrahlung and anisotropic emission of the photoelectrons are discussed and a general comparison of thick and thin target methods is made.

§1. INTRODUCTION

Ellis and Aston in 1930 in a paper to be referred to as I, described a quantitative method for estimating the intensities in a γ-ray spectrum by using the photoelectrons ejected from a thick target. They gave the following relation between the γ-ray intensity I^γ and the height h_{K} of the photoelectron line recorded in a magnetic spectrometer:

$$h_{\mathrm{K}} = I^\gamma \tau_{\mathrm{K}} H\rho \beta^3 f(\beta) \times \text{constant}. \qquad \ldots\ldots(1)$$

Here h_{K} is the number of K photoelectrons recorded per second at the peak of the line, and I^γ the number of quanta emitted per second. τ_{K} is the photoelectric absorption coefficient for absorption in the K shell of the target atom. $\beta = v/\mathbf{c}$, where v is the speed of the electron of momentum $p = H\rho\mathbf{e}/\mathbf{c}$. $f(\beta)$ is a slowly varying function of β taken from the classical theory of stopping-power of Bohr (1915).

$f(\beta)$ can now be given a quantum-mechanical form and it is of interest to see if the additional stopping-power due to radiation losses may be neglected. The error due to electron scattering can also be estimated; it is clearly small if the resolving power of the apparatus is sufficiently high, because then the peak of the line is formed by photoelectrons coming only from a thin layer at the surface of the target. Should the target be too thin to build up the peak to its maximum height, equation (1) does not apply and we have the alternative 'thin target' method. In both methods serious error may be caused by the variation with quantum energy of the anisotropy of photoelectric emission.

Equation (1) may be of use in interpreting experiments on the natural β-ray lines from sources of low specific activity. The height of a conversion line is given by (1) if $I^\gamma \tau_{\mathrm{K}}$ is replaced by P_β, the intensity of the line in electrons per disintegration. For this application the source must be thicker than Δx, the 'contributing depth', given by equation (5) below.

§2. THE QUANTUM-MECHANICAL FORM OF EQUATION (1)

$f(\beta)$ is related to the rate of loss of momentum of a photoelectron by collisions with the electrons in the target by

$$-d(H\rho)/dx = \text{constant}/\beta^3 f(\beta), \qquad \ldots\ldots(1a)$$

where x is measured along the path. An approximate relativistic expression for the collision loss in ergs/cm. is (Heitler 1936, p. 219)

$$-dE/dx = \tfrac{3}{4} nZ\phi_0 \frac{\mathbf{m}\mathbf{c}^2}{\beta^2}\left[\ln \frac{WE^2v^2}{I^2Z^2\mathbf{m}\mathbf{c}^4} + 1 - \beta^2\right]. \qquad \ldots\ldots(2)$$

Here n is the number of target atoms of atomic number Z per cm^3 and I is 13·5 electron volts, so that IZ is an average ionization energy for the atom.

$$\phi_0 = (8\pi/3)(\boldsymbol{e}^2/\boldsymbol{mc}^2)^2 = 6{\cdot}57 \times 10^{-25}\,\mathrm{cm}^2$$

is the Thomson cross section and $E(=\epsilon \boldsymbol{mc}^2)$ is the photoelectron energy including the rest energy $\boldsymbol{mc}^2$.

W is the largest single collision loss which contributes to dE/dx in (2); for our purpose it is chosen so that a larger loss could not affect the observed retardation of the peak of an initially mono-energetic group of electrons because it would remove the electron from the neighbourhood of the peak. Thus a collision is excluded if it causes a fractional loss of momentum exceeding $R = \Delta(H\rho)_0/H\rho$, where $\Delta(H\rho)_0$ is the interval in the photoelectron spectrum between the peak of a line and its high energy limit. A larger loss does not concern us because it is certain to bring the photoelectron to the low energy side of the line.

From the relations $p = \eta \boldsymbol{mc} = \boldsymbol{m}v/(1-\beta^2)^{\frac{1}{2}}$ and $dp/dE = 1/v$, we get $\mathrm{W} = vRp$ and

$$-\frac{d(H\rho)}{dx} = \tfrac{3}{4} nZ\phi_0 \frac{\boldsymbol{mc}^2}{\boldsymbol{e}\beta^3}\left[\ln \frac{R\boldsymbol{m}^2\boldsymbol{c}^4\beta^4}{I^2Z^2(1-\beta^2)^{3/2}} + 1 - \beta^2\right]. \quad \ldots\ldots(3)$$

Writing $F(R, \beta, Z)$ for the expression in the square brackets and making use of (1a), we find that equation (1) becomes

$$h_{\mathrm{K}} = \frac{I^{\gamma}\tau_{\mathrm{K}} H\rho\, \beta^3 \times \text{constant}}{nZF(R,\, \beta,\, Z)}. \quad \ldots\ldots(4)$$

The fraction R is a measure of the resolution of the apparatus and, in an instrument of constant ρ, is nearly the same for all the lines. It equals $\Delta(H\rho)/H\rho$ if scattering is absent, where $\Delta(H\rho)$ is the width of the base of the narrow line formed by unretarded photoelectrons from the outer surface of the target. $\Delta(H\rho)/H\rho$ is fixed by the finite width of the target and slits. Its constant value may in practice exceed $R(=\Delta(H\rho)_0/H\rho)$ because the actual broad line may be sharpened by scattering which reduces the more retarded contributions coming from greater depths in the target.

§ 3. THE DEPTH Δx OF THE CONTRIBUTING SURFACE LAYER

If scattering is small the path x in the target will equal the depth of origin below the surface measured in the direction of the beam focused by the spectrometer. Only electrons starting in a thin layer at the surface can contribute to the height of the peak because the others will be retarded by more than $\Delta(H\rho)_0$. The maximum contributing depth Δx is

$$\Delta x = -\Delta(H\rho)_0 \Big/ \frac{d(H\rho)}{dx} = \frac{4}{3}\frac{R\eta\beta^3}{nZ\phi_0 F}, \quad \ldots\ldots(5)$$

where $\eta = H\rho/1704{\cdot}2$ and $3nZ\phi_0/4 = 2{\cdot}32\,\mathrm{cm}^{-1}$ for gold.

$23{\cdot}2\Delta x/\eta R$ is plotted against $\log\epsilon$ $(=\log E/\boldsymbol{mc}^2)$ in Figure 1 for a gold target. If the target is thicker than Δx the height of the line will not be increased but its low energy side will be broadened, thus obscuring the resolution of close lines. If possible therefore the target thickness should equal Δx for the hardest γ-ray studied in the experiment and any underlying mounting of the target should have small Z in order to add only Compton electrons to the spectrum.

§4. THE EFFECT OF SCATTERING

It was remarked in I that if there were no scattering there should be little apparent absorption of photoelectrons coming from the deeper layers in the target. The theory of retardation and straggling would then predict a line shape in the momentum spectrum having a steep rise from the high energy limit up to a long plateau extending to low energies. In contrast, the observed lines are well defined and their steep fall on the low energy side must be mainly due to scattering, which would seem to operate so as to give them all nearly the same shape. This is clear from Figure 3 of the preceding paper (Martin and Richardson 1950), to be referred to as II, where several lines have been plotted with the relative displacement in momentum as abscissa. If the shapes are identical it follows that the heights must all be reduced in the same ratio by scattering and the relative intensities will be given correctly by equation (4).

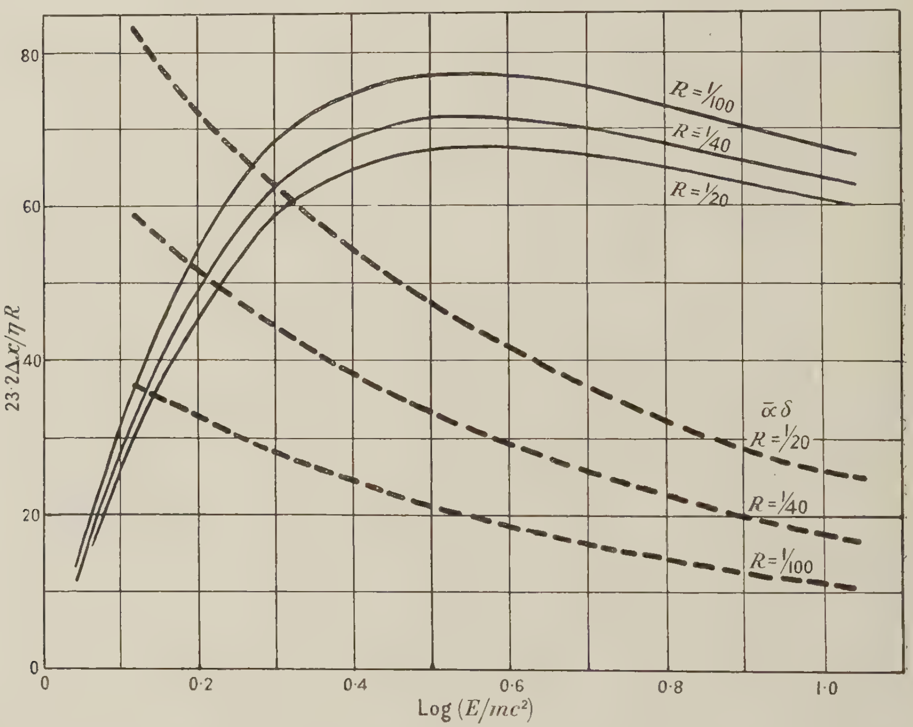

Figure 1. Energy dependence of $23{\cdot}2\ \Delta x/\eta R$ (continuous curves) and of $\bar{\alpha}\delta$ (broken curves). $\bar{\alpha}\delta$ is the mean projected deflection in degrees, in gold ($Z=79$). The thicknesses Δx of the scattering layer are such as to give mean retardations $R=\delta(H\rho)/H\rho$ of 1/20, 1/40 and 1/100.

It is of interest to see if the similarity in shape can be due to compensation of the greater scattering per centimetre of slow β-rays by their smaller contributing depths Δx.

A convenient treatment of multiple scattering is that of Williams (1940) in which the angles are measured in a unit δ given by

$$\delta = 2Z' r_0 (nt)^{\frac{1}{2}} / \beta^2 \epsilon \text{ radians}, \qquad \ldots\ldots(6)$$

where $r_0 = \mathbf{e}^2/\boldsymbol{mc}^2$, t is the thickness of the scatterer and $Z' = (Z^2 + Z)^{\frac{1}{2}}$.

The deflections are given projected on a fixed plane containing the initial direction. The mean projected deflection $\bar{\alpha}$ (in units δ) is

$$\bar{\alpha} = 0{\cdot}80(\ln M)^{\frac{1}{2}} + 1{\cdot}45, \qquad \ldots\ldots(7)$$

where $M = 0{\cdot}64\pi n t (Z')^{4/3}(\hbar/\boldsymbol{mc})^2\beta^{-2}$, the mean number of collisions. The probability of a projected deflection α is

$$G(\alpha) = (1 - \pi/2\phi_2^{\,2})(2/\pi\alpha_{\mathrm{m}})\exp(-\alpha^2/\pi\alpha_{\mathrm{m}}^{\,2}), \qquad \ldots\ldots(8)$$

where $\phi_2 = 5{\cdot}1(\ln M)^{\frac{1}{2}} - 4{\cdot}0$ and $\alpha_{\mathrm{m}} = (\bar{\alpha} - \pi/\phi_2)/(1 - \pi/2\phi_2^{\,2})$.

The formulae are only accurate for deflections less than 10° for which $\sin\alpha\delta \simeq \alpha\delta$, but they give a rough guidance at larger angles.

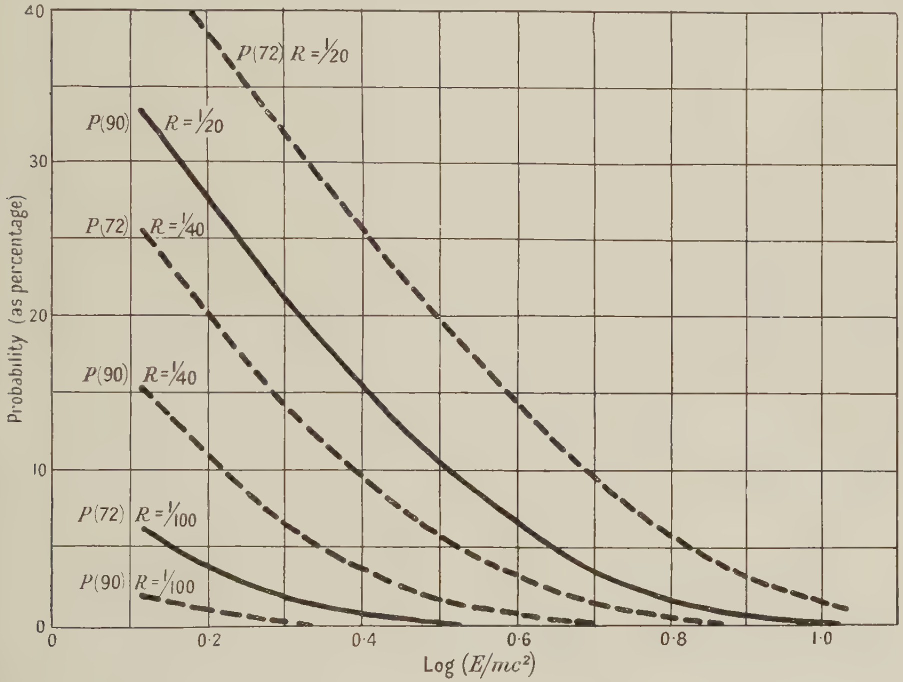

Figure 2. Energy dependence of the probability P of scattering through more than 90° ($P(90)$), and more than 72° ($P(72)$), in a path x giving retardations R of 1/20, 1/40 or 1/100.

Putting $t = \Delta x$, from (5), in (6), it will be seen that there is some compensation of the energy variation. We have

$$\delta^2 = 2R(Z+1)/\pi\epsilon F. \qquad \ldots\ldots(9)$$

Thus δ varies quite slowly, nearly as $\epsilon^{-\frac{1}{2}}$.

For the ideal case of zero straggling we may trace a narrow outgoing pencil of focused rays backward into the target. Then those rays having the same retardation $\delta(H\rho)$ will all have the same path-length x and, owing to scattering, their points of origin will lie in a cup-shaped volume having cylindrical symmetry about the pencil. Owing to the reversibility of elastic scattering, conditions inside the target will be the same as for a pencil of incoming rays each scattered in a total path-length x. The cup-shaped volume will extend rapidly with x and eventually part of it will protrude forward through the target surface. This part, having no sources of photoelectrons in the actual experiment, will be non-contributing. The fraction of rays excluded in this way will obviously depend on the inclination of the focused pencil to the target surface, but it is clear that some line sharpening will always occur and that it will be more pronounced when the focused pencil leaves the target nearly at grazing angles.

There may be other less direct ways in which scattering reduces the low energy side of a line, but it seems likely that they will cause little variation with energy and that rays scattered out of the beam will often be replaced by rays scattered in. In view of the possible presence of such further factors, the probability $P(90)$ of a projected deflection greater than 90° may underestimate the loss by scattering even for normally emergent pencils and so $P(72)$ has also been plotted in Figure 2 where

$$P(72)=\int_{72^\circ/\delta}^{\infty} G(\alpha)\,d\alpha.$$

The values are given for three path-lengths x causing three retardations $\delta(H\rho)/H\rho$ of 1/20, 1/40 and 1/100 in gold ($Z=79$).

In so far as extrapolation of (8) to such large angles is valid, the curves suggest that in an apparatus with the high resolution of 1/100 the scattering loss is negligible, but for the low resolution of 1/20 it is quite large. Even for this resolution it varies fairly slowly with energy so the heights of close lines will have the correct ratio. At 0·15 Mev. a retardation of 1/40 in gold may cause a scattering loss of 25%, whereas at 2·5 Mev. the loss is negligible. The decrease in line heights at 0·15 Mev. with a resolution $\Delta(H\rho)_0/H\rho$ of 1/40 will, however, be less than 25% because the mean path x of the contributing photoelectrons is about $\Delta x/2$, giving an average retardation of only 1/80.

A variation of 20% in scattering loss should cause a small change with energy in the shape of the photoelectron lines near their peaks. Close study of Figure 3 of II shows that the lines of the 2·6 Mev. γ-ray are perhaps 0·7% of $H\rho$ broader than the others in the region just below the peak. (The 0·47 Mev. M line in thorium also shows a small broadening which can be given another explanation, namely the presence of the unresolved weak line of 20 kv. more energy ejected by the 0·51 Mev. γ-ray from the L shell.)

The error due to neglect of the small difference in the sharpening of the peaks by scattering could be avoided by comparing the slopes of the lines on their high energy sides, instead of the heights. The electrons here come from such small depths that $\bar{\alpha}\delta$ will be less than about 20°. In the experiments of II no significant difference could be found between the ratios of the slopes and the heights.

§ 5. LARGE COLLISION LOSSES

Collision losses greater than the critical value W, which occur in the contributing layer Δx, will remove photoelectrons which would otherwise contribute to the height h.

The probability in Δx of a loss greater than W is given by the classical Thomson formula (Jánossy 1948, p. 100, Bohr 1948).

$$P(W)\Delta x=\tfrac{3}{4}nZ\phi_0\frac{mc^2}{\beta^2}\left(\frac{1}{W}-\frac{1}{W_{\max}}\right)\Delta x. \qquad \ldots\ldots(10)$$

In our case the reciprocal of $W_{\max}$, the maximum possible loss, can be neglected.

Then since $\Delta x = -W(dE/dx)$, we have from (2) and (3)

$$P(W)\Delta x = 1/F. \qquad \ldots\ldots(11)$$

For $R=1/40$ and $Z=79$, $P(W)\Delta x$ varies from $1/8{\cdot}4$ to $1/13{\cdot}7$ in the range $\boldsymbol{h}\nu = 0{\cdot}24$ MeV. to $\boldsymbol{h}\nu = 2{\cdot}6$ MeV. Thus the fraction of photoelectrons originating in the contributing layer but removed in large collisions is about 8% and is too independent of energy to cause error.

§ 6. BREMSSTRAHLUNG LOSSES

At high energies, radiation losses make an appreciable contribution to the stopping-power of media of large atomic number. These losses must reduce h, first, by increasing the number of single losses smaller than W which cause the mean retardation of the peak, and second, for losses greater than W, by removing electrons which would otherwise contribute to its height. The stopping-power of the losses less than W is

$$-\left(\frac{dE}{dx}\right)_{\mathrm{rad}}^{<W} = n\int_0^{W/(E-\boldsymbol{mc}^2)} k\phi_k\, d\{k/(E-\boldsymbol{mc}^2)\}, \qquad \ldots\ldots(12)$$

where $k=\boldsymbol{h}\nu$ and $\phi_k\, d\{k/(E-\boldsymbol{mc}^2)\}$ is the cross section of a target atom for a radiation loss between k and $k+dk$.

The dependence of ϕ_k on E and k has been given by Heitler (1936, fig. 14, p. 170). For $k<W\ll E$, the small losses are numerous and are due to collisions of large impact parameter for which the screening of the nucleus by the atomic electrons is nearly complete. For this case the quantity $k\phi_k/E\bar{\phi}$ is independent of both the energies E and k. We have

$$\bar{\phi} = \frac{1}{137}\left(\frac{Z\boldsymbol{e}^2}{\boldsymbol{mc}^2}\right)^2 = Z^2 \times 5{\cdot}71\times 10^{-28}\,\mathrm{cm}^2$$

and

$$k\phi_k/E\bar{\phi} = (4/3)(4\ln 183 Z^{-1/3} + 1/3) = 15{\cdot}8 \text{ for } Z=79.$$

Integrating (12)

$$-\left(\frac{dE}{dx}\right)_{\mathrm{rad}}^{<W} = 15{\cdot}8 n\bar{\phi}EW/(E-\boldsymbol{mc}^2) = A(\epsilon+1), \qquad \ldots\ldots(13)$$

where $A = 15{\cdot}8 n\bar{\phi}R\boldsymbol{mc}^2$.

For $\epsilon \gg 1$ the stopping power is effectively $A\epsilon$ and for $\epsilon=1$ it is $2A$. For $\epsilon=6$ and $R=1/40$ the contribution of (13) is about 2% of that due to inelastic electronic collisions given by (2) so that the effect can be ignored except at very high energies.

The second effect, due to large losses, is given by the probability $P(W)_{\mathrm{rad}}\,\Delta x$ of a radiation loss greater than W occurring in the contributing layer Δx. We have (Heitler 1936, p. 171)

$$P(W)_{\mathrm{rad}}\,\Delta x = n\Delta x \int_{W/(E-\boldsymbol{mc}^2)}^{1} \phi_k\, d\{k/(E-\boldsymbol{mc}^2)\}.$$

An approximation for ϕ_k is $k^{-1}E\bar{\phi}\exp\{-2{\cdot}2k/(E-\boldsymbol{mc}^2)\}$ which gives

$$P(W)_{\mathrm{rad}}\,\Delta x = \frac{n\bar{\phi}\Delta x E}{E-\boldsymbol{mc}^2}\int_{2\cdot 2W/(E-\boldsymbol{mc}^2)}^{2\cdot 2} e^{-z}\,dz/z, \qquad \ldots\ldots(14)$$

where $z = 2{\cdot}2k/(E-\boldsymbol{mc}^2)$.

For $E=6\boldsymbol{mc}^2$ and $R=1/40$ the probability (14) is about 2×10^{-3} so that the reduction in height is negligible.

§7. THE THIN TARGET METHOD AND THE EFFECT OF PHOTOELECTRIC ANISOTROPY

Deutsch, Elliott and Evans (1944) have described a method in which the target is thinner than Δx so that h_K does not reach its maximum value and is not given by equation (4).

In this method the intensities of two γ-rays may be compared by finding the areas of their lines in the momentum spectrum. However there is now no compensation to reduce the energy variation of scattering and the line of lower energy will lose more of its area than the comparison line unless $\bar{\alpha}\delta$ is kept small. In practice $(\ln M)^{\frac{1}{2}}$ is fairly constant so that it suffices to choose a target thickness t, giving δ less than about 0·25 radians. For example, for the F-line of ThB in gold, if $t = 1{\cdot}33 \times 10^{-4}$ cm. (2·6 mg/cm^2), we have from (6) that $\delta = 0{\cdot}228$, giving $P(90) = 2\%$ and $P(72) = 6\%$.

For this thickness the scattering is negligible, however poor the resolution, but lines due to hard γ-rays will be of very small intensity because of the decrease of the absorption τ_K with increasing energy.

In contrast, the thick target method gives a valuable intensification of the high energy lines due to the growth of the contributing depth Δx and, if R is kept small by using a high resolving power and a small target, the scattering error is again negligible.

In both methods the anisotropy in the photoelectric emission will not be smoothed out under conditions of small scattering.

It therefore seems desirable to use a collimated beam of γ-rays and to replace τ_K by the differential photoelectric cross section integrated over the solid angle focused by the spectrometer, as has been done by Latyshev, Companeetz, Borisov and Gusak (1940) in the case of Compton electrons. Where collimation is not possible the calculation should still use the integral taken over a limited solid angle because in practice the γ-ray flux is not isotropic.

When a thin magnetic lens is used the predominant flux is in the direction of the focused electron beam so that small angles of emission θ will be collected preferentially. This intensifies hard γ-rays relatively to soft ones, for which the probable value of θ is 90°. In the case of the 180° spectrometers of I and II the γ-flux has a larger component across the beam, but even here there is little or no contributing flux in the backward direction so that hard γ-rays giving forward momentum to the electron are still favoured. Thus in all practical cases the errors due to anisotropy and scattering both over-emphasize the hard γ-rays.

REFERENCES

Bohr, N., 1915, *Phil. Mag.*, **30,** 178; 1948, *D. Kgl. Danske Vid. Sel. Math. fys. Medd.*, XVIII, **8,** 1–144.

Deutsch, M., Elliott, M. G., and Evans, R. D., 1944, *Rev. Sci. Instrum.*, **15,** 178.

Ellis, C. D., and Aston, G. H., 1930, *Proc. Roy. Soc.* A, **129,** 180.

Heitler, W., 1936, *Quantum Theory of Radiation*, 1st edition (Oxford : University Press).

Jánossy, L., 1948, *Cosmic Rays* (Oxford : University Press).

Latyschev, G. D., Companeetz, A. F., Borisov, N. P., and Gusak, I. M., 1940, *J. Phys. U.S.S.R.*, **3,** 251.

Martin, D. G. E., and Richardson, H. O. W., 1950, *Proc. Phys. Soc.* A, **63,** 223.

Williams, E. J., 1940, *Phys. Rev.*, **58,** 292.

Note on the Fluctuation Problem of Cascades

By L. JÁNOSSY
Dublin Institute for Advanced Studies

MS. received 7th November 1949

ABSTRACT. Diffusion equations governing the fluctuations of nucleon cascades and also of electron–photon cascades are given. The electron cascade is treated at first in the usual approximation, but it is shown that the approximations are not essential for the treatment. The diffusion equations appear in the form of integro-differential equations which can be solved directly using numerical integration. It is hoped to present numerical solutions in a later publication.

§ 1. INTRODUCTION

In two previous publications (Heitler and Jánossy 1949) we have considered collisions of nucleons. A primary nucleon is considered to suffer a number of collisions; in each collision a recoil nucleon is supposed to be emitted and the primary loses some energy. The number of particles thus increases by one in every collision and a cascade develops. In the present paper we consider the mathematical problem of the fluctuations of such a cascade.

It will be seen that the problem of the fluctuation of the nucleon cascade is mathematically very similar to that of the fluctuation of an electron–photon cascade. We present a formalism for both types of cascades in the present paper and hope to give numerical results in a future publication. The theory of such stochastic processes has been outlined, for example, by Arley (1949).

In §§ 2 and 3 we deal with generating functions of the actual distribution, in § 4 we discuss the determination of the distributions from generating functions, and in § 5 we show how certain restrictions in the assumptions can be eliminated.

§ 2. NUCLEON CASCADE

We assume, as in the previous publications, that the cross section for nuclear collision is a homogeneous function of primary and secondary energies. Thus we assume

$$w(E_0;\ E', E'')\,dE'\,dE''\,dx = w\left(\frac{E'}{E_0},\ \frac{E''}{E_0}\right)\frac{dE'\,dE''}{E_0^{\,2}}\,dx \quad \ldots\ldots (1)$$

is the probability that a primary of energy E_0 suffers a collision along dx so that the resulting particles are in the intervals $E', E'+dE'$ and $E'', E''+dE''$. We assume

$$w(\epsilon',\epsilon'')=0, \qquad \epsilon'+\epsilon''>1, \quad \ldots\ldots (2a)$$

$$w(\epsilon',\epsilon'')=0, \qquad \epsilon'<\epsilon'', \quad \ldots\ldots (2b)$$

and thus the total collision probability per unit path is

$$\int_0^1\int_0^1 w(\epsilon',\epsilon'')\,d\epsilon'\,d\epsilon''=\alpha. \quad \ldots\ldots (3)$$

The cascade shall be described by a function

$$\phi(\epsilon, n_1, n_2, x).$$

This function gives the probability that after a depth x a primary of energy E_0 has given rise to n_1 particles energy above ϵE_0, and n_2 particles energy below ϵE_0; for brevity we describe the n_1 particles as 'fast' and the n_2 particles as 'slow'.

To obtain a diffusion equation for ϕ we consider the first collision the primary particle suffers. The probability that the primary travels a distance $x-\xi$ without collision is $\exp\{-\alpha(x-\xi)\}$. The probability that along the next interval $d\xi$ there should be a collision dividing the energy into amounts inside intervals $d\epsilon'$ and $d\epsilon''$ is $d\xi\, w(\epsilon', \epsilon'')\, d\epsilon'\, d\epsilon''$. In order to end up with a cascade of n_1 fast particles and n_2 slow particles, the particles of energies ϵ' and ϵ'' have to develop into cascades giving rise to n_1' and n_1'' fast particles and n_2' and n_2'' slow particles with

$$n_1' + n_1'' = n_1 \quad \text{and} \quad n_2' + n_2'' = n_2.$$

Summing over all possible depths of $d\xi$ and all possible divisions of the cascade we obtain

$$\phi(\epsilon, n_1, n_2, x) = \int_0^x \exp\{-\alpha(x-\xi)\}\,.\,d\xi \sum_{\substack{n_1'+n_1''=n_1\\ n_2'+n_2''=n_2}} \int_0^\infty\int_0^\infty \phi\left(\frac{\epsilon}{\epsilon'}, n_1', n_2', \xi\right) \times \phi\left(\frac{\epsilon}{\epsilon''}, n_1'', n_2'', \xi\right) w(\epsilon', \epsilon'')\, d\epsilon'\, d\epsilon''. \quad \ldots\ldots (4)$$

We introduce a generating function

$$G(\epsilon, x, U) = \sum_N \phi(\epsilon, N, x) U^N \quad \ldots\ldots (5)$$

in which we have written, for the sake of compactness, U for u_1, u_2; N for n_1, n_2; U^N for $u_1^{n_1} u_2^{n_2}$.

From (4) and (5) we find

$$G(\epsilon, x, U) = \int_0^x \exp\{-\alpha(x-\xi)\} \int_0^\infty \int_0^\infty G\left(\frac{\epsilon}{\epsilon'}, \xi, U\right) G\left(\frac{\epsilon}{\epsilon''}, \xi, U\right) w(\epsilon', \epsilon'')\, d\epsilon'\, d\epsilon''. \quad \ldots\ldots (6)$$

If we multiply (6) by $e^{\alpha x}$, differentiate with respect to x, and multiply by $e^{-\alpha x}$, we find

$$G_x(\epsilon, x, U) + \alpha G(\epsilon, x, U) = \int_0^\infty \int_0^\infty G\left(\frac{\epsilon}{\epsilon'}, x, U\right) G\left(\frac{\epsilon}{\epsilon''}, x, U\right) w(\epsilon', \epsilon'')\, d\epsilon'\, d\epsilon'', \quad \ldots\ldots (7)$$

where $G_x = \partial G/\partial x$.

Equation (7) is an integro-differential equation which can be solved by numerical integration, provided an initial condition is imposed. The initial condition is obtained from the assumption that at $x=0$ there is one particle of energy E_0, i.e. with $\epsilon=1$, and no other particle. Thus

$$\phi(\epsilon, n_1, n_2, 0) = \begin{cases} \delta(1-n_1)\delta(n_2) & \text{for } \epsilon < 1, \\ \delta(n_1)\delta(1-n_2) & \text{for } \epsilon > 1, \end{cases}$$

and, therefore,

$$G(\epsilon, u_1, u_2, 0) = \begin{cases} u_1 & \text{for } \epsilon < 1, \\ u_2 & \text{for } \epsilon > 1. \end{cases} \quad \ldots\ldots (8)$$

The solution of the system (7) and (8) can be found by the well-known methods of numerical integration. The procedure is quite straightforward, except that for fixed values of the u_1 and u_2 one must compute for all values of ϵ ranging from

0 to ∞ simultaneously. This procedure is greatly simplified by the fact that for $\epsilon>1$ $G(\epsilon, U, x)$ can be obtained explicitly. We note that there are no particles with $\epsilon>1$ and we can therefore write $G(\epsilon, x, U)=g(x, U)$ for $\epsilon>1$. Introducing this into (7) we find

$$g_x(x, U)+\alpha g(x, U)=\alpha g^2(x, U) \qquad \text{for } \epsilon>1;$$

thus

$$\frac{1}{g(x, U)}-\frac{1}{\alpha}\frac{\partial}{\partial x}\left(\frac{1}{g(x, U)}\right)=1$$

and

$$g(x, U)=\frac{1}{Ae^{\alpha x}+1}. \qquad \ldots\ldots(9)$$

From (8) and (9) we have $1/(A+1)=u_2$ and

$$G(\epsilon>1, x, U)=g(x, U)=\frac{e^{-\alpha x}}{1-u_2(1-e^{-\alpha x})}. \qquad \ldots\ldots(10)$$

Equation (10) gives thus the values of G for $\epsilon>1$ and only the values $\epsilon<1$ have to be determined by numerical integration. Developing the right-hand expression of (10) into powers of u_2, we find incidentally

$$\phi(\epsilon>1, n_1=0, n_2=n, x)=e^{-\alpha x}(1-e^{-\alpha x})^{n-1}.$$

The above expression gives the probability of finding exactly n particles (of any energy) at x.

§ 3. THE ELECTRON CASCADE

1. We describe the electron cascade by a function $\phi^{(i)}(\epsilon, N, x)$ where $i=1$ for a primary electron, $i=2$ for a primary photon, $N=n_1, n_2, n_3, n_4$; $n_1, n_2=$ number of electrons of energy $>, <\epsilon E_0$, $n_3, n_4=$ number of photons of energy $>, <\epsilon E_0$. $\phi^{(i)}(\epsilon, N, x)$ is the probability that a cascade of N members be found at x. Considering the 'approximation A' for the moment (e.g. full screening and negligible ionization loss), the function ϕ does not depend explicitly on the primary energy E_0. For the cross sections we use the well-known Bethe–Heitler expressions and write $w^{(1)}(\epsilon)\, d\epsilon\, dx$ for the probability of an electron E to emit along dx a photon of energy $E\epsilon$ in the interval $Ed\epsilon$, and $w^{(2)}(\epsilon)\, d\epsilon\, dx$ the corresponding expression for the emission of a pair one partner having the energy ϵE. We write

$$\int_0^1 w^{(i)}(\epsilon)\, d\epsilon=\alpha_i, \quad i=1, 2. \qquad \ldots\ldots(11)$$

Because of the divergence of the Bremsstrahlung cross section the integral diverges for $i=1$; we avoid this purely mathematical difficulty by postulating

$$w^{(1)}(\epsilon)=0, \quad 0<\epsilon<k, \qquad \ldots\ldots(12)$$

where k is a small quantity. In all physically interesting applications it will be possible to use the limit $k\to 0$ for the solutions.

The diffusion equation can thus be written

$$\phi^{(i)}(\epsilon, N, x)=\int_0^x \exp\{-\alpha_i(x-\xi)\} \sum_{N'+N''=N} \int_0^1 \phi^{(3-i)}\left(\frac{\epsilon}{\epsilon'}, N', \xi\right) \times \phi^{(1)}\left(\frac{\epsilon}{1-\epsilon'}, N'', \xi\right) w^{(i)}(\epsilon')\, d\epsilon'\, d\xi.$$

Introducing the generating function

$$G^{(i)}(\epsilon, U, x) = \sum_N \phi^{(i)}(\epsilon, N, x) U^N, \qquad \ldots\ldots(13)$$

where $U = u_1, u_2, u_3, u_4$, etc., we have

$$G^{(i)}(\epsilon, U, x) = \int_0^x \exp\{-\alpha_i(x-\xi)\}\, d\xi \int_0^1 G^{(1)}\left(\frac{\epsilon}{\epsilon'}, U, \xi\right) G^{(3-i)}\left(\frac{\epsilon}{1-\epsilon'}, U, \xi\right) w^{(i)}(\epsilon')\, d\epsilon', \qquad \ldots\ldots(14)$$

and differentiating in the same manner as before,

$$G_x^{(i)}(\epsilon, U, x) = \int_0^1 \left\{ G^{(1)}\left(\frac{\epsilon}{\epsilon'}, U, x\right) G^{(3-i)}\left(\frac{\epsilon}{1-\epsilon'}, U, x\right) - G^{(i)}(\epsilon, U, x) \right\} w^{(i)}(\epsilon')\, d\epsilon', \qquad \ldots\ldots(15)$$

where again $G_x^{(i)} = \partial G^{(i)}/\partial x$.

We have replaced α_i by $\int w^{(i)}(\epsilon')\, d\epsilon'$ and transferred the term $\alpha_i G^{(i)}$ from the left to the right-hand side and placed it under the integral.

2. The equation (15) can be integrated for a given initial condition. We note, however, that owing to our approximations the number of electrons or photons *below* a given energy is infinite in the limit $k \to 0$. Physically only those states are of interest which contain a given number of electrons or photons *above* an energy ϵE_0 together with an arbitrary number of electrons and photons below ϵE_0. We introduce therefore the probabilities

$$\phi^{(i)}(\epsilon, n', n'', x) = \sum_{n_2,\, n_4 = 0}^{\infty} \phi^{(i)}(\epsilon, n', n_2, n'', n_4, x).$$

The corresponding generating functions are

$$g^{(i)}(\epsilon, u, v, x) = \sum_{n',\, n''=0} \phi^{(i)}(\epsilon, n', n'', x) u^{n'} v^{n''} \equiv G^{(i)}(\epsilon, u, 1, v, 1, x);$$

the generating functions $g^{(i)}$ are special cases of $G^{(i)}$, and thus also obey equation (15). To obtain the initial condition for the $g^{(i)}$ we note that for $x = 0$, $i = 1$ there is one electron present, while for $x = 0$, $i = 2$ there is one photon present. Thus

$$\phi^{(1)}(\epsilon, 1, 0, x=0) = \phi^{(2)}(\epsilon, 0, 1, x=0) = 1 \qquad \epsilon < 1,$$

$$\phi^{(1)}(\epsilon, 0, 0, x=0) = \phi^{(2)}(\epsilon, 0, 0, x=0) = 1 \qquad \epsilon > 1;$$

all other $\phi^{(i)}$'s are 0 for $x = 0$, and, therefore,

$$g^{(i)}(\epsilon, u_1, u_3, x=0) = 1 \qquad \epsilon > 1 \qquad \ldots\ldots(16)$$

and

$$g^{(1)}(\epsilon, u_1, u_3, x=0) = g^{(2)}(\epsilon, u_3, u_1, x=0) = u_1 \qquad \epsilon < 1. \qquad \ldots\ldots(17)$$

As at any depth there are no photons or electrons with energies exceeding the primary energy, we can generalize (16) to

$$g^{(i)}(\epsilon, u_1, u_3, x) = 1 \qquad \epsilon > 1. \qquad \ldots\ldots(18)$$

Examining (15) we find, with help of (18), that the integrand remains finite when approaching $\epsilon' \to 0$, $(k = 0)$ if the specialized $g^{(i)}$'s are used. Thus, considering electrons and photons above ϵE_0, the right-hand side of expression (15) has a finite limit for $k \to 0$. $g^{(i)}$ is the generating function of the simultaneous distributions of electrons and photons above ϵE_0. We may average over the photons or over the electrons and thus obtain the distributions of electrons accompanied by an undetermined number of photons or the number of photons accompanied by an undetermined number of electrons. We write

$$\left.\begin{aligned} \phi^{(i,1)}(\epsilon, n, x) &= \sum_{v=0}^{\infty} \phi^{(i)}(\epsilon, n, v, x) \\ \text{and} \qquad \phi^{(i,2)}(\epsilon, n, x) &= \sum_{v=0}^{\infty} \phi^{(i)}(\epsilon, v, n, x); \end{aligned}\right\} \qquad \ldots\ldots(19)$$

the four functions $\phi^{(i,k)}$ $i, k=1, 2$ represent thus the probabilities of finding given numbers of electrons or photons in cascades initiated by electrons or photons. The first index refers to the nature of the primary, the second to the nature of secondaries under consideration. The corresponding generating functions are

$$g^{(i,k)}(\epsilon, u, x) = \sum_{n=0}^{\infty} \phi^{(i,k)}(\epsilon, n, x) u^n. \qquad \ldots\ldots(20)$$

$$i, k = 1, 2.$$

The $g^{(i,k)}$ are again special values of the $G^{(i)}$, namely

$$\left.\begin{aligned} g^{(i,1)}(\epsilon, u, x) &= G^{(i)}(\epsilon, u, 1, 1, 1, x), \\ g^{(i,2)}(\epsilon, u, x) &= G^{(i)}(\epsilon, 1, 1, u, 1, x). \end{aligned}\right\} \qquad \ldots\ldots(21)$$

§4. DISCUSSION OF THE GENERATING FUNCTION

1. From the definitions (15) and (21) of the generating function, it follows that

$$g^{(i,k)}(\epsilon, 1, x) = 1, \qquad i, k = 1, 2. \qquad \ldots\ldots(22)$$

This condition is compatible with the diffusion equation (14) or (15). Differentiating equation (20) with respect to u, we find for $u=1$

$$\begin{aligned} \left(\frac{\partial g^{(i,k)}(\epsilon, u, x)}{\partial u}\right)_{u=1} &= \sum_{v=0}^{\infty} v \phi^{(i,k)}(\epsilon, v, x) \\ &= \langle n(i, k;\ \epsilon, x)\rangle. \end{aligned} \qquad \ldots\ldots(23)$$

The latter expression signifies the average number of electrons or photons with energy $>\epsilon E$ at a depth x given rise to by an electron or photon. Similarly we can get higher momenta of the distribution

$$\left(\frac{\partial^p g^{(i,k)}(\epsilon, u, x)}{\partial^p (\log u)}\right)_{u=1} = \Sigma v^p \phi^{(i,k)}(\epsilon, v, x), \qquad \ldots\ldots(23\,a)$$

or mixed momenta

$$\left(\frac{\partial^{p+q} g^{(i)}(\epsilon, u, v, x)}{\partial^p (\log u) \partial^q (\log v)}\right)_{u=1,\ v=1} = \Sigma v'^p v''^q \phi^{(i)}(\epsilon, v', v'', x). \qquad \ldots\ldots(23\,b)$$

We note that differentiating (14) and introducing (23) we have, with the help of (22), replacing G by g,

$$\begin{aligned} \frac{\partial}{\partial x} \langle n(i, k;\ \epsilon, x)\rangle = -\langle n(i, k;\ \epsilon, x)\rangle \int_0^1 w(\epsilon')\, d\epsilon' + \int_0^1 \langle n(1, k;\ \frac{\epsilon}{\epsilon'}, x)\rangle w(\epsilon')\, d\epsilon' \\ + \int_0^1 \langle n(3-i, k;\ \frac{1-\epsilon'}{\epsilon}, x)\rangle w(\epsilon')\, d\epsilon'. \end{aligned} \qquad \ldots\ldots(24)$$

The above equation is equivalent to the well-known diffusion equation of the theory neglecting the ionization term.

Similarly, the second derivative with respect to u of (15) gives the diffusion equation for the mean square spread; such equations were investigated by Nordsieck, Lamb and Uhlenbeck (1940).

2. The fact that the equations (15) can be reduced in a special case to the ordinary diffusion equations for average numbers sheds some light on the amount of work necessary to integrate the system (15). To build up the solution of (15) for a fixed value of u is about equivalent to integrating numerically equation (24). Such an integration is somewhat cumbersome as it is necessary to compute simultaneously solutions for all values of ϵ above the required value of ϵ. However, for the purpose of a complete tabulation of the functions $\langle n(i,k;\epsilon,x)\rangle$ etc. this procedure is not essentially more elaborate than it would be to integrate some ordinary differential equation numerically and to get solutions for all values of ϵ one after the other.

We are of the opinion therefore that for the purpose of tabulating the cascade functions comprehensively the direct numerical integration of the diffuse equations is not essentially more elaborate than computation by the well-known analytical methods.

To tabulate the generating functions a procedure similar to direct numerical integration of, say, (24) has to be repeated for several values of the argument U.

3. The actual probabilities $\phi^{(i)}(\epsilon,n',n'',x)$ or $\phi^{(i,k)}(\epsilon,n,x)$ can be obtained for small values of n by differentiating the generating function. Thus

$$\frac{1}{n'!\;n''!}\left(\frac{\partial^{n'+n''}g^{(i)}(\epsilon,u,v,x)}{\partial u^{n'}\partial v^{n''}}\right)_{u=v=0}=\phi^{(i)}(\epsilon,n',n'',x)$$

and
$$\frac{1}{n!}\left(\frac{\partial^{n}g^{(i,k)}(\epsilon,u,x)}{\partial u^{n}}\right)_{u=0}=\phi^{(i,k)}(\epsilon,n,x).$$

The derivatives can be obtained either by numerical differentiation or alternatively by successive integrations with respect to x of the derivatives into u of the equation (15). Differentiating (15) n times into u, we get a recursion formula which permits determination of the nth derivative of g with help of the lower derivatives. As an example we consider a case, of particular importance in practice, namely, $\phi^{(1,1)}(\epsilon,1,x)$, i.e. the probability of an electron passing through an absorber and emerging from it accompanied by photons and low energy electrons only. We have for this probability

$$\phi^{(1,1)}(\epsilon,1,x)=\left(\frac{\partial g^{(1,1)}(\epsilon,u,x)}{\partial u}\right)_{u=0}.$$

The diffusion equation for this quantity is obtained from (15) and its derivative into u with the following initial conditions (see (16), (17) and (21)):

$$g^{(1,1)}(\epsilon,u=0,x=0)=\begin{cases}0 & \epsilon<1\\ 1 & \epsilon>1\end{cases}$$

$$g^{(2,1)}(\epsilon,u=0,x=0)=\;1\ \text{any}\ \epsilon$$

$$\left(\frac{\partial g^{(1,1)}(\epsilon,u,x=0)}{\partial u}\right)_{u=0}=\begin{cases}1 & \epsilon<1\\ 0 & \epsilon>1\end{cases}$$

$$\left(\frac{\partial g^{(2,1)}(\epsilon,u,x=0)}{\partial u}\right)_{u=0}=\;0\ \text{any}\ \epsilon.$$

4. For large values of n it is impracticable to evaluate the high-order derivatives of the generating function step by step. Such cases can be dealt with using complex integrals. We have

$$\phi^{(i,\,k)}(\epsilon, n, x) = \frac{1}{2\pi i}\oint_{u=0} u^{-n-1} g^{(i,\,k)}(\epsilon, u, x)\,du,$$

and similar expressions for other probabilities. The complex integrals can as a rule be deformed to a path parallel to the imaginary u axis and the integrals can be evaluated by the saddle-point method. This procedure requires the values of $g^{(i,\,k)}(\epsilon, u, x)$ and both their first and second derivatives into u.

Similarly probabilities of the simultaneous presence of specified numbers of electrons and photons can be obtained by double complex integrals, which can be reduced to double saddle-point integrals. We hope to return to the details of this procedure in a later publication.

§ 5. EQUATIONS FOR ARBITRARY CROSS SECTIONS AND IONIZATION LOSS

1. In the previous sections we have assumed that the differential cross section is a homogeneous function of the energies, and we have also neglected ionization loss. Neither of these assumptions is essential to the formalism; these assumptions have, however, the advantage of reducing the number of independent variables. Instead of the two variables of the exact procedure, namely the primary energy E_0 and the final energy E, we have in the approximate procedure only their ratio ϵ as an independent variable.

If the simplifying assumptions are dropped we have thus to deal with functions and generating functions *

$$\phi^{(i)}(E_0, E, N, x), \quad G^{(i)}(E_0, E, U, x).$$

The diffusion equations for a general cross section $w^{(i)}(E_0, E', E'')$ in the case of electron cascades without ionization loss is thus

$$G^{(i)}(E_0, E, U, x) = \int_0^x \exp\{-\alpha_i(E_0)(x-\xi)\}\,d\xi \int_0^\infty\int_0^\infty G^{(1)}(E', E, U, \xi) \times G^{(3-i)}(E'', E, U, \xi)\, w^{(i)}(E_0;\, E', E'')\,dE'\,dE'' \qquad \ldots\ldots (25)$$

with
$$\alpha_i(E) = \int_0^\infty\int_0^\infty w^{(i)}(E;\, E', E'')\,dE'\,dE''.$$

We integrate separately over E' and E'' as for actual collisions $E' + E''$ is not exactly equal to E on account of recoil of the nucleus.

From (25) we get the differential equation

$$G_x^{(i)}(E_0, E, U, x) = \int_0^\infty\int_0^\infty \{G^{(1)}(E', E, U, x) G^{(3-i)}(E'', E, U, x) - G^{(i)}(E_0, E, U, x)\} \times w(E_0;\, E', E'')\,dE'\,dE''. \qquad \ldots\ldots (26)$$

The equation (26) can be integrated in the same way as (15). For a fixed value of E one has to compute simultaneously all the values of E_0 between E and the desired value.

---

* For the electron cascade $i=1, 2$ most of the following formulae apply to the case of nucleon cascades when the index i is omitted, and accordingly the number of equations reduced.

2. Ionization loss can be included into the formalism by remembering that the primary of energy E_0 has at the time of its first collision at $x-\xi$ an energy $E_0-\beta_i(x-\xi)$, where β_1 is rate of ionization loss of an electron, $\beta_2=0$. Thus we have in the case of homogeneous w, i.e. for $\alpha_i(E_0)=\alpha_i$ (independent of E_0),

$$G^{(i)}(E_0, E, U, x) = \int_0^x \exp\{-\alpha_i(x-\xi)\}\, d\xi \int_0^\infty \int_0^\infty G^{(1)}(E', E, U, \xi) G^{(3-i)}(E'', E, U, \xi)$$
$$\times w^{(i)}(E_0-\beta_i(x-\xi), E', E'')\, dE'\, dE''.$$

Multiplying by $\exp(\alpha_i x)$ and differentiating with respect to x, we find in the usual way

$$G_x^{(i)}(E_0, E, U, x) = \int_0^\infty \int_0^\infty \{G^{(1)}(E', E, U, x) G^{(i-3)}(E'', E, U, x) - G^{(i)}(E_0, E, U, x)\}$$
$$\times w^{(i)}(E_0, E', E'')\, dE'\, dE'' - \beta_i \frac{\partial G^{(i)}(E_0, E, U, x)}{\partial E_0}. \quad \ldots\ldots (27)$$

3. As the operation $\partial/\partial E_0$ for large values of E_0 reduces the order of $w^{(i)}$, the second term on the right-hand side is small for $E_0 \gg \beta_1$; thus it is small provided the primary energy much exceeds the initial energy.

An approximate solution of (27) is the solution without ionization loss. Denoting this by G_0, we put

$$G^{(i)}(E_0, E, U, x) = G_0^{(i)}(E_0, E, U, x) + \beta_1 g_1^{(i)}(E_0, E, U, x) + \beta_1{}^2 g_2^{(i)}(E_0, E, U, x) + \ldots .$$

In the first order of β we have from (27)

$$\frac{\partial g_1^{(i)}(E_0, E, U, x)}{\partial x} = -\frac{\beta_i}{\beta_1} \frac{\partial G_0^{(i)}(E_0, E, U, x)}{\partial E_0} + \int_0^\infty \int_0^\infty \{G_0^{(1)}(E', E, U, x)$$
$$\times g_1^{(3-i)}(E'', E, U, x) + g_1^{(3-1)}(E', E, U, x) . G_0(E'', E, U, x)$$
$$- g_1^{(i)}(E_0, E, U, x)\} w^{(i)}(E_0, E', E'')\, dE'\, dE''. \quad \ldots\ldots (27a)$$

The equation (27*a*) can be integrated if $G_0^{(i)}$ is known. The integration requires the same amount of work as the integration of (27) itself, which gives the exact solution directly. The practical advantage of (27*a*) over (27) is, however, this: If $w(E_0, E', E'')\, dE'\, dE''$ is a function of E'/E_0 and E''/E_0 only, then G_0 is also a homogeneous function; further, writing

$$G_0(E_0, E, U, x) = \overline{G}_0(\epsilon, U, x), \qquad \epsilon = E/E_0,$$

we have

$$\frac{\partial G_0}{\partial E_0} = -\frac{\partial \overline{G}_0}{\partial \epsilon} \frac{E}{E_0{}^2} = \frac{1}{E_0} \times \text{function of } \epsilon.$$

Thus

$$g_1^{(i)}(E_0, E, U, x) = \frac{\text{function of } (E/E_0)}{E_0},$$

and $g_1^{(i)}$ needs to be evaluated for various values of the ratio of E/E_0 only.

4. Finally, for the sake of completeness, we give the diffusion equation, including ionization loss for arbitrary $w(E_0, E', E'')$.

The probability for a primary to lose energy by ionization only down to a depth $x-\xi$ is

$$P^{(i)}(E_0, x-\xi) = \exp\left\{-\int_0^{x-\xi} \alpha_i(E_0-\beta_i\eta)\, d\eta\right\}.$$

Thus the integral equation for the generating function may be written

$$G^{(i)}(E_0, E, U, x) = \int_0^x \exp\left\{-\int_0^{x-\xi} \alpha_i(E_0-\beta_i\eta)\,d\eta\right\} d\xi \int_0^\infty \int_0^\infty G^{(1)}(E', E, U, \xi)$$
$$\times\, G^{(3-i)}(E'', E, U, \xi)\, w^{(i)}(E_0-\beta_i(x-\xi)E', E'')\, dE'\, dE''. \quad \ldots\ldots (28)$$

Multiply (28) by
$$\exp\left\{\int_0^x \alpha_i(E_0-\beta_i\eta)\,d\eta\right\},$$

differentiate, and divide by the same factor. This procedure gives

$$\frac{\partial G^{(i)}(E_0, E, U, x)}{\partial x} = \int_0^\infty \int_0^\infty G^{(1)}(E', E, U, x) G^{(3-i)}(E'', E, U, x) w^{(i)}(E_0, E', E'')$$
$$- G^{(i)}(E_0, E, U, x) w^{(i)}(E_0-\beta_i x, E', E'')\, dE'\, dE''$$
$$- \beta_i \frac{\partial G^{(i)}(E_0, E, U, x)}{\partial E_0}. \quad \ldots\ldots (29)$$

Equation (29) can be integrated numerically for a given initial condition, as all previous equations. Again, as in the preceding section, it is possible to approximate the exact solution by a series of homogeneous functions.

REFERENCES

Arley, N., 1949, *On the Theory of Stochastic Processes* (New York : John Wiley and Sons).
Heitler, W., and Jánossy, L., 1949, *Proc. Phys. Soc.* A, **62,** 374, 669.
Nordsieck, A., Lamb, W. E., Jr., and Uhlenbeck, G. E., 1940, *Physica*, **7,** 344.
Scott, W. T., and Uhlenbeck, G. E., 1942, *Phys. Rev.* **62,** 407.

Some Observations on the Nuclear Disintegrations caused by Cosmic Rays in Photographic Emulsions

By NORA PAGE

The Physical Laboratories, The University, Manchester

Communicated by G. D. Rochester; MS. received 2nd November 1949, *and in amended form 21st December* 1949

ABSTRACT. An account is given of a study of 2,150 stars in Ilford C2 plates and 312 stars in Kodak NT4 plates exposed under different conditions. Possible values for the cross section for star-producing collisions are discussed. It is concluded that this collision cross section is equal to the geometrical cross section of the nuclei, and that the stars producing particles are non-catastrophically absorbed, leading to the observed absorption cross sections. It is shown that nuclear transparency could not account for the observed results. It is estimated that 17% of all stars and 40% of stars from which two or more lightly ionizing particles are emitted are caused by ionizing primary particles. The size distributions for stars caused by ionizing and non-ionizing particles are given, and possible explanations for the difference between them are considered. The experimental observations are in agreement with the theory that the star-producing particles are mainly neutrons and protons secondary to the primary cosmic rays.

The variation with star size of the proportion of doubly charged to singly charged particles is found, and for stars of more than six prongs is in agreement with Le Couteur's extension of the evaporation theory. A value of 0·54 is deduced for the proportion of doubly charged particles from disintegrations in the light elements of the emulsion.

An increase in the proportion of lightly ionizing tracks is observed for stars of more than eight prongs, and is ascribed to the creation of mesons.

---

§1. INTRODUCTION

The fundamental problems requiring elucidation in the study of nuclear disintegrations caused by cosmic rays are the nature of the star-producing radiation and the mechanism of disintegration of the nucleus. It is now thought that the radiation responsible for most low energy stars (i.e. < 200 MEV.) consists of neutrons, and for high energy stars fast neutrons and protons, with a cross section for star production proportional to the geometrical cross section. The disintegration of the nucleus is thought to involve the emission of a number of relatively slow particles with energies and an angular distribution typical of evaporation, and a smaller number of particles of high energy (i.e. > 50 MEV.) which form a 'tail' to the evaporation spectrum. These particles probably consist of the incident nucleon, knock-on nucleons and mesons created in nucleon–nucleon collisions.

A study of 2,450 stars formed in Ilford C2 and Kodak NT4 nuclear research emissions has recently been completed and the main results are summarized in this paper. The conclusions regarding the nature of the star-producing radiation confirm those of other workers. The results on the mechanism of disintegration of the nucleus afford a test of Le Couteur's (1950) extension of the evaporation theory of nuclear disintegrations, and where it can be applied this theory is found to be in substantial agreement with the experimental results.

§ 2. EXPERIMENTAL DETAILS

Details of plates, exposure times etc. are given in Table 1.

Table 1

Type of plate	Thickness of emulsion (μ)	Area (cm²)	Altitude (m.)	Duration of exposure	Number of stars
Ilford C2	100	200	3450	75 days	2000
Ilford C2	100	160	12000	2 hours	150
Kodak NT4	200	51·4	3450	14 days	192
Kodak NT4	400	36	2800	6 days	120

The large group of 2,000 stars was obtained from a group of plates of which one-third was placed horizontally, one-third vertically, and one-third vertically under 10 cm. of lead. All the other plates were exposed vertically. Moreover, all the plates were kept at 0° c. in thin air-tight containers, and they were developed within a few days of the end of the exposure. Except for the Ilford plates exposed at 3,450 m. the fading was negligible, but even in this case it was estimated that less than 3% of the stars were lost. These plates were fully developed to give uniform development to the bottom of the emulsion, and ionizations down to 3·5 times minimum (corresponding to protons of energy 100 Mev.) could be detected. The plates exposed at 12,000 m. were under-developed to facilitate particle discrimination and energy measurements; for these plates ionizations down to 7 times minimum, or protons of 40 Mev., were recorded. The electron-sensitive plates were developed by the freezing method of Dilworth, Occhialini and Payne (1948) and minimum ionization tracks were easily detected, their average grain density being about 400 grains per mm.

All the plates were scanned with great care and checks indicated that less than 1% of the stars were missed. The electron-sensitive plates were scanned with oil immersion objectives. Radioactive stars and possible cases of scattering were excluded.

§ 3. THE STAR-PRODUCING RADIATION

(i) *The Total Flux at Different Altitudes*

The Kodak NT4 plates exposed at an altitude of 3,450 m. under no absorber recorded $13{\cdot}4 \pm 1$ stars/cm³/day. Of these approximately 1·0/cm³/day, or 8%, could not have been observed on the C2 plates because they would have appeared as single tracks or large angle scatterings. Since the fading on NT4 plates was negligible and the scanning very carefully carried out, it is justifiable to assume that this figure represents the true rate of production of stars. The rate of production of stars in the Ilford C2 plates would be expected to be about 8% less, but in fact the measured value was almost the same, i.e. $13{\cdot}5 \pm 0{\cdot}5$/cm³/day for plates exposed under the same conditions. It is assumed that this indicates that fading was small and the scanning adequate. The figure of $13{\cdot}5 \pm 0{\cdot}5$ stars/cm³/day may therefore be taken as the rate of star production at 3,450 m. Moreover, the number of stars with three or more prongs was found to be $12{\cdot}2 \pm 0{\cdot}6$ which is not appreciably different from the figure of $14{\cdot}2 \pm 0{\cdot}5$ given by Cortini and Manfredini (1949).

From the observed rate of star production at 3,450 m., it is possible to calculate the flux of the star-producing particles at this altitude provided that the cross section for star production in the emulsion is known. Consider one component r of the emulsion, with density ρ_r and atomic weight A_r of which there are N_r atoms per cm³. Then the number of stars dn_r formed in the atoms of the element r, per day, in 1 cm² of emulsion dx cm. in thickness is

$$\frac{dn_r}{n_0} = N_r \sigma_r \, dx,$$

where n_0 is the total flux of star-producing particles/cm²/day, and σ_r is the cross section for star production in the element r. Summing over all the components of the emulsion we have, since $N_r = \frac{N_0 \rho_r}{A_r}$, where N_0 is Avogadro's number,

$$\frac{dn}{n_0} = N_0 \Sigma_r \frac{\sigma_r \rho_r}{A_r} \, dx, \qquad \ldots\ldots (1)$$

where dn is the total number of stars per day in 1 cm² of emulsion dx cm. thick. In this summation the hydrogen in the emulsion is excluded, since collisions with hydrogen atoms will not in general give recognizable stars.

Before calculating the flux of star-producing particles it is therefore necessary to determine the values of σ_r. Now the cross section for absorption of the star-producing radiation has been found for air, carbon and lead by George and Jason (1949) and for lead and aluminium by Bernardini *et al.* (1949). In all cases it is equal to half the geometrical cross section of the absorbing nuclei (taking the nuclear radius to be $1{\cdot}42 \times 10^{-13} A^{1/3}$ cm., where A is the atomic weight).

An increase in absorption cross section with atomic weight may be obtained in two ways. In the first place the cross section for star-producing collisions may be equal to the geometrical cross section of the absorbing nuclei. This implies that the mean free path of the star-producing particles in nuclear matter is small compared with the nuclear radius. The fact that the absorption cross section is only half the geometrical cross section would then be accounted for if the collisions were not catastrophic, each star-producing particle causing on the average two disintegrations.

The alternative explanation is that the nucleus is not completely opaque to the star-producing radiation, that is, the mean free path in nuclear matter is of the same order of magnitude as the nuclear radius. In order to explain the quantitative results it must then be assumed that the primary particle passes on the average through two nuclei before producing a star, giving a cross section for star-producing collisions equal to half the geometrical cross section. The absorption and star-producing collision cross sections would then be equal. This means that the mean probability for the primary particle to pass through a nucleus without being absorbed is equal to one half. It follows from an analysis first given by Cocconi (1949, equation (7)) that if this probability is a constant for all elements, the mean free path of the star-producing radiation in nuclear matter must be directly proportional to the nuclear radius of the element. This is most probable and it is therefore not possible to explain the experimental results satisfactorily by nuclear transparency. We are then left with the first explanation, namely that the cross section for star-producing collisions is equal to the geometrical cross section. This will give a value of the flux which differs by a factor of two from that calculated using the absorption cross section (see George and Jason 1949).

Equation (1) then becomes

$$\frac{dn}{n_0} = N_0\pi(1{\cdot}42\times10^{-13})^2\, \Sigma_r \frac{\rho_r}{A_r^{1/3}}\, dx.$$

Using the observed values for *dn* the total flux at 3,450 m. is found to be 366 particles/cm²/day, and at 12,000 m., 11,000 particles/cm²/day. If exponential absorption is assumed the total flux at sea level is 28 particles/cm²/day.

(ii) *The Nature of the Star-producing Radiation*

It is generally agreed that the majority of star-producing particles at altitudes below approximately 4,000 m. are energetic neutrons, whilst the charged particles observed to cause stars may be protons or σ mesons (George and Jason 1949). Using the NT4 plates exposed at 2,800 m. and 3,450 m. an attempt was made to find the relative numbers of stars formed by ionizing and non-ionizing particles, and to discover any characteristic features of the two types of star. There is inevitably some uncertainty in identifying a particle as the primary, but although there are doubtless errors in individual cases, the general conclusions are believed to be valid. The criteria used to distinguish an ionizing primary were somewhat similar to those outlined recently by Brown *et al.* (1949 a), i.e. tracks less than 90° to the vertical, on the axis of symmetry of emitted fast particles and with ionization less than 1·5 times minimum. It was found that the angular distribution of ionizing primary particles selected by these criteria obeyed a cosine squared law, within the limits of statistical errors.

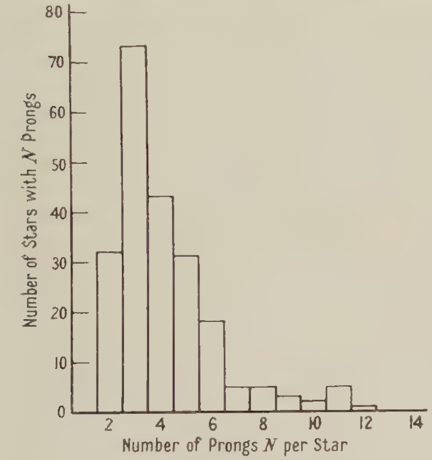

Figure 1 (*a*).
Stars caused by non-ionizing primary particles.

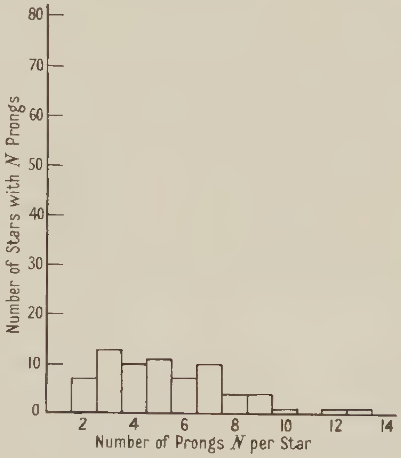

Figure 1 (*b*).
Stars caused by ionizing primary particles.

In agreement with other workers it was found that ionizing primary particles caused $17\pm3\%$ of all the stars, and 40% of the stars from which two or more lightly ionizing particles were emitted. If it is assumed that the cross section for star production is the same for charged and uncharged primary particles this means that at 3,450 m. the flux of charged star-producing particles is 62/cm²/day, and uncharged is 304/cm²/day, or 1·4% and 6·6% respectively of the total charged corpuscular radiation at this height.

The differential size distributions for stars caused by non-ionizing and ionizing particles are shown in Figure 1, and are in good agreement with the results of

Brown *et al.* (1949b). This observed difference in size distribution may be due to the two types of star-producing particle having different energy spectra. Alternatively the results might be accounted for if the cross section for star-producing collisions were different in the two cases or varied with the energy of the incident particle in different ways for charged and uncharged particles. Thirdly, the probability of a certain energy dE being transferred to the nucleus by a particle of energy E, whilst traversing a distance dl through the nucleus, might not be the same for charged and uncharged primary particles.

If the non-ionizing primary particles are neutrons and the ionizing are, for example, σ mesons, it is probable that the observed size distribution can only be accounted for by considering all three factors. However, if the star-producing particles are assumed to be mainly neutrons and protons the last two explanations are not so plausible as the first one, i.e. a difference in the energy spectra. The proton spectrum would be expected to contain a greater proportion of high energy particles than the neutron spectrum since the protons with energies less than 10^9 ev. lose energy very rapidly by ionization.

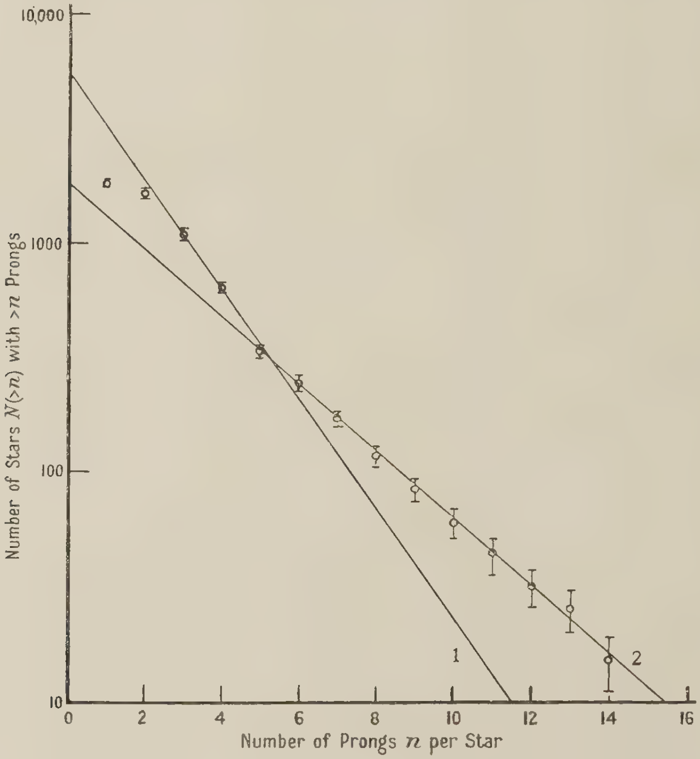

Figure 2. (1) $N(>n)=A\exp(-0{\cdot}521n)$. (2) $N(>n)=0{\cdot}38A\exp(-0{\cdot}331n)$. (All observations on C2 plates.)

The size distribution of stars on Ilford C2 plates at 3,450 m., is shown in Figure 2. $N(>n)$ is the number of stars with more than n prongs, and A is a constant. It appeared from the size distribution at 3,450 m. and 12,000 m. that the proportion of large stars increased at the higher altitude. Thus at 3,450 m., the proportions of stars with more than 9 prongs is $0{\cdot}045 \pm 0{\cdot}005$ whilst at 12,000 m. it is $0{\cdot}100 \pm 0{\cdot}028$. This increase would be expected if the average energy of the star-producing nucleons increased with height.

§4. THE MECHANISM OF DISINTEGRATION OF THE NUCLEUS

(i) *The Evaporation Theory*

As stated in §1 the disintegration of the nucleus involves the emission of a number of slow particles (i.e. <50 MEV.), and a smaller number of fast particles, which may consist of the primary nucleon, knock-on nucleons and created mesons. The slow particles arise as a result of the excitation or heating up of the nucleus by the fast particles and, as is well known, their emission is analogous to evaporation. This evaporation theory for the production of the secondary particles was due to Bohr and Kalckar (1937) and extended by Bethe (1937) and Weisskopf (1937). It was applied by Bagge (1938, 1946) and in greater detail by Harding *et al.* (1949) to the low energy particles observed in stars. They found, using the Fermi gas model of the nucleus and making due allowance for cooling and barrier penetration, that the theory gave a good account of the energy spectrum. The evaporation theory has recently been extended further by Le Couteur (1950) by taking into account the thermal expansion of the nucleus and the effect of the neutron excess. Le Couteur has obtained the energy distribution of evaporated particles and has calculated the probability for the emission of protons, neutrons, deuterons, tritons, ^{3}He, and α-particles as a function of the excitation energy. Since the excited nucleus is assumed to be always in approximate thermodynamic equilibrium the calculations have not been extended beyond energies of the order of 600 MEV. Thus the maximum star size to which the theory can be applied is about 14 prongs. Moreover, since this model can only be applied to heavy nuclei, stars which originate in the light nuclei, carbon, nitrogen and oxygen, should be excluded. This means the exclusion of all stars of less than about 6 prongs. Thus, strictly, the theory may be applied only to stars of between 6 and 14 prongs, but in actual fact a short extension of the limits is permissible.

The proof that the light nuclei do not contribute appreciably to stars of more than 6 prongs is as follows. (1) The plot of the logarithm of the integral size distribution against star size (i.e. number of prongs n) consists of two straight lines with a clear break at approximately $n=6$. (2) The size distribution of 50 stars produced in a cloud chamber filled with air, water vapour and alcohol, by a beam of 90 MEV. neutrons by Horning and Baumhoff (1949) in Berkeley shows a negligible proportion of stars of more than 5 prongs. It is reasonable to assume that the size distribution of stars formed in carbon, nitrogen and oxygen does not vary considerably with the energy of the incident particle if this is in excess of 90 MEV., since these nuclei are relatively easily broken up into α-particles.

The two main features of the theory which may most easily be checked are (i) the energy spectrum of evaporated particles, (ii) the ratio of doubly to singly charged particles. An energy analysis has been made of a group of 17 stars from 7 to 17 prongs in the C2 plates. The proton energy spectrum as deduced from this analysis combined with the results of Perkins have been shown by Le Couteur (1950) to be in good agreement with his theory, which also accounts for the α-particle spectrum. The experimental determination of the ratio of doubly to singly charged particles will now be described.

(ii) *The Ratio of Doubly to Singly Charged Particles*

The proportion of doubly charged particles emitted was found for all stars in the Ilford C2 plates and the results are shown in Figure 3. These results appear to be confirmed by those of Addario and Tamburino (1949). They differ somewhat from the latest (unpublished) results of Perkins although the differences are not as much as three times the standard deviations.

The proportion of doubly charged particles decreases with increasing star size, remaining more or less constant for stars of above 6 prongs. There are 392 stars with more than 6 prongs with an average size of 10 prongs and the value of the ratio is 0·271 ± 0·008. This is in excellent agreement with the values obtained by Le Couteur, who found an average value of 0·27. Le Couteur predicts a variation of from 0·25 for 2-pronged stars in heavy elements, to 0·28 for large stars.

These figures may be used, with the experimental results, to give a value for *K*, the proportion of doubly charged particles from the disintegration of carbon, nitrogen or oxygen, if *K* is assumed constant for stars of from 2 to 6 prongs.

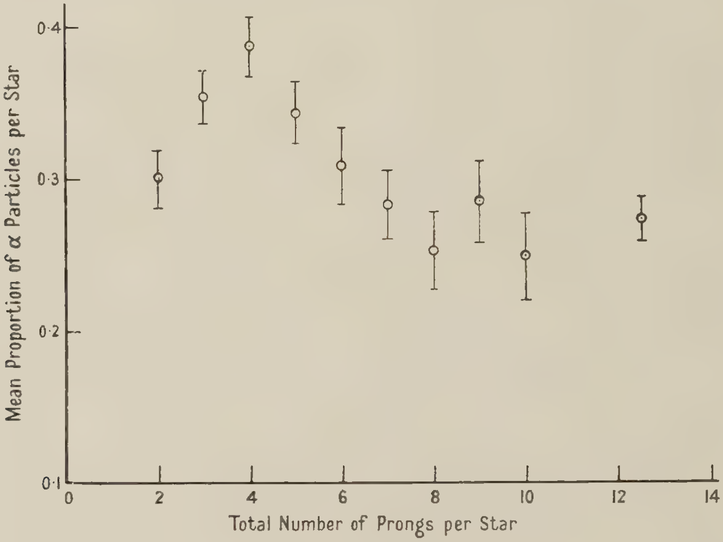

Figure 3.

This value may then be compared with that obtained by Perkins (1949) from a study of stars in a gelatine sandwich plate.

Using Le Couteur's figure for stars in silver and bromine the relative number of stars formed in the light elements of the emulsion may be calculated in terms of *K*. If the relative number of stars formed in the different elements of the emulsion is proportional to the geometrical cross section of the nuclei of the elements, approximately 27% of the total number of stars in the emulsion will be formed in light nuclei. Harding (1949) has recently made a direct determination of this quantity by comparing the stars formed in gelatine and in ordinary emulsion. He finds approximately 36 ± 4·5% of all stars are formed in the light nuclei, a result in reasonable agreement with the above value.

A figure of 27% for the proportion of stars formed in carbon, nitrogen and oxygen is found, if *K* is assumed to be 0·54. Perkins (1949) from a study of stars in gelatine found for *K* a value of 0·5.

On the Le Couteur theory, approximately 28% of all singly charged particles emitted from stars should be deuterons or tritons. From the relative numbers of protons, deuterons and tritons from stars which ended in the emulsion it was estimated that approximately 25% of all emitted singly charged particles were heavier than protons, and Harding *et al.* (1949) give a value of 30%. This may be taken as a further confirmation of the theory.

§ 5. THE HIGH ENERGY PARTICLES

The 312 stars in the electron-sensitive emulsion were analysed for high energy particles in the following way. The particles were divided according to their energies, those with energy corresponding to an ionization greater than 7 times minimum, those between 7 and 3·5 times minimum, and those of less than 3·5 times minimum. For protons these ionization values correspond to energies of 40 MeV. and 100 MeV. The numbers of particles in the three groups are shown in Table 2.

Table 2. Relative Number of Particles with given Value of Ionization

Ionization (× minimum)	>7	3·5–7	<3·5
Stars with 8 or less evaporated particles	1	0·103±0·010	0·156±0·013
Stars with more than 8 evaporated particles	1	0·079±0·026	0·380±0·063
All stars	1	0·100±0·010	0·180±0·013

This grouping was chosen to give statistically significant results, and because the proportion of high energy particles was observed to increase for stars with more than eight evaporated particles. Charged primary particles have not been included.

It was found that 56 ± 10% of the particles with ionization less than 3·5 times minimum emitted from stars with *less* than nine prongs had ionization below 1·5 times minimum. This is in agreement with the value of 56 ± 8% calculated from the results of Brown *et al.* (1949 b) for stars with *more* than seven evaporated particles.

It can be seen from Table 2, that whilst the proportion of particles with ionization between 3·5 and 7 times minimum does not vary within the limits of error, there is an increase in the proportion of those with ionization less than 3·5 times minimum for large stars. Now the ratio of the number of directly ejected protons to the number of charged evaporated particles should not vary appreciably with the energy involved in the disintegration (Rosenfeld 1948). This experimental increase may therefore be due to the creation of mesons, since the probability of this occurring will be greater in high energy disintegrations.

In the absence of scattering measurements it is difficult to estimate the proportion of tracks with ionization less than 7 times minimum which may be ascribed to created mesons and the proportion which may be ascribed to recoil protons. A small number of mesons with energies of a few MeV. are certainly emitted, and it is known from penetrating showers that very high energy mesons are also created.

It is of interest to note that the proportion of particles with ionization lower than 3·5 times minimum which have an ionization less than 1·5 times minimum is the same (56%) for small and large stars. If, as suggested above, a large proportion of particles in the group may be ascribed to mesons in the case of large stars, this indicates that some 60% of such mesons have ionizations less than 1·5 times minimum (or energies in excess of 60 MeV. if π mesons) and about 40% are slow mesons (i.e. if π mesons, of energies less than 60 MeV.).

Further, the fact that the proportion of particles with ionization between 3·5 and 7 times minimum does not appear to vary much with star size may indicate that only a small proportion of these are due to mesons, and the majority are recoil protons of energy 40–100 MeV.

ACKNOWLEDGMENTS

I wish to thank Professor P. M. S. Blackett for the facilities to do this work and for his interest and advice. I also wish to express my thanks to Dr. G. D. Rochester for valuable discussion, help and advice, and to Dr. Le Couteur for discussion on the theoretical aspects involved. Miss M. Blundell has developed and scanned many of the plates and assisted at all stages of the work, and I wish to express my thanks to her and to all those who assisted in scanning the plates. I am indebted to Dr. G. P. S. Occhialini of Brussels for exposing and developing the plate at 2,800 m., to the Staff of the Scientific Station, Jungfraujoch, for their co-operation in exposing the plates at 3,450 m., and to the staff of the R.A.F. at Benson, Oxon., for making the exposures at 12,000 m. I should also like to thank the staffs of Messrs. Ilford and Messrs. Kodak, who have supplied us with the plates and advised us on their processing.

REFERENCES

Addario, M. M., and Tamburino, S., 1949, *Reports of the Como Conference* (in the press).

Bagge, E., 1938, *Ann. Phys., Lpz.*, **33,** 389; 1946, *Cosmic Radiation* (edited by Heisenberg) (New York: Dover Publications), p. 128.

Bernardini, G., Cortini, G., and Manfredini, A., 1949, *Cosmic Radiation*, Colston Papers, p. 22.

Bethe, H. A., 1937, *Rev. Mod. Phys.*, **9,** 69, 245.

Bohr, N., and Kalckar, F., 1937, *Proc. Cop.*, **14,** No. 10.

Brown, R. H., Camerini, U., Fowler, P. H., Muirhead, H., Powell, C. F., and Ritson, D. H., 1949 a, *Nature, Lond.*, **163,** 47.

Brown, R. H., Camerini, U., Fowler, P. H., Heitler, H., King, D. T., and Powell, C. F., 1949 b, *Phil. Mag.*, **40,** 862.

Cocconi, G., 1949, *Phys. Rev.*, **75,** 1074.

Cortini, G., and Manfredini, A., 1949, *Nature, Lond.*, **163,** 991.

Dilworth, C. C., Occhialini, G. P. S., and Payne, R., 1948, *Nature, Lond.*, **162,** 103.

George, E. P., and Jason, A. C., 1949, *Cosmic Radiation*, Colston Papers, p. 31.

Harding, J. B., 1949, *Nature, Lond.*, **163,** 440.

Harding, J. B., Lattimore, S., and Perkins, D. H., 1949, *Proc. Roy. Soc.* A, **196,** 325.

Horning, W., and Baumhoff, L., 1949, *Phys. Rev.*, **75,** 370.

Le Couteur, K. J., 1950, *Proc. Phys. Soc.* A, **63,** 259.

Perkins, D. H., 1949, *Phil. Mag.*, **40,** 601.

Rosenfeld, L., 1948, *Nuclear Forces* (Amsterdam: North Holland Publishing Co.), p. 266.

Weisskopf, J., 1937, *Phys. Rev.*, **52,** 295.

The Evaporation Theory of Nuclear Disintegrations

By K. J. Le COUTEUR*
University of Manchester

Communicated by P. M. S. Blackett; MS. received 15*th August* 1949

ABSTRACT. The relationship between nuclear temperature and excitation energy is discussed taking into account the thermal expansion of the nucleus and the effect of the neutron excess. Using these results, the evaporation theory is put into a form suitable for the treatment of highly excited nuclei. The competition between the emission of proton, neutron, deuteron, triton and α-particle is considered in detail, using Weisskopf's method of detailed balance.

Detailed numerical values are calculated for the disintegrations of silver bromine observed in photographic plates. The main points of comparison with experiment are (i) the energy distribution of the evaporated particles, and (ii) the ratio of emission of singly and doubly charged particles. The comparison yields close information about the relationship of nuclear energy and temperature; the agreement with theory is as good as can be expected. It is necessary to assume that the Coulomb potential barrier is reduced at high excitation energies.

§ 1. INTRODUCTION

NUCLEAR disintegrations of high energy, initiated by cosmic rays, have been studied extensively by the photographic emulsion technique. The recent papers of Harding, Lattimore and Perkins (1949), referred to as H.L.P., and Page (1950) contain sufficient statistical evidence to provide an effective test of some points of nuclear theory.

The early work on disintegration stars was reviewed by Bagge (1943). From this and subsequent researches (H.L.P.) it has been recognized that the emitted particles can be divided roughly into two groups, namely (i) a few particles of high energy, and (ii) a greater number of slow particles with an energy spectrum typical of nuclear evaporation. Of course there is no clear-cut distinction between the groups; if the energy spectrum is plotted (i) appears as a high energy tail added to (ii). Qualitatively it is clear that the fast particles must consist of nucleons which have come into direct collision with the primary particle, often a fast neutron, initiating the star, and of mesons created as the Bremsstrahlung of these collisions. The theory of such processes is not yet in a satisfactory state, for example Zwanikken (1948) shows that the static nuclear forces cannot account for the large energy transfer from the primary particle to the nucleus: presumably the difference must be attributed to velocity dependent forces of which little is known. Before finally escaping, these fast particles must lose energy to the nucleus and so leave it in a highly excited state. Further particles are emitted until the final nucleus is stable; it is these secondary particles which one attempts to treat by nuclear evaporation theory.

The statistical treatment of nuclear disintegrations, initiated by Bohr and Kalckar (1937) and amplified by Bethe (1937) and Weisskopf (1937), can be applied to the secondary process (Bagge 1938, H.L.P.) and leads to definite predictions. But the excitation energies involved in large stars are very much higher than those envisaged by the theory, which assumes that the excited nucleus is always in approximate thermodynamic equilibrium. This requires that the interval between the emission of successive particles is longer than the time required for the convection of energy across the nucleus. This condition is probably satisfied since, for all but the largest stars, the mean kinetic energy of the evaporated particles (perhaps 13 MeV.) is much less than the kinetic energy ($\simeq$22 MeV.) of the nucleons at the top of the zero-point Fermi distribution, which is mainly responsible for the convection of energy. There is also the requirement that the excitation energy should be much less than the total binding energy of the nucleus. For this reason, dealing with the stars created in silver and bromine with an average mass number of 100, it has not been thought worth while to extend the calculations to excitation energies above 600 MeV. Though this figure is a high one, it must be remembered that the nucleus cools down as particles are emitted so that most of the particles are emitted when the excitation energy is much lower and under conditions to which evaporation theory may be applied. Because of these limitations, one should not apply evaporation theory to stars with more than about 14 prongs. On the other hand, in photographic emulsions, stars with less than 7 prongs may originate in the light elements and so cannot be compared with the theory. However there remains a useful range of star sizes and the greater part of the experimental evidence actually falls within this range. H.L.P. have verified that, for such stars, the particles are emitted with random direction as would be expected for an evaporation process.

---

* Now at University of Liverpool.

Much of the experimental evidence to which reference has been made was derived from photographic plates which, for various reasons, were insensitive to fast particles. Energies above 40 MeV. were not measured by Page. Thus the available data chiefly concern the secondary particles which are best treated by evaporation theory. The main features which can be compared with experiment are (i) the energy distribution of the evaporated particles, (ii) the relative numbers of particles of charge e and charge $2e$. Much more experimental evidence exists for (ii) than for (i) because different charges can be distinguished at sight whereas energy measurements are difficult. By combining both types of evidence one obtains fairly precise information about some of the basic parameters of nuclear disintegration.

The most important relationship of nuclear thermodynamics is that connecting the temperature τ and excitation energy U. The 'Fermi gas' model, corrected by Bardeen's (1937) method, has been used and is discussed in § 2 where it is extended to take account of the thermal expansion of the nucleus and of the neutron excess. It is reasonable to use something resembling a free particle model at these high excitation energies. The alternative 'liquid drop' model (Bethe 1937) is not very suitable for high excitation as it gives $U = a\tau^{7/3} + b\tau^4$ and, since the number of degrees of freedom is only 3A this formula must be restricted to low values of τ. It could be amended by Debye's method and the 'critical temperature' is found to be about 15 MeV.; as appreciable corrections are required at less than half the critical energy the method is not very attractive. The 'liquid drop' formula, without emendation, was tested by H.L.P. and found to be unsatisfactory.

The theory has been used to calculate the expected numbers of evaporated neutrons, protons, deuterons and ^{3}H, ^{3}He and ^{4}He nuclei. Heavier particles could be considered but the emission probabilities are quite small. Weisskopf's (1937) method is to derive the differential emission probabilities by consideration of detailed balance in a state of thermodynamic equilibrium. With the assumption that, apart from the well-known dependence upon energy and upon the Coulomb barrier, all these particles have the same cross section for capture by the residual nucleus, it is not necessary to introduce explicit factors to represent the 'probability of existence' of compound particles within the nucleus. It would not be possible to obtain agreement with the observed ratio of singly and doubly charged particles if further small factors for the existence of α-particle and triton were introduced into the formulae.

§ 2. THE STATISTICAL MODEL OF EXCITED NUCLEI

2.1 *The Hartree Approximation*

The thermodynamics of an excited nucleus is completely determined if the total energy is known as a function of the temperature and volume. From this information, together with the boundary condition of zero external pressure, one can for example determine the equilibrium volume or radius at any temperature. In principle it should be possible to derive these quantities directly from the nuclear forces, but in practice, even for the ground state of the nucleus, the calculations are not very reliable.

While the statistical mechanics of a number of independent particles in a fixed field of force is well known, the mechanics of particles in interaction hardly exists. Therefore to proceed with the problem it is necessary to adopt Hartree's approximation and assume that the force between nucleons can be represented by an average potential field. Then the different nucleons are supposed to occupy individual quantum states in the field and, at any nuclear temperature τ (measured in energy units), the probable number n_s of particles in the sth state is given by Fermi's formula

$$n_s = \frac{1}{\exp\{(\epsilon_s - \epsilon')/\tau\} + 1}, \qquad \ldots\ldots(1)$$

where ϵ_s is the energy of the state and ϵ' is the Fermi energy. Use of this result involves the assumption that the Hartree field is unchanged by small changes in the occupation numbers n_s. In the nuclear problem there is some justification for this step since only very low temperatures are considered and so only a few particles at the top of the zero-point Fermi distribution can be excited; this should not greatly change the mean potential field which is chiefly due to the particles in the lower part of the distribution. This use of a Hartree approximation leads to a close resemblance between the calculations for excited nuclei and the well-known calculation for the ground state of the nucleus (Bethe and Bacher 1936, Rosenfeld 1948).

It is necessary to sum various functions over the distribution (1); by introducing the density in energy $g(\epsilon)$ of the individual quantum states their sums may be written as

$$Q(\tau) = \Sigma_s \frac{q_s}{\exp\{(\epsilon_s - \epsilon')/\tau\} + 1} = \int_{\epsilon_-}^{\infty} \frac{q(\epsilon) g(\epsilon) d\epsilon}{\exp\{(\epsilon - \epsilon')/\tau\} + 1}, \qquad \ldots\ldots(2)$$

where ϵ_- is the energy of the lowest individual state. The integral can be evaluated by Sommerfeld's method by splitting the range of integration at ϵ' and the result is

$$Q(\tau) = \int_{\epsilon_-}^{\epsilon'} qg\, d\epsilon + \frac{\tau^2 \pi^2}{6} \left(\frac{dqg}{d\epsilon}\right)_{\epsilon=\epsilon'} + \tau^4 \frac{7\pi^4}{360} \left(\frac{d^3 qg}{d\epsilon^3}\right)_{\epsilon=\epsilon'} + \ldots . \qquad \ldots\ldots(3)$$

ϵ' is itself dependent on τ; if ϵ_0 is the value of ϵ' at zero temperature one has, neglecting terms proportional to τ^4 and higher powers of τ,

$$Q(\tau)=\int_{\varepsilon_-}^{\varepsilon_0} qg\,d\epsilon+(\epsilon'-\epsilon_0)(qg)_{\varepsilon_0}+\frac{\tau^2\pi^2}{6}\left(q\frac{dg}{d\epsilon}+g\frac{dq}{d\epsilon}\right)_{\varepsilon=\varepsilon_0}. \qquad \ldots\ldots(4)$$

The value of $\epsilon'-\epsilon_0$ is fixed by the condition that, since the total number of particles is fixed, the special choice $q=1$ must lead to $Q(\tau)=Q(0)$. Therefore (4) reduces to

$$Q(\tau)=Q_0+\frac{\tau^2\pi^2}{6}g_0\left(\frac{dq}{d\epsilon}\right)_0, \qquad \ldots\ldots(5)$$

with $Q_0=Q(0)$ etc. It also follows that $\epsilon'-\epsilon_0$ is of order τ^2. In particular by putting $q=\epsilon$ one obtains the total energy as a function of temperature,

$$E(\tau)=E_0+\frac{\tau^2\pi^2}{6}g_0. \qquad \ldots\ldots(6)$$

In this approximation the dependence of $E(\tau)$ on the volume of the nucleus appears as a dependence on the extensive parameter, x say, which fixes the linear scale of the Hartree field; it is sometimes convenient to denote this explicitly by writing E as $E(\tau,x)$. Then from (6), one obtains the free energy $F(\tau,x)$ as

$$F(\tau,x)=E_0(x)-\frac{\tau^2\pi^2}{6}g_0(x). \qquad \ldots\ldots(7)$$

In the absence of external pressure, at temperature τ the equilibrium value x_τ of x must satisfy the condition

$$\frac{dF(\tau,x)}{dx}=\frac{dE_0(\tau,x)}{dx}-\frac{\tau^2\pi^2}{6}\frac{dg_0(x)}{dx}=0, \qquad \ldots\ldots(8)$$

and so, if x_0 is the value of x_τ for the ground state,

$$x_\tau-x_0=\frac{\tau^2\pi^2}{6}\left(\frac{dg_0(x)/dx}{d^2E_0(x)/dx^2}\right). \qquad \ldots(9)$$

This is the law of linear expansion for the nucleus.

It remains to calculate $g_0(x)$ and $E_0(x)$ which requires a more specific approximation. With plane wave functions and a Gaussian potential, $g_0(x)$ has been calculated by Bardeen (1937) and (d^2E_0/dx^2) by Bethe (1937, equation 318). (d^2E_0/dx^2) determines the compressibility of nuclear matter and, according to Feenberg (1947), can to some extent be checked by an examination of nuclear regularities. It is necessary to extend Bardeen's work a little to take account of the volume expansion and to apply it to nuclei with unequal numbers N and Z of neutrons and protons. It is found that the expression for $g_0(x)$ can be put into a more simple form by a method equivalent to use of the virial theorem.

2.2 *Plane Wave Approximation*

The individual wave functions are approximated by plane waves periodic in a box of volume $v=4\pi R^3/3$ equal to that of the nucleus. In terms of the wave number k the density of individual states of proton or neutron is

$$g(\epsilon)=\frac{v}{\pi^2}k^2\frac{dk}{d\epsilon}. \qquad \ldots\ldots(10)$$

With N and Z unequal it is necessary to replace ϵ' by two parameters ϵ_{n} and ϵ_{p} given by

$$N = \frac{v}{\pi^2}\int \frac{k^2 dk}{\exp\{(\epsilon-\epsilon_{\mathrm{n}})/\tau\}+1}, \qquad Z = \frac{v}{\pi^2}\int \frac{k^2\, dk}{\exp\{(\epsilon-\epsilon_{\mathrm{p}})/\tau\}+1}, \qquad \ldots\ldots(11)$$

and so at zero temperature all states are occupied which have wave numbers below

$$k_{\mathrm{n}0} = k_0 n^{1/3} \quad \text{and} \quad k_{\mathrm{p}0} = k_0 p^{1/3}, \qquad \ldots\ldots(12)$$

where $$n = 2N/A, \quad p = 2Z/A \quad \text{and} \quad N+Z = A = 2vk_0{}^3/3\pi^2. \qquad \ldots\ldots(13)$$

In the ground state the total potential energy of the nuclear forces (strictly the volume contribution only),

$$V = V_{\mathrm{pn}} + \tfrac{1}{4}V_{\mathrm{pp}} + \tfrac{1}{4}V_{\mathrm{nn}}, \qquad \ldots\ldots(14)$$

is determined from certain 'mixed densities' of the form

$$\rho_{\mathrm{n}}(\mathbf{r}_1, \mathbf{r}_2) = \frac{1}{v}\Sigma_s \exp\{i\mathbf{k}\,.\,(\mathbf{r}_1-\mathbf{r}_2)\} = \left(\frac{\sin kr - kr\cos kr}{\pi^2 r^3}\right)_{\mathrm{n}0}, \qquad \ldots\ldots(15)$$

with $r = |\mathbf{r}_1 - \mathbf{r}_2|$, by equations ($\alpha, \beta = n$ or p)

$$V_{\alpha\beta} = \int \rho_\alpha(\mathbf{r}_1, \mathbf{r}_2) J_{\alpha\beta}(\mathbf{r}_1, \mathbf{r}_2)\rho_\beta(\mathbf{r}_1, \mathbf{r}_2)\, d^3r_1\, d^3r_2. \qquad \ldots\ldots(16)$$

In this equation J_{pn} represents the mean proton–neutron interaction after the spin summation has been carried out, J_{pp} and J_{nn} have similar interpretations. Thus the expectation value of the total energy $\epsilon_{\mathrm{p}}(k)$ of a proton of wave number k is

$$\begin{aligned}\epsilon_{\mathrm{p}}(k) &= \frac{\hbar^2}{2M}k^2 + \int e^{ikr}J_{\mathrm{pn}}(r)\rho_{\mathrm{n}}(r)\, d^3r + \tfrac{1}{2}\int e^{ikr}J_{\mathrm{pp}}(r)\rho_{\mathrm{p}}(r)\, d^3r \\ &= \frac{\hbar^2}{2M}k^2 + \int \frac{\sin kr}{kr}J_{\mathrm{pn}}\rho_{\mathrm{n}}\, d^3r + \tfrac{1}{2}\int \frac{\sin kr}{kr}J_{\mathrm{pp}}\rho_{\mathrm{p}}\, d^3r. \qquad \ldots\ldots(17)\end{aligned}$$

Then $$\left(\frac{d\epsilon}{dk}\right)_{\mathrm{p}0} = \frac{\hbar^2}{M}k_{\mathrm{p}0} - \left(\frac{\pi}{k_{\mathrm{p}0}}\right)^2 \int (\rho_{\mathrm{p}}J_{\mathrm{pn}}\rho_{\mathrm{n}} + \tfrac{1}{2}\rho_{\mathrm{p}}J_{\mathrm{pp}}\rho_{\mathrm{p}})r^2\, d^3r, \qquad \ldots\ldots(18)$$

and

$$\left(k^2\frac{d\epsilon}{dk}\right)_{\mathrm{p}0} + \left(k^2\frac{d\epsilon}{dk}\right)_{\mathrm{n}0} = \frac{\hbar^2}{M}(k_{\mathrm{p}0}^3 + k_{\mathrm{n}0}{}^3) - 2\pi^2\int (\rho_{\mathrm{p}}J_{\mathrm{pn}}\rho_{\mathrm{n}} + \tfrac{1}{4}\rho_{\mathrm{p}}J_{\mathrm{pp}}\rho_{\mathrm{p}} + \tfrac{1}{4}\rho_{\mathrm{n}}J_{\mathrm{nn}}\rho_{\mathrm{n}})r^2\, d^3r. \qquad \ldots\ldots(19)$$

For a Gaussian potential

$$J_{\mathrm{pn}} = -B\exp(-r^2/a^2), \qquad J_{\mathrm{pp}} = J_{\mathrm{nn}} = -C\exp(-r^2/a^2), \qquad \ldots\ldots(20)$$

the last equation, after multiplication by $v/3\pi^2$, takes the simple form

$$Z\left(\frac{d\epsilon}{k\,dk}\right)_{\mathrm{p}0} + N\left(\frac{d\epsilon}{k\,dk}\right)_{\mathrm{n}0} = \frac{\hbar^2}{M}(Z+N) + \frac{2}{3}\left(\frac{\partial V}{\partial a^{-2}}\right)_{R\ \mathrm{const.}} \qquad \ldots\ldots(21)$$

Bethe and Bacher express V in terms of a parameter $x = ak \propto a/R$ and then

$$\left(\frac{\partial V}{\partial a^{-2}}\right)_R = -a^4\left(\frac{\partial V}{\partial a^2}\right)_R = -a^2x^2\frac{\partial V}{\partial x^2}.$$

Thus $$\frac{Z}{A}\left(\frac{d\epsilon}{k\,dk}\right)_{\mathrm{p}0} + \frac{N}{A}\left(\frac{d\epsilon}{k\,dk}\right)_{\mathrm{n}0} = \frac{\hbar^2}{M}\left(\frac{Z+N}{A}\right) - \frac{2}{3A}a^2x^2\frac{\partial V}{\partial x^2}. \qquad \ldots\ldots(22)$$

Since the range of the force is fixed, x is an extensive parameter for the nucleus. Therefore, if T is the total kinetic energy, the value of $\partial V/\partial x^2$ for the ground state follows at once from

$$\frac{d}{dx^2}(T+V)=0 \quad \text{for} \quad x=x_0. \qquad \ldots\ldots(23)$$

Now

$$T=\frac{3}{5}\frac{\hbar^2}{2M}(Nk_{\mathrm{n}0}^2+Zk_{\mathrm{p}0}^2)=\frac{3\hbar^2 A}{20M}(n^{5/3}+p^{5/3})k_0^2, \qquad \ldots\ldots(24)$$

which gives for $x=x_0$,

$$-\frac{2}{3A}a^2x^2\frac{\partial V}{\partial x^2}=\frac{2x^2}{3A}\frac{\partial T}{\partial k_0{}^2}=\frac{x^2}{5}\frac{\hbar^2}{M}\left(\frac{n^{5/3}+p^{5/3}}{2}\right).$$

Thus

$$\left(\frac{d\epsilon}{k\,dk}\right)_{\mathrm{n}0}=\frac{\hbar^2}{M}(1+\tfrac{1}{5}x_0{}^2n^{2/3})=\frac{\hbar^2}{M}\gamma_{\mathrm{n}}. \qquad \ldots\ldots(25)$$

With $n=p=1$, this reduces to

$$\gamma=1+\tfrac{1}{5}x_0{}^2, \qquad \ldots\ldots(26)$$

which, because of (23), is equivalent to Bardeen's more complicated expression. By inserting (25) into (10), the basic result (6) for $E(\tau)$ can be written explicitly as

$$E(\tau)=E_0+\frac{\tau^2\pi^2}{6}\frac{v}{\pi^2}\frac{M}{\hbar^2}k_0\left(\frac{n^{1/3}}{\gamma_{\mathrm{n}}}+\frac{p^{1/3}}{\gamma_{\mathrm{p}}}\right),$$

$$=E_0+\frac{\tau^2\pi^2 A}{4\zeta}\left(\frac{n^{1/3}}{2\gamma_{\mathrm{n}}}+\frac{p^{1/3}}{2\gamma_{\mathrm{p}}}\right), \qquad \ldots\ldots(27)$$

where $\zeta=(\hbar^2k_0/2M)$ is the kinetic energy corresponding to k_0, empirically $\zeta\simeq 22$ MEV. With $\gamma_{\mathrm{n}}=\gamma_{\mathrm{p}}=1$, equation (27) reduces to Bethe's formula for the free particle model.

2.3 *The Coefficient of Expansion*

To determine the expansion from (9) one needs dg_0/dx which must be calculated from (22) as it is not permissible to differentiate (25). It is sufficient to consider only the simple case $n=p=1$. Then

$$g_0=\frac{3A}{2k_0{}^2}\left(\frac{k\,dk}{d\epsilon}\right)_0=\frac{3Aa^2}{2x^2}\left(\frac{k\,dk}{d\epsilon}\right)_0.$$

So

$$\frac{1}{g_0}=\frac{2}{3A}\left(\frac{\hbar^2x^2}{Ma^2}-\frac{x^3}{3A}\frac{\partial V}{\partial x}\right).$$

Also

$$E=A\left(\frac{3\hbar^2}{10Ma^2}x^2+\frac{V}{A}\right).$$

Bethe and Bacher give

$$\frac{V}{A}=-\pi^{-\frac{1}{2}}(B+\tfrac{1}{2}C)x^{-3}\{2-3x^2+(x^2-2)\exp(-x^2)+\pi^{\frac{1}{2}}x^3\Phi(x)\}.$$

Then, with $D=Ma^2(B+\frac{1}{2}C)/\hbar^2$,

$$\left[\frac{d}{dx}\left(\frac{1}{g}\right)\Big/\frac{d^2E}{dx^2}\right]_0=\frac{2}{3A^2}\left\{\frac{2x+\pi^{-\frac{1}{2}}D[1+2x^{-2}-\exp(-x^2)(3+2x^{-2}+2x^2)]}{\frac{3}{5}+\pi^{-\frac{1}{2}}D\,6\,[x^{-3}-4x^{-5}+\exp(-x^2)(3x^{-3}+4x^{-5}+x^{-1})]}\right\}$$

$$=\frac{2\mu}{3A^2}. \qquad \ldots\ldots(28)$$

Hence
$$\left(\frac{dg_0/dx}{d^2E/dx^2}\right)_0 = -g_0{}^2\frac{2\mu}{3A^2} = -\frac{6\mu}{(4\zeta\gamma)^2}.$$

There (9) gives the law of expansion as
$$\frac{R-R_0}{R_0} = -\frac{(x_\tau - x_0)}{x_0} = \frac{\tau^2\pi^2}{(4\zeta\gamma)^2}\frac{\mu}{x_0}. \qquad \ldots\ldots(29)$$

For convenience this result is stated as an expansion of the mean nuclear radius but, since it is derived from the simple statistical model, it must be understood as giving the change of mean density of the nucleus with increase of temperature.

2.4 *The Excitation Energy*

The excitation energy $U(\tau)$ required to raise the nucleus to temperature τ is defined as
$$U(\tau) = E(\tau, x_\tau) - E(0, x_0). \qquad \ldots\ldots(30)$$

Now, according to (8),
$$F(\tau, x_\tau) = F(\tau, x_0) + \mathrm{O}(\tau^4). \qquad \ldots\ldots(31)$$

Thus
$$E(\tau, x_\tau) = E(0, x_0) + \frac{\tau^2\pi^2}{6}(2g_0(x_\tau) - g_0(x_0)) + \mathrm{O}(\tau^4)$$
$$= E(\tau, x_0) + \mathrm{O}(\tau^4), \qquad \ldots\ldots(32)$$

since $g_0(x_\tau) - g_0(x_0)$ is of the order τ^2. Therefore, from (30) and (27),
$$U(\tau) = \tau^2\frac{\pi^2 A}{4\zeta}\left(\frac{n^{1/3}}{2\gamma_{\mathrm{n}}} + \frac{p^{1/3}}{2\gamma_{\mathrm{p}}}\right). \qquad \ldots\ldots(33)$$

Since $n-1=(N-Z/A)=\theta$ is small, it is convenient to expand the right-hand side in powers of θ. From (25) and (26),
$$\left(\frac{n^{1/3}}{2\gamma_{\mathrm{n}}} + \frac{p^{1/3}}{2\gamma_{\mathrm{p}}}\right) = \frac{1}{\gamma}\left\{1 - \frac{\theta^2}{9}\left(1 + \frac{x^2}{5\gamma} - \frac{4x^4}{25\gamma^2}\right)\right\}. \qquad \ldots\ldots(34)$$

Also ζ and γ depend on $x_0{}^2$ which is itself dependent on θ. According to Bethe and Bacher (1936) *, the nuclear radius is given by
$$R = r_0 A^{1/3}(1 + 0{\cdot}5\,\theta^2), \qquad \ldots\ldots(35)$$

so that, if $\bar{x}_0$ is the value of x_0 corresponding to $\theta = 0$ and $\bar{\zeta}, \bar{\gamma}$ the corresponding ζ, γ,
$$x_0 = \bar{x}_0(1 - 0{\cdot}5\,\theta^2)$$

and
$$\frac{\bar{\zeta}\bar{\gamma}}{\zeta\gamma} = \frac{\bar{x}_0{}^2(1+\frac{1}{5}\bar{x}_0{}^2)}{x_0{}^2(1+\frac{1}{5}x_0{}^2)} = 1 + \theta^2\left(1 + \frac{x_0{}^2}{5\gamma}\right). \qquad \ldots\ldots(36)$$

---

* The numerical coefficient 0·5 in (35) is less than the coefficient 0·66 given by Bethe and Bacher; the smaller value is obtained by taking account of the forces between like particles. According to Bethe and Bacher, the interaction parameters must satisfy $B + \frac{1}{2}C = 70$ Mev., also Rosenfeld (1948, § 11.11, Table 2) states that in a charge-independent theory B and C must be equal. Thus we take $B = C = 47$ Mev. These parameters lead to the value $\beta' = 22$ Mev. for the coefficient (equation (43) below) which expresses the dependence of binding energy on isotopic number. This agrees better with the empirical value, 20·5 Mev., than does that derived by Bethe and Bacher with weaker forces between like particles. Since the parameter y, introduced in (38), is very closely related to β', it can be assumed that y also is given fairly accurately by the theory.

Therefore the final result is, from (33), (34), (36),

$$U(\tau,\theta)=\frac{\tau^2\lambda^2}{4}(1+\theta^2 y)=\frac{\tau^2\Lambda^2}{4} \qquad \ldots\ldots(37)$$

with
$$y=1+\frac{x_0{}^2}{5\gamma}-\frac{1}{9}\left(1+\frac{x_0{}^2}{5\gamma}-\frac{4x_0{}^4}{25\gamma^2}\right)\simeq 2-\frac{1}{\gamma} \qquad \ldots\ldots(38)$$

and
$$\lambda^2=\pi^2 A/\bar{\zeta}\bar{\gamma}. \qquad \ldots\ldots(39)$$

The entropy S, of the nucleus is given by

$$S(\tau,\theta)=\int_0^\tau \frac{dU}{\tau}=\tfrac{1}{2}\tau\Lambda^2=\Lambda\sqrt{U}, \qquad \ldots\ldots(40)$$

and, according to Bethe (1937, equation 281), the density ρ of the nuclear levels and the average spacing D between levels are given by

$$D(U)=\frac{1}{\rho(U)}=\tau\left(2\pi\frac{dU}{d\tau}\right)^{1/2}e^{-S}$$
$$=\left(\frac{8\pi}{\Lambda}\right)^{1/2}U^{3/4}e^{-S}. \qquad \ldots\ldots(41)$$

Λ is the most important parameter of nuclear thermodynamics.

2.5 *Numerical Values and Discussion*

The nuclear radius R is taken as $R=r_0A^{1/3}$ with $r_0=1{\cdot}47\times10^{-13}$ cm.; this leads to $\zeta=22$ MeV.

Rosenfeld (1948, p. 153) quotes $a=1{\cdot}9\times10^{-13}$ cm. for the range of the Gaussian potential as derived by analysis of two nucleon systems. This gives $x=1{\cdot}5a/r_0=1{\cdot}93$ and $\gamma=1{\cdot}75$.

The present work has been carried out with the Hartree model for large nuclei and it may be more consistent to use force parameters chosen so that this model yields the correct binding energy. Bethe and Bacher, using the first approximation only, arrive at $x=2{\cdot}7$ which leads to $\gamma=2{\cdot}46$. This is probably an over-estimate since it is known that the method requires very strong force parameters; thus all that can be said is that γ should lie in the range 1·75 to 2·46.

The results of the theory have been expressed in terms of the ratio of energies $(\tau/\zeta\gamma)$ and one must regard $\zeta\gamma$ as the characteristic energy for thermal effects. Now the calculations deal only with the volume energy and could not easily be extended to include the surface energy in a rigorous way. But the latter is not negligible, for $A=80$ the volume energy is $-14{\cdot}46$ and the surface energy $+3{\cdot}58$ MeV. per nucleon. As a rough correction it seems reasonable to suppose that the surface contribution varies with energy in the same way as the volume contribution; from this point of view the characteristic energy $\zeta\gamma$ should be reduced in the ratio (total energy)/(volume energy), which for $A=80$ gives a factor 0·75. Leaving ζ unchanged this is equivalent to a reduction of γ from 2·46 to 1·85 or from 1·75 to 1·31.

We shall see that a value of γ of about 1·5, giving $\zeta\gamma=33$, is quite consistent with the data on disintegration stars and it also agrees reasonably well with the older data on nuclear reactions at low energy.

The degeneracy parameter for the Fermi statistics is, in effect, $\tau/\zeta\gamma$. Now, even for an excitation energy as high as 400 MeV., with $A=100$ and $\gamma=1{\cdot}5$, equation (37) gives $\tau\simeq 7$ MeV. so that $\tau/\zeta\gamma\simeq 0{\cdot}22$. Stoner (1936) has shown that for such small values of the parameter the error in the energy due to the neglect of terms in $(\tau/\zeta\gamma)^4$ etc. is negligible.

With Bethe's values, $x=2{\cdot}7$ and $D=9{\cdot}6$ equation (28) gives $\mu/x_0=4{\cdot}15$ and the law of expansion becomes

$$R=R_0\{1+0{\cdot}25(\tau/\zeta\gamma)^2\}. \qquad \ldots\ldots(42)$$

Thus in the above example with $\tau/\zeta\gamma\simeq 0{\cdot}2$, the expansion of the mean radius is about 10% corresponding to a reduction in mean density of 30%. Equation (38) now gives $y=1{\cdot}3$; with this value of y the dependence of $S(\tau,\theta)$ on θ is almost negligible in all applications.

So far nothing has been said about the Coulomb forces. For a given nuclear volume the total Coulomb energy is obviously independent of temperature, therefore equation (27) and the subsequent equations for the excitation energy remain true when the Coulomb interaction is taken into account. Strictly speaking, the Coulomb term should be included in the expression for d^2E/dx^2 used to calculate the expansion, but the effect is negligible.

§ 3. NUCLEAR EVAPORATION

3.1 *The Energy Balance*

It is necesssary to use the semi-empirical representation of the binding energy of a nucleus in its ground state

$$E_0(\theta)=\overline{E}+\beta' A\theta^2+\frac{3e^2}{5r_0}Z^2A^{-1/3} \qquad \ldots\ldots(43)$$

$$=-\alpha A+\beta A(\theta-\theta_{\mathrm{e}})^2. \qquad \ldots\ldots(44)$$

For values of A in the range 70–100 with which we are chiefly concerned, it is best to take $\alpha=8{\cdot}6$ MeV. The empirical value of β' is 20·5 MeV. which gives $\beta=23$ MeV. Also the value of θ for the most stable nucleus N_{e}, Z_{e} of mass A is well represented by the empirical formula

$$\theta_{\mathrm{e}}=A^{2/3}/(A^{2/3}+131) \qquad \ldots\ldots(45)$$

and, at $A=80$, this gives

$$d\theta_{\mathrm{e}}/dA=0{\cdot}0009 \quad \text{and} \quad dN_{\mathrm{e}}/dZ_{\mathrm{e}}=1{\cdot}5. \qquad \ldots\ldots(46)$$

Then from (44), one gets

$$\frac{\partial E_0(N,Z)}{\partial N}=-\alpha+2\beta_{\mathrm{n}}(\theta-\theta_{\mathrm{e}}), \qquad \frac{\partial E_0(N,Z)}{\partial Z}=-\alpha-2\beta_{\mathrm{p}}(\theta-\theta_{\mathrm{e}}), \qquad \ldots\ldots(47)$$

with

$$\beta_{\mathrm{n}}=\beta\left(1-A\frac{d\theta_{\mathrm{e}}}{dA}-\frac{\theta+\theta_{\mathrm{e}}}{2}\right)\simeq 0{\cdot}8\beta,$$

$$\beta_{\mathrm{p}}=\beta\left(1+A\frac{d\theta_{\mathrm{e}}}{dA}+\frac{\theta+\theta_{\mathrm{e}}}{2}\right)\simeq 1{\cdot}2\beta. \qquad \ldots\ldots(48)$$

Suppose that a nucleus a, with excitation energy U_a emits a fragment (n, z) leaving a residual nucleus b with excitation energy U_b. If the kinetic energy of the fragment is T and its binding energy is w, the energy relation is

$$U_a + E_0(a) = U_b + E_0(b) - w + T$$

or

$$U_b = U_a - Q(a, b) - T, \qquad \ldots\ldots(49)$$

where

$$Q(a, b) = \alpha(n+z) - 2(\theta - \theta_e)(n\beta_n - z\beta_p) - w \qquad \ldots\ldots(50)$$

is the threshold energy for emission from the nucleus of a fragment (n, z) with zero kinetic energy.

3.2 *The Emission Probabilities*

Weisskopf (1937) has derived a formula for the probability per unit time of emission of a particle with kinetic energy T from a nucleus a leaving a residual nucleus b,

$$P(T)\,dT = \gamma \frac{\sigma}{\sigma_0} \frac{T\rho(b)}{\rho(a)}\,dT, \qquad \ldots\ldots(51)$$

where $\gamma = \sigma_0 g m/\pi^2\hbar^3$ and ρ is the level density. Here g is the number of spin states and m the mass of the particle. σ_0 is the geometrical cross section of the residual nucleus and σ is the total cross section for capture of the particle by b. For neutral particles is it usual to assume $\sigma = \sigma_0$ but for positively charged particles the capture process is opposed by the Coulomb interaction; if V is the height of the potential barrier the classical theory gives

$$T\sigma/\sigma_0 = T - V, \qquad \ldots\ldots(52)$$

which in conjunction with (51) implies that particles of kinetic energy less than V cannot be emitted from the excited nucleus. Quantum mechanics leads to a larger cross section because charged particles can to some extent penetrate the potential barrier, thus one gets

$$T\sigma/\sigma_0 = T - V', \qquad 0 < V' < V. \qquad \ldots\ldots(53)$$

The theory has been worked out and applied to nuclear reactions by Bethe (1937) and Bethe and Konopinski (1938) and has been invoked by H.L.P. to account for the emission of low-energy charged particles from cosmic-ray stars. With this expression for σ, the emission probability becomes, after use of (41),

$$P(T)\,dT = \gamma(T - V')(U_b/U_a)^{-3/4} \exp(S_b - S_a)\,dT. \qquad \ldots\ldots(54)$$

To determine the total emission probability and mean energy of emission it is necessary to evaluate

$$\int_{V'}^{U_a - Q} (T - V')^n P(T)\,dT = \gamma U_a^{3/4} \exp(-S_a) \int_{V'}^{U_a - Q} U_b^{-3/4}(T - V')^{n+1} \exp S_b\,dT. \qquad \ldots\ldots(55)$$

With the notation $U - Q - V' = R = y_0^2$ and $U_b = y^2$ this becomes

$$2\gamma U_a^{3/4} \exp(-S_a) \int_0^{y_0} y^{-1/2}(y_0^2 - y^2)^{n+1} \exp(\Lambda y)\,dy$$

$$= 2\gamma U_a^{3/4} \exp(-S_a + \Lambda y_0) \int_0^{y_0} y_0^{n+1/2} 2^{n+1} x^{n+1} (1 - x/y_0)^{-1/2}$$

$$\times (1 - x/2y_0)^{n+1} \exp(-\Lambda x)\,dx,$$

with $x = y_0 - y$. The integration may be carried out after expansion of the binomial. Since $\Lambda \simeq 5$ terms in $\exp(-\Lambda y_0)$ may be neglected for $R > 1$ Mev. Thus, the emission probability per unit time is

$$P(T)\,dT = \int_{V'}^{U_a - Q} P(T)\,dT = 4\gamma U_a^{3/4} \exp(-S_a + \Lambda\sqrt{R}) \frac{R^{1/4}}{\Lambda^2}\left(1 + \frac{3}{4{y_0}^2\lambda^2} + \ldots\right). \qquad \ldots\ldots(56)$$

In this equation Λ must be calculated for the residual nucleus b. Similarly

$$\int_{V'}^{U_a - Q} (T - V')\,P(T)\,dT = 8\gamma U_a^{3/4} \exp(-S_a + \Lambda\sqrt{R}) \frac{R^{3/4}}{\Lambda^3}\left(2 - \frac{3}{y_0\Lambda} + \frac{3}{{y_0}^2\Lambda^2} \ldots\right). \qquad \ldots\ldots(57)$$

Thus the mean energy $\overline{T}$ of emission is given by

$$\overline{T} - V' = \frac{2R^{1/2}}{\Lambda}\left(2 - \frac{3}{y_0\Lambda} + \frac{3}{{y_0}^2\Lambda^2} + \ldots\right) \Big/ \left(1 + \frac{3}{4{y_0}^2\Lambda^2} \ldots\right)$$

or

$$\overline{T} = V' + \frac{4}{\Lambda}\sqrt{R} - \frac{6}{\Lambda^2} + \frac{3}{y_0\Lambda^3} + \ldots. \qquad \ldots\ldots(58)$$

The first term in this expression corresponds to the simple formula $\overline{T} = V' + 2\tau$, the correction term $6/\Lambda^2$ is relatively small. The terms involving negative powers of y_0 or R in (56) and (58) are negligible for $R > 1$ Mev,; since in any case the integrals behave in a perfectly regular way as $y_0 \to 0$ it is best to omit these terms altogether.

3.3 *Competition between Emission Processes*

The equations of § 3.2 can be used to determine the probability of emission of various types of particle from an excited nucleus. There is competition between the different possibilities; it is sufficient to consider only the emission of neutrons, protons, deuterons and ^3H, ^3He, ^4He nuclei which are respectively denoted by n, p, d, t, **t**, α.

According to (51) the relative weight factors γ are

$$\gamma_n = \gamma_p = \gamma_d, \qquad \gamma_t = \gamma_{\mathbf{t}} = 3\gamma_p, \qquad \gamma_\alpha = 2\gamma_p, \qquad \ldots\ldots(59)$$

and it will be seen that the factor 3 leads to an appreciable probability for triton emission.

The formulae of § (3.2) involve the parameter R_x which represents the excitation energy of the residual nucleus left after the excited nucleus a has emitted a particle x (n, p, ... α) with kinetic energy V_x'. It is useful to collect together the values R_x of $R = U - Q - V'$ as

$$\left.\begin{array}{ll} R_n = U_a - 8{\cdot}6 + 1{\cdot}6\beta(\theta - \theta_e) & R_t = U_a - 17{\cdot}4 + 0{\cdot}8\beta(\theta - \theta_e) - V_t', \\ R_p = U_a - 8{\cdot}6 - 2{\cdot}4\beta(\theta - \theta_e) - V_p' & R_{\mathbf{t}} = U_a - 18{\cdot}1 - 3{\cdot}2\beta(\theta - \theta_e) - V_{\mathbf{t}}', \\ R_d = U_a - 15 - 0{\cdot}8\beta(\theta - \theta_e) - V_d' & R_\alpha = U_a - 6{\cdot}2 - 1{\cdot}6\beta(\theta - \theta_e) - V_\alpha'. \end{array}\right\} \qquad \ldots\ldots(60)$$

Also if the initial nucleus a is A, θ the Λ values for the various residual nuclei are, with $\Lambda = \Lambda(A-1, \theta)$,

$$\left.\begin{aligned} \Lambda_{\mathrm{n}} &= \Lambda(1 - y\theta/A) & \Lambda_{\mathrm{t}} &= \Lambda(1 - 1/A - y\theta/A), \\ \Lambda_{\mathrm{p}} &= \Lambda(1 + y\theta/A) & \Lambda_{\mathbf{t}} &= \Lambda(1 - 1/A + y\theta/A), \\ \Lambda_{\mathrm{d}} &= \Lambda(1 - 1/2A) & \Lambda_{\alpha} &= \Lambda(1 - 3/2A). \end{aligned}\right\} \qquad \ldots\ldots(61)$$

Now from (56), the relative probabilities of neutron and proton emission from the excited nucleus are

$$\frac{P_{\mathrm{n}}}{P_{\mathrm{p}}} = \left(\frac{R_{\mathrm{n}}}{R_{\mathrm{p}}}\right)^{1/4} \left(\frac{\Lambda_{\mathrm{p}}}{\Lambda_{\mathrm{n}}}\right)^{2} \exp\left(\Lambda_{\mathrm{n}}\sqrt{R_{\mathrm{n}}} - \Lambda_{\mathrm{p}}\sqrt{R_{\mathrm{p}}}\right) \qquad \ldots\ldots(62)$$

and

$$\begin{aligned} \Lambda_{\mathrm{n}}\sqrt{R_{\mathrm{n}}} - \Lambda_{\mathrm{p}}\sqrt{R_{\mathrm{p}}} &= \tfrac{1}{2}(\Lambda_{\mathrm{n}} + \Lambda_{\mathrm{p}})(\sqrt{R_{\mathrm{n}}} - \sqrt{R_{\mathrm{p}}}) + \tfrac{1}{2}(\Lambda_{\mathrm{n}} - \Lambda_{\mathrm{p}})(\sqrt{R_{\mathrm{n}}} + \sqrt{R_{\mathrm{p}}}) \\ &= \frac{\Lambda_{\mathrm{n}} + \Lambda_{\mathrm{p}}}{4\sqrt{R_{\mathrm{np}}}}(R_{\mathrm{n}} - R_{\mathrm{p}}) + (\Lambda_{\mathrm{n}} - \Lambda_{\mathrm{p}})\sqrt{R_{\mathrm{np}}}, \qquad \ldots\ldots(63) \end{aligned}$$

where R_{np} is defined by $\sqrt{R_{\mathrm{n}}} + \sqrt{R_{\mathrm{p}}} = 2\sqrt{R_{\mathrm{np}}}$. ......(64)

The factor $(R_{\mathrm{n}}/R_{\mathrm{p}})^{1.4}$ in (62) may be expressed as $\exp(R_{\mathrm{n}} - R_{\mathrm{p}}/4R_{\mathrm{np}})$ and, since $\Lambda \simeq 5$, is always negligible in comparison with the last factor. The terms which appear in (63) may be taken from (60) and (61) and so the relative emission probabilities take the form

$$\frac{P_{\mathrm{n}}}{P_{\mathrm{p}}} = \exp\left\{\frac{\Lambda}{\sqrt{R_{\mathrm{np}}}}\left[2\beta(\theta - \theta_{\mathrm{e}}) + \tfrac{1}{2}V_{\mathrm{p}}' - 2y\frac{\theta}{A}R_{\mathrm{np}}\right]\right\}, \qquad \ldots\ldots(65\,a)$$

$$\frac{P_{\mathrm{d}}}{P_{\mathrm{p}}} = \exp\left\{\frac{\Lambda}{\sqrt{R_{\mathrm{dp}}}}\left[-3{\cdot}2 + 0{\cdot}8\beta(\theta - \theta_{\mathrm{e}}) + \tfrac{1}{2}(V_{\mathrm{p}}' - V_{\mathrm{d}}') - \left(\frac{1}{2A} + y\frac{\theta}{A}\right)R_{\mathrm{dp}}\right]\right\}, \qquad \ldots\ldots(65\,b)$$

$$\frac{P_{\mathrm{t}}}{P_{\mathrm{p}}} = 3\exp\left\{\frac{\Lambda}{\sqrt{R_{\mathrm{tp}}}}\left[-4{\cdot}4 + 1{\cdot}6\beta(\theta - \theta_{\mathrm{e}}) + \tfrac{1}{2}(V_{\mathrm{p}}' - V_{\mathrm{t}}') - \left(\frac{1}{A} + 2y\frac{\theta}{A}\right)R_{\mathrm{tp}}\right]\right\}, \qquad \ldots\ldots(65\,c)$$

$$\frac{P_{\mathbf{t}}}{P_{\mathrm{p}}} = 3\exp\left\{\frac{\Lambda}{\sqrt{R_{\mathbf{t}\mathrm{p}}}}\left[-4{\cdot}7 - 0{\cdot}4\beta(\theta - \theta_{\mathrm{e}}) + \tfrac{1}{2}(V_{\mathrm{p}}' - V_{\mathbf{t}}') - \frac{1}{A}R_{\mathbf{t}\mathrm{p}}\right]\right\}, \qquad \ldots\ldots(65\,d)$$

$$\frac{P_{\alpha}}{P_{\mathrm{p}}} = 2\exp\left\{\frac{\Lambda}{\sqrt{R_{\alpha\mathrm{p}}}}\left[1{\cdot}2 + 0{\cdot}4\beta(\theta - \theta_{\mathrm{e}}) + \tfrac{1}{2}(V_{\mathrm{p}}' - V_{\alpha}') - \left(\frac{3}{2A} + y\frac{\theta}{A}\right)R_{\alpha\mathrm{p}}\right]\right\}. \qquad \ldots\ldots(65\,e)$$

The interpretation of the terms in these emission ratios is of interest as some of them represent strange effects which are important only at high energies. Thus equation (65 *a*) shows at once that

(i) the potential barrier V favours neutron emission,

(ii) the term $2\beta(\theta - \theta_{\mathrm{e}}) = 92(N - N_{\mathrm{e}})/A$ favours neutron or proton emission according as $N - N_{\mathrm{e}}$ is positive or negative. It thus acts as a 'governor' controlling the emission in such a way that $N - N_{\mathrm{e}}$ never becomes very large. This term arises because the energy available for emission of particles is greatest if the isotopic number of the residual nucleus is that of maximum stability. In stars with several evaporated particles this effect requires that more neutrons than protons are emitted,

(iii) the term $-2y\theta R/A$ favours proton emission if θ is positive; thus it endeavours to increase the value of $|N-Z|$, reflecting the fact that the density of levels of the residual nucleus increases with $|N-Z|$.

The order of magnitude of $\frac{1}{2}V_p'$ is 1 to 3 Mev., depending on assumptions about the temperature dependence of the potential barrier; so for a nucleus of $A \simeq 80$, the first and second terms become comparable when $N-N_e$ lies between 1 and 3. The third term is relatively small; with $y=1{\cdot}3$, $\theta=0{\cdot}13$ and $A=80$ it becomes $0{\cdot}4R/100$ and so becomes comparable with the first two only when $R_{np} > 300$ Mev.

The relative probability of α emission contains the term

$$(3/2A + y\theta/A)R \simeq 1{\cdot}67R/A$$

which is important because it increases with excitation energy. The contribution $3R/2A$ arises from the dependence of the level density of the residual nucleus upon its mass number, which discourages the emission of heavy particles. For excitations above 100 Mev., this is the most important single term determining P_α/P_p. It is obvious from the form of (65 *e*) that P_α/P_p has a rather flat maximum, which occurs at $R \simeq 100$ Mev.; this has the important consequence that over a considerable range of star sizes the ratio of α to proton emission from silver or bromine remains almost constant. In the absence of the term $3R/2A$, the ratio P_α/P_p would increase steadily with energy ultimately approaching the limit 2. Thus the ratio of α to proton emission would increase steadily with star size, very much in disagreement with experiment.

3.4 *Integration of the Equations of Emission*

The emission process is treated as a continuous one. The mean reduction in excitation due to emission of a particle of type x(x = n, p....) is given by (49) and (58) as

$$H_x = Q_x + V_x' + (4/\Lambda)\sqrt{R_x} - 6/\Lambda^2. \qquad ......(66)$$

Thus the mean number of particles emitted per unit drop of excitation is $(\bar{H})^{-1}$ where

$$\bar{H} = \frac{\Sigma_y H_y P_y}{\Sigma_y P_y} \qquad ....(67)$$

and the mean number of particles of type x emitted per unit drop of excitation

$$\delta n_x = \frac{P_x}{\bar{H}\Sigma_y P_y} = \frac{P_x/P_p}{\bar{H}\Sigma_y P_y/P_p}. \qquad ......(68)$$

Of course the right-hand side of this equation depends on what particles have already been emitted. We have here a set of six simultaneous integral equations governing the emission of the six kinds of particle considered; strictly speaking one should integrate these numerically, working downwards from the initial excitation energy, a separate integration being required for each value of the initial excitation. However the equations are coupled mainly through the θ terms in (65) and it is possible to arrive at an approximate solution for θ which is not very sensitive to the initial excitation energy. Then one has only to integrate the six independent emission equations rather than a set of six simultaneous equations.

3.5 *The Equation for the Neutron Excess*

The rate of change of $\theta=(N-Z)/A$ due to the emission of particles is

$$\frac{d\theta}{dt}=-\frac{1}{A}(P_{\mathrm{n}}-P_{\mathrm{p}}+P_{\mathrm{t}}-P_{\mathbf{t}})-\frac{\theta}{A}\frac{dA}{dt}. \qquad \ldots\ldots(69)$$

Let r be the total number of particles (n, p, d....) emitted by the nucleus up to the time when its excitation energy has fallen to U, then $dr/dt=\Sigma P_{\mathrm{x}}$ and

$$\frac{d\theta}{dr}=-\frac{1}{A}\frac{P_{\mathrm{n}}-P_{\mathrm{p}}+P_{\mathrm{t}}-P_{\mathbf{t}}}{\Sigma P_{\mathrm{x}}}-\frac{\theta}{A}\frac{dA}{dr}. \qquad \ldots\ldots(70)$$

Now $$\frac{P_{\mathrm{n}}-P_{\mathrm{p}}}{P_{\mathrm{n}}+P_{\mathrm{p}}}\simeq\tfrac{1}{2}\log\frac{P_{\mathrm{n}}}{P_{\mathrm{p}}} \quad\text{and}\quad \frac{P_{\mathrm{t}}-P_{\mathbf{t}}}{P_{\mathrm{t}}+P_{\mathbf{t}}}\simeq\tfrac{1}{2}\log\frac{P_{\mathrm{t}}}{P_{\mathbf{t}}}$$

are given by (65) and may be treated as equal. Then, with the notation,

$$a=(P_{\mathrm{n}}+P_{\mathrm{p}}+P_{\mathrm{t}}+P_{\mathbf{t}})/\Sigma P_{\mathrm{x}}=1-(P_{\mathrm{d}}+P_{\alpha})/\Sigma P_{\mathrm{x}}, \qquad \ldots\ldots(71)$$

one finds

$$\bar{H}\frac{d}{dU}(\theta-\theta_{\mathrm{e}})=-\frac{d}{dr}(\theta-\theta_{\mathrm{e}})$$

$$=\frac{a\Lambda}{2A\sqrt{R_{\mathrm{pn}}}}\left\{2\beta(\theta-\theta_{\mathrm{e}})+\tfrac{1}{2}V_{\mathrm{p}}'-2y\frac{\theta}{A}R_{\mathrm{np}}\right\}+\left(\frac{\theta}{A}+\frac{d\theta_{\mathrm{e}}}{dA}\right)\frac{dA}{dr}.$$

By writing

$$x=\sqrt{R_{\mathrm{pn}}},\quad \frac{H}{a}=p+qx \quad\text{and}\quad \frac{2A}{\Lambda}\left(\frac{\theta}{A}+\frac{d\theta_{\mathrm{e}}}{dA}\right)\frac{1}{a}\frac{dA}{dr}=-b, \qquad \ldots\ldots(72)$$

this becomes

$$(p+qx)\frac{d}{dx}2\beta(\theta-\theta_{\mathrm{e}})-\frac{2\beta\Lambda}{A}\{2\beta(\theta-\theta_{\mathrm{e}})-G(x)\}=0, \qquad \ldots\ldots(73)$$

where $$G(x)=bx+2y\theta x^2/A-\tfrac{1}{2}V_{\mathrm{p}}'. \qquad \ldots\ldots(74)$$

In equation (73) one can treat $p, q, \Lambda/A, \theta_{\mathrm{e}}/A$ as constants. Then, neglecting derivatives of G beyond the second, the solution is, with $\mu=2\beta\Lambda/Aq$,

$$2\beta(\theta-\theta_{\mathrm{e}})=J(x)+K(p+qx)^{\mu}, \qquad \ldots\ldots(75)$$

where $$J(x)=G(x)+\frac{(p+qx)}{q(\mu-1)}\frac{dG}{dx}+\frac{(p+qx)^2}{q^2(\mu-1)(\mu-2)}\frac{d^2G}{dx^2} \qquad \ldots\ldots(76)$$

and K is a parameter determined by the initial conditions.

In this form the solution is sufficiently general to take account of the increase of b with excitation energy and also of the possible decrease of the potential barrier V' with increasing energy. According to Bagge (1938), the potential barrier should fall off approximately linearly with increase of energy, that is $V=V_0-cx^2$.

With any given assumption about V and Λ one can estimate a, b, p, q, numerically by use of equations (65); then the solutions (76) can be worked out explicitly. Figure 1 shows results obtained in this way using various parameters (detailed in §4.1 below) and for several different values of the initial excitation energy. The coefficient q is rather larger than the value 4Λ suggested by (66) because as the energy is increased the emission of heavy particles becomes more probable, therefore $\overline{H}$ increases faster than H_n or H_p and a decreases with energy; both factors lead to a more rapid increase of $\overline{H}/a$ with energy.

The variation of $2\beta(\theta-\theta_e) \simeq N-N_e$ as the nucleus cools down is easily understood. To maintain the neutron–proton balance of the residual nucleus roughly 1·5 times as many neutrons as protons must be emitted during the evaporation. But, starting with $\theta=\theta_e$ at an initial excitation energy of say 400 MeV. ($x \simeq 20$), neutron and proton emission are at first about equally probable, therefore the neutron excess of the residual nucleus increases at first rapidly and then more slowly as the 'controlling term' comes into play; later when the excitation has fallen below about 100 MeV. the potential barrier leads to a further increase of neutron emission so that eventually, at $x=0$, the residual nucleus has a deficit of between 1 and 2 neutrons. It will be noticed that this final value is almost independent of the initial excitation energy.

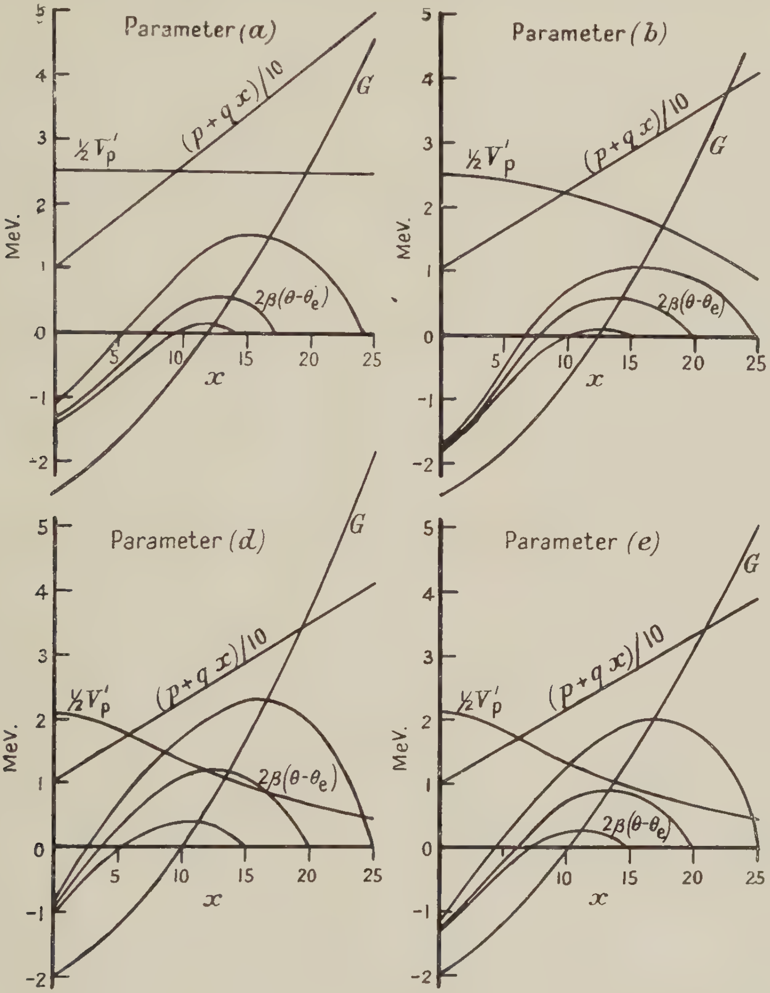

Figure 1. Variation of the neutron excess during evaporation. $2\beta(\theta-\theta_e) \simeq N-N_e$ as a function of $x \simeq \sqrt{U}$ for three different initial values of the excitation energy U. Also the auxiliary functions V_p', $G(x)$ and $p+qx$ of § 3.5.

3.6 *The Emission of Low-Energy Particles*

The results of the previous section for the term $2\beta(\theta-\theta_e)$ have an important physical consequence. Figure 1 (*b*) gives $-1{\cdot}7$ MeV. for the value of $2\beta(\theta-\theta_e)$ at $x=0$. By inserting this value into the expression (50) or (60) for Q, one finds that the excitation energy necessary to release the last particle with zero kinetic energy is Q_x, given by

$$Q_n = 10\,\text{MeV.},\qquad Q_p = 6{\cdot}6\,\text{MeV.},\qquad Q_\alpha = 4{\cdot}9\,\text{MeV.}\qquad \ldots\ldots(77)$$

Thus when the excitation energy has fallen below 10 MeV. neutrons cannot be emitted but charged particles can, even though they must penetrate the potential barrier. There is however competition from two other processes, namely γ-ray emission and β-decay by K capture. Estimates of the radiation width for γ emission are a little uncertain, Bethe (1937, equation 729 *b*) suggests a width of approximately $\frac{1}{2}$ volt which represents a lifetime of 10^{-15} sec., very much less than the time required for a β process. Protons and α-particles can be emitted in less than 10^{-15} sec. only if their 'penetration probabilities' for the potential barrier are greater than 10^{-10} and 10^{-6} respectively. With $A=66$, $Z=29$, which are reasonable values for the residual nucleus of a star of about 12 prongs, Bethe's table XXXVII shows that these probabilities are exceeded if the proton and α-particle are emitted with kinetic energies greater than 0·5 MeV. and 4 MeV. respectively. Therefore the threshold energies (77) for neutron, proton and α-emission become

$$Q_n = 10\,\text{MeV.},\qquad Q_p = 7\,\text{MeV.},\qquad Q_\alpha = 9\,\text{MeV.}\qquad \ldots\ldots(78)$$

However, when the excitation energy is 9 MeV., proton emission is very much more likely than α-emission.

These results show that if after emission of the penultimate nucleon the excitation energy lies between 10 and 7 MeV. a proton is emitted, if it lies below 7 MeV. γ-rays are emitted. There is then a probability $(10-7)/10=0{\cdot}3$ that the last heavy particle emitted by the nucleus is a proton with kinetic energy between 0·5 and 3·5 MeV.*

On the average, with the nuclear parameters *b*, this process contributes 0·3 protons per star with energies in the range 0·5 to 3·5 MeV. With the parameters *d* or *e* the contribution is 0·15 protons per star with energy in the range 0·5 to 1·5 MeV.

Some very slow protons are observed experimentally. Classically this cannot be understood since Weisskopf's formula (52) forbids emission of particles with energy below the barrier height V, in this case about 6 MeV. Harding, Lattimore and Perkins (1949) have pointed out that slower particles can be emitted by ordinary barrier penetration, and this has been allowed for crudely by replacing V by V' in (54). The penetration formulae of Bethe and Konopinski (1938) lead to $V_p' = 0{\cdot}7\,V$, thus this process allows protons with energies down to about 4 MeV. Protons with lower energies can be attributed to the 'trick' mechanism described above.

The mechanism of this section has been proposed independently by Fujimoto and Yamaguchi (1949). It is difficult to say from the short publication available how far their methods of calculation are similar to those of this paper†.

---

* At these low energies one should take account of the dependence of binding energy on the even–odd characteristics of the nuclei. However this leads to the same result.

† The author does not agree with their statement that γ-emission is negligible.

The experimental evidence shows that this cannot be the full theory of the emission of low-energy particles, for it does not explain the emission of low-energy α-particles. If one takes for the potential barrier $V_\alpha=12$ Mev., the penetration effect gives $V_\alpha'=10$ Mev. but many α-particles of lower energy are emitted (H.L.P., Page (1950)). It seems necessary to assume with Bagge (1938)that the potential barrier is lowered at high excitation energies.

3.7 *Final Value of the Neutron Excess*

With $A=70$, the value -1 of $2\beta(\theta-\theta_e)$ at $x=0$ gives $N-N_e=-0{\cdot}75$. Since on the average 0·2 protons are emitted in the subsequent process described in §3.6, one has then $N=N_e-0{\cdot}5$, a very slight neutron deficit. The residual nucleus, which may have 1 Mev. or so of excitation energy then reaches stability by γ-emission or perhaps by a β-transition with K-capture.

Thus, according to this theory, the way to estimate the unobservable neutron emission from a star is to calculate the charge of the final nucleus and to assume that its neutron content corresponds to maximum stability. The experimental data have usually been analysed by assuming that equal numbers of neutrons and single protons are emitted. The present author's procedure would lead to higher estimates of the energy associated with stars of a given number of prongs.

This prediction can to some extent be checked experimentally. For, if equal numbers of neutrons and protons were emitted, the residual nucleus would have a large neutron excess and would reach stability by β-transition with emission of electrons of about 1 Mev. Two or three electrons would be expected from a star of 10 prongs. These would be recorded in the new photographic emulsions but have not been observed.

§4. NUMERICAL RESULTS

4.1 *Nuclear Parameters and Method of Integration*

The main experimental data to be compared with the theory concern stars with an average of 10 prongs. Allowing for the preliminary ejection of a few fast particles, it is assumed that for this star size the evaporation proper starts at about $A=98$ and terminates at $A=68$. Thus during the evaporation the average value of A is about 83. The previous discussion has taken explicit account of all factors which depend on differences between values of A; therefore for the calculation of Λ which varies only as $\sqrt{A}$ it is sometimes sufficient to use the mean value $A=83$.

The equations of emission have been integrated for various sets of parameters, namely

$$a\ \ \Lambda=4 \qquad V_p'=V_d'=V_t'=5\ \text{Mev.} \qquad V_t'=V_\alpha'=10\ \text{Mev.}$$

$$\left.\begin{array}{l} b\ \ \Lambda=5\simeq\sqrt{(A/3{\cdot}3)} \\ c\ \ \Lambda=5{\cdot}5\simeq\sqrt{(A/2{\cdot}7)} \end{array}\right\} V_p'=V_d'=V_t'=\tfrac{1}{2}V_t'=\tfrac{1}{2}V'_\alpha=5(1-U/1000)\ \text{Mev.}$$

$$\left.\begin{array}{l} d\ \ \Lambda=\sqrt{(A/3{\cdot}3)} \\ e\ \ \Lambda=\sqrt{(A/2{\cdot}9)} \end{array}\right\} \begin{array}{l} V_p'=0{\cdot}7V,\quad V_d'=0{\cdot}77V,\quad V_t'=0{\cdot}8V,\quad V_t'=1{\cdot}6V, \\ \qquad V_\alpha'=1{\cdot}66V\quad\text{and}\quad V=6/(1+U/200)\ \text{Mev.} \end{array}$$

The reduction of potential barrier with excitation energy assumed in b and c is roughly that predicted by Bagge (1938). The more drastic reduction d seems to be required to explain the emission of slow α-particles. The relationship between V and V' assumed in d, e is a fair approximation to the penetration formulae of Bethe and Konopinski.

The evaluation of the term $2\beta(\theta-\theta_e)$ was discussed in §3.5 and the results are plotted in Figure 1. These values can be inserted into the emission ratios 65. None of the ratios b, c, d, e, with the possible exception of c, is at all sensitive to the term in $\beta(\theta-\theta_e)$; therefore the dependence of this term on the initial excitation has been ignored and all the emission ratios (65) have been calculated using values derived from an initial excitation of 400 MEV. The slight error in ^{3}H emission thus introduced is of no importance since ^{3}H emission is in any case small compared to that of protons and the experimental check (ii) on the emission ratios involves only $(P_\alpha+P_t)/\Sigma P_x$. Of course, (65 a) is more sensitive to the θ terms, but as the total neutron emission has already been determined, P_n is required only for the calculation of ΣP_x and $\Sigma H_x P_x$ and the approximataion is adequate for this purpose. To illustrate these points the evaluation of (65 e) for P_α/P_p with parameters b is given in the Table. The second line is the value of the expression in square brackets in that equation.

U	30	50	100	200	300	400	500	600
Bracket [ ]	1·76	1·99	2·95	4·56	6·11	7·6	8·95	9·8
$\left\{\frac{A}{\sqrt{R_{\alpha p}}}[\,]\right\}$	1·84	1·40	1·33	1·45	1·63	1·79	1·92	2·00
P_α/p_p	0·31	0·49	0·53	0·47	0·39	0·33	0·29	0·27

These values illustrate the existence of a maximum, already mentioned in §3.3, in the table of ratios P_α/P_p and also show the dominance of the term $1{\cdot}67\,R/A$ at high energies. It is clear that small errors in the θ terms are of no consequence.

Integration of the equations of emission determines the total number of evaporated particles of each kind as a function of the initial excitation energy. The results are given in Figure 2, the contribution of § 3.6 to the proton emission being included. The full curves are shown as they give some insight into the evaporation process but the results may not be very accurate for stars of less than 6 prongs since the calculation has presumed initial conditions appropriate to larger stars.

The theoretical ratio of the number of doubly charged tracks to the total number of tracks is plotted in Figure 4 as a function of star size. Experimental points given by Page (1950) are shown. The observed excess of α-emission for the small stars of six or less prongs is attributed to the disintegration of the light elements carbon, nitrogen and oxygen which are present in the emulsion. For stars of more than six prongs the agreement is satisfactory.

H.L.P. (§4 b) also mention that the proportion of protons to all singly charged particles is $55/79=0{\cdot}7$. Thus the proportion of deuterons and ^{3}H must be $0{\cdot}3\pm0{\cdot}07$. For 10-prong stars the theoretical results are

$$a=0{\cdot}37,\qquad b=0{\cdot}28,\qquad c=0{\cdot}25,\qquad d=0{\cdot}28,\qquad e=0{\cdot}26,$$

which is satisfactory enough. The number of singly charged particles ending in the emulsion is not sufficient for a precise check on this point.

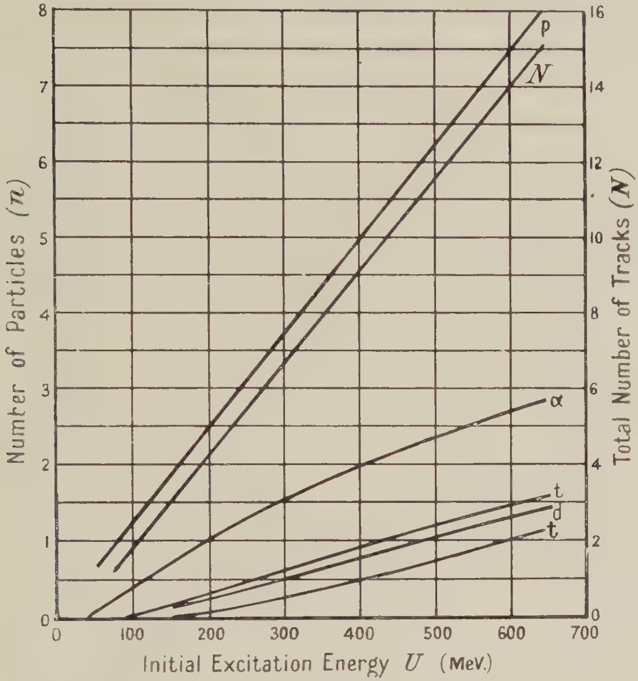

Figure 2. The total number N of tracks and the numbers n of protons, deuterons, tritons, and α-particles evaporated from a nucleus with initial excitation energy U. Parameters : mean of d and e.

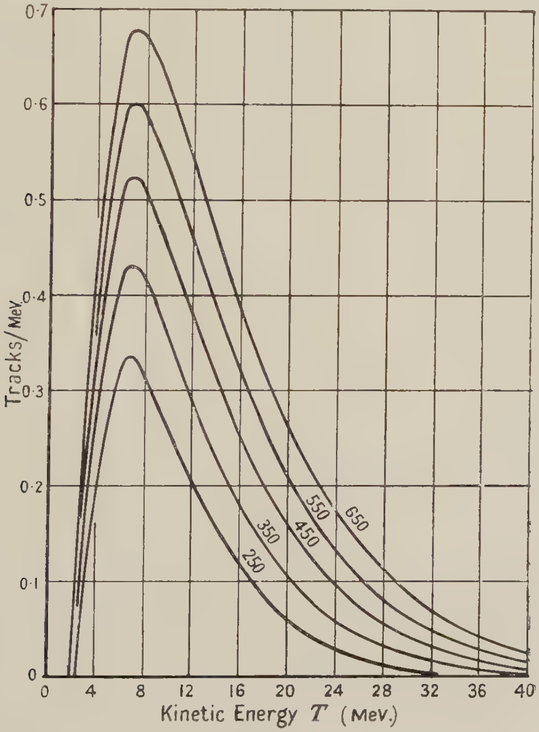

Figure 3. The energy spectrum of the evaporated particles of charge e for five different values of the initial excitation energy. Parameters : mean of d and e.

The energy spectrum of the emitted particles has been derived from equation (54), which for this purpose can be put into the form

$$P(T)\,dT=\frac{T-V'}{\tau^2}\exp\{-(T-V')/\tau\}\,dT \quad \text{with} \quad \tau=(2\sqrt{R})/\Lambda, \quad \ldots\ldots(79)$$

by averaging over the whole emission process. The results are shown in Figure 3 for various values of the initial excitation energy. All the singly charged particles have been grouped together since experimentally full identification of particles is not usually possible; similarly for the doubly charged particles. The slow protons of § 3·6 have not been included in the energy spectrum. In working out these curves it is worth while to take account of the dependence of Λ on *A* since initially, when the excitation is large, *A* and so Λ are above average ; this has the effect of reducing the high energy tail of the integrated energy spectrum.

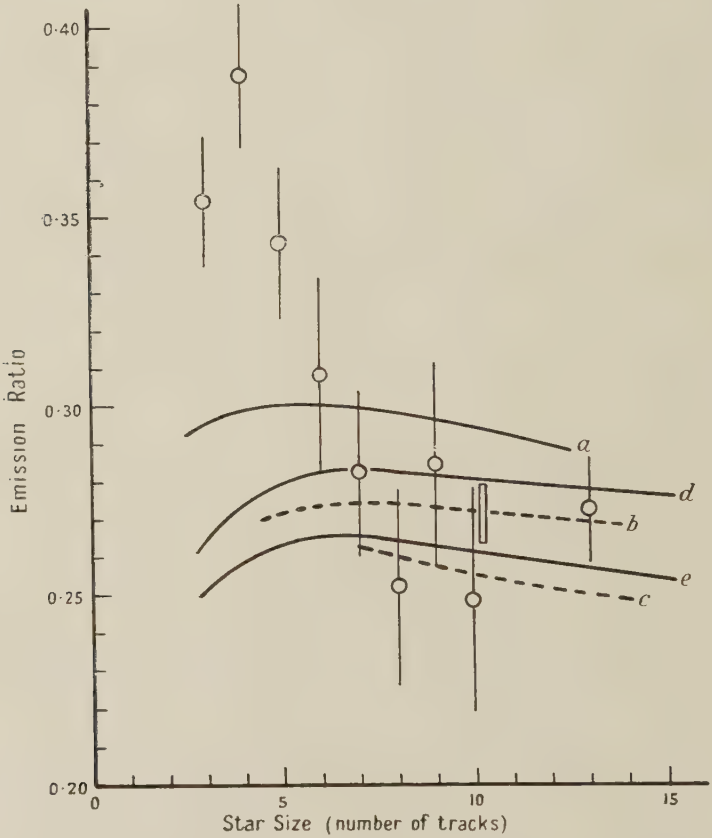

Figure 4. Theoretical and experimental values (Page) of the emission ratio (number of tracks of charge 2*e*/total number of tracks) as a function of star size. The rectangle indicates the mean and standard error of the experimental results for stars of 7 or more tracks.

The experimental data for stars with an average of 10 prongs, due to H.L.P. and Page, are shown in Figures 5 and 6 for comparison with the theoretical curves. These stars have on the average one fast particle which falls outside the evaporation distribution, and the curves therefore represent the theoretical evaporation spectrum for 9-prong stars. The amount of experimental data available for the α-spectrum is exaggerated in Figure 6 since the observations of H.L.P. have been increased by their correction factor f to allow for the 'loss' of long tracks.

4.3 *Discussion of Parameters*

a. The *a priori* parameters *a* give a surprisingly good estimate of the proportion of doubly charged tracks. The value is a little high, and the energy spectrum (not plotted in Figure 5 but worse than *b*) contains too many high energy particles. Both these results show that the Λ value is too small. Attempts to correct the emission ratio, with this value of Λ, by raising the potential barrier would lead to a very bad energy spectrum.

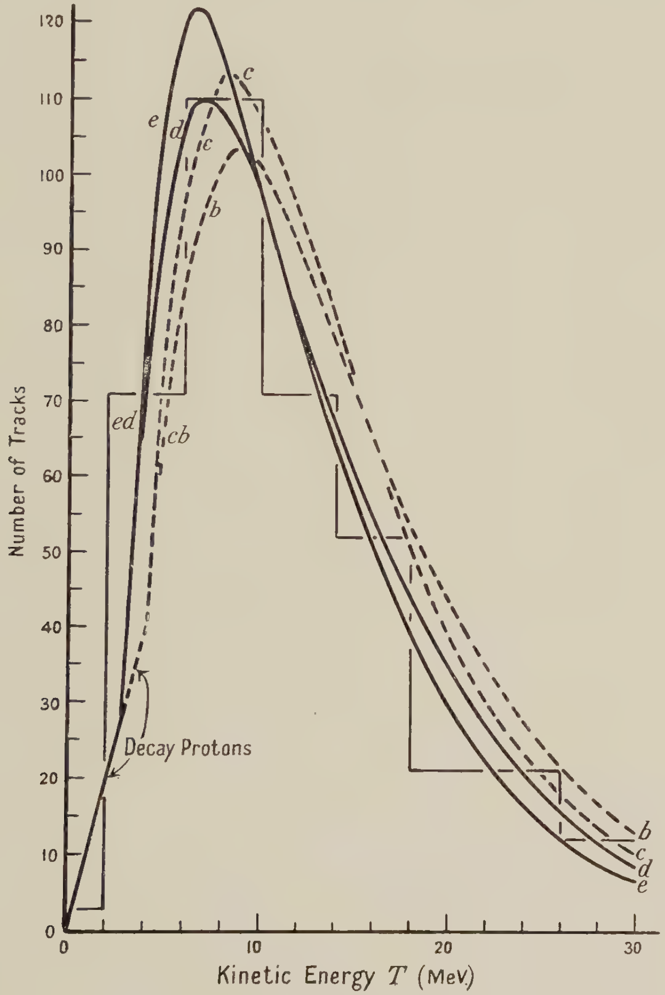

Figure 5. Theoretical and experimental (H.L.P. and Page) results for the energy spectrum of particles of charge e evaporated from stars with an average of 10·2 prongs. The slow 'decay protons' from the process of § 3.6 are included.

b, c. Increased values of Λ are combined with a reduced potential barrier to give a small decrease in the emission ratio and a greater improvement in the energy spectrum. Since for the ground state of the nucleus the height of the potential barrier is approximately known, the reduction must occur at high excitation energies only. This provides evidence, independent of that previously derived from the α spectrum, in support of Bagge's calculation. Figure 5 shows that the theoretical energy spectrum still contains rather too many fast particles of charge e. Curve c is better than b and larger values of Λ would lead to further improvement but Figure 4 shows that the emission ratio would then be much too small. As the α spectrum (Figure 6) contains far too few particles of low energy, a further reduction of the potential barrier is suggested and this will at the same time improve the spectrum of the singly charged particles.

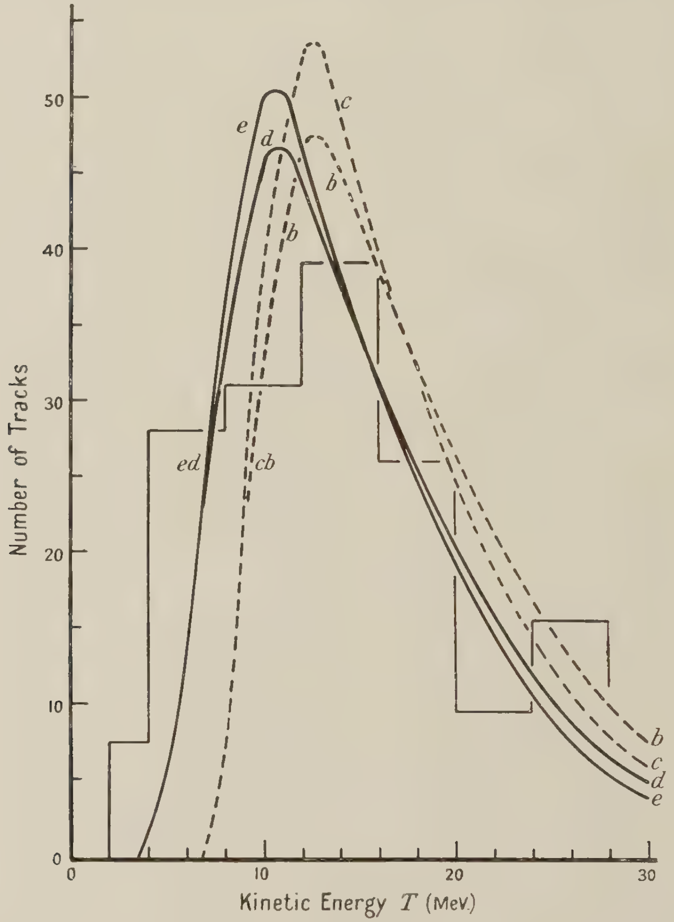

Figure 6. Theoretical and experimental results for the energy spectrum of evaporated particles of charge $2e$. Stars as in Figure 5.

d, *e*. Parameters *d* and *e* have been introduced to improve the energy spectrum. There is now sufficient emission of low energy α-particles. In contrast, it will be noticed that the lowered potential barrier does not greatly increase the emission of slow protons since the increased contribution from states of high excitation is partly compensated by a reduced contribution from the process of § 3.6; the high energy side of the spectrum is however much improved.

Figure 4 shows that, for stars with over 7 prongs, the calculated emission ratio decreases linearly with star size. This simplifies the comparison with experiment.

Page (1950) has determined the mean value of this ratio as $0{\cdot}271 \pm 0{\cdot}008$ for 392 stars with an average of 10·2 prongs. For this size *d* gives 0·278 and *e* gives 0·260. Thus, on this evidence, the correct value of Λ lies midway between those assumed in *d* and *e* which represent the limits of uncertainty of this parameter. This conclusion is in full agreement with the independent evidence from the energy spectrum.

The experimental data therefore indicate a value $3{\cdot}1 \pm 0{\cdot}2$ Mev. for the coefficient $\zeta\gamma/\pi^2$ which determines Λ. This value falls well within the limits arrived at in §2.5.

The value $V = 6$ Mev. for the residual nucleus is reasonable. But the reduction of potential barrier with increase of energy assumed in *d* and *e* is much larger than would follow from the small uniform expansion calculated in §2.5 and a little larger than that derived by Bagge as a consequence of the formation of surface waves of large amplitude. However the values are certainly required by the experimental data and are not *a priori* unreasonable. The dependence on energy could be less marked if one started from a lower potential barrier in the ground state of the nucleus and assumed the same value for the excited nucleus. The author's value $V = 6$ Mev., is actually higher than Bethe's value $V = 5{\cdot}3$ Mev. derived from his larger estimate of the nuclear radius. The above estimate of $\zeta\gamma$ would also be consistent with a slightly larger nuclear radius, which would have to be combined with a value of γ nearer to the upper limit of §2.5. However this work provides no grounds for a choice of nuclear radius.

§ 5. CONCLUSIONS

A detailed investigation of the nuclear evaporation theory shows that it can give a consistent account of the main features of disintegration stars.

It has been necessary to make rather *ad hoc* assumptions about the potential barrier but comparison of the results for *b*, *c* and *d*, *e* shows that the experimental estimate of the parameter Λ, which (equation (37)) connects nuclear energy and temperature, does not much depend on these assumptions. Thus it is legitimate to check the theoretical estimate of Λ against the experimental data. The agreement is as good as can be expected.

This investigation yields information on one point of principle. Factors to represent explicitly the 'probability of existence' of compound particles (α, triton) within the nucleus do not enter explicitly into Weisskopf's evaporation formulae. The 'existence' is completely taken into account through the dependence of the emission probabilities P_α, P_t upon the binding energies w_α, w_t of these compound particles. In the formulae, such as (56), this effect is expressed by the dependence of R on w. The calculations support this point of view, for it would not have been possible to obtain agreement with experiment if additional factors to represent small 'probabilities of existence' had been introduced into the emission formulae. The Table shows that to maintain the correct proportion of doubly charged particles, a factor $\frac{1}{2}$ for their existence within the nucleus would have to be compensated by halving the value of Λ. This would give an incorrect energy distribution, the width of the proton spectrum would approximately be doubled. The situation in this problem is quite different from that existing in the theory of natural α-radioactivity (Bethe 1937) where, because of the dominance of the penetration factor and its critical dependence on barrier height, large factors against the existence of the α-particle can be compensated by small changes in the nuclear radius.

ACKNOWLEDGMENTS

The author would like to thank Dr. Page and Dr. Perkins for the generous supply of experimental results and Professor Rosenfeld for his kind interest in this work.

REFERENCES

Bagge, E., 1938, *Ann. Phys., Lpz.*, **33**, 389; 1943, *Cosmic Radiation* (Ed. Heisenberg) (reprinted 1946 by Dover Publications, New York), p. 128.
Bardeen, J., 1937, *Phys. Rev.*, **51**, 799.
Bethe, H. A., 1937, *Rev. Mod. Phys.*, **9**, 69.
Bethe, H. A., and Bacher, R., 1936, *Rev. Mod. Phys.*, **8**, 82.
Bethe, H. A., and Konopinski, E. J., 1938, *Phys. Rev.*, **54**, 130.
Bohr, N., and Kalckar, F., 1937, *K. Danske Vidensk. Selskab*, **24**, 10.
Feenberg, E., 1947, *Rev. Mod. Phys.*, **19**, 239.
Ferretti, B., 1948, *Nuovo Cim.*, **5**, 36.
Fujimoto, Y., and Yamaguchi, 1949, *Phys. Rev.*, **75**, 1276.
Harding, J. B., Lattimore, S., and Perkins, D. D., 1949, *Proc. Roy. Soc.* A, **196**, 325.
Page, N., 1950, *Proc. Phys. Soc.* A, **63**, 250.
Rosenfeld, L., 1948, *Theory of Nuclear Forces* (Amsterdam : North Holland Publishing Co.).
Stoner, E. C., 1936, *Phil. Mag.*, **21**, 159.
Weisskopf, V., 1937, *Phys. Rev.*, **52**, 295.
Zwanikken, G. C. J., 1948, *Physica*, **14**, 530.

Note added in proof. My attention has been drawn to a paper by Ferretti (1948) on meson-induced disintegrations, in which the importance of the neutron excess in nuclear evaporation is discussed.

The Correction of Specific β-Radioactivity for Self-Absorption

By C. H. COLLIE, P. F. D. SHAW and H. J. GALE
Clarendon Laboratory, Oxford

MS. received 4th August 1949

ABSTRACT. The self-absorption of β-rays in radioactive films between 5 and 100 mg/cm^2 superficial density has been investigated. The marked departures from the exponential absorption law are shown to be due to scattering of the β-rays in the film. The use of very thin films to avoid the correction for self-absorption is not recommended as a routine method.

§ 1. INTRODUCTION

In using β-radioactive elements as tracers one often needs to correct observed readings (particles per minute per mg.) for self-absorption in the specimen to a specific activity for a thin film. This is particularly important in modern work using end-on counters since the restricted window area leads to the use of thicker preparations than were commonly used with cylindrical counters. An empirical correction curve can be constructed, but this can be very time-consuming if the specific activities involved are low, and a good understanding of the processes contributing to the self-absorption is very desirable. Extensive experimental work on this subject (Broda *et al.* 1948) has shown that for thick films an exponential absorption law is well obeyed. In the course of some measurements using radioactive silver iodide (Shaw and Collie 1949) two of the present authors found that no appreciable correction for self-absorption was necessary below a superficial density of 50 mg/cm^2, a result which greatly simplified the experimental work. It was later realized that this result was not in agreement with the exponential absorption usually assumed, according to which the correction should have been 15%. An examination of the published data showed that few measurements had been made below 25 mg/cm^2, and that most of the work had been done on films thicker than 50 mg/cm^2. The object of the present work is to investigate this anomaly.

§ 2. SELF-ABSORPTION OF THIN FILMS

To measure the self-absorption a stock of dry radioactive powder was prepared and suitable amounts were weighed out into the specimen holder. This consisted of a brass plate with a 1 cm. diameter hole in it closed by a piece of 'Cellotape' placed across the bottom of the plate. After introduction of the powder the cavity was closed with a further piece of 'Cellotape' and the whole pressed with a well fitting plunger to make the preparation as homogeneous as possible. Specimens made in this way gave results which were well reproducible. The specimen holder fitted into a lead castle below a G.E.C. end-on counter (Type G.M. 2) for measurement. The usual corrections for decay and paralysis time were made, and the sensitivity of the counter was controlled by the repeated measurement of an uranium oxide source. Two positions for the source were available, an upper and a lower one, distant 0·4 cm. and 2·4 cm. respectively from the window of the counter.

The results obtained are shown in Figure 1, curves *b* and *g*, and disclose a very shallow maximum in the self-absorption curve. Similar curves, *c*, *a* and *f*, were obtained using films of radioactive silver bromide and barium phosphate respectively. It was at first thought that the phenomenon was to be explained in terms of some specific property of silver iodide which is reported (Broda *et al.* 1948) to show an absorption curve anomalous in other respects. However, since radio-phosphorus emits no γ rays, and radio-bromine and radio-iodine have very different β-ray spectra, the phenomenon is clearly a general one, not to be explained in terms of some specific property of silver iodide. The maximum is sufficiently shallow to require rather accurate counting to establish it with certainty, but an examination of the self-absorption curve for radio-sulphur, ^{35}S, in barium sulphate obtained by Hendricks *et al.* (1943) shows an ill-defined maximum at about 0·3 mg/cm^2. A similar phenomenon has been briefly reported by Solomon *et al.* (1947) for thin films of barium carbonate, Ba^{14}CO$_3$. The latter at first attributed the phenomenon to the loss of the very small amounts of barium carbonate (0·65 mg/cm^2) involved, but Glendenin (see Solomon *et al.* 1947) suggested that the observations could be explained in terms of scattering.

The existence of a maximum indicates the interplay of two opposing phenomena, the one causing an increase in specific activity with superficial density and the other, which is presumably the exponential absorption dominant for thicker films, causing a decrease.

It was at first thought that the phenomenon causing the increase was back scattering. For a thin film the electrons which are counted are those initially projected forward together with those scattered back from the support, which is either 'Cellophane' and air or 'Cellophane' and brass, according to the method of supporting the film. Since a large part of electron scattering is nuclear and so, according to Rutherford's law, is proportional to Z^2, the back scattering in silver iodide is more than in brass, and it is possible that this might account for the phenomenon. The exponential external absorption of β rays is sufficiently well established by experiment for it to be usual to quote the absorption coefficient μ/ρ in the literature. The theoretical explanation of this is uncertain since a stream of homogeneous electrons is not absorbed exponentially. The conditions under which exponential absorption will be observed have been discussed *inter alia* by Feather (1944). The occurrence of exponential external absorption over a limited range accounts for the observed self-absorption, provided that all effects due to scattering are neglected, as they can be for thick films. A theoretical treatment of the effect of scattering is extremely complicated, but the self-absorption

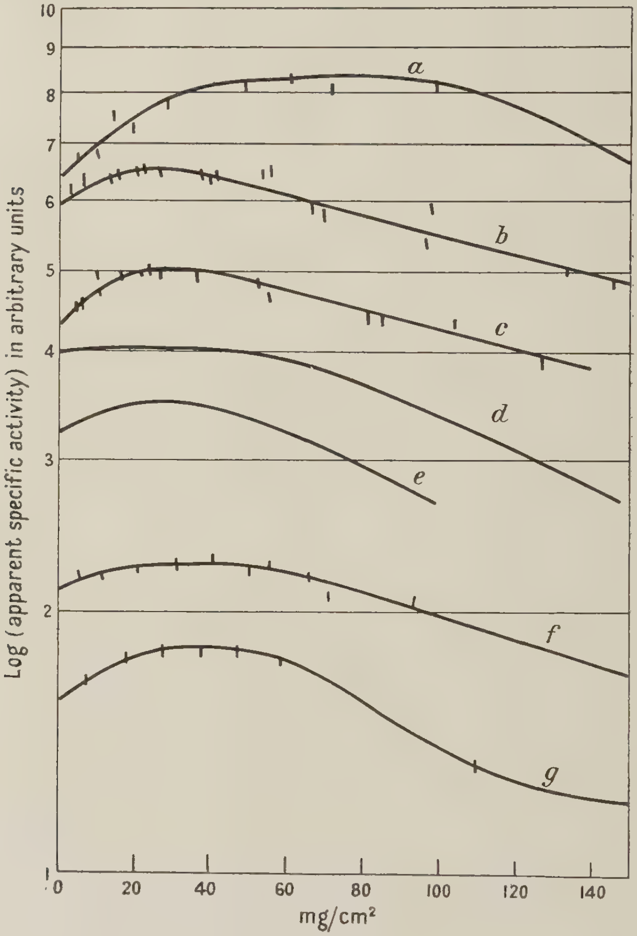

Figure 1. Self-absorption curves.

a. ^{32}P β's in barium phosphate (lower position, no backing).
b. ^{128}I β's in silver iodide (upper position, brass backing).
c. ^{82}Br β's in silver bromide (upper position, brass backing).
d. Calculated self-absorption curve for ^{128}I β's in silver iodide assuming exponential absorption (upper position).
e. Calculated self-absorption curve for ^{128}I β's in silver iodide using measured external absorption curve (upper position).
f. ^{32}P β's in barium phosphate (upper position, no backing).
g. ^{128}I β's in silver iodide (upper position, no backing).

curve can be constructed by graphical integration if the external absorption curve and the back-scattering curve are known. Accordingly the effect on the observed activity of a thin film of active silver iodide of backing it with increasing thicknesses of inactive silver iodide was measured. The maximum amount of back scattering is approximately 26%, and the shape of the curve agrees generally with what was to be expected from the work of Yaffe (1949) and Zumwalt and Lloyd (1947). By combining this curve with an exponential external absorption curve one can determine what the self-absorption curve should be. Imagine a layer of active material divided up into n equal sections, and consider one of the inner sections of activity $2I$. From the mth layer radiation I will proceed towards the counter; $\alpha_m I$ will reach the counter, and $\beta_m I$ will be scattered back. Thus the downward radiation from the layer is $I(1+\beta_m)$, of which $I(1+\beta_m)\gamma_m$ will be scattered back. The total radiation reaching the counter which started in the mth layer is thus

$$I\alpha_m + I\alpha_m(1+\beta_m)\gamma_m[1+\beta_m\gamma_m+\beta_m^2\gamma_m^2\ldots] = I\alpha_m + \frac{I\alpha_m\gamma_m(1+\beta_m)}{1-\beta_m\gamma_m},$$

and the total activity of the film is given by

$$I\sum_{m=1}^{m=n}\left\{\alpha_m + \frac{\alpha_m\gamma_m(1+\beta_m)}{1-\beta_m\gamma_m}\right\},$$

in which expression α_m is to be read from the external absorption graph and β_m and γ_m from the graph of back scattering against superficial density at the thickness corresponding to the value of m. The result of such a graphical integration (using 5 mg. steps) assuming exponential absorption in the layer is shown in Figure 1, curve *d*. Although the effect of taking back scattering into account is seen to be considerable, there is no maximum in the curve, as is found experimentally. The assumption that the external absorption remains exponential for thin layers of absorber can be investigated by direct experiment. This was done using weighed layers of silver iodide and a thin active silver iodide source. In the upper position the use of silver iodide was impracticable and sheets of tin foil, which has the same scattering power, were used instead. The results are shown in Figure 2, curves *a*, *b*, *c*; it is at once apparent that the simple absorption law obeyed for thick absorbers breaks down for thin ones, and indeed that the effect of a thin absorbing foil is to increase and not decrease the measured activity.

If the experimental absorption curve is combined with the observed back-scattering curve to give a calculated self-absorption curve, the result, shown in Figure 1, curve *e*, is seen to be in as good agreement with experiment as could be expected when the rather coarse steps in the graphical integration are taken into account.

It is quite easy to account for the maximum in the external absorption curve in terms of electron scattering. Electrons are heavily scattered in layers of material in which the absorption is small. It is therefore not unreasonable to consider a small thin film in which absorption can be neglected. If the film is thin enough to allow scattering to be neglected as well, the polar diagram of the electrons emitted into a solid angle Ω will be independent of the angle θ between the direction of Ω and the normal to the film.

For a thicker film the angular distribution of the electrons will approximate to the usual $\cos\theta$ distribution: since there is no absorption in the film the total number of electrons emitted is constant. As a result of this, a counter subtending any angle less than 2π at the film will count a greater fraction of the electrons from a thick film, and in the extreme case of a counter subtending a small solid angle about the normal to the specimen the observed activity will be increased, due to scattering, by a factor two. This is a large effect well able to mask the effect of absorption and so give a maximum in the absorption curve. The general correctness of this explanation is confirmed by the increased sharpness of the maximum which is shown when thin foils of platinum (which has a larger atomic number and, therefore, shows more large angle scattering) are used as the absorber (Figure 2, curves *d*, *e*). The matter may be looked upon in another way. Electrons which start off towards the counter have a good chance of getting there because the thickness of film through which they have to pass is small. On the other hand, electrons emitted nearly parallel to the film are quite likely to be scattered through a large angle out of the film into the counter. Thus increasing the thickness of the scattering layer will increase the recorded count until the film is thick enough

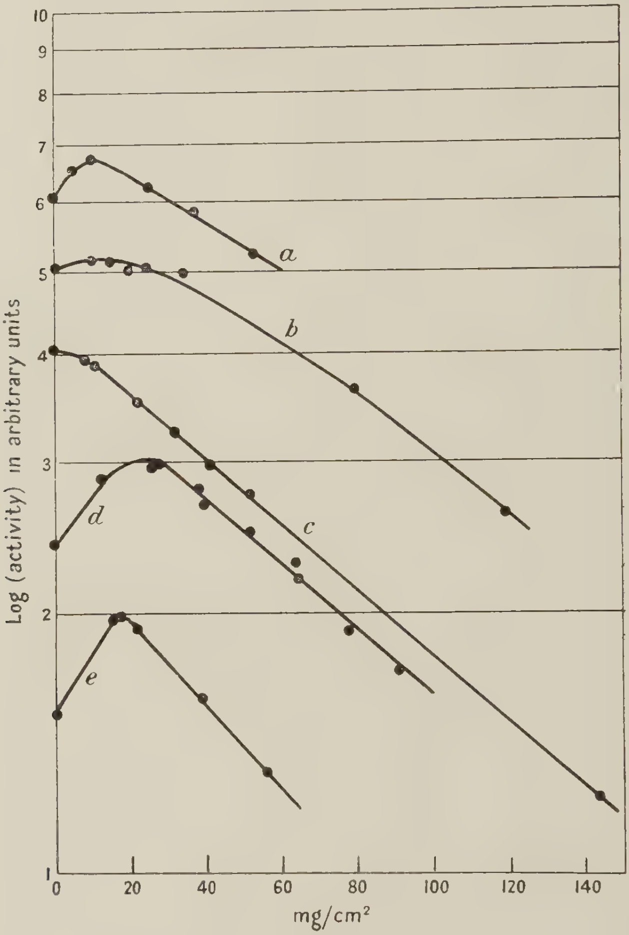

Figure 2. External absorption curves.

a. ^{128}I β's in silver (lower position, brass backing).
b. ^{128}I β's in silver iodide (lower position, no backing).
c. ^{128}I β's in tin (upper position, no backing).
d. ^{32}P β's in silver (lower position, aluminium backing).
e. ^{32}P β's in platinum (lower position, aluminium backing).

for the probability of scattering to be large whatever the initial direction of the β particle. To verify that this effect was taking place in films under consideration whose superficial density lay in the range 0–50 mg/cm² the apparatus shown in Figure 3 was constructed.

It consisted of an evacuated space in which a small source could be mounted as freely as possible on a light wire frame, which could be rotated on a ground joint. Electrons in a selected solid angle entered an external counter after traversing the thin mica window at the top of the apparatus. An aluminium diaphragm ensured that electrons scattered from the aluminium-lined walls could not enter the counter unless they had been scattered at least twice. The sources consisted of active barium phosphate on a 1 cm. diameter filter paper mounted on a 'Cellophane' strip. Coherence was given to the specimens by a final wash with dilute collodion, and the superficial density was determined after the measurement by incineration in the usual way.

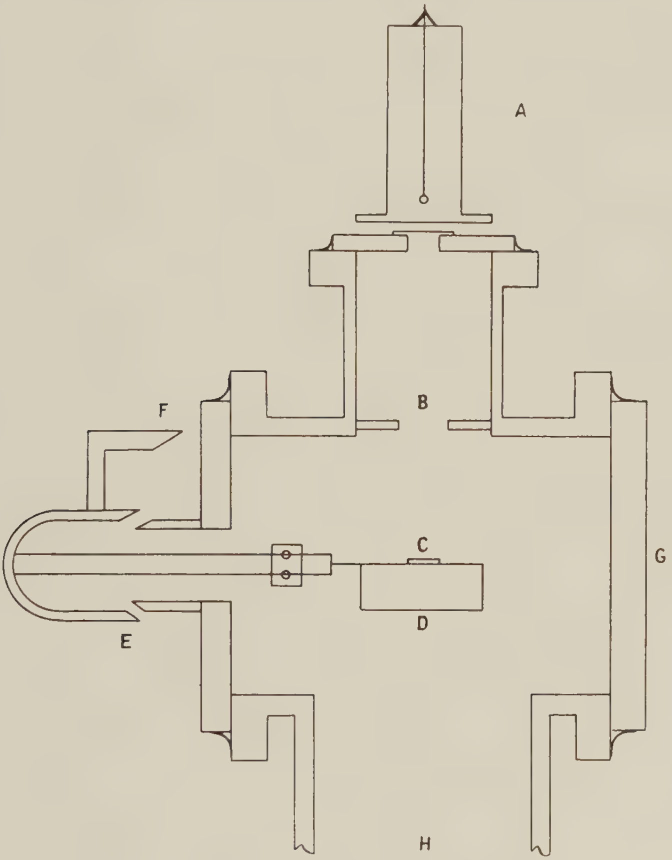

Figure 3. Apparatus for measuring the angular distribution of electrons from a source. A. Geiger-Müller counter. B. Diaphragm. C. Source. D. Aluminium frame. E. Ground joint. F. Scale of degrees. G. Inspection window. H. Vacuum pump.

The electron distributions obtained are given in Figure 4 and show the expected change in the angular distribution of the electrons from independence of θ to dependence according to a $\cos\theta$ law in just the range of superficial densities considered. There can be no doubt that this phenomenon must be taken into account in explaining the observed self-absorption curves, and that it will give rise to a maximum if the true absorption is small and the solid angle subtended by the counter is appreciably less than 2π.

§ 3. DISCUSSION

The accuracy with which the polar diagrams represent the true angular distribution of the electrons from the source is rather difficult to assess. Removal of the diaphragm increased the readings by about 30% and began to affect the shape of the curves at about 60° azimuth. This indicates that the baffle is effective in preventing scattered electrons from entering the counter. Another test was made using a very thin active phosphate film made by evaporating a drop of separated phosphate on to a 12μ ‘Styrafoil’ sheet. This was supported on a frame in such a way that the scattering due to the frame when the film was nearly vertical was intercepted by the walls and the baffle. The results obtained are shown in Figure 4(*a*). The bulge between 45° and 80° represents the effect of scattering in

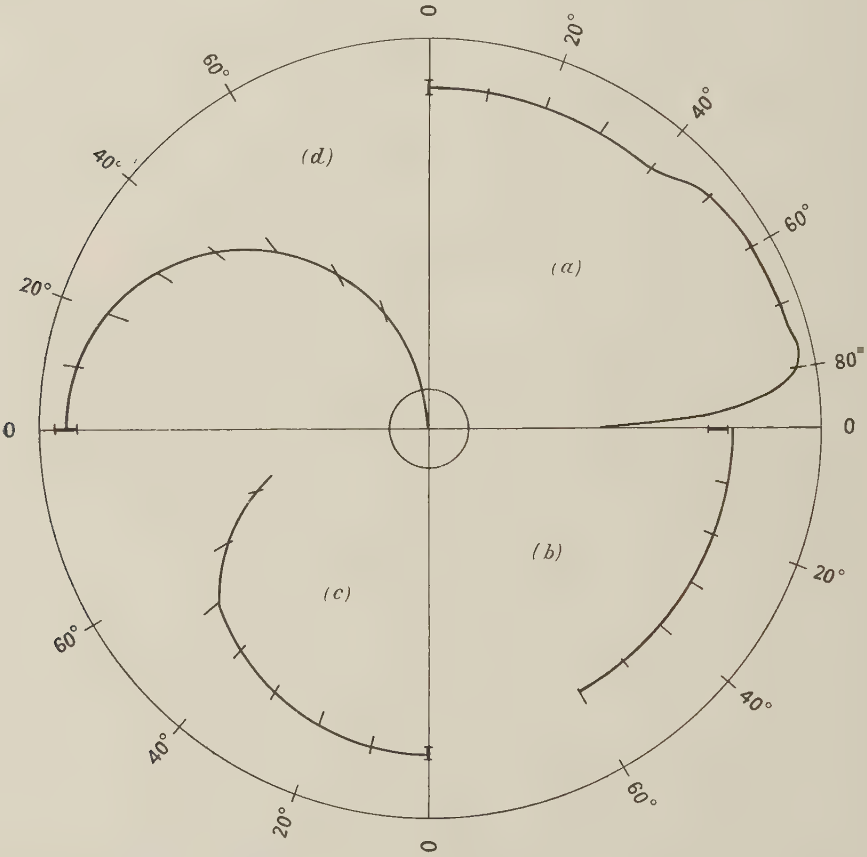

Figure 4. Angular distribution of β-particles from a plane source.

Each quadrant refers to a separate experiment, and θ increases uniformly from 0–90° clockwise. Readings were taken every 10° and are represented by radial lines whose length represents the statistical error of the readings.

(*a*) ^{32}P on 12 μ ‘ Styrafoil ’. (*b*) ^{32}P in barium phosphate 8 mg/cm^2. (*c*) ^{32}P in barium phosphate 22 mg/cm^2. (*d*) ^{32}P in barium phosphate 70 mg/cm^2. Full line represents a cos θ distribution.

the film, of electrons initially directed in its plane. Evidence in favour of this view can be obtained by a graphical integration of the polar diagram to obtain the total number of electrons emitted from the source. If ω is the mean solid angle subtended by the counter at the source, and n is the rate of counting of particles in the spherical part of the polar diagram, then the total number of particles emitted forward from the source is

$$\frac{2\pi n}{\omega}=\frac{2\pi}{\omega}(1388\pm 8)\text{ electrons/minute.}$$

This number can also be obtained by graphical integration of the complete polar diagram. This gives $(2\pi/\omega)(1387\pm 8)$ particles/minute. Agreement within the statistical error is fortuitous, but does show that general scattering from the walls of the containing vessel cannot be seriously distorting the true angular distribution of the β particles.

It remains to see to what extent one can reconstruct the self-absorption curve from the now empirically known elements of absorption scattering and back scattering.

The most suitable case for a quantitative comparison is that of barium phosphate observed with the source some distance from the counter, for which the self-absorption curve is given in Figure 1, curve *a*. The maximum occurs at about 80 mg/cm^2 when the apparent specific activity is about 30% above that found for a very thin film. Using our empirical data one can calculate the solid angle which the counter must subtend at the specimen to give this result and compare this with the measured solid angle.

The thin source (of activity say 100 units) will be giving an approximately spherical distribution while the thick sources will have passed over to the $\cos\theta$ distribution. The 130 units of radiation observed with the thick source have been reduced by self-absorption, and if the film had been an ideal one showing only scattering the observed activity would have been 157 units. This increase is, on our assumptions, entirely due to changes in the angular distribution of the electrons.

Let θ be the effective angle subtended by the counter and let $4\pi I$ β particles be emitted from the ideal source. Then for a uniform angular distribution $2\pi I(1-\cos\theta)$ will enter the counter and after redistribution by scattering $\pi I(1-\cos 2\theta)$ will enter the counter. Thus in the case being considered θ is given by the equation

$$\frac{\pi I(1-\cos 2\theta)}{2\pi I(1-\cos\theta)}=1{\cdot}57,$$

whence $\theta=35°$.

The measured value of θ is approximately 26°. This agreement is as close as can be expected when the approximate nature of the assumptions and of the methods of calculation involved is considered: for example, no correction was made for scattering due to the brass plate surrounding the source; a reasonable allowance for this makes the agreement between measured and calculated angles much closer.

It remains to discuss the practical application of these results to tracer work. It is quite clear that the specific activity obtained by correcting a measurement made on a thick preparation of moderate activity is different from, and cannot be compared at all easily with, the specific activity measured on a thin specimen.

It appears that there is no particular advantage in working with extremely thin preparations as this does not avoid the need for applying a correction. The most satisfactory procedure seems, in comparative work, to be to measure near the maximum in the apparent specific activity curve. By arranging for the counter to subtend a large solid angle this maximum can be made so flat that except for work of very great accuracy using very strong preparations (to avoid the statistical error) no correction is needed.

ACKNOWLEDGMENTS

The authors wish to thank Lord Cherwell for his continued interest in the work, and the Director of the Tin Research Institute for some absorption foils. Thanks are also due to the Nuffield Trustees and the Department of Scientific and Industrial Research for financial assistance.

REFERENCES

Broda, E., Grummitt, W. E., Guéron, J., Kowarski, L., and Wilkinson, G., 1948, *Proc. Phys. Soc.*, **60**, 460.
Feather, N., 1944, B.R. 504.
Hendricks, R. H., Bryner, L. C., Thomas, M. D., and Ivie, J. O., 1943, *J. Phys. Chem.*, **47**, 469.
Shaw, P. F. D., and Collie, C. H., 1949, *J. Chem. Soc.*, **264**, 1217.
Solomon, A. K. Gould, R. G., and Anfinsen, C. B., 1947, *Phys. Rev.*, **72**, 1097.
Yaffe, L., 1949, *J. Chem. Soc.*, Supplement II (Symposium at Oxford).
Zumwalt, L. R., and Lloyd, R., 1947, M.D.D.C. 1346.

The Magneto-Resistance of the Alkali Metals

By D. K. C. MacDONALD
Clarendon Laboratory, University of Oxford

Communicated by F. E. Simon; *MS. received 4th January* 1950

ABSTRACT. The magneto-resistive effect has been examined experimentally in the alkali metals at low temperatures. It is concluded that deviations from the free electron gas model become considerable in the case of the heavier metals, caesium and rubidium.

If one neglects the possibility of quantization of the orbits of the conduction electrons in a magnetic field (e.g. Țițeica 1935), then the change of resistance of a metal in a magnetic field arises from the departure of the electronic behaviour from that of the ideal free electron model. Sommerfeld and Frank (1931) analysed the *very* small effect that does in fact arise for free electrons, but Peierls (1930, 1931) first showed that the observable change springs from the non-ideal behaviour which may also be expressed as a departure of the Fermi surface from the spherical surface in momentum space characteristic of a free electron gas. The detailed analysis of the magneto-resistive effect is still today by no means complete, but measurements of its magnitude should offer a means of comparing how far different metals of similar type depart from the free electron model.

I have examined experimentally the relative magneto-resistive effect in all the alkali metals; these would be expected *a priori* to present the closest approximation to the ideal case. The magnitude of the change anticipated depends essentially on the ratio of the field strength, H, to the electrical resistance, R_T, at the temperature T. This dependence, often known as Kohler's Rule, was indicated originally by Peierls (1930, 1931) and by Bethe (1931). Low temperatures are then particularly valuable in yielding a satisfactory magneto-resistive change even for moderate fields (10^3–10^4 gauss) because of the low value of resistivity attainable in pure samples of metal. The experiments were carried out at temperatures between 4·2 and 20° K., and the results are shown in the accompanying figure. The ordinate exhibits the percentage change in resistance observed, $100(\Delta R_T/R_T)$, while as abscissa we have H/r_T where r_T is the ratio $R_T/R_{0^\circ\text{C.}}$. To provide a perhaps more valid comparative abscissa for different metals one might use instead of r_T the parameter $\mathrm{r}_T = R/_T R_\Theta$ where

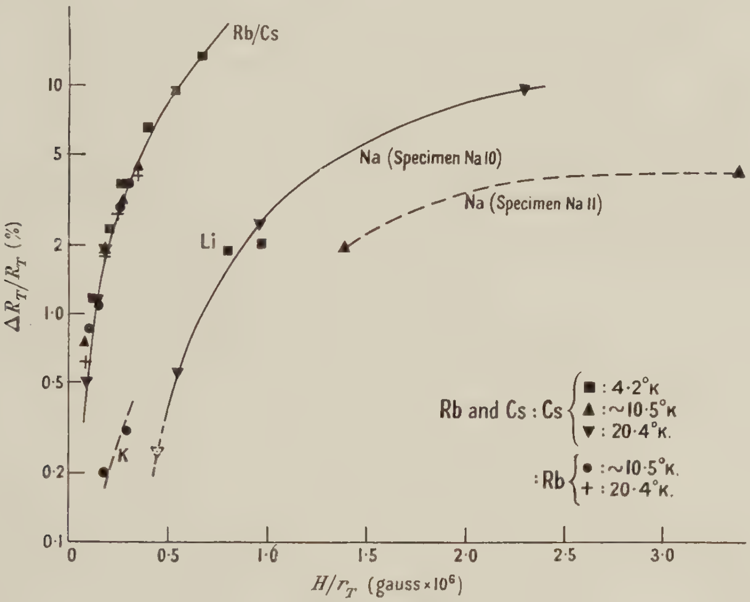

Magneto-resistance of the alkali metals.

Θ is the Debye temperature for the metal concerned; difficulty arises, however, due to the uncertainty in the value of Θ. Justi (1948) has used this parameter in a recent publication in this field, but unfortunately so many slips occur in the relevant part of his paper that useful comparison of the results has not been found possible. Another choice of abscissa which suggests itself (cf. MacDonald and Mendelssohn 1950) is obtained through multiplication of r_T by the factor $\Omega/l_{0^\circ\text{C.}}$, where Ω is the atomic volume of the metal concerned and l the electronic mean free path. This factor yields the values below for the alkali metals, when normalized to unity for sodium:

Metal	Li	Na	K	Rb	Cs
$\Omega/l_{0^\circ\text{C.}}$	1·6	1·0	1·74	3·6	6·2

The modification of the abscissa, however, in either of these ways only serves to emphasize more strongly the difference between the alkali metals demonstrated in the Figure.
]

The results on all specimens except Na10 may be regarded as essentially appropriate to polycrystalline metal since no appreciable variation in $\Delta R_T/R_T$ was observed with angular rotation of the specimens in the field.

The increasing departure from the free electron model as one goes from sodium towards the heavier members of the alkali group is in agreement with the conclusions drawn from detailed experimental comparisons of the low temperature variation of the conductivity with the theoretical Bloch–Grüneisen law by MacDonald and Mendelssohn (1948, 1950). It was found there in particular that the theory was obeyed very closely by sodium, but deviations—becoming particularly strong in the case of rubidium and caesium—were observed in all the other metals.

Further work in this field, particularly on single crystals, is at present in progress, having as its ultimate goal a more precise knowledge of the characteristics of the Fermi surface structure.

REFERENCES

Bethe, H., 1931, *Nature, Lond.*, **127**, 336.

Justi, E., 1948, *Ann. Phys., Lpz.*, **3**, 183.

MacDonald, D. K. C., and Mendelssohn, K., 1948, *Nature, Lond.*, **161**, 972; 1950, *Proc. Roy. Soc.* A, in the press.

Peierls, R., 1930, *Ann. Phys., Lpz.*, **4**, 120; 1931, *Ibid.*, **10**, 97.

Sommerfeld, A., and Frank, N. H., 1931, *Rev. Mod. Phys.*, **3**, 1.

Țițeica, Ș., 1935, *Ann. Phys., Lpz.*, **22**, 129.

LETTERS TO THE EDITOR

The Radiations of Praseodymium-142

The 19·3 hour activity of ^{142}Pr has been investigated by a number of authors (De Wire *et al.* 1942, Cork *et al.* 1948, Jurney 1949, Mandeville 1949) who have given rather inconsistent results for the energies of the beta and gamma radiations. This activity, in a sample of spectroscopically pure Pr_2O_3 irradiated in the Harwell Pile, has been examined here in a semicircular magnetic spectrometer of 12 cm. radius and geometrical resolution of 2% in the course of other work, and the results of this investigation are given below.

Figure 1 shows the beta-ray spectrum which, when examined by means of a Fermi plot, gives end points for the soft and hard components of 0·66±0·02 and 2·23±0·04 MeV. respectively. Since a very thin source was used, and since the counter window was of mica of the order of 1 mg/cm² thick, the soft end of the spectrum should not be appreciably distorted and a comparison of the areas under the two components indicates that the hard beta-rays outnumber the soft by a factor of about four to one. It is also interesting to note

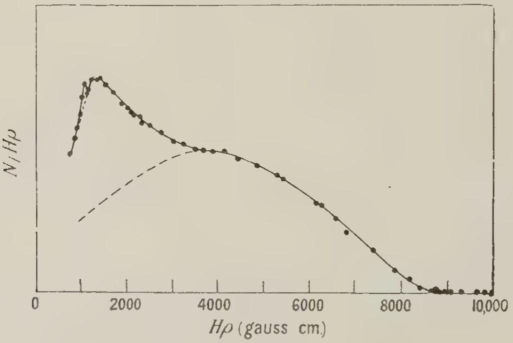

Figure 1. The beta-ray spectrum of ^{142}Pr.

that the end point of the soft component (0·66 Mev.) is not inconsistent with the experimental points of Jurney from which he derived an end point of 0·35 Mev., especially as it can be shown that, with a coincidence circuit of any reasonable resolving time, it would be extremely difficult, using an absorption method, to determine the end point of a spectrum of this nature because of the very large number of accidental coincidences due to the background of hard beta-rays. In the case of the hard component of the beta-ray spectrum, the agreement between the experimental values for the end point given by the various authors is much more satisfactory and the value obtained here is in reasonable agreement with the only other spectrometer determination, that of De Wire *et al.*, of 2·14±0·02 Mev.

The spectrum of the secondary electrons ejected from a thick copper cylinder covered with a thin (0·0015 in.) lead foil by the gamma-rays of ^{142}Pr is shown in Figure 2 and the estimated energy of the hard gamma-ray is 1·59±0·04 Mev. There is a suggestion of the presence of a weak soft radiation with an energy of about 0·14 Mev., and this is confirmed by the presence of a very weak conversion peak in the beta-ray spectrum which gives the energy of this soft line as 0·135±0·005 Mev. and shows that even if this is of electric dipole origin, its intensity cannot be greater than about 20% of that of the hard gamma-ray. Since this peak appears to decay with a similar period to that of the other radiations, it seems likely that it is, in fact, the same line as that reported by Cork *et al.* as having an energy of 0·134 Mev., the conversion lines of the harder radiations at 0·329, 0·490 and 0·624 Mev. being invisible in this instance on account of their much smaller conversion coefficients.

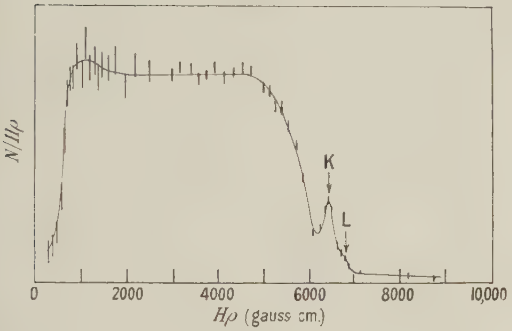

Figure 2. Momentum spectrum of electrons ejected from a thick-walled copper cylinder covered with a thin lead foil by the gamma-rays of ^{142}Pr.

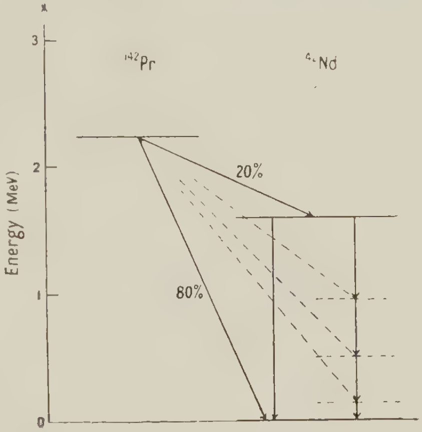

Figure 3. Energy level diagram for the beta-decay of ^{142}Pr.

Since the four soft gamma-rays reported by Cork *et al.* add up in energy to 1·58 Mev., it seems likely that the transition from the level at 1·59 Mev. to the ground state of the ^{142}Nd nucleus may either be made directly or else by way of three intermediate levels, thus giving rise to four soft gamma-rays in cascade. These cascade gamma-rays would account for the small number of gamma–gamma coincidences reported by Mandeville and Jurney. It is also possible that there are subsidiary beta-ray transitions directly to these intermediate levels which would be too weak to be observed against the strong 2·23 Mev. component. It would therefore appear that the complete decay scheme must be similar to that shown in Figure 3 in which one possible arrangement of the intermediate levels is given. The transitions actually observed are indicated by full lines and the possible subsidiary beta-ray transitions by dotted lines.

Department of Natural Philosophy,
University of Glasgow.
29th November 1949.

E. R. Rae.

Cork, J. M., Shreffler, R. G., and Fowler, C. M., 1948, *Phys. Rev.*, **74,** 1657.
De Wire, J. W., Pool, M. L., and Kurbatov, J. D., 1942, *Phys. Rev.*, **61,** 564.
Jurney, E. T., 1949, *Phys. Rev.*, **76,** 290.
Mandeville, C. E., 1949, *Phys. Rev.*, **75,** 1287.

The Angular Distribution of Gamma-Rays from ^{7}Li(p, p$'$)^{7}Li*

The nuclear level of ^{7}Li at 0·48 Mev. is of considerable theoretical interest; owing to its relative simplicity, this nucleus should form a useful test case for any proposed model of nuclear structure. The most convenient interpretation of the low-lying level is that it forms a ^{2}P spin doublet (Inglis 1936) with the ground state, which is known to have spin 3/2. On this basis the spin of the excited state should be 1/2. There are, however, some experimental facts and theoretical considerations difficult to reconcile with this view (Devons 1949, Hanna and Inglis 1949).

To study the problem further, the angular distribution of gamma radiation from the reaction ^{7}Li(p, p$'$)^{7}Li* has been measured. If the spin of ^{7}Li* is indeed 1/2, this distribution must be isotropic in the centre of mass system, whereas in general some correlation between the directions of the bombarding proton and the gamma-ray would be expected for all spin assignments other than 1/2.

The gamma detectors used were scintillation counters, and the bombarding energies on the thin ($\sim$80 kev.) Li_2CO_3 target ranged from the effective threshold value (800 kev.) to 1,080 kev. Under these conditions the contribution to the counting rates from the 17 Mev. gamma-ray due to ^{7}Li(p, γ)^{8}Be was negligible.

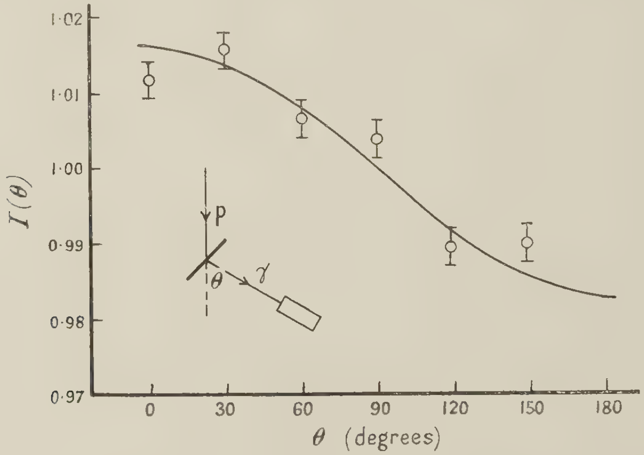

The accompanying diagram shows the experimental results at 980 kev.; essentially the same distribution was obtained at the other bombarding energies used. The points have been superimposed on the curve $I(\theta)=I_0(1+A\cos\theta)$, with $A=0{\cdot}016$; this would be the expected distribution in laboratory space if the gamma-ray were emitted isotropically from a nucleus still moving with the full ' recoil ' velocity. The results of Elliott and Bell (1948) indicate that the nuclei are not slowed down much in the target material during the life-time of the excited state. Approximate isotropy is assumed for the inelastically scattered protons, so that the momentum carried away by them is, on the average, zero.

The experimental points fit the curve well, so that the upper limit of any undetected anisotropy can be placed at $A=0{\cdot}005$. Although a full theoretical analysis has not yet been made, it would appear difficult to reconcile this result with any spin assignment to ^{7}Li* other than 1/2.

Full details of this work will be published in due course. I am indebted to Dr. S. Devons for suggesting the problem and for valuable discussion.

Cavendish Laboratory,
Cambridge.
16th December 1949.

R. M. Littauer.

Devons, S., 1949, *Proc. Phys. Soc.* A, **62**, 580.
Elliott, L. G., and Bell, R. E., 1948, *Phys. Rev.*, **74**, 1869.
Hanna, S. S., and Inglis, D. R., 1949, *Phys. Rev.*, **75**, 1767.
Inglis, D. R., 1936, *Phys. Rev.*, **50**, 783.

On the Production of Penetrating Showers in Nuclear Collisions

In a recent paper Heitler and Jánossy (1949) have given a rigorous theory of meson production, and applied it to the absorption of the particles that produce local penetrating showers. Their calculations are based on the assumption that the probability w of an energy loss ϵ by a nucleon of energy E in a collision follows a law of the form

$$w(\epsilon, E)\, d\epsilon = w(\epsilon/E)\, d\epsilon/E,$$

and it is shown that in order to comply with experimental results w must be a fairly broad distribution, favouring rather low values of ϵ/E. This assumption for w was suggested by analogy only; other laws are being considered as well. It is the purpose of this communication to point out additional evidence which could be interpreted as supporting that particular choice.

In the analysis of experimental results on penetrating showers, in general only two factors are taken into account: the fact that while the collision cross section for fast nucleons is equal, or very nearly equal, to the geometrical nuclear cross section, the absorption cross section is only about one-half of that value; and the absence of an appreciable geomagnetic effect (Appapillai and Mailgavanam 1948), at least in sea-level observations. One would believe that the first is explained by any theory which permits the average primary to undergo about two collisions before it becomes incapable of further shower production, and the second by any theory in which the bulk of the shower-producing particles at sea level are descendants of high-energy primaries capable of surviving repeated collisions without too much energy loss. A third criterion appears to be more sensitive, namely, the total intensity of the shower-producing radiation.

Recent experiments carried out at an altitude of 3,260 m. gave a result of

$$(1{\cdot}6 \pm 0{\cdot}3) \times 10^{-5}\ \mathrm{cm}^{-2}\ \mathrm{sec}^{-1}\ \mathrm{sterad}^{-1}$$

for the vertical intensity of the charged particles which produce, in lead, showers containing at least three particles capable of penetrating more than 200 gm/cm^2 Pb. This value, while slightly larger than the estimate of Hazen, Randall and Tiffany (1949), seems to agree well with experiments both at sea level and mountain altitudes of other authors (Broadbent and Jánossy 1947, Cocconi 1949), if in comparing them Tinlot's (1948, 1949) value for the absorption mean free path in air is used. However, extrapolation with the same absorption coefficient to the top of the atmosphere gives a primary flux of shower-producing particles of only $0{\cdot}55 \times 10^{-2}\ \mathrm{cm}^{-2}\ \mathrm{sec}^{-1}\ \mathrm{sterad}^{-1}$, or only about one-tenth of the total primary intensity. Thus it would appear that even if no multiplication process of nucleons takes place, only a fraction of all primaries give rise to penetrating showers. In fact, however, we know from the existence of such showers produced by neutral particles that fast nucleons are ejected in nuclear collisions: a process disregarded in the computations of Heitler and Jánossy, but probably of considerable importance.

This surprisingly small intensity could be explained in three ways: Firstly, low-energy primaries, that is, primaries of less than about $1{\cdot}5 \times 10^{10}$ ev. if the integral energy spectrum follows a power law with an exponent of the order of 1·8, may be more rapidly absorbed than faster particles, and may thus not contribute to showers observed even at mountain or aeroplane altitudes. Secondly, the total energy which a shower-producing particle dissipates in the production of a penetrating shower in lead may be much higher than the 2–3 $\times 10^9$ ev. observed in the form of charged secondaries. Thirdly, particles in the lower-energy region may undergo predominantly collisions in which no hard secondaries are emitted, so that again their contribution to the production of penetrating showers is negligible.

The first assumption of more efficient elimination of slower than of fast particles could be understood if in each collision on the average there was dissipated a constant amount of energy rather than a more or less constant fraction of the incident energy. However, this would make the absorption by nuclear collisions of the primaries resemble ionization losses, and would not lead to an exponential absorption curve. Only with very artificial assumptions could one combine 'selective' absorption of lower-energy primaries with an exponential absorption law.

The second assumption would obviously require a much larger fraction of the total incident energy to go into neutral instead of charged particles. Even if all observed charged shower particles were protons, the inclusion of neutrons could only about double the amount of 2–3×10^9 ev. carried by the charged particles; a large fraction of neutral mesons would be required to account for the rest, and owing to the decay of these particles all penetrating showers would be accompanied by an energetic cascade shower. While such events are known to occur, they are by no means common and typical.

There remains, finally, the third assumption which demands that the slower primaries in the majority of their collisions will not transfer sufficient energy to generate a penetrating shower. The same fractional energy transfer ϵ/E would, however, suffice for the production of an observable penetrating shower if the primary energy was high. In other words: while *every* collision of *fast* particles initiates a local hard shower, only a *small fraction* of the collisions of *slower* particles does so, while the rest of these collisions will be of a more star-like character. This assumption corresponds exactly to the distribution function of Heitler and Jánossy, with large probability for small ϵ/E. Hence the experimental evidence that only a fraction of all incident primaries appears to produce penetrating showers lends support to that rather than to other transfer laws.

Physics Department, Syracuse University, K. Sitte.
Syracuse, New York.
28th December 1949.

Appapillai, V., and Mailgavanam, A. W., 1948, *Nature, Lond.*, **162**, 887.
Broadbent, D., and Jánossy, L., 1947, *Proc. Roy. Soc.* A, **190**, 497.
Cocconi, G., 1949, *Phys. Rev.*, **75**, 1074; **76**, 984.
Hazen, W. E., Randall, C. A., and Tiffany, O. L., 1949, *Phys. Rev.*, **75**, 694.
Heitler, W., and Jánossy, L., 1949, *Proc. Phys. Soc.* A, **62**, 374.
Tinlot, J., 1948, *Phys. Rev.*, **73**, 1476; 1949, *Ibid.*, **74**, 1197.

Some Decay Effects of Mesons in Penetrating Showers observed in a High-Pressure Wilson Cloud Chamber

Penetrating showers produced by cosmic-ray particles are now known to contain a small number (i.e. one to thirty) of fast particles that are created in a single nuclear explosion or star. In these stars, slow π-mesons are sometimes observed (Brown *et al.* 1949), and there is further evidence of the presence of neutral particles (Rochester and Butler 1947, Kaplon, Peters and Bradt 1949). The Plate shows a photograph of a penetrating shower of six particles which was obtained with a counter-controlled Wilson cloud chamber containing nitrogen at a pressure of 60 atmospheres. The shower, which has originated in a lead plate placed above the cloud chamber, shows two interesting events. Firstly, one of the particles (track ABC) can be identified as a slow π-meson decaying in flight at B, and secondly, a particle (track DE) starts in the gas as if it came directly (or nearly so) from the star.

The velocity v of the particle along AB can be estimated in two ways: (*a*) from the number of short electron branches on AB, (*b*) from the branch electron near A. The first method gives the limiting values of v as $0{\cdot}46\boldsymbol{c}$ and $0{\cdot}62\boldsymbol{c}$, whilst the second yields $0{\cdot}5\boldsymbol{c}$ and $0{\cdot}7\boldsymbol{c}$. The second value is probably less reliable than the first, and it is not unreasonable to take $0{\cdot}55\boldsymbol{c}$ as the mean. To estimate the mass M of the particle, the deflection due to multiple scattering along the length AB has been measured (Williams 1940), and the limiting values of $0{\cdot}5\boldsymbol{c}<v<0{\cdot}7\boldsymbol{c}$ give $60\,m_e<M<600\,m_e$. The particle can therefore be safely assumed to be a meson.

At B there is a single deflection of 23°, although the probability of the scattering of a meson through an angle greater than 20° is only 10^{-4} per cm. of path. Thereafter along BC the track is perceptibly thinner and straighter than before and, furthermore, only one electron branch is observed in the 3·3 cm. length BC, whereas one per cm. is observed in AB. This is consistent with the assumption that the particle velocity of the meson, just before B, is less than its value just after, and thus it is reasonable to assume that it has suffered decay at B. Since the time of flight of the meson in the chamber is only of the order of 10^{-9} sec., the event is unlikely to represent the decay, in flight, of a μ-meson whose half-life is of the order of 2×10^{-6} sec.; on the other hand, it can well be an example of the decay, in flight, of

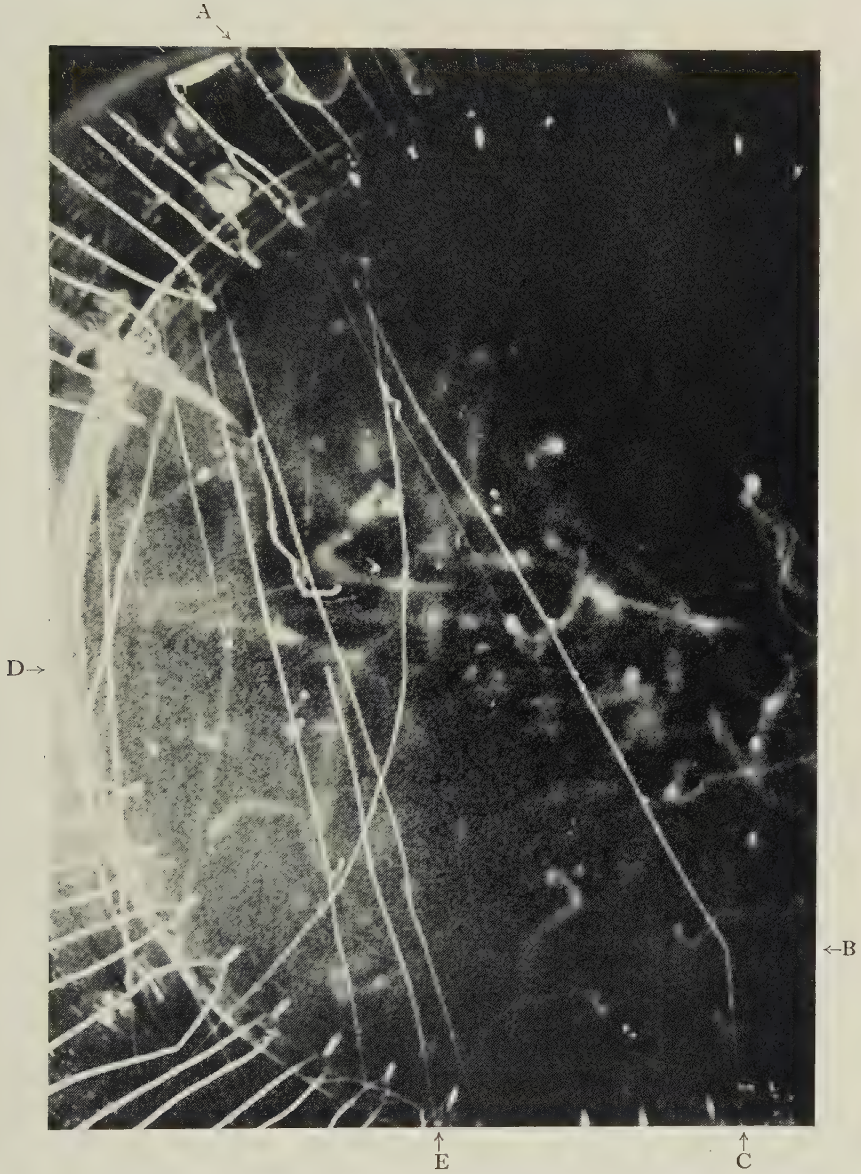

A high-pressure Wilson cloud-chamber photograph of a penetrating shower, showing (*a*) track ABC, representing the decay of a π-meson in flight, (*b*) track DE, a particle starting in the gas as if it came directly from the origin of the shower.

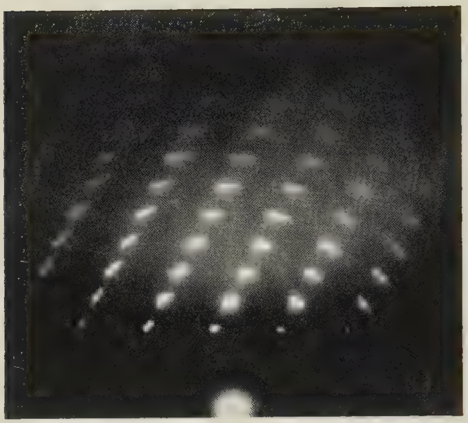

Figure 1. Oxidized zinc-blende cleavage face; beam parallel to cube-face diagonal.

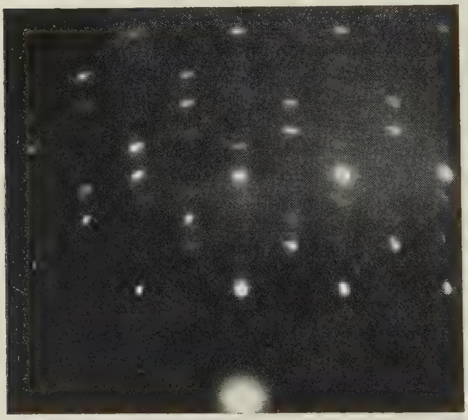

Figure 2. Oxidized zinc-blende cleavage face of Figure 1; beam along the cube edge.

a π- into a μ-meson. It can be estimated that the velocity of the latter along BC is within the range $0{\cdot}6c$ to $0{\cdot}8c$, and a simple calculation gives the velocity, v_μ, of the μ-meson in the frame of reference in which the π-meson is at rest to be $0{\cdot}29c < v_\mu < 0{\cdot}50c$; this velocity has been found by other methods to be $0{\cdot}28c$ (Lattes, Occhialini and Powell 1948). It can be shown that with these values of v_μ the μ-meson would be projected at right angles to the original direction of the π-meson. To sum up this much can be said: it is exceedingly probable that the track ABC represents the decay, in flight, of a meson whose half-life cannot greatly exceed 10^{-9} sec., and that most likely it represents the decay of a π-meson.

Turning now to consider the track DE, the particle starting in the gas leaves a track similar to the other shower particles, and this means that it is either an electron whose energy is of the order of $50mc^2$ or a heavier particle whose velocity is at least $0{\cdot}8c$. It cannot represent the track of a proton, since the deflection in this case due to multiple scattering would be negligible. The particle is therefore assumed to be either an electron or a meson. If it is an electron, then one explanation of this event would be that it is a Compton recoil electron. It can be shown that in this case the energy of the incident photon must be less than $100mc^2$ and greater than $50mc^2$. If its energy is greater than $100mc^2$, it is more likely that an electron pair would be produced, whilst if it is less than $50mc^2$ it would only rarely happen that the recoil electron would be projected at such a small angle (i.e. 5° or less) to the original direction of the photon (Heitler 1935). Now if this event can be interpreted as a Compton effect, it is interesting to consider the source of the γ-radiation. If it comes from the star, it is difficult to understand why there are so few electrons coming from the walls of the chamber, which are of steel of thickness 6 cm. It is only in large electron showers that recoil electrons of such energy are observed starting in the gas, and then only in small numbers representing less than 2% of the total number present. It therefore seems that the photon is created either in the steel or in the chamber itself, or, in other words, it must have been created in some secondary process in which the other fragments of the star are involved. Now no experimental evidence has yet been found for the existence of γ-radiation arising from the decay of charged π- or μ-mesons; on the other hand, it has been suggested that neutral mesons, if they exist, would, in decaying, give rise to two photons, and on this view the event under consideration might be interpreted as due to the scattering of one of these photons. While this is a possible interpretation, there are a number of objections to it. Firstly, the number of photons produced in this way should be about equal to the number of charged mesons in the shower; secondly, the scattering cross section in nitrogen for photons of energy $50mc^2$ is small. Finally, the striking feature of the photograph is the fact that the particle is projected forwards as if coming directly from the star. On the whole it appears that this hypothesis is unsatisfactory, and it may well be that some hitherto unsuspected nuclear reaction is taking place, whereby a neutral meson, coming directly from the star, is able to acquire a charge without at the same time exchange of energy taking place. If there were an exchange of energy, other effects must result, and it would certainly not be expected that the recoil particle would be projected forwards.

The experiments are being continued in an attempt to ascertain the identity of the recoil particle.

The work was carried out with the aid of a research grant from the Department of Scientific and Industrial Research; one of us (T.C.G.) is also indebted to this Department for a maintenance allowance. We wish to thank Professor P. M. S. Blackett of the University of Manchester and Professor R. M. Davies of the Department of Physics at Aberystwyth for their help and encouragement in this work.

Physics Department,
University College of Wales,
Aberystwyth.
22nd December 1949.

G. R. EVANS.
T. C. GRIFFITH.

BROWN, R. H., CAMERINI, U., FOWLER, P. H., HEITLER, H., KING, D. T., and POWELL, C. F., 1949, *Phil. Mag.*, **40**, 862.
HEITLER, W., 1935, *Quantum Theory of Radiation* (Oxford : University Press).
KAPLON, M. F., PETERS, B., and BRADT, H. L., 1949, *Phys. Rev.*, **76**, 1735 (L).
LATTES, C. M. G., OCCHIALINI, G. P. S., and POWELL, C. F., 1948, *Proc. Phys. Soc.*, **61**, 173.
ROCHESTER, G. D., and BUTLER, C. C., 1947, *Nature, Lond.*, **160**, 855.
WILLIAMS, E. J., 1940, *Phys. Rev.*, **58**, 292.

Epitaxial Strain and Disorientation in Crystals Growing on Single-Crystal Substrates

The electron-diffraction patterns, Figures 1 and 2, were obtained by one of us (D.M.E.) from a zinc-blende {110} cleavage face after heating in air. The crystal was a transparent pale yellow and was raised from room temperature to approximately 520° c. in air during 45 minutes, kept at 520° c. for a further 30 minutes, and then allowed to cool in the oven for about 10 minutes before removal and transference to the electron-diffraction camera. Figure 1 was obtained with the electron beam grazing the surface along the cube-face diagonal of the ZnS substrate, and Figure 2 was from the same surface with the beam along the ZnS cube edge (for Figures 1 and 2 see Plate opposite p. 297).

Apart from the pronounced arcing (6°) shown in Figure 1, apparently not observed previously, the diffraction patterns confirm the {103} ZnO orientation indicated by the experiments of Yamaguti (1935), Aminoff and Broomé (1936, 1938), and Uyeda, Takagi and Hagihara (1941) (see also Seifert 1940). This difference is probably due to the higher temperature (red heat) of oxidation which they used.

The initial pattern from the crystal which yielded Figures 1 and 2 showed the high perfection and atomically smooth cleavage surface of the crystal; and after etching away the ZnO–ZnS surface layer by nitric acid a sharp spot pattern was obtained, showing the zinc-blende substrate to be still undistorted at a short distance below the interface.

Recent work submitted for publication in July 1949 (also Wilman 1950) by one of the authors (H.W.) demonstrated the common occurrence of rotational slip as a new kind of deformation process in crystals. The above results (Figures 1 and 2) are now explained satisfactorily as being due to this kind of deformation, caused by the epitaxial stress between the substrate and overgrowth crystals, due to their different lattice constants. Thus the strong arcing in Figure 1, but the inappreciable arcing in Figure 2, shows clearly that the lattice disorientation is, in this case, simply a rotation about an axis parallel to the cube-face diagonal of the {110} ZnS surface. This could therefore correspond to rotational slip of the {103}-orientated ZnO crystals, or of parts of the ZnS substrate, on the planes which are normal to this rotation axis, i.e. $\{11\bar{2}0\}$ in the ZnO (since ⟨100⟩ ZnO is parallel to $\langle 1\bar{1}0\rangle$ ZnS) or {110} in the ZnS. In the ZnS, at least, this plane is a direction of especially perfect cleavage, and thus according to the previous results it should indeed be a direction of easy rotational slip; and it should also be similarly easy on the corresponding $\{11\bar{2}0\}$ planes of the ZnO, which has a structure differing from that of zinc blende only in the hexagonal type of superposition of its (0001) layers.

This constitutes the first clear example of rotational slip caused by epitaxial stresses, since we have also verified experimentally that zinc blende does undergo easily a lattice rotation on {110} planes. For example, when a cleavage face was abraded along the cube-edge direction, a strong (~30°) lattice rotation occurred in the surface region, about an axis in the surface and normal to the abrasion direction, corresponding to rotational slip on the $\{1\bar{1}0\}$ planes which were parallel to the abrasion direction and normal to the surface.

We have similarly demonstrated extensive rotational slip in a copper crystal on {001}, $\{1\bar{1}0\}$ and $\{1\bar{1}1\}$ planes, by abrasion of an anodically polished {110} face in directions parallel to these planes respectively, which were normal to the surface. In this case there is no possibility of interpretation in terms of flexural translational slip, since such slip in copper is well authenticated as being along $\langle 1\bar{1}0\rangle$ in {111}.

Rotations of this kind, due to abrasion of {001} cleavage faces along ⟨100⟩, were noted in PbS by Germer (1936) and Beukers (1939) and also in NaCl by Raether (1947). Raether followed Germer's interpretation, which entirely neglected the possibility of lateral cohesion between the rotated blocks (in these cases cleavage blocks) on their common faces which are normal to the rotation axis.

In order to present a possible picture of the way in which the rotational slip arises in orientated overgrowth crystals, let us consider Figure 3 (*a*). ABCD and A′B′C′D′ represent the corners of neighbouring rotational-slip lamellae as part of an overgrowth crystal before the stress is relieved by its subdivision. The part near CD adjoining the substrate is held under tension (or compression) parallel to CD owing to the atomic forces of the substrate on the overgrowth crystal, while further from the substrate, i.e. along AB, the lattice dimensions tend to their normal values. It thus seems possible that relief of the tension (or compression) near CD, by a slip at the overgrowth-substrate interface, may occur unevenly over the contact surface, so that, for example, the lamella ABCD may remain held near C and contract (or expand) from D towards C, while A′B′C′D′ may be held near D′ and contract (or expand) in the direction C′D′. This motion, oppositely directed in the two parts of the crystal, may thus result in a relative rotational slip which in general will not be fully reversed as the interface slip proceeds; thus there will be left both a residual rotational-slip deformation and a residual but reduced strain near the interface (Figure 3 (*b*)).

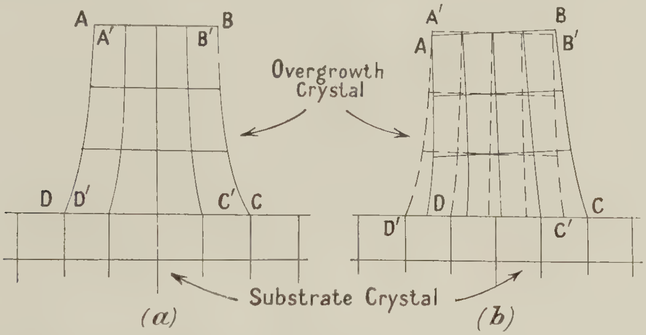

Figure 3. Schematic representation of a possible way in which an epitaxially strained overgrowth crystal (*a*) may have its strain partially relieved by a lamellar subdivision by rotational slip (*b*) on the plane ABCD.

The nearly uniform intensity along the arcs in Figure 1 suggests that, in actual fact, a fine-lamellar subdivision of the ZnO crystals occurred, initiated by a sudden release along one lamellar region and thereby passing on rotational motion to neighbouring regions as in normal rotational slip, but also triggering their partial release at the interface region.

It is hoped to publish a fuller account of the above experiments in the near future.

Applied Physical Chemistry Laboratories,
Imperial College, London S.W.7.
28th December 1949.

D. M. Evans.
H. Wilman.

Aminoff, G., and Broomé, B., 1936, *Nature, Lond.*, **137,** 995; 1938, *Kungl. Svenska Vetenskapsakad. Handl.*, 3rd series, **16.**
Beukers, M. C. F., 1939, *Rec. Trav. Chim. Pays-Bas*, **58,** 435.
Germer, L. H., 1936, *Phys. Rev.*, **50,** 659.
Raether, H., 1947, *Metaux et Corrosion*, **22,** 2 (No. 257).
Seifert, H., 1940, *Z. Kristallogr.*, **102,** 183.
Uyeda, R., Takagi, S., and Hagihara, H., 1941, *Proc. Phys. Math. Soc., Japan*, **23,** 1049.
Wilman, H., 1950, *Nature, Lond.* (to be published in February).
Yamaguti, T., 1935, *Proc. Phys. Math. Soc., Japan*, **17,** 443.

Corrigendum

"Time Dependence of Electronic Processes in Dielectrics", by H. Fröhlich and J. O'Dwyer (*Proc. Phys. Soc.* A, 1950, **63,** 81).

Equation (8), page 83, *should read*

$$\frac{\tau_c}{N_{\mathrm{cs}}}\frac{dN_{\mathrm{cs}}}{dt}=1-\left(\frac{N_{\mathrm{cs}}}{N(T)}\right)^{\alpha-1}$$

instead of

$$\frac{\tau_c}{N_{\mathrm{cs}}}\frac{dN_{\mathrm{cs}}}{dt}=1-\left(\frac{N_{\mathrm{cs}}}{(NT)}\right)^{\alpha}.$$

REVIEWS OF BOOKS

The Structure of Matter, by F. O. Rice and E. Teller. Pp. xiii+361. 1st Edition. (New York: John Wiley and Sons; British Agents: Chapman and Hall, 1949.) 30*s*.

The great successes achieved by quantum theoretical methods in the rationalization and understanding of physical and chemical phenomena have raised inevitable difficulties in the teaching of physics and, particularly, of chemistry. The phenomena of molecular structure and of chemical reactions involving simple systems are now amenable to quantitative interpretation in terms of concepts such as energy levels, wave functions, degenerate states, bonding orbitals, spin functions, reaction complexes, and so on, but the understanding of these concepts requires some knowledge of quantum mechanics, and this in turn requires a mathematical equipment well beyond the elementary calculus with which most students of physics and chemistry can be assumed to be equipped.

The work under review aims at providing an introduction to the study of theoretical chemistry and related topics while keeping the mathematical formalism to a minimum. As an indication of the success achieved, the authors manage to express in a lucid and imaginative way some of the most fruitful (and difficult) concepts of quantum theory without once stating the Schrödinger Equation.

The book however deals, not with the concepts themselves, but with their application to atomic and molecular structure, the chemical bond, atomic and molecular spectra, molecular vibrations and related topics. Chapters are also included on nuclear chemistry and the state of matter in stars. The presentation is stimulating throughout and the book represents a notable contribution to the teaching of quantum chemistry. Students of physics and chemistry in the third year of their course, and graduate students alike, will find it of great value.

This book is the first in the Wiley " Structure of Matter " Series and sets a very high standard both in subject matter and in technical excellence of production. E. H. S. B.

The Adsorption of Gases on Solids, by A. R. Miller. Pp. xi+133. Cambridge Monographs on Physics, 1st Edition. (Cambridge: University Press). 12*s*. 6*d*.

Ten years ago J. K. Roberts wrote a monograph called *Some Problems in Adsorption* giving a live account of his own recent researches, experimental and theoretical, on the adsorption of gases (hydrogen and oxygen) as monolayers at the surface of a clean metal (tungsten). This monograph was then, is still, and will remain a valuable, instructive and faithful first-hand record of how an outstanding physicist plans and directs the exploration of a new field. Unfortunately the monograph is out of print.

The editors instead of reprinting Roberts' monograph asked his pupil A. R. Miller to ' revise ' it. The result is the book now under review. The ' revision ' consisted of (*a*) omission of some bits of theory and substitution of others (the essentially new matter is equivalent to rather more than a chapter), (*b*) some changes in the order of presentation, (*c*) replacement of an accurately descriptive title by a thoroughly misleading one, (*d*) substitution of the reviser's name for the author's.

The reviewer is not at all clear what is gained by thus revising this kind of monograph. The product is no longer an authoritative description of how a great researcher works. It is certainly not the sort of book that Roberts himself might have written now had he been alive, for his outstanding characteristic was progress, not stagnation. He would have discarded the clumsy statistical methods used ten years ago in favour of the simpler and more direct methods developed meanwhile and incidentally used elsewhere by Miller himself. Still less can the book be regarded as a comprehensive textbook on the adsorption of gases on solids. Perhaps it is merely the book which the editors or the reviser would have wished Roberts to write. E. A. G.

Les Spectres Moléculaires, Colloques Internationaux, Paris, May 1947. Pp. 176. (Paris: Centre Nationale de la Recherche Scientifique; British Agents: H. K. Lewis, 1948). 16*s*.

Collected in this book are the 46 papers which were presented at an international conference held in Paris in May 1947, and which have since been reprinted either in the *Journal de Physique* or in the *Journal de Chimie Physique*. A few papers discuss topics in the spectroscopy of diatomic molecules—for example, the demonstration of septet–septet transitions in the manganese halides, and the question of interchange of rotational and translational energy between AlH and He—but most of the work can be described as the application of infra-red and Raman spectroscopy to structural problems of polyatomic molecules. Notable here are the studies of crystals which seek information about questions as diverse as those of symmetry, dynamics and hydrogen-bonding. Earlier established subjects are not neglected, and there are articles on the improvement of vibrational potential functions, measurements of absolute intensities and the use of isotopic substitution. The progress here is illustrated by the account of the first singlet excited state of benzene, which fits so happily with what is known theoretically of the electronic structure of this species.

Although the work of some of the most active laboratories in this field is not represented, so that there is, for example, no mention of microwave spectroscopy, the book does provide both an interesting picture of the directions in which the subject is moving and a useful key to some of the literature—there are about 300 references, many to work done or published during the war years. R. F. B.

Electron Tubes, by the LABORATORIES OF THE RADIO CORPORATION OF AMERICA. Volume I (1935–41). Pp. x+475. Volume II (1942–48). Pp. x+454. 1st Edition. (Princeton, New Jersey: R.C.A. Review, 1949.) $2.50 each volume.

These two volumes form the ninth and tenth in the *R.C.A. Technical Book Series* and are the first to be devoted entirely to electron tubes. They are made up of reprints of some of the most important papers published by workers at the Radio Corporation of America, together with abstracts of some other papers and a complete bibliography of all the publications of the Laboratory on this subject.

The material presented in Volume I, which covers the period 1935–41, is by now fairly well known, and the collection here presented will probably be of most interest to workers in the subject, partly as an historical account and partly as containing some of the key papers on important aspects of tube design. The series of five papers by Thomson, North and Harris on " Fluctuations in Space-charge Currents at moderately high Frequencies " are by now classical and provide a good introduction to the problems of ' noise ' in electron tubes. The paper by Linder on " Excess-energy Electrons and Electron Motion in high-vacuum Tubes " deals with excess energy electrons in magnetrons and the excessive ' noise ' produced by them. The subject is of present-day interest, not only because magnetrons are still ' noisy ' but also because mechanisms of the type described here are being suggested as possible causes of ' noise ' radiation from sunspots. The papers on " Beam Power Tubes " by Schade and " The Secondary Emission Multiplier " by Zworykin, Morton and Malter are well known.

Volume II (1942–48) is likely to be of more general interest, not only because the subject-matter is newer but also because many radio workers, not immediately concerned with problems of vacuum tubes, had not time during the war years to follow the literature on the subject. For them it is valuable to have a collected series of reprints of the kind here presented. The papers on " Grounded Grid Amplifiers " (M. C. Jones), " Excess Noise in Cavity Magnetrons " (R. L. Sproull), " Maximum Efficiency of Reflex Klystrons " (Linder and Sproule), " Beam Deflection Control for Amplifier Tubes " (Kilgore), " Small Signal Analysis of Travelling-wave Tubes " (Shulman and Heagy) and " Analysis of a Simple Model of Two-beam Growing Wave Tube " (Nergaard) all deal with important fundamental principles. It is of interest to note that work on the ‘ growing wave tube ’ appears to have started simultaneously and independently at R.C.A., by Haeff at the Naval Research Laboratory, and at the Bell Telephone Laboratories.

Naturally the volumes present a one-sided view of the development of electron tubes, but since the R.C.A. Laboratories have played such a great part in this development the papers cover most aspects of the subject, with only a few important gaps, amongst which the problem of the cavity magnetron is most noticeable. These volumes will find a place in all laboratories dealing with the design of electron tubes, and Volume II can well be read by the radio engineer with wide interests, at least until the subject is really well written up in textbook form.

J. A. RATCLIFFE.

Reprints of Papers in the ‘Proceedings of the Physical Society’

In general, reprints of papers published in the *Proceedings of the Physical Society* are not available at the Offices of the Society, but may occasionally be obtained from the authors of the papers concerned. The address of the author is given at the head of each paper.

Exceptions to this are the special Lectures delivered before the Society, such as the Guthrie Lecture, the Presidential Address, the Charles Chree Lecture and the Rutherford Lecture.

CONTENTS FOR SECTION B

PAGE

Dr. G. G. Haselden. The Deposition of Ice Crystals on Cooling Surfaces in Low Temperature Plant 157

Mr. T. S. Moss. A Relationship between the Refractive Index and the Infra-Red Threshold of Sensitivity for Photoconductors 167

Dr. R. Cooper. Capacitance Measurements on Selenium Rectifiers : Evidence of Anomalous Dispersion 176

Mr. J. W. Warren, Mr. W. Hopwood and Dr. J. D. Craggs. On Dissociation Processes in certain Gases of High Dielectric Strength 180

Dr. R. C. Parker and Mr. D. Hatch. The Static Coefficient of Friction and the Area of Contact 185

Prof. E. N. da C. Andrade and Dr. R. F. Y. Randall. The Thermal Etching of Single Crystals of Cadmium 198

Mr. H. D. Keith. The Lattice-Parameters of Clear Crystalline Quartz . . 208

Letters to the Editor :

Dr. J. Collard, Mr. G. R. Nicoll and Dr. A. W. Lines. Discrepancies in the Measurement of Microwave Power at Wavelengths below 3 cm. . . 215

Reviews of Books 216

Corrigenda 221

Contents for Section A 222

Abstracts for Section A 222

ABSTRACTS FOR SECTION B

The Deposition of Ice Crystals on Cooling Surfaces in Low Temperature Plant, by G. G. HASELDEN.

ABSTRACT. A study is made of the conditions governing the deposition of ice crystals from a moist air stream on to the inside surface of a cooled tube. The promoting effect of impurities such as oil vapour in the air stream is demonstrated. Series of experiments were made to establish the effect of air velocity, and of the temperature difference between the tube wall and air stream, on the amount of deposition. In the flow range tested (Reynolds' number 11,000 to 27,000) it was observed that increasing the air velocity increased the percentage deposition; at the lower velocities there was no evidence of progressive deposition. The effect of temperature difference on the percentage adhesion in the range 7° to 14° C. was small, but an experiment at a value of 4·6° C. showed a decrease in the amount of condensed snow deposited. In most experiments a glass tube was used but in others use of a brass tube gave similar results.

A Relationship between the Refractive Index and the Infra-Red Threshold of Sensitivity for Photoconductors, by T. S. MOSS.

ABSTRACT. It is shown that for photoconductive compounds the long wavelength ' threshold ' of sensitivity λ should be related to the refractive index n of the photoconductor, and analysis of the available data shows that for the more highly refractive compounds n^4/λ always has a value close to 77. As a consequence of this relation, an explanation can be given for the change of the threshold wavelength with temperature which is observed for lead sulphide and similar materials. Suggestions are made as to what materials ought to be suitable for photoconductive detectors at longer wavelengths in the infra-red, and some confirmation of the ideas is shown by results obtained with cadmium arsenide, the properties of which are briefly described.

Capacitance Measurements on Selenium Rectifiers: Evidence of Anomalous Dispersion, by R. COOPER.

ABSTRACT. The paper presents evidence showing that, contrary to the generally accepted view, the capacity of a selenium rectifier at audio frequencies may vary with the frequency of measurement. The magnitude of the variation depends on the metal used as counter-electrode. Thus in the frequency range 300–2,000 c/s. little variation occurs with antimony or bismuth, but with cadmium there is a considerable decrease in capacitance. The effect is considered due to polarization arising from the relative motion in the selenium lattice of the negatively charged impurity centres and positive ions which diffuse into the selenium from the counter-electrode.

On Dissociation Processes in certain Gases of High Dielectric Strength, by J. W. WARREN, W. HOPWOOD and J. D. CRAGGS.

ABSTRACT. The dissociation processes, due to electron collisions, in certain polyatomic gases such as CCl_4, CCl_2F_2 are discussed with reference to the unusually high dielectric strength of certain of these gases. Possible explanations of the latter are then suggested in terms of these dissociation processes.

The Static Coefficient of Friction and the Area of Contact, by R. C. PARKER and D. HATCH.

ABSTRACT. An apparatus for measuring the static coefficient of friction has been designed in which the forces tending to disturb the contact area are minimized and which further enables the contact area to be viewed throughout the experiment. Application of a tangential load, less than that required to give limiting friction, has been shown to give rise to a growth of both the real and apparent contact areas and to produce a relative displacement of the surfaces to an extent governed by the tangential load. An examination of the surface topography, by means of an electron microscope, has shown that the earlier type of slip ceases because surface scratches extend the boundaries of real contact. Both the force of adhesion and the tangential force vary linearly with the real and apparent areas of contact. These results are in accord with a cohesive theory of friction, and offer no support for the theory on which friction is attributed to the formation of welded junctions.

The Thermal Etching of Single Crystals of Cadmium, by E. N. DA C. ANDRADE and R. F. Y. RANDALL.

ABSTRACT. The heating of single crystal wires of cadmium in circumstances that permit free evaporation produces a development of crystalline planes. When the basal plane makes a small angle with the axis of the wire there is a characteristic formation of hexagonal pits, the bottoms of which are mirror-like basal planes : when the basal planes make larger angles, characteristic elliptical traces appear, reminiscent of those formed by mechanical extension. The thermal etching reveals, by the formation of steps, thin laminae existing in the unstrained wire : the thickness of these, of the order of 1 μ, is the same as the spacing of the glide planes revealed by mechanical extension. The etched figures, in general, indicate that the substructure revealed by straining is already present in the unstrained crystal. The secondary pyramidal faces revealed agree with the calculations of Stranski, Kaischew and Krastanov.

The mirror-like basal planes are sufficiently large to permit the application of an optical method to reveal a scatter in their inclination to the axis. This method shows that there is a variation, of round about 20 minutes, of orientation among the basal planes about the direction of growth of the crystals, which were grown by the method of Andrade and Roscoe and showed good single crystal properties by the usual criteria.

The Lattice-Parameters of Clear Crystalline Quartz, by H. D. KEITH.

ABSTRACT. Some experimental results are presented showing that the calibration of Debye–Scherrer X-ray diffraction cameras by means of clear crystalline quartz may lead to appreciable errors unless the parameters of the quartz are first determined by a direct method. The parameters of a sample of clear Brazilian quartz have been found to be in serious disagreement with the accepted values, and variations in the parameters of synthetic quartz, with an apparent dependence on growth temperature, have also been observed. Taken in conjunction with previous results of other workers, the experiments show that quartz parameters vary from sample to sample by amounts as large as 0·01% according to the impurity content. The previously proposed quartz calibration standard is rejected.

PHYSICAL SOCIETY PUBLICATIONS

Fellows and Student Members of the Society may obtain ONE copy of each publication at the price shown in brackets. In most cases the cost of postage and packing is extra.

Noise and Sound Transmission. Report of the 1948 Summer Symposium of the Acoustics Group of the Physical Society. Pp. 200. In paper covers. 17*s*. 6*d*. (10*s*. 6*d*.) Postage 6*d*.

Resonant Absorbers and Reverberation. Report of the 1947 Summer Symposium of the Acoustics Group of the Physical Society. Pp. 57. In paper covers. 7*s*. 6*d*. (5*s*.) Postage 6*d*.

The Emission Spectra of the Night Sky and Aurorae, 1948. Papers read at an International Conference held under the auspices of the Gassiot Committee in London in July 1947. Pp. 140. In paper covers. 20*s*. (12*s*. 6*d*.) Postage 6*d*.

The Strength of Solids, 1948. Report of Conference held at Bristol in July 1947. Pp. 162. In paper covers. 25*s*. (15*s*. 6*d*.) Postage 8*d*.

Report of International Conference on Fundamental Particles (Vol. I) *and Low Temperatures* (Vol. II), 1947. Conference held at Cambridge in July 1946. Pp. 200 (Vol. I), pp. 184 (Vol. II). In paper covers. 15*s*. each vol. (7*s*. 6*d*.) Postage 8*d*.

Meteorological Factors in Radio-Wave Propagation, 1947. Report of Conference held jointly with the Royal Meteorological Society in April 1946. Pp. 325. In paper covers. 24*s*. (12*s*.+postage 1*s*.)

Handbook of the 34th Exhibition of Scientific Instruments and Apparatus, 1950. Pp. 270 (approx.). In paper covers. 5*s*. (2*s*. 6*d*.) Postage 1*s*.

Handbook of the 33rd Exhibition of Scientific Instruments and Apparatus, 1949. Pp. 272. In paper covers. 5*s*. (2*s*. 6*d*.) Postage 1*s*.

Catalogue of the 32nd Exhibition of Scientific Instruments and Apparatus, 1948. Pp. 288. In paper covers. 5*s*. (2*s*. 6*d*.) Postage 1*s*. (Half price from 5th April 1949).

Catalogue of the 31st Exhibition of Scientific Instruments and Apparatus, 1947. Pp. 298. In paper covers. 2*s*. 6*d*. (1*s*. 6*d*.) Postage 1*s*.

Report on Colour Terminology, by a Committee of the Colour Group. Pp. 56. In paper covers. 7*s*. (3*s*. 6*d*.)

Report on Defective Colour Vision in Industry, by a Committee of the Colour Group. 1946. Pp. 52. In paper covers. 3*s*. 6*d*. (1*s*. 9*d*.+postage 4*d*.)

Science and Human Welfare. Conference held by the Association of Scientific Workers, Physical Society and other bodies. 1946. Pp. 71. In paper covers. 1*s*. 6*d*. (9*d*.) Postage 4*d*.

Report on the Teaching of Geometrical Optics, 1934. Pp. 86. In paper covers. 6*s*. 3*d*. Postage 6*d*.

Report on Band Spectra of Diatomic Molecules, 1932. By W. Jevons, D.Sc., Ph.D. Pp. 308. In paper covers, 25*s*.; bound in cloth, 30*s*. (15*s*.) Postage 1*s*.

Discussion on Vision, 1932. Pp. 327. In paper covers. 6*s*. 6*d*. (3*s*. 3*d*.) Postage 1*s*.

Discussion on Audition, 1931. Pp. 151. In paper covers. 4*s*. (2*s*.) Postage 1*s*.

Discussion on Photo-electric Cells and their Application, 1930. Pp. 236. In paper covers. 6*s*. 6*d*. (3*s*. 3*d*.) Postage 8*d*.

The Decimal Bibliographic Classification (*Optics, Light and Cognate Subjects*), 1926. By A. F. C. Pollard, D.Sc. Pp. 109. Bound in cloth. 4*s*. (2*s*.) Postage 8*d*.

Motor Headlights, 1922. Pp. 39. In paper covers. 1*s*. 6*d*. (9*d*.) Postage 4*d*.

Report on Series in Line Spectra, 1922. By A. Fowler, C.B.E., Sc.D., F.R.S. Pp. 182. In paper covers. 30*s*. (15*s*.) Postage 8*d*.

A Discussion on the Making of Reflecting Surfaces, 1920. Pp. 44. In paper covers. 2*s*. 6*d*. (1*s*. 3*d*.) Postage 4*d*.

Reports on Progress in Physics. Vol. XII (1948–49). Pp. 382. Bound in cloth. 42*s*. (25*s*.) Postage 1*s*.

Reports on Progress in Physics. Vol. XI (1946–48). Pp. 461. Bound in cloth. 42*s*. (25*s*.) Postage 1*s*.

Reports on Progress in Physics. Vols. IV (1937, reprinted 1946) and X (1944–45). Bound in cloth. 30*s*. each. (15*s*.) Postage 1*s*.

The Proceedings of the Physical Society. From Vol. I (1874–75), excepting a few parts which are out of print. Prices on application to Messrs. Wm. Dawson Ltd., 102 Wigmore St., London W.1.

The Transactions of the Optical Society. Vols. 1 (1899–1900) –33 (1931–32), excepting a few parts which are out of print. Prices on application to Messrs. Wm. Dawson Ltd., 102 Wigmore St., London W.1.

Orders, accompanied by remittances, should be sent to

THE PHYSICAL SOCIETY

1 Lowther Gardens, Prince Consort Road, London S.W.7

The
PHILOSOPHICAL
MAGAZINE
(First Published 1798)

A Journal of
Theoretical Experimental
and Applied Physics

EDITOR:
PROFESSOR N. F. MOTT,
M.A., D.Sc., F.R.S.
EDITORIAL BOARD:
SIR LAWRENCE BRAGG,
O.B.E., M.C., M.A., D.Sc., F.R.S.
ALLAN FERGUSON,
M.A., D.Sc.
SIR GEORGE THOMSON,
M.A., D.Sc., F.R.S.
PROFESSOR A. M. TYNDALL,
C.B.E., D.Sc., F.R.S.

ANNUAL SUBSCRIPTION
£5 2s. 6d.
OR
10s. 6d.
EACH MONTH
POST-FREE

Contents for March 1950

FEODORA BERZ on "Potentials Derived from Axial Values in Electron Optics".

H. FRÖHLICH, H. PELZER & S. ZIENAU on "Properties of Slow Electrons in Polar Materials".

A. B. PIPPARD on "The Kinetics of the Phase Transition in Superconductors".

CLAUDE E. SHANNON on "Programming a Computer for Playing Chess".

B. L. COLEMAN on "The Propagation of Electromagnetic Disturbances along a Thin Wire in a Horizontally Stratified Medium".

D. M. MacKAY on "The Quantal Aspects of Scientific Information".

BOOK REVIEWS.

ALERE FLAMMAM
Established 150 Years

TAYLOR & FRANCIS LTD., Red Lion Court, Fleet St., LONDON, E.C.4

Printed by Taylor and Francis, Ltd., Red Lion Court, Fleet Street, London E.C.4